SOMATOSTATIN NEURONS IN PREFRONTAL CORTICAL MICROCIRCUITS IN SCHIZOPHRENIA

by

Samuel James Dienel

Bachelor of Science, Neuroscience, University of Pittsburgh 2014

Submitted to the Graduate Faculty of the

Dietrich School of Arts and Sciences in partial fulfillment

of the requirements for the degree of

Doctor of Philosophy

University of Pittsburgh

2022

UNIVERSITY OF PITTSBURGH

DIETRICH SCHOOL OF ARTS AND SCIENCES

This dissertation was presented

by

Samuel James Dienel

It was defended on

July 13, 2022

and approved by

Cameron S. Carter, MD, Department of Psychiatry,
University of California, Davis

Kenneth N. Fish, PhD, Department of Psychiatry

Caroline A. Runyan, PhD, Department of Neuroscience

William R. Stauffer, PhD, Department of Neurobiology

Committee Chair: Stephen D. Meriney, PhD, Department of Neuroscience

Dissertation Advisor: David A. Lewis, MD, Department of Psychiatry

SOMATOSTATIN NEURONS IN PREFRONTAL CORTICAL MICROCIRCUITS IN SCHIZOPHRENIA

Samuel James Dienel, Ph.D.

University of Pittsburgh, 2022

Certain cognitive functions, including working memory, are impaired in individuals with schizophrenia. These cognitive impairments are key predictors of functional outcomes in this patient population, but there are no available therapeutic options to ameliorate these impairments. Only postmortem studies of the brain can reveal alterations in the cortical circuitry in schizophrenia that could underlie these cognitive disturbances and inform therapeutic intervention. Proper working memory function requires robust resistance to distracting information, and it appears that working memory deficits in schizophrenia reflect, at least in part, heightened susceptibility to distractors. The capacity for working memory generally, and especially for filtering out distracting information, is heavily dependent on activity in the dorsolateral prefrontal cortex (DLPFC). Convergent lines of evidence suggest that within the DLPFC, dendritic inhibition, provided from GABA neurons expressing the neuropeptide somatostatin (SST), is crucial for mediating distractor resistance in the DLPFC. The DLPFC, relative to other cortical regions, is enriched for SST mRNA, supporting the idea that SST neurons contribute to a distractor-resistant circuit. In schizophrenia, SST mRNA levels are markedly lower in the DLPFC, suggesting that impairment of these neurons in the disorder render these individuals more susceptible to distractors during working memory. Here, this dissertation work elucidates the *basis* for these differences in mRNA levels. In the first chapter, we find that higher SST in the DLPFC relative to the primary visual cortex reflects a greater proportion of SST neurons in the DLPFC,

rather than SST levels per neuron. In contrast, in the second chapter, we find that deficits in SST mRNA in the DLPFC of schizophrenia primarily reflect lower gene expression per neuron without a deficit in neuron density. Finally, in the third chapter, we find that SST neurons exhibit lower levels of key GABA synthesizing enzymes in schizophrenia, indicating that these neurons have an impaired capacity to provide inhibition. The results of this dissertation reveal the *nature* of SST neuron disturbances in the DLPFC in schizophrenia, inform the putative impact of these alterations in the context of working memory, and offer insight for novel therapeutic interventions aimed at ameliorating the cognitive burden in the disorder.

TABLE OF CONTENTS

LIST OF TABLES

LIST OF FIGURES

ABBREVIATIONS

BDNF: brain-derived neurotrophic factor

CB: calbindin

CCK: cholecystokinin

CR: calretinin

CHODL: chondrolectin

DAPI: 4',6-diamidino-2-phenylindole

DLPFC: dorsolateral prefrontal cortex

FISH: fluorescent *in situ* hybridization

fMRI: functional magnetic resonance imaging

GABA: γ-aminobutyric acid

GABRA1: $GABA_A$ receptor subunit α1

GABRA2: $GABA_A$ receptor subunit α2

GAD65: glutamic acid decarboxylase, 65 kilodalton isoform

GAD67: glutamic acid decarboxylase, 67 kilodalton isoform

GAT1: GABA membrane transporter 1

mRNA: messenger ribonucleic acid

MRS: magnetic resonance spectroscopy

NPY: neuropeptide Y

NOS1: nitric oxide synthase 1

PET: positron emission topography

PV: parvalbumin

PVBC: parvalbumin basket cell

qPCR: quantitative polymerase chain reaction

SOX6: SRY-Box transcription factor 6

SST: somatostatin

TAC1: tachykinin 1 (alias, substance P)

TACR1: tachykinin 1 receptor

VGAT: vesicular GABA transporter

VIP: vasoactive intestinal peptide

ACKNOWLEDGEMENTS

It is fitting that this thesis begins with a statement about all of those who have devoted themselves to my betterment, as this accomplishment would not exist without them. I am grateful to all the programs and institutional support throughout my pursuit of the physician-scientist life: to the Translational Neuroscience Program (TNP) in the Department of Psychiatry, of which I have been a part of for 8 years, for incubating my intellectual and scientific development and the extraordinary opportunities for learning; to the Center for Neuroscience at the University of Pittsburgh (CNUP), for the many faculty members who are extremely generous with their time and knowledge and commitment to graduate training; to the Medical Scientist Training Program (MSTP), for the outstanding guidance of the next generation of physician-scientists, of which I am a great beneficiary.

In particular, I am indebted to the members of my thesis committee: Stephen Meriney, Cameron Carter, Caroline Runyan, and Bill Stauffer. I wanted all of you as members of my committee because of your demonstrated commitments to scientific excellence and the passage of that excellence onto the next generation of scientists. Your thoughtful feedback and facilitation of my graduate training has been invaluable to my development, and I am deeply grateful for your time. I look forward to the many more conversations we will have in the future, and hope that this is only the beginning of many years of collaborations.

I am grateful to Richard Steinman, for your consistent and unwavering commitment to training physician-scientists at the University of Pittsburgh. Your generosity and graciousness towards myself and the other students does not go unnoticed, and we are all thankful for your commitment to mentoring. Additionally, I am grateful to the mentoring provided by Elias

Aizenman, my career advisor, and for all the time you have spent meeting with me throughout my MSTP career. I am also grateful to my undergraduate research mentor, Charles Horn, for taking me into the lab as a freshman in college and instilling in me a love for science that pushed me to pursue the MSTP path.

I am so grateful for the members of the Lewis lab. In particular, I want to thank Kiley Laing and Kelly Rogers, my first managers when I started at the TNP in 2014, as well as Mary Ann Kelly, Holly Bazmi, and Dominique Arion. You have all been a part of my TNP experience from when I started there in 2014 and have contributed so significantly to every project described in this thesis. I cannot begin to thank you enough for your generosity with your time. Additionally, I want to thank Jill Glausier, Matt MacDonald, Melanie Grubisha, Rob Sweet, Marianne Seney, Zach Freyberg, John Enwright, David Volk, Takanori Hashimoto, Sohei Kimoto, and Guillermo Gonzalez-Burgos for all your support and many wonderful conversations about science in the hallways of the 16th floor and virtually. I want to thank Mary Brady for all her amazing work over the years with figure creation for articles and chapters and Amy Noll, Sharon Slovenec, and Lisa Murphree for all their support over the entire time I've been a part of the TNP.

Many friends have supported me throughout this journey, both inside and outside the lab. From the MSTP: Michael Granovetter, Ali Butler, Alex Layden, Ansen Burr, Eileen Nguyen, and Roger Tieu. You have all provided tremendous support over the years, and I am grateful to be going through this journey with you. From the TNP: Wonjae Chung, Kirsten Schoonover, Kevin Dowling, Youjin Chung, Silas Buck, Kirsten Wade, Julia Vespoli, Amy Liu, Tyler Myers, Gil Hoftman, and Dibs Datta. You have all been tremendous collaborators and friends, aiding on the various projects described within, and I feel very lucky to have crossed paths with each of you in this journey. In addition, I want to thank Matt Humes, Lisa Zimmerman, Abby Pipcho, Rachael

Viehman, Sue Johnston, Jenna Lindsay, Jean Miewald, Zack Barile, Matty Maier, Tori Detweiler, Rhea Lipscomb, Daley Favo, Mikaela Fenn, Kenny Clark, Andy Ciesielski, Kyle Terrill, Liban Dinka, Alicia Locker, Elizabeth Profozich, and Matty Maier. You have all, in different ways, been committed to the work in this dissertation and to my development as a scientist. Outside of the lab, I am especially grateful to Kurt Werner, Jonathan Cunningham, Tyler Lucas, Kyle Irwin, Dan Bendit, Cody Sandahl, and Dennis Allan. Your friendship, wisdom, and constant support of me is one of the greatest gifts I've received.

I am thankful to Ken Fish who is not only a committee member, but a co-mentor. None of the work described in this dissertation would have been possible without all the time you devoted to me and these projects. Your tenacity and commitment to technical advances have allowed us to answer questions in the lab in a time frame not conceivable even a year ago. Thank you for the endless hours of conversations in the lab and over the phone, all the hours spent troubleshooting and fixing microscopes, and providing unfettered access to their use.

I am so incredibly indebted to my dissertation advisor, Dave Lewis. You have been a paragon of scientific mentorship over the years, providing tremendous opportunities for me inside and outside of the lab, supporting and challenging my ideas, providing the space and resources necessary to carry out these experiments, and always putting my interests above your own. Thank you for your partnership in the shared mission of this research. More importantly, thank you for your unwavering friendship over the years in all times, and for the cherished times meeting on Wednesday mornings over the years. Thank you for agreeing to take me into the lab back in 2013; that providential experience that you provided has profoundly changed the trajectory of my life, for the better. My hope is that it does the same for the field of psychiatric and neurosciences in the future.

I want to thank my uncles, Gerry Dienel and Nick Dienel, who have both provided so much love and support for my journey, and provided so much mentoring and advice through their own careers as a neuroscientist and physician. I'm deeply grateful for all the conversations that we've had throughout the years and for your love and support.

My parents, Phil and Nancy Dienel, have been so profoundly supportive of me throughout this journey, and to any degree that I can be proud of the work contained within this document, I reflect that back to them for how they raised in and continue to love and support me. Thank you for everything you sacrificed to raise me as you did and for all that you continue to sacrifice for me. I will never be able to thank you enough for all you did.

I am only here today because of all that my beloved aunt, Kathy Roberts, did for me. Thank you for everything you did to make my childhood such a glowing and enriching experience. Thank you for your commitment to fun, to excellence, to new ideas, to cooking, and for passing all of that onto me. I truly believe that all the work in this dissertation has a direct through-line to those late nights working on school projects together, to the way you included me in everything you were doing, the obsession with details, and the pride we had in the finished projects. You are loved, and you are deeply missed.

I am forever grateful to my partner and wife, MaryJane Anderson. Your love and support is unceasing, and I am grateful for how you have continuously supported my career and passion. You are the light of my life, the one who I most want to share everything with, and I feel so lucky to have met you. Thank you for being on this journey with me to understand the world.

Finally, I am grateful to God, who I believe called me onto this journey and has never wavered in revealing the path forward. We are not long here, but I hope that in my short time, I can participate in the mission of providing healing and shalom for those afflicted by brain diseases.

We seek the truth; but if some voice told us that a few years more would see the end of our journey, that the clouds of uncertainty would be dispersed, and that we should perceive the whole truth about the physical universe, the tidings would be by no means joyful. In science as in religion, the truth shines ahead as a beacon, showing us the path; we do not ask to attain it, it is better far that we be permitted to seek.

—Sir Arthur Eddington

Science and the Unseen World, 1929

Through it, he is a minister of progress, a priest of truth, and a confidant of the Creator. He is devoted entirely to understanding something of that mysterious language that God has written in nature. He alone is allowed to penetrate the marvelous works of Creation. He renders to the Absolute the most pleasing and acceptable homage—studying His prodigious handiwork so as to know, admire, and revere him through it.

—Santiago Roman y Cajal

Advice for a Young Investigator, 1897

1.0 GENERAL INTRODUCTION

Diseases that afflict the brain often rob us of the most crucial functions that define our sense of being in the world. The human brain, the most complex organ in the known universe, is the vehicle by which we effectuate our personhood, interact with others, and solve problems that seem only within the reach of humans. Whether those problems involve the mundane: planning your day, carrying out work that contributes to the local or global economy, or integrating oneself into the social milieu; or the complex: developing massive social structures that organize our society and define our sense of justice, pushing the boundaries of human knowledge, or engineering the newest structural, biological, and chemical entities that manipulate the world around us; all of these depend on the brain. This complexity comes at a cost: like all biological entities, the brain is subject to disease, disorder, and decay, and these processes incapacitate our ability to participate in all the activities that define the human condition.

This thesis focuses on one such brain disorder, schizophrenia. Schizophrenia is a global scourge that annually robs approximately one million new people worldwide of some of the key functions that are emergent properties of the human brain. Individuals diagnosed with schizophrenia experience a wide range of impairments in key aspects of reality testing, mood regulation, and cognition. In the following sections, I describe the burden of schizophrenia, illuminated by epidemiological findings, the contribution of cognitive dysfunction to that burden, and the specific types of cognition that have been studied in detail and appear particularly disturbed in schizophrenia.

1.1 OVERVIEW OF SCHIZOPHRENIA

The presenting signs and symptoms of schizophrenia typically emerge during the second and third decades of life; the zenith of vitality and excitement for the future for many individuals. In a stereotyped disease course of schizophrenia, a person will themselves present or be taken by family members, friends, or law enforcement to a psychiatric hospital with a range of abnormal behavior, including endorsement of hallucinations or delusions and a range of disorganized thinking or behavior (Marder & Cannon, 2019). This period, considered the active phase of the disease course of schizophrenia, is the most striking aspect of schizophrenia and is the basis for clinical presentation. Here, I provide an overview of schizophrenia with special attention to the burden of the disorder at societal and individual levels, the epidemiology and etiology of the disorder, as well as the clinical features and currently available therapeutic interventions (Marder & Cannon, 2019). While these averages attempt to capture the general aspects of the disorder, individuals with schizophrenia are not a monolith; there is wide heterogeneity in symptom severity and level of functioning, as would be expected from the underlying heterogeneity in human hosts in which the disease process takes place.

1.1.1 Burden of schizophrenia

The burden of schizophrenia is heavy and endured by millions of people in the US and worldwide, as well as their family members and caregivers (Szkultecka-Dębek et al., 2016). The burden endured by those with schizophrenia include difficulty maintaining gainful employment (Evensen et al., 2016), self-care (Holmberg & Kane, 1999), or personal relationships (Ritsher et al., 2003). Estimates of the lifetime prevalence of schizophrenia are generally just under 1% of the

world population and is consistently ranked as one of the top causes of years of life lived with disability (James et al., 2018; Chong et al., 2016). There are many indices that substantiate this claim: the estimated cost of schizophrenia in the United States alone have significantly increased over the past 20 years: from $62.7 billion in 2002 (Wu et al., 2005), to $155.7 billion in 2013 (Cloutier et al., 2016), and has most recently been estimated at $330.6 billion in 2019 (Kadakia et al., 2022a). These costs reflect direct and indirect medical expenditures as well as years of lost productivity (Evensen et al., 2016; Chong et al., 2016).

Reduced life expectancy is perhaps the most illuminating feature for understanding the burden of schizophrenia. Indeed, persons with schizophrenia live 1-3 decades shorter than those without a major mental disorder: a burden that has been equated to heavy smoking (Chesney et al., 2014). In fact, the prevalence of smoking is substantially higher among persons with schizophrenia relative to other psychiatric disorders or the unaffected population (Diwan et al., 1998; Goff et al., 1992), contributing to higher mortality from pulmonary and cardiovascular disease (Olfson et al., 2015). Further contributing to this number is the heightened incidence of comorbid substance and alcohol use disorders, both further adding to measures of all-cause mortality (Olfson et al., 2015). Finally, individuals with schizophrenia are more likely to attempt (20% of those with schizophrenia) or complete (5% of those with schizophrenia) suicide (Hawton et al., 2005; Hor & Taylor, 2010). Together, these numbers reflect the reality of the human cost beyond the financials of the burden that schizophrenia has on individuals, their family members, and society.

During their life, individuals with schizophrenia are also more likely to endure many other challenges as a consequence of this mental disorder. For example, although schizophrenia is estimated to affect under 1% of the US population, the prevalence of schizophrenia among unhoused persons is strikingly higher (13.7% across individuals carrying a diagnosis of

schizophrenia or schizoaffective disorder; (Ayano et al., 2019)). In addition, individuals diagnosed with schizophrenia endure repeated and unrelenting stigmatization in society (Ritsher et al., 2003). One example of the stigma is the perception that individuals with schizophrenia, and indeed broadly those with a mental disorder, are more prone to exhibit violent behavior towards others, especially strangers. On the contrary, the convergence of findings from criminology suggests that persons with schizophrenia are no more likely to commit acts of violence than the psychiatrically unaffected population when compared in the same neighborhoods and localities (Wehring & Carpenter, 2011). Many of these studies point to the fact that there are likely underlying demographic (male sex, young) and societal factors (poverty, etc.) that are significantly better predictors for violent behavior than a diagnosis of schizophrenia (Appelbaum et al., 2000; Monahan, 2002; Steadman et al., 2015; Elbogen & Johnson, 2009). On the contrary, individuals with schizophrenia appear to be much more likely to be *victims* of violent crime than their psychiatrically unaffected counterparts (Maniglio, 2009; Teplin et al., 2005), although not all studies show evidence of this, and findings might vary by country (Sariaslan et al., 2020).

1.1.2 Epidemiology and etiology of schizophrenia

Schizophrenia is estimated to affect 0.25-0.75% of the population (Charlson et al., 2018; Lewis & Lieberman, 2000; McGrath et al., 2008). The disease course for schizophrenia is typically divided into three stages: prodromal, active, and residual phases. The prodromal phase can occur over the course of years and is characterized by subtle changes in behavior, social withdrawal, and impairments in work and school. The active phase is typically the clinically presenting phase, with the emergence of the diagnostic psychotic features of the disorder that onset between the late teen years and mid-30's. The residual phase is defined as the phase that might also be associated with

some ‘remittance’ of symptoms, with occasional re-emergence of psychotic symptoms. In the following section, I describe the epidemiological features of schizophrenia and some of the proposed etiological and risk factors associated with the disorder.

1.1.2.1 Sex and race differences in schizophrenia: a re-examination of dogma

Historically, schizophrenia has been reported to be more prevalent in males than females with a ratio estimated at 1.4:1, respectively (Aleman et al., 2003; McGrath et al., 2008). Recently, however, there are challenges to this dogma, with new findings that there are no differences in prevalence between sexes (Charlson et al., 2018; Saha et al., 2005). Moreover, the reported sex differences vary depending on diagnostic criteria used: diagnoses based on the Diagnostic and Statistical Manual of Mental Disorders (DSM) are more likely to result in a heightened male: female ratio of schizophrenia compared to diagnoses made based on the International Classification of Diseases (ICD)-9 (Beauchamp & Gagnon, 2004). However, it does seem clear that males and females have distinct disease courses: males are diagnosed earlier (early 20’s) relative to females (late 20’s/early 30’s) and tend to have worse functional outcomes (i.e., employment, marital status, or housing) compared to females (Sommer et al., 2020; Cotton et al., 2009; Hanlon et al., 2017).

Schizophrenia has been diagnosed across cultures, societies, and eras, but some culturally specific elements might be evident. For example, the content of delusions, including the perception of their prosecutorial and violatory nature, vary across cultures (Luhrmann et al., 2015; Luhrmann et al., 2021; Campbell et al., 2017). Moreover, the functional outcomes of individuals with schizophrenia might vary by cultures and societies, possibly reflecting of differences in the social support across government systems (Harvey et al., 2009) and localities (Marwaha et al., 2007). In 1986, a World Health Organization (WHO) collaborative study put forward the provocative

finding that persons with schizophrenia living in ‘developing’ nations exhibit better course and outcomes compared to those in ‘developed’ nations (Sartorius et al., 1986), a pattern that held in a reanalysis almost two decades later (Hopper & Wanderling, 2000). This distinction has been called into question (Patel et al., 2006b; Burns, 2009; Kulhara et al., 2009), both because of the imprecision in defining countries based on these terms and the more likely scenario that these terms simply capture a significant portion of unexplained variance that was not accounted for in these studies (Cohen et al., 2007).

One example of a contributory factor to cultural differences in the outcome of schizophrenia can be attributable to stigmatization across cultures. For example, in China, the concept of ‘face’ is the moral lodging of one’s status in community and is contingent on the interpersonal relationships in that community. Given the perception that individuals with schizophrenia act dangerously and unpredictably, those individuals are not viewed as fully participatory in social life, leading to the internalization of stigma (Yang & Kleinman, 2008). The disruption introduced by schizophrenia to this moral lodging introduces deep internalization of stigma by those diagnosed with schizophrenia and their caregivers (Wong et al., 2018b). This stigma is tied directly to certain functional outcomes, such as employment (Sum et al., 2021). Thus, differences in the internalization of stigma are just one example of an unexplained variable that could contribute to differences in outcomes in schizophrenia across countries. Importantly for this example, the negative impact of stigma has motivated efforts to introduce new terminology for schizophrenia in Asian cultures (Sartorius et al., 2014) and elsewhere (Brown, 2021).

Issues of race, ethnicity, and ancestry with regard to a diagnosis of schizophrenia are complex and interwoven with societal and cultural structures (Harnett & Ressler, 2021; Neighbors et al., 1989). It has been historically thought, perhaps emanating from a premature but widely cited

conclusion of the WHO collaborative study in 1986, that "schizophrenic (*sic*) illnesses occur with comparable frequency in different populations," (Sartorius et al., 1986). This quote has contributed to the myth that schizophrenia is an 'egalitarian disorder' (McGrath, 2005b; McGrath, 2005a). More recently, however, it has become clear that Black Americans are estimated as being 2.4 – 4 times more likely than White Americans to be diagnosed with schizophrenia (Olbert et al., 2018; Bresnahan et al., 2007; Schwartz, 2014;). Some of these racial differences might be attributable to the racial discrepancies, as a function of structural racism, in the exposure to certain risk factors that increase the likelihood for schizophrenia. These risk factors include trauma and stress during pre- and perinatal periods of pregnancy, among others (Anglin et al., 2021).

In addition, these differences appear to reflect, at least in part, biases intrinsic to the clinician-patient interaction and do not seem clearly attributable to heightened genetic risk reflecting ancestry differences in Black and White individuals (Calkins et al., 2010; Wiener et al., 2009). For example, after interviews, clinician-perceived honesty, which was lower in Black compared to White patients, partly mediated the racial differences in a diagnosis of schizophrenia (Eack et al., 2012). Additionally, similar to the United States, Black persons in England (where Black persons constitute a racial minority) are more likely to be diagnosed with schizophrenia related to White persons (Kirkbride et al., 2012; Halvorsrud et al., 2019), but this might not be true in places where Black persons are not part of the racial minority (Schwartz, 2014). Finally, while psychotic symptoms are more likely to be diagnosed in Black Americans, concurrent mood symptoms in Black Americans are less likely to be diagnosed relative to their White counterparts (Gara et al., 2019). An example of this phenomenon comes from one study that systematized the presentation of patients with and without racial cues in the prompts. The authors found, consistent with the clinical literature, that psychiatrists assessed psychosis as the first-rank symptom in Black

Americans more frequently than mood symptoms when racial cues were included in the transcripts, but equivalently when the clinicians were blind to racial cues (Strakowski et al., 2003).

Finally, it is worth noting that racism in psychiatric diagnoses, especially in the diagnosis of 'insanity' and schizophrenia, is deeply rooted in the ignominious past of this Nation's history. To provide two brief examples spanning 100 years of our country's short history, Dr. Samuel Carthwright, in the antebellum South in the 1850's, formed the pseudoscientific basis for psychiatric disorders such as 'drapetomania', or the insanity ascribed to Black slaves for running away from the plantation (Willoughby, 2018). In the Civil Rights era of the 1960's and 70's, the perception that those with paranoid schizophrenia exhibited 'hostile' and 'aggressive' behavior is embedded in the text of the second edition of the Diagnostic and Statistical Manual of Mental Disorders (published in 1968). This provided the professional justification for the institutional of Black male Civil Rights activists during this era and led to psychiatrists coining terms like "protest psychosis", coupling delusions and hallucinations with a rejection of 'white values' and 'civil society' (Metzl, 2010). Thus, a careful examination of present-day social and structural influences is required in our perception of mental disorders.

1.1.2.2 Etiology of schizophrenia

Risk factors for schizophrenia are well-established to consist of both genetic and environmental causes (Marder & Cannon, 2019; Torrey & Yolken, 2019). The genetic risk architecture for schizophrenia is complex and includes small contributions from many common polygenic variants (Psychiatric Genomics Consortium, 2009; Psychiatric Genomics Consortium, 2018; Fromer et al., 2014; Trubetskoy et al., 2022) , copy number variants (Marshall et al., 2017; Pocklington et al., 2015; Singh et al., 2017; Purcell et al., 2014), the latter which might be specifically associated with poorer cognition in schizophrenia (Hubbard et al., 2021). However,

schizophrenia is not a fully heritable disorder, and certain environmental risk factors appear to interact with the genetic risk to lead to the emergence of schizophrenia.

Some of the environmental risk factors for the later emergence of schizophrenia appear to be prevalent as early as gestation, with maternal immune insults in utero (Estes & McAllister, 2016; Kępińska et al., 2020) and obstetric complications (Lewis & Murray, 1987) being associated with schizophrenia risk. The finding of increased risk of schizophrenia as a consequence of maternal immune activation draws attention to the yet-unknown risk of the ongoing COVID-19 pandemic for the offspring of mothers during this period. Other oft-cited environmental risk factors for the emergence of schizophrenia include childhood trauma, urbanicity, minority group position, and cannabis use during adolescence (Marder & Cannon, 2019; van Os et al., 2010), with early and heavy adolescent cannabis use being very strongly associated with later psychosis risk (Albaugh et al., 2021; Curran et al., 2016; Marconi et al., 2016; Murray et al., 2017; Gage et al., 2016).

1.1.3 Clinical features and treatment paradigms for schizophrenia

Clinically, schizophrenia is diagnosed based on a set of signs and symptoms that have been grouped into three dimensions (American Psychiatric Association, 2022; Andreasen, 1995; Marder & Cannon, 2019): the psychosis dimension, the negative dimension, and the disorganization dimension. Symptoms within the psychosis domain include perceptual disturbances like hallucinations and delusions. Delusions, or fixed, false beliefs that persist in the face of contradictory evidence, are present in the vast majority of individuals diagnosed with schizophrenia and frequently assume a persecutory nature (Andreasen, 1987). Hallucinations, or sensory perceptions in the absence of external stimulation, can occur across sensory modalities but

are most frequently auditory in nature, occurring in ~75% of patients (Andreasen, 1987). The negative symptoms, a broad term that encompasses the concept of absence of normal brain functions, include diminished emotional expression and avolition (Black & Andreasen, 2014), as well as alogia and anhedonia. Together, these symptoms indicate that those with schizophrenia do not exhibit the range of emotional expression (for positive or negative experiences), goal-directed behavior, or spontaneous speech.

Another dimension of schizophrenia is known as the disorganization dimension, or formal thought disorders, encompassing the range of possible disorganized speech or behavior seen in these patients. Most often, these manifest as loose associations (switching from one topic to another) or tangentiality (unrelated responses to questions). Infrequently, disorganized thought and speech can manifest in such a manner that it manifests as aphasias observed in Wernicke's aphasia (generating 'word salads') (American Psychiatric Association, 2022). Other forms of formal thought disorder can include perseveration, distractibility, clanging (use of words together based on sound, not association), neologisms (new words), echolalia (meaningless repetition of another's' words), and blocking (interruption of speech in the middle without explanation, as if there was some internal interruption).

Finally, the cognitive symptoms refer to the constellation of impairments in certain executive functions (Kerns et al., 2008), including selective attention, working memory, episodic memory, and language comprehension. One interpretation of the constellation of altered executive functions is a generalized deficit in a concept known as cognitive control (Lesh et al., 2011), or the ability to use contextual information to guide behavior in the face of habitual (or prepotent) responding (Barch et al., 2008). Cognitive control and working memory are closely related

constructs, and cognitive control requires the maintenance of contextual information held in working memory (Smucny et al., 2022).

Among the constellation of symptoms and signs described above, the following are required for clinical diagnosis: A. Two or more of the following: delusions, hallucinations, disorganized speech, grossly disorganized or catatonic behavior, and negative symptoms, and at least one has to include delusions, hallucinations, or disorganized speech. B. Level of functioning in major areas of work, relationships, or self-care is markedly below the level achieved prior to the onset of the disease. C. Continuous signs of the disturbances for >6 months. Further, the diagnosis cannot be attributable to other conditions (i.e., substance induced psychoses), and the distinction between schizophrenia and schizoaffective disorder (meeting criteria for schizophrenia with a concurrent major mood episode, either depressive or manic).

Notably, none of these diagnostic criteria require the presence of cognitive dysfunction. However, the concept of cognitive dysfunction as the core feature of the disorder is strongly supported by the clinical literature (Kahn & Keefe, 2013). Additionally, nearly all treatment paradigms focus on the (often successful) treatment of psychotic symptoms using antipsychotic medications. However, none of the available antipsychotic therapies appear to ameliorate cognitive disturbances in schizophrenia (Keefe et al., 2007; Mishara & Goldberg, 2004). Thus, treatment of the cognitive symptoms in schizophrenia remains a major unmet need.

1.2 COGNITIVE DYSFUNCTION IS A CORE FEATURE OF SCHIZOPHRENIA

Since the very first descriptions of schizophrenia, cognitive impairments have been observed to be a core feature of the disorder. Emil Kraepelin, a German psychiatrist who, during

the late 19th and early 20th century, first described *dementia praecox*, or precocious dementia. Hagiographies have been written lauding Kraepelin's importance (Ebert & Bär, 2010) in developing the notion that certain psychiatric disorders can be grouped into symptom clusters, rather than singular symptoms–a concept that continues to pervade our modern conception of psychiatric diagnoses and as defined by the DSM. Diagnostic distinctions between *dementia praecox*, which Eugen Bleuler later updated and relabeled as *schizophrenia*, from manic-depressive insanity, known now as bipolar disorder, was "by far the most important, […] yet at the same time also the most difficult," (Kraepelin, 1921). Although Kraepelin describes multiple distinctions between these two disorders, one of the key distinctions is related to conversation: "In dementia praecox again conversation is frequently altogether senseless and incoherent in spite of very slight excitement, while even in the most violent raving mania we seldom quite lose an at least approximate understanding of the manic train of thought." (Kraepelin, 1921). Further, Kraepelin distinguished dementia praecox from *hysteria* (an antiquated term with no clear modern equivalent) as follows: "In hysteria whole regions of the psychic life may temporarily be forced out of connection with consciousness; but they still go on working approximately as at other times, something like separated choirs. In dementia praecox that connection remains preserved, but the psychic faculties lose their mutual inner contact like an orchestra without a conductor," (Kraepelin, 1921). Indeed, the cognitive dysfunctions observed in schizophrenia are as central to the disorder as a conductor is to an orchestra.

Bleuler, in support of Kraepelin's observations, also theorized that in schizophrenia, the "loosening of continuity in associations" was a fundamental symptom, while delusions and hallucinations were accessory symptoms (Bleuler, 1950; Green & Harvey, 2014). Additionally, Bleuler also noted that "the peculiar intellectual characteristics often induce the comrades of these

candidates for schizophrenia to regard them as ‘crazy’ at a rather early stage,” (Bleuler, 1950). Indeed, cognitive symptoms in schizophrenia frequently precede the onset of psychosis by a decade (Bora & Murray, 2014)–evidenced by lower IQ and reduced scholastic performance in school in those who go on to develop schizophrenia (Reichenberg et al., 2010; Gur et al., 2014; Jonas et al., 2022;). The few longitudinal studies suggest that this deficit is evident as early as age 13 and continues to decline through the adolescent years in those who later present with schizophrenia (Reichenberg et al., 2010; MacCabe et al., 2013). Indeed, cognitive impairments are evident in individuals with their first episode of psychosis and appear to be, generally speaking, relatively stable of the course of the disorder (Reichenberg et al., 2010; Zanelli et al., 2022; Niendam et al., 2018; Mollon et al., 2018).

It might be most appropriate to think about the cognitive dysfunction in persons with schizophrenia from a framework of the deviation from expectations with or without a diagnosis of schizophrenia. Of course, the answer to this question cannot be known for certain, as nature provides no opportunity to test the direct effect of schizophrenia given the same host background. However, multiple studies indicate that individuals with schizophrenia cognitive underperform compared to expectations based on family members (Glausier et al., 2020b). For example, monozygotic twins with schizophrenia perform worse on cognitive tests relative to their unaffected twin (Goldberg et al., 1990). Moreover, when compared to parental achievement in education and other neuropsychological indices, approximately half of the unaffected population falls below expectation (i.e., chance), but 98% of individuals with schizophrenia fall below expectations (Keefe et al., 2005). Of course, individuals with schizophrenia exhibit significant heterogeneity in terms of cognitive capacity and functional independence. However, these findings strongly suggest

(but cannot prove) that cognitive capacity of a given individual with schizophrenia seems to fall below what that capacity would have been in the absence of the disease process of schizophrenia.

Finally, the severity of cognitive impairments is a key predictor of functional outcomes in persons with schizophrenia (Bowie & Harvey, 2006; Bowie et al., 2006; Strassnig et al., 2018; Green, 1996; Palmer et al., 2002). Patient-centered outcomes, such as the ability to maintain employment (Gold et al., 2002), living independently, and developing fulfilling social relationships (Green et al., 2019; Silberstein & Harvey, 2019; Hofer et al., 2005) are all related to the degree of cognitive impairments. Moreover, the societal economic burden of schizophrenia is significantly accounted for by the degree of cognitive impairment (Kadakia et al., 2022b). Together, these separate lines of evidence support the initial observations by Bleuler and Kraepelin: cognitive dysfunction in schizophrenia is the core feature of the disorder, and treatment of this dysfunction remains a major unmet need (Gold, 2004; Keefe et al., 2013).

1.2.1 Working memory deficits are a prototypical cognitive impairment in schizophrenia

Among the multiple domains of cognitive skills that are deficient in schizophrenia, working memory deficits are prototypical of these alterations. Alterations in different domains of cognition in schizophrenia can be distinguished from one another using batteries of neuropsychological testing. Working memory, a concept crystallized by Alan Baddeley in the late 20th century (Baddeley, 1983; Baddeley, 2012), is the ability to maintain and manipulate limited amounts of information in memory in order to guide thought or behavior. In the model of working memory, the capacity to manipulate transiently distinguishes it from short-term memory, and the limited nature of working memory and the ability to clear contents for subsequent tasks place this function clearly within the domain of cognition rather than association or recall functions (Baddeley, 2012).

Working memory deficits in schizophrenia were first reported by in 1992 by Park and Holtzman (Park & Holzman, 1992) and widely replicated since (Aleman et al., 1999; Fleming et al., 1997). Two meta-analyses of multiple studies of working memory in schizophrenia find that individuals with the disorder exhibit deficits that are, on average, ~1 standard deviation below the psychiatrically unaffected population (Forbes et al., 2009; Lee & Park, 2005). These deficits are evident in a variety of working memory tasks that depend on distinct sensory modalities (i.e., vision and hearing); therefore, the most plausible explanation is that a shared neural circuit, underlying multiple forms of working memory, is affected in schizophrenia (Smucny et al., 2022). Additionally, these deficits in working memory are independent of differences in IQ, the duration of the delay period, and, to a large extent, the duration of illness (Lee & Park, 2005; Forbes et al., 2009).

These deficits in working memory have been hypothesized to underlie the cognitive deficits observed in other domains (Johnson et al., 2013). For example, deficits in working memory in men with schizophrenia were significantly correlated with deficits in a multitude of other neuropsychological batteries, including memory for objects and faces, executive functions, and complex sensorimotor function (Silver et al., 2003). These correlations were not observed in psychiatrically unaffected comparison individuals. One possible interpretation of these differences is that working memory deficits in schizophrenia are 'rate-limiting' and therefore contribute to deficits in other cognitive tasks.

1.2.2 Multiple subprocesses are involved in working memory

A classical test of visuospatial working memory is the oculomotor delayed response task (**Figure 1**). In this task, the research subject learns to focus on a central fixation point. In the

periphery of that focus point, an object flashes on-screen for a second or so, after which the object disappears. After some set delay period of a few seconds, the central fixation point disappears, cuing the participant to make a saccade toward the direction where the point appeared. Successful completion of the task occurs when the individual makes the visual saccade to the location of the original object, after which the central fixation point re-appears to start the task anew. During the task, the individual is required to maintain the location of the object during the delay period—referred to as *maintenance* of the information. Afterwards, this information must be cleared from memory in order to execute the subsequent task which involves a new object location. Importantly, this task can be tested in both humans and monkeys (Keefe et al., 1995), providing an important opportunity for translational research.

Working memory tasks can be subdivided into three core component parts: encoding, maintenance, and retrieval—all of which are required to execute working memory tasks (Jonides et al., 2008). First, encoding, or the process of bringing the memorandum into mind or focus, has to occur. Encoding specifically involves the generation of the mental representation of the object that is to be remembered. Second, that mental representation must stay online during the delay period of the working memory, when the object is no longer being presented. This fact, although simple, is perhaps one of the most fascinating aspects of working memory: the idea that the brain clearly represents something that is no longer present. Third, that information has to be retrieved at the proper time, in order to send the motor action plan necessary to indicate that the memorandum has been kept online successfully. During each of these stages, especially during encoding and maintenance phases, information about the location of the stimulus must be robust to the effect of intervening distractors (Awh et al., 2006; Lorenc et al., 2021; McNab & Dolan, 2014). Distractors are defined as the presentation of related stimuli that are not required to

complete the task at hand but do compete for neural resources (Marshall & Bays, 2013; Zanto & Gazzaley, 2009).

The psychological literature has long suggested that the ability to resist distractors is a core component of working memory. Individuals in the general population can be separated into high and low working memory capacity based on their ability to resist distracting stimuli (Vogel et al., 2005; Minamoto et al., 2010; Conway et al., 2001). Likewise, the likelihood of successful completion of a working memory task is directly associated with the individual ability to limit interference from distracting information (Zanto & Gazzaley, 2009). While all components of a working memory task are required for its successful execution, the ability to reduce the intervening effects of distracting stimuli is clearly a crucial component of working memory processing.

1.2.3 Schizophrenia likely involves disturbances to multiple components of working memory, including the ability to filter out distracting information

Attempts to isolate the core component of working memory that is deficient in persons with schizophrenia could identify the best options for therapeutic intervention. The first evidence that persons with schizophrenia display specific impairments in the ability to filter out distractor information come from carefully conducted psychological studies in the 1960's. One key finding of these studies is that when comparing the deficit in working memory performance between a neutral 6-item digit span task and a 6-item digit span task with distractors, individuals with schizophrenia clearly demonstrated a much larger deficit in performance (Lawson et al., 1967). Moreover, while both unaffected individuals and those with schizophrenia show deterioration on working memory tasks when distractors were introduced, those with schizophrenia showed more rapid deterioration (Oltmanns & Neale, 1975; Oltmanns, 1978).

While it does not appear that the deficits in working memory in schizophrenia are fully accounted for by an impaired ability to filter out distractors (Erickson et al., 2014), there are many lines of evidence to suggest that this contributes in part to the deficit in schizophrenia. For example, relative to psychiatrically unaffected participants, those with schizophrenia exhibit deficits in working memory that are exaggerated when distractors are introduced into the task (Silver & Feldman, 2005). Additionally, like the psychiatrically unaffected population, the ability to filter out distractor stimuli predicts performance on working memory tasks in schizophrenia (Mayer et al., 2012). In general, relative to the unaffected population, persons with schizophrenia appear to be less resilient to the effect of intervening distractors (Starc et al., 2017; Murray et al., 2014b; Hahn et al., 2010; Guimond et al., 2018; Gold et al., 2020).

Not all evidence clearly points to an impaired ability to resist distractors in working memory in persons with schizophrenia (Luck et al., 2019b). One research group has put forward a "hyperfocusing" hypothesis (Luck et al., 2019a), based on findings that in some tests, individuals with schizophrenia exhibit an intense and narrow focusing of processing resources during cognitive tasks, like working memory. This intense focus is still predicted to be detrimental to cognitive function generally, as it does not permit task flexibility required in both real-world circumstances and neuropsychological testing (Luck et al., 2019a). This notion of hyperfocusing was even observed by Kraepelin a century ago: "With this loss of capacity to follow a lead is connected to a certain unsteadiness of attention; the patients digress, do not stick to the point, let their thoughts wander without voluntary control in the most varied directions. On the other hand, the attention is often rigidly fixed for a long time, so that patients stare at the same point, or the same object, continue the same line of thought, or do not let themselves be interrupted in some definite piece of work," ((Kraepelin, 1921), p. 6). Interestingly, Hahn, Luck, and Gold posit that

both hyperfocusing and impaired ability to filter out distractors are operative in schizophrenia in different contexts. Specifically, attentional control is diminished when there is significant challenge to that control by requiring identification of lower salience stimuli but enhanced when attention is the least challenged and individuals are required to identify the higher salience target (Hahn et al., 2021). While further dissection of these complex cognitive processes is required, it seems clear that the ability to resist distracting stimuli in schizophrenia is altered, and this partly contributes to the overall deficit in working memory.

1.3 ROLE OF THE DORSOLATERAL PREFRONTAL CORTEX IN WORKING MEMORY

Working memory function has been extensively studied because of the translatability between laboratory tasks testing these functions in both non-human primates and humans (without and without schizophrenia) (Keefe et al., 1995). Much has been elucidated about the neural substrate of working memory over the past century, and these methodologically diverse studies clearly converge on the key role of the dorsolateral prefrontal cortex (DLPFC) in mediating working memory.

1.3.1 Evidence for the role of the DLPFC in working memory

The first investigations into the neuropsychological consequences of frontal lobe lesions in humans provided early clues as to its role in working memory. An early detailed investigation into Patient A, on whom neurosurgeon Walter Dandy performed bilateral frontal lobectomies in 1930,

suggested the role of the frontal lobes in certain cognitive functions. Richard Brickner, a clinical neurologist, subsequently completed an extraordinarily detailed monograph of clinical neuropsychological testing and everyday conversations with this patient, offering a detailed, albeit narrow, insight into the functional deficits endured by individuals without a frontal lobe. However, other investigators failed to identify specific deficits in other functions after frontal lobectomies (Hebb, 1945). This reported absence of gross deficits after frontal lobectomies may have contributed to an erroneous and now-maligned view of using frontal lobotomies (leucotomies) as a therapeutic strategy for various psychiatric disorders (Boettcher & Menacho, 2017). At the time, this "riddle of the frontal lobe" (Teuber, 2009) proved difficult to resolve even as multiple conferences and meetings brought together many who studied individuals without frontal cortices and noted findings from absolutely no functional deficits to subtle, yet reproducible deficits in cognition. For his part, Brickner stated that these deficits were "quantitative, not qualitative," while also noting that "A can make simple syntheses perfectly well—that is, syntheses composed of only a few elements. A can even sustain a fairly prolonged conversation, if its elements are sufficiently simple. But he fails in making complex syntheses," ((Brickner, 1936), p. 120). Thus, some of the absence of gross deficits might have reflected the relative simplicity of some neurocognitive tests.

Although studies of human frontal lobectomies offered clues as to the role of the frontal lobes in synthesizing "complex sets of information," a deeper understanding of the role of the frontal lobes in working memory function specifically came from studies of frontal lobectomies in non-human primates by Carlyle F. Jacobsen. After removal of the frontal lobes, Jacobsen found these monkeys could no longer remember the location of food hidden under a cup for even 5 seconds, while previously being able to remember for nearly 90 seconds. He concluded: "basic change associated with lesions of the prefrontal area is the loss of capacity for immediate or for

recent memory," (Jacobsen, 1935). Indeed, his 1935 report on the functional deficits of these primates was prescient in later descriptions of working memory function: "Temporal patterning fails because the subject can no longer remember a single experience for even a few seconds in the face of new incoming sensory data. The loss is not unlike […] organic dementia—an inability to keep in mind a number of separate elements and at the same time to manipulate them in thought," (Jacobsen, 1935). Lesions to other cortical areas, including temporal, parietal, and premotor areas, failed to reproduce this effect (Jacobsen et al., 1936; Breslaw et al., 1934). These studies provided the first causal evidence of the role of the prefrontal cortex in mediating working memory function.

Stronger support for the distinct role of the DLPFC, rather than the frontal lobes broadly, in working memory came decades later through the work of Brenda Milner (Kolb, 2021). Milner, a neuropsychologist working with Wilder Penfield's neurosurgical patients, performed extensive testing on individuals with much more circumscribed lesions of the DLPFC than previously studied. Strikingly, and unlike the subtle alterations on a variety of tasks for individuals with frontal lobectomies, she found that these individuals performed significantly worse on the Wisconsin Card-Sorting task, a task thought to specifically interrogate working memory function. Importantly, Milner had the opportunity to study these patients before and after their surgery, finding that these patients performed normally on this task prior to the removal of the DLPFC (Milner, 1963). This groundbreaking work set the stage to further interrogate the specific role of the DLPFC in working memory function. More recent reviews of multiple studies of humans with lesions in various aspects of the frontal lobe due to neurosurgical intervention, cerebrovascular accidents, or extraneous trauma, confirm these findings and elucidate distinct roles that anatomical regions of the prefrontal cortex have in subserving different domains of cognitive processing. (Szczepanski & Knight, 2014; D'Esposito & Postle, 1999).

Similarly in non-human primates, it was found that the minimal lesion site necessary to reproduce deficits in working memory were circumscribed to the area surrounding the principal sulcus (Passingham, 1985; Butters & Pandya, 1969; Butters et al., 1972; Buckley et al., 2009). Further, it was shown specifically that lesions to the dorsal and ventral bank of the middle third of the principal sulcus in monkeys introduced deficits that were specific to the introduction of delays into the task, rather than a generalized deficit on visual processing (Goldman & Rosvold, 1970). While these lesion studies are crucial for understanding the localized role of regions of the DLPFC for specific aspects of working memory tasks, lesions are irreversible and may introduce collateral damage that clouds interpretation. Reversible mechanisms for dampening DLPFC activity, such as electrical stimulation (Stamm, 1969) or reversible cooling of the cortex (Fuster & Alexander, 1970; Chafee & Goldman-Rakic, 2000) further substantiates the notion that this region of the DLPFC in primates is necessary for working memory, and, specifically, the ability to maintain information online during the delay period.

Finally, evidence of functional activation of the DLPFC in humans and monkeys substantiates lesion studies which first revealed the crucial role of the DLPFC in working memory. For example, in monkeys performing working memory tasks, 2-deoxy-D-glucose functional mapping studies (Sokoloff et al., 1977) indicate that there was significantly higher local cerebral glucose utilization in the DLPFC (and posterior parietal cortex, but not auditory cortex) relative to monkeys performing control tasks that only depended on associational, and not working, forms of memory (Friedman & Goldman-Rakic, 1994). In human functional imaging studies with greater temporal resolution, multiple studies reveal robust working memory-dependent activation of the DLPFC (D'Esposito et al., 1998; Petrides et al., 1993; Jonides et al., 1993; McCarthy et al., 1996) and a linear relationship between the number of items held in working memory and the magnitude

of activation in the DLPFC (Braver et al., 1997; Callicott et al., 1999). Together, the functional findings coupled with lesion studies converge on the notion that the DLPFC is an indispensable node in the working memory circuit.

1.3.2 The DLPFC has a critical role in distractor resistance during working memory

These early studies of frontal lobectomies and DLPFC lesions in humans and primates also provide the first clues into the specific role that the DLPFC has in filtering out intervening distractors during working memory. Even in the earliest studies of frontal lobectomies in neurosurgical patients, Brickner noted that "One of the most frequently described symptoms, in cases of frontal lobe injury, is difficulty in fixing the attention, or in keeping it fixed." Note here the similarity in description to patients with schizophrenia by Kraepelin: "It is quite common for them to lose both inclination and ability on their own initiative to keep their attention fixed for any length of time. It is often difficult enough to make them attend at all," (p. 6, (Kraepelin, 1921)). Robert Malmo, performing similar frontal lobectomies in non-human primates as Jacobsen, controlled the amount of extraneous information in the setting where these animals were performing tasks that depended on working memory. Strikingly, the performance on these tasks dropped dramatically when the lights in the room were on relative to when lights were off. In the lights-on condition, the animal could perceive multiple extraneous stimuli in the visual field that were not necessary to complete the working memory task at hand, and the performance on this task subsequently dropped to chance (Malmo, 1942). As summarized by Malmo: "The difference between normal and operated monkeys with respect to [delayed response] performance is not one of presence or absence of the capacity for delayed response, but rather the difference is one of degree of susceptibility to the interfering effects of extraneous stimuli occurring during the delay

interval." Consistent with these findings in monkeys, when individuals with frontal lobe lesions perform working memory tasks, their impaired performance is *further* impaired with the introduction of distractors into the task (Chao & Knight, 1995; Rueckert & Grafman, 1996; D'Esposito & Postle, 1999; Thompson-Schill et al., 2002). This effect appears specific to lesions of the frontal, and not temporal, lobes (Smith et al., 1995). Finally, transient inactivation of the DLPFC, but not the posterior parietal cortex, leads to heightened sensitivity of distractors in monkeys (Suzuki & Gottlieb, 2013). Together, lesion studies strongly suggest that at least some of the impairment in working memory tasks might be related to the inability to suppress distracting information during these tasks.

One framework for thinking about how the DLPFC might provide resistance to distractor stimuli is to compare how it responds during a working memory task relative to other cortical regions. For example, during the visuospatial working memory task, the primary visual cortex (V1), a primary sensory area, must faithfully track the appearance of any stimuli that is present in the visual field. Neurons in this region respond regardless of the stimuli's particular relevance to a given task. Obviously, this is the crucial first step in cognitive processing during the encoding phase of working memory, and V1 would be expected to encode both relevant and irrelevant stimuli with equivalent fidelity. However, during a working memory task, neurons within the DLPFC likely encode the rules necessary to complete the working memory task (i.e., remember the location of the first stimulus while ignoring the second) (Wallis et al., 2001), and appear to be insensitive to the effects of intervening distractors (Lennert & Martinez-Trujillo, 2011; Suzuki &

Gottlieb, 2013; Everling et al., 2002)[1]. Moreover, the distractor-resistant nature of the DLPFC can provide top-down control over other cortical regions that prevents responsiveness to task-irrelevant stimuli (Crowe et al., 2013). In functional imaging studies of humans during a working memory task, there is increased DLPFC activity when challenged with distractors (Dolcos et al., 2007; Sakai et al., 2002), and the sustained DLPFC activation corresponds to the filtering of distractors and successful completion of the task (Sakai et al., 2002). In both studies, the heightened activation of the DLPFC was not evident in the posterior parietal cortex. Other studies support the idea that neurons in the DLPFC exhibit limited responses to task-irrelevant distractor stimuli (Rainer et al., 1998); properties that are not true of neurons in the posterior parietal, motor, or temporal cortices (Miller et al., 1996; Qi et al., 2010; di Pellegrino & Wise, 1993). One interpretation of these studies is that the DLPFC, when successfully suppressing the activation related to distractors, leads to successful execution of the motor plan for the task at hand.

[1] The cited studies suggest that activation of the DLPFC is limited during distractor presentation. However, another study found in a test of numerosity that the primate DLPFC does encode distractor stimuli during their presentation, but restores target information after the distractor presentation ends, which predicted correct behavioral decision making (Jacob & Nieder, 2014). Even if the DLPFC does encode some distractors, it is able to resume firing for task-relevant activity quickly.

1.4 A DORSOLATERAL PREFRONTAL CORTICAL MICROCIRCUIT MEDIATES WORKING MEMORY IN PRIMATES

Based on the clear role of the DLPFC in working memory, later elegant studies at the level of resolution of individual cells reveal the cellular basis for this regional function (Goldman-Rakic, 1995). Specifically, these studies identified neurons that exhibit 'delay period activity'—that is, these neurons continue to fire in the absence of ongoing presentation of the stimulus, thus representing the neural substrate subserving working memory function. This microcircuitry is thought to consist of neurons within the superficial layers of the DLPFC (layers 2, 3, and 4). The laminar-specificity of this circuit is supported layer-specific functional magnetic resonance imaging in humans, demonstrating higher levels of activity in the superficial layers of the DLPFC during working memory (Finn et al., 2019). In addition, layer-specific recording probes in monkeys reveals that activity associated with working memory is principally generated in the superficial layers (Bastos et al., 2018). As described below, DLPFC layer 3 pyramidal neurons and their interconnected GABA neurons appear to be the neural substrate for working memory in primates.

1.4.1 Delay-period active cells are pyramidal neurons that predominantly reside in layer 3

The cellular resolution of working memory within the DLPFC, starting with work from the labs of Joaquin Fuster and Garrett Alexander and later by Patricia Goldman-Rakic, provided the initial evidence of neurons that were specifically active during working memory. Recordings of these neurons in the DLPFC during working memory tasks in primates identified those that became active with stimulus presentation and remained active during the delay interval of working memory

(Fuster & Alexander, 1971; Funahashi et al., 1989). In the context of a visuospatial working memory task, neurons that fire selectively with the presentation of a visual stimulus in a specific orientation relative to the central fixation point are referred to as *tuned* neurons. These neurons exhibit selectivity for a given stimulus and begin firing during the presentation of that stimulus but *continue to fire in the absence of ongoing presentation of the stimulus.* Additionally, failure to successfully identify the location of the stimulus during working memory behaviorally is associated with cessation of the delay-period activity in DLPFC pyramidal neurons. Thus, the ongoing activity of these neurons during the delay period of working memory tasks appears to represent the maintenance of the information online.

Morphological evidence further supports the notion that these layer 3 pyramidal neurons are the neural substrate for working memory in primates. In human and non-human primates, layer 3 pyramidal neurons in the DLPFC have large somal bodies and dendritic arbors. In addition, the dendritic arbors are covered in dendritic spines, and layer 3 pyramidal neurons in the primate DLPFC exhibit a much greater spine density relative to layer 3 pyramidal neurons in other cortical regions (Gonzalez-Burgos et al., 2019; Amatrudo et al., 2012). These differences may be species specific—across the cortical hierarchy, layer 3 pyramidal neurons in monkeys exhibit markedly higher spine densities than those in V1, while the spine densities are comparable between layer 2/3 pyramidal neurons in both regions in mice (Gilman et al., 2017). Thus, the large cell bodies and dendritic arbors of primate DLPFC layer 3 pyramidal neurons appear to be able to support a wide diversity of synaptic inputs, positioning these neurons as 'integrative' neurons, incorporating inputs locally and from other cortical regions (Elston, 2000).

In addition to being able to integrate multiple synaptic inputs from many cortical and subcortical areas, excitatory layer 3 pyramidal neurons also form multiple connections locally,

within the DLPFC at a distance from the cell body and to other brain regions (Barbas, 1986). Layer 3 pyramidal neurons furnish a principal axon that projects through the white matter to other cortical regions in the working memory network, as well as local axon collaterals that primarily target dendritic spines of other layer 3 pyramidal neurons (Melchitzky et al., 2001). These axon collaterals form 'stripes' of clusters of interconnected pyramidal neurons, with those clusters separated from one another by approximately ~200-300 μm (Kritzer & Goldman-Rakic, 1995; Pucak et al., 1996; Levitt et al., 1993). At a distance from the location of the cell body of a layer 3 pyramidal neuron (i.e., between stripes), these collaterals nearly exclusively target the dendritic spines of other pyramidal neurons (Melchitzky et al., 2001). Near the location of the cell body, approximately 50% of these collaterals target other dendritic spines, and the other 50% appear to target inhibitory GABA neurons. The local axon collaterals formed by layer 3 pyramidal neurons are thought to form a recurrently excitatory network with other pyramidal neurons in this layer (González-Burgos et al., 2000), and thus be positioned to recurrently and continuously excite each other to maintain working memory information online in the absence of ongoing stimulus presentation. This hypothesis is supported by computational models of recurrent excitatory networks (Compte et al., 2000; Camperi & Wang, 1998). Thus, these neurons are anatomically and functionally positioned to mediate the recurrent excitation necessary to keep information online during working memory (**Figure 1**).

While the available data seem to clearly support a role of layer 3 pyramidal neurons in mediating working memory, exactly how they perform this function remains a matter of debate. The initial findings from recordings of pyramidal neurons during working memory seemed to suggest these neurons persistently fire during the delay period, and this is the neural mechanism for the maintenance of information online during working memory (Constantinidis et al., 2018).

Others have suggested that these neurons remain active during the delay period but do not fire continuously; rather, their activity is periodically 'refreshed' during the delay period of working memory task (Lundqvist et al., 2018). Support for the former hypothesis comes from studies such as those reviewed above, demonstrating that persistent activity of neurons in the DLPFC is necessary and sufficient for the maintenance of the memorandum online during the delay period of working memory (Wang, 2021). Evidence for the latter hypothesis is based on bioenergetic considerations (it is metabolically expensive for neurons to continuously fire) as well as technical considerations of averaging spike events across trials, making it appear as those the activity is persistent even though it might be more sparse on individual trials (Lundqvist et al., 2016; Miller et al., 2018). Finding a model that explains the totality of neurophysiological observations over the past 50 years remains ongoing work. Regardless, it seems clear that sustained activity of these neurons during the delay period of working memory tasks is required to keep the memory online.

1.4.2 Inhibitory GABA neurons in the local DLPFC circuit modulate layer 3 pyramidal neuron activity

Evidence that pharmacologic antagonism at $GABA_A$ receptor in the DLPFC impaired working memory in (Sawaguchi et al., 1989) first suggested that working memory depended not only on the excitatory activity of pyramidal neurons but also on their interconnected inhibitory GABA neurons. Later, $GABA_A$ receptor antagonists were shown to disrupt the spatial preference-related activity of pyramidal neurons tuned for a specific stimulus during working memory, while also shaping the tuning of other untuned pyramidal neurons (Rao et al., 2000). Additionally, GABA neurons facilitated the interactions between different groups of neurons that are active at discrete periods of a working memory task in nonhuman primates, including transitions between

the presentation of the cue, the delay period, and the response period (Constantinidis et al., 2002). Moreover, GABA neurons are similarly tuned as their neighboring pyramidal neurons, rather than simply providing nonspecific modulation of pyramidal neuron activity (Wilson et al., 1994; Rao et al., 1999) Thus, GABA signaling shapes the tuning of pyramidal neurons necessary for working memory and facilitates transitions between distinct epochs of the working memory tasks.

GABA neurons in the cerebral cortex can be divided into different subclasses based on electrophysiological, morphological, and molecular properties. Most frequently, these neurons are referred to based on distinct molecular markers they express, and these molecular markers, especially calcium-binding proteins and neuropeptides (Jones & Hendry, 1986; Hendry et al., 1984) seem to reliably map onto the physiological and morphological properties of those neurons. With few exceptions, distinct populations of GABA neurons in the primate neocortex tend to express calcium binding proteins, including parvalbumin (PV), calbindin (CB), and calretinin (CR) (Condé et al., 1994; Andressen et al., 1993). PV-containing GABA neurons have fast-spiking physiological properties; that is, these neurons exhibit a nearly constant interval between spikes. This feature is in contrast to other populations of GABA neurons, which tend to show an adapting spiking pattern such that with increasing stimulus duration, the interval between spikes gets longer, possibly reflecting an increasing refractory period. Morphologically, PV neurons can be subdivided into two main classes: basket cells, whose axons tend to target the soma and proximal dendrites of pyramidal neurons or other PV basket cells, and chandelier cells, whose axon terminals form distinctive vertical arrays, termed cartridges, that exclusively target the axon initial segment of pyramidal neurons. In primates, PV neurons are present in layers 2-6, with the highest density in deep layer 3 and layer 4 but are not present in layer 1 or the underlying subcortical white matter.

The group of non-fast spiking GABA neurons are molecularly heterogenous, but a few molecular markers appear to capture the vast majority of this diversity. CR-expressing neurons constitute a large proportion (~50%) of GABA neurons in the primate neocortex (Condé et al., 1994; Gabbott & Bacon, 1996), and tend to express other neuropeptides such as vasoactive intestinal peptide (VIP) and cholecystokinin (CCK). Additionally, the primate neocortex also appears to have a smaller population of cells that express CCK and exhibit a morphology similar to PV basket cells, but do not express CR or VIP (Curley & Lewis, 2012). CCK basket cells preferentially appear to target the somas of pyramidal neurons as well as other PV neurons, positioning them to both inhibit and disinhibit excitatory cells. CR/VIP neurons preferentially appear to target other GABA neuron populations in the rodent and primate neocortex, positioning this population of cells to provide disinhibitory control over cortical circuits (Pfeffer et al., 2013; Meskenaite, 1997). In general, CR/VIP and CCK neurons are enriched in the superficial layers of the neocortex, especially layers 1-superficial 3.

Finally, a separate population of GABA neurons, constituting approximately ~25% of all GABA neurons, are defined based on their expression of the neuropeptide somatostatin (SST). SST neurons classically furnish axons that synapse onto the distal dendrites of pyramidal neurons, positioning SST neurons to provide an inhibitory 'gate' to the excitatory inputs received by pyramidal neurons at their dendrites (Stokes et al., 2014; Chiu et al., 2013; de Lima & Morrison, 1989; Melchitzky & Lewis, 2008). In the primate DLPFC, SST neurons are present throughout all layers of the neocortex but are enriched in layers 2-superficial 3, layer 5, and the subcortical white matter (Lewis et al., 1986). Although both express SST, those in the subcortical white matter are dramatically different in transcriptome, morphology, and physiology from those in the superficial gray matter. For example, SST neurons in superficial gray matter frequently express CB, while

those in the subcortical white matter do not express CB. Moreover, the white matter SST neurons frequently express strikingly high levels of SST relative to those in the superficial gray matter. These subcortical white matter neurons also express high levels of other neuropeptides, including neuropeptide Y (NPY), and tachykinin 1 (TAC1). Rather than participating in dendritic inhibition and microcircuit processing, SST neurons in the subcortical white matter appear to have distinct roles in sleep homeostasis (Kilduff et al., 2011) and cerebral blood flow (Krawchuk et al., 2020; Lee et al., 2020; Ruff, 2021). Finally, the majority of GABA neuron axons synapse with their target locally, and not over long-distances (hence the moniker *interneuron* so frequently used interchangeably with GABA neurons); SST neurons in the subcortical white matter appear to be an exception to this rule. Subcortical white matter neurons tend to form axons that project to other cortical regions in rodents and primates (Tomioka & Rockland, 2007).

1.4.3 Perisomatic-targeting PV neurons likely synchronize the activity of groups of pyramidal neurons necessary for the maintenance of working memory

DLPFC PV neurons, especially PV basket cells, have been most extensively studied in the context of working memory, and their role in this function comes from divergent lines of evidence using models at multiple levels. At the cellular level, PV basket cells in layer 3-4 receive a robust complement of excitatory inputs from layer 3 pyramidal neurons: the ~50% of local axon collaterals of layer 3 pyramidal neurons that form synapses onto GABA-containing dendrites do so onto PV-expressing dendrites (Melchitzky & Lewis, 2003). Additionally, PV basket cells make multiple contacts onto the perisomatic region of pyramidal neurons and also provides inputs to multiple pyramidal cells (Williams et al., 1992). This pattern of innervation enables PV basket cells to exert strong inhibitory control over large numbers of pyramidal neurons, so that the firing

of a single PV basket cell transiently silences multiple pyramidal neurons. The synchronous decay of inhibition over an identical time frame across pyramidal neurons, enabling them to fire in concert. The coordinated firing of large groups of pyramidal neurons then depolarizes PV basket cells, providing reciprocal, feedback inhibition. The repetition of synchronized firing creates oscillatory activity in the DLPFC at gamma frequency (30–80 Hz) (reviewed in (Gonzalez-Burgos et al., 2015)). Gamma oscillatory activity that is strongly associated with working memory in humans (Howard et al., 2003; Cho et al., 2006), and nonhuman primate models report that DLPFC gamma oscillatory activity specifically responsible for working memory is generated in the superficial layers of the cortex (Bastos et al., 2018) (**Figure 1**).

Compared to other interneurons, the fast-spiking activity of PV basket cells is most closely coupled with gamma oscillations. *In vitro* studies of hippocampal and neocortical organotypic slices first demonstrated a causal role for PV neurons in the generation of gamma oscillatory activity (Buzsaki & Wang, 2012; Gulyás et al., 2010). Additionally, a causal role for PV neurons in the generation of gamma oscillations was shown *in vivo* in rodent models using optogenetics (Cardin et al., 2009; Sohal et al., 2009). In addition to the fast-spiking properties of PV basket cells, the synapses from these neurons are primarily formed onto $GABA_A$ receptors enriched in the $\alpha 1$ subunit. These $GABA_A$ receptors mediate fast postsynaptic decay kinetics of the inhibitory postsynaptic potential that is consistent with the frequency of gamma oscillations (Gonzalez-Burgos et al., 2015; Farrant & Nusser, 2005). Thus, while PV chandelier cells are also fast spiking, chandelier cell cartridges are mainly formed onto GABAA receptors that predominantly uses $\alpha 2$, not $\alpha 1$, (Farrant & Nusser, 2005) and mediate slow decay kinetics (Woodruff et al., 2010). Thus, the role of PV chandelier cells in mediating gamma oscillations might be more limited compared to the basket cell counterparts. Together, these findings suggest that PV basket cells are responsible

for gamma oscillatory activity in the DLPFC, and this activity, in turn, is necessary for the mediation of working memory.

1.4.4 Dendritic-targeting SST neurons might play a critical role in mediating distractor resistance in the DLPFC

Unlike PV cells, SST neurons are distinct in that many SST neurons supply inhibitory inputs onto pyramidal neuron dendrites, rather than the perisomatic region (de Lima & Morrison, 1989; Melchitzky & Lewis, 2008). Dendritic inhibition has been posited to be critical for distractor resistance in the DLPFC during working memory (Yang et al., 2016; Wang et al., 2004). It is important to note that there is a dearth of causal evidence linking a direct role of DLPFC SST neurons in mediating distractor resistance, especially in primate models. However, given the causal evidence from rodent models that prefrontal cortical SST neurons have in working memory (Abbas et al., 2018), it is worth considering their role in the working memory circuit. Here, I hypothesize, based on computational models put forward by Xiao-Jing Wang and others (Yang et al., 2016; Wang et al., 2004; Riley & Constantinidis, 2015), that DLPFC SST neurons are crucial mediators of distractor resistance.

First, the preferential targeting of pyramidal neuron dendrites by SST neurons mediates disynaptic lateral inhibition between pyramidal neurons (Obermayer et al., 2018; Silberberg & Markram, 2007; Zilberter et al., 1999). Dendritic inhibition exerts a critical role in the integration of inputs received by pyramidal neurons and regulates their firing (Bloss et al., 2016; Chiu et al., 2019; Lovett-Barron et al., 2012; Chiu et al., 2013; Gidon & Segev, 2012). Thus, these neurons are anatomically positioned to control the firing of pyramidal neurons based on external excitatory input received at their dendrites.

Second, it appears that SST neurons have a much higher propensity for firing compared to other types of interneurons, making them well-suited to provide blanket inhibition to pyramidal neuron dendrites. In rodent cortex, it has been shown that SST neurons are spontaneously active at baseline (Gentet et al., 2012; Urban-Ciecko et al., 2015). This spontaneous activity was masked from prior studies of *in vitro* slice preparation that utilize artificial cerebrospinal fluid (aCSF) with a relatively high concentration of magnesium ions, which introduce a persistent block in N-methyl-D-aspartate (NMDA) receptors. This normally serves to keep slice activity tonically low during recordings. When brain slices are bathed with aCSF with a magnesium ion concentration closer to physiologic levels, SST neurons (along with other neurons), are active at baseline (Maffei et al., 2004; Urban-Ciecko et al., 2015). This network feature of tonically active SST neurons reflects the finding that individual SST neurons are 'low-threshold spiking.' Together with a high input resistance (Zaitsev et al., 2009), the strength of excitation needed to make SST neurons active is much lower compared to the needed activation of other interneurons.

Third, excitatory synapses onto SST neurons are thought to be highly variable relative to other interneurons (Campagnola et al., 2022; Urban-Ciecko et al., 2018), possibly reflecting the asynchronous release of glutamate onto SST neurons (Deng et al., 2020; Mendonça et al., 2022). Moreover, excitatory inputs onto SST neurons tend to be 'facilitating', meaning the postsynaptic potential evoked by presynaptic glutamate release increases in the presence of ongoing stimulation (in contrast to fast-spiking cells, which tend to show synaptic depression in response to ongoing stimulation; (Pala & Petersen, 2015; Reyes et al., 1998; González-Burgos et al., 2004; Lu et al., 2007)). In response to stimulation, SST neurons are considered facilitating or continuous adapting (Zaitsev et al., 2009). In the presence of ongoing stimulation, continuously adapting cells will exhibit a progressively extending interspike interval. The nature of their slow adaptation means

that these neurons can provide tonic inhibition in a more sustained manner relative to some other interneurons (with the exception of PV neurons, which do not demonstrate any adaptation; (Zaitsev et al., 2009)). Because these excitatory-to-SST neuron synapses are so variable, they can be tuned to provide both tonic inhibition at baseline, as well as highly specific inhibition to render the circuit more resistant to incoming excitatory inputs encoding distractor stimuli.

Finally, the connectivity of SST neurons is quite broad, such that recordings of any pyramidal and SST neuron within 200 μm of each other reveals a nearly 100% probability of being synaptically connected (Fino & Yuste, 2011; Karnani et al., 2014). While this feature of connectivity is also true for PV neurons, there is some evidence that PV neurons are more likely to form reciprocal connections to the pyramidal neurons that excite them compared to other GABA neuron types, including SST cells (Yoshimura & Callaway, 2005; Otsuka & Kawaguchi, 2009).

Together, the low-threshold necessary to induce SST neuron firing, coupled with facilitation of synaptic efficacy from glutamatergic synapses and broad postsynaptic connectivity, seems to support the idea that these neurons can remain tonically active and provide baseline inhibition onto pyramidal neuron dendrites. One possibility is that the activation of calretinin (CR)-expressing GABA neurons, either through neuromodulatory extracortical inputs (i.e., dopamine or acetylcholine) or from glutamatergic afferents from other cortical regions (Medalla & Barbas, 2009). At least in primate visual cortex, CR neurons make frequent contacts on CB-containing GABA neurons (DeFelipe et al., 1999), many of which also express SST. Moreover, at least in rodent, the long-range excitatory corticocortical connections frequently form onto VIP-expressing cells but rarely onto SST neurons (Naskar et al., 2021). Thus, long-range afferents to the DLPFC might disinhibit the pyramidal neurons in that region through activation of CR/VIP neurons, shutting down dendritic inhibition by SST neurons.

Here, I posit a model such that baseline, tonically active dendritic inhibition mediated by SST neurons prevents the inputs to DLPFC pyramidal neuron from activating those neurons. During encoding, these neurons are disinhibited through activation of the CR/VIP population of GABA neurons, permitting the excitation of DLPFC pyramidal neuron dendrites and the proper encoding of the information during working memory. The coordinated activity of pyramidal neurons responsive to a particular working memory memorandum might more strongly activate SST neurons outside of the microcolumn of similarly tuned pyramidal neurons. The more robust activation of SST neurons provides stronger dendritic inhibition to pyramidal neurons that would encode other stimuli that are distractors and not necessary to complete the task at hand (**Figure 1**).

Interestingly, some neurons recorded in the monkey DLPFC during working memory do exhibit 'inverted-tuning', such that the activity of those neurons is significantly diminished for a particular stimulus (Wang et al., 2004). In support of the model where SST neurons subserve this function, the relative proportion of neurons that exhibit this behavior in monkey DLPFC is consistent with the relative proportion of CB/SST neurons in this region, and there are more neurons that exhibit this behavior in the DLPFC relative to the posterior parietal cortex (Zhou et al., 2012), consistent with the pattern of SST expression across the cortical hierarchy (DLPFC > PPC > primary sensory areas) (Tsubomoto et al., 2019) and might contribute to the distractor-resistant properties of the DLPFC (Qi et al., 2010). However, it is unclear whether the regional enrichment in SST expression actually reflects a relatively higher proportion of SST neurons in this region (in support of the specific role of the DLPFC in distractor resistance) or higher SST mRNA levels per neuron (**2.0**). Together, these convergent lines of evidence support the idea that dendritic inhibition, mediated by SST neurons, has a role in distractor resistance in the DLPFC during working memory.

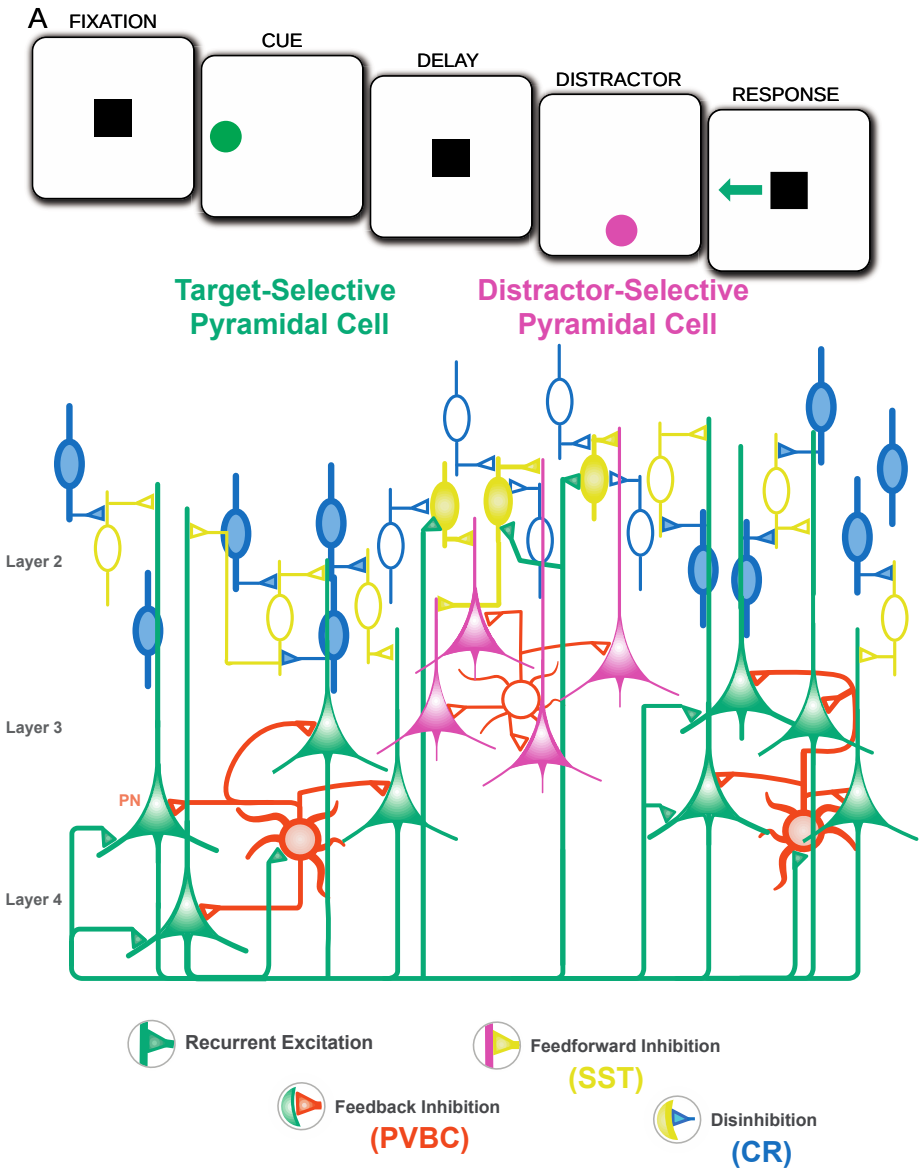

Figure 1. Schematic of primate superficial DLPFC microcircuitry subserving working memory.
A) Phases of an oculomotor delayed response task that requires the subject to respond with an eye saccade towards the location of the cue and ignore the presence of the distractor during the delay interval. **B)** Pyramidal neurons tuned to the cue (green) maintain recurrent excitation among other tuned neurons wtihin the cluster and with other pyramidal neurons located at a distance that are similarly tuned. Within this column, parvalbumin basket cells (PVBCs, orange), which receive excitatory inputs from local pyramidal neurons, provide feedback inhibition that synchronizes the activity of pyramidal neurons within a column. **C)** Pyramidal neurons that are activated by the distractor stimulus are inhibited by feedforward inhibition from somatostatin (SST) neurons (yellow). **D)** Other pyramidal neurons similarly tuned to the cue (green) are disinhibited by activity of calretinin (CR) neurons (blue) that preferentially form synapses onto SST neurons. Filled cells indicate those hypothesized to be active during this stimulus and open cells indicate those hypothesized to be silenced.

1.5 IN VIVO STRATEGIES FOR INVESTIGATING DLPFC DYSFUNCTION IN SCHIZOPHRENIA

One of the strengths of *in vivo* studies of individuals with schizophrenia are the ability to directly relate the activity in the DLPFC to certain cognitive tasks, such as working memory. In the following section, I describe the currently available modalities from the clinical neurosciences for investigating DLPFC alterations in research participants diagnosed with schizophrenia.

1.5.1 Neuroimaging studies reveal alterations at the regional level in the DLPFC specifically associated with working memory in persons with schizophrenia

As indicated from functional mapping studies in primates (Friedman & Goldman-Rakic, 1994), activation of the DLPFC during working memory is associated with an upregulation in glucose utilization by neurons in this region. Concomitantly, cerebral blood flow increases to match the energetic demands of the neurons in this region during working memory in a process known as neurovascular coupling. Indeed, functional magnetic resonance imaging (fMRI) studies clearly find a task-dependent upregulation of cerebral blood flow during working memory in the DLPFC in humans (Callicott et al., 1999). However, schizophrenia is associated with diminished upregulation in local blood flow in the DLPFC during working memory (Weinberger et al., 1986; Carter et al., 1998; Minzenberg et al., 2009; Perlstein et al., 2001), indicative of its dysfunction during these tasks (**Figure 2A**). Moreover, functional imaging studies reveal alterations in DLPFC activation in the context of other executive functioning tasks thought to depend on this region (Yoon et al., 2008). Thus, functional imaging studies reveal an impaired ability to upregulate cerebral blood flow in response to working memory tasks. Whether this impairment reflects an

issue of ‘demand’ (an inability for neurons to fire or synchronize their activity appropriately and thus require less upregulation in local blood flow) or ‘supply’ (an inability for the mechanisms that regulate neurovascular coupling to appropriately upregulate cerebral blood flow in response to demands) remains unclear (see section **5.3.2** for further discussion of this topic).

Functional neuroimaging studies are an indirect assessment of neuronal activity during tasks such as working memory, and more direct assessment of neuronal firing can be interpreted from electroencephalographic (EEG) studies of the DLPFC during these tasks. During working memory tasks, the model posited above suggests that groups of pyramidal neurons that specifically encode the memoranda online during working memory have coordinated firing rates in synchrony. The synchrony of this activity can be detected at the scalp using EEG or magnetic encephalographic recordings (Gonzalez-Burgos et al., 2015). During working memory, these recordings are called *gamma oscillations* given their periodic firing at gamma frequency, between 30-80 Hz (Uhlhaas & Singer, 2010). Gamma oscillatory activity is clearly related to working memory activity in the DLPFC in human and non-human primates: the power of gamma oscillations increases proportionally in response to the number of items to be maintained in working memory (Howard et al., 2003; Jensen et al., 2007), and individuals with schizophrenia show a diminished ability to increase gamma power in response to working memory demands (Cho et al., 2006; Minzenberg et al., 2010) (**Figure 2B**, **Figure 2C**). Moreover, the power of gamma activation in the DLPFC might specifically encode the number of task-relevant items, while ignoring the presence of distractors (Roux et al., 2012).

At a neural level, the activity of PV basket cells seems to be most closely linked to the activity of gamma oscillations. PV firing is both necessary and sufficient to drive gamma oscillatory activity in cortical circuits (Sohal, 2022), and exhibit the physiological properties and

synaptic connectivity pattern necessary to mediate fast, synaptic, inhibition required to coordinate the activity of large groups of pyramidal neurons. Although some studies have linked the activity of SST neurons to gamma oscillations (Veit et al., 2017), those findings have been challenged on the basis of the physiological firing properties of SST neurons, which appears to slow to operate in the high gamma range and is instead sustained at high beta/low gamma frequency (15-30 Hz) (Chen et al., 2017). Thus, alterations to PV basket cells specifically in the DLPFC of schizophrenia might underlie gamma oscillatory alterations reported in the disorder (**Figure 2D**).

1.5.2 In vivo approaches for quantifying alterations in excitatory and inhibitory neuron function in schizophrenia

Both fMRI and EEG studies of the DLPFC in schizophrenia reveal a basis for its dysfunction, and specifically tie this dysfunction to activity in working memory. Other *in vivo* strategies allow for some interrogation into alterations at the level of excitatory and inhibitory neurotransmission. One of these approaches, magnetic resonance spectroscopy (MRS), is able to measure the levels of certain metabolites and neurotransmitters in the functioning cortex, with regional specificity, offering significant promise for biomarker development (Schoonover et al., 2020). In MRS, the strength of the magnetic field used in the study directly determines the capacity to dissociate spectral peaks that are specific to a given metabolite or neurotransmitter (Maddock & Buonocore, 2012).

Two recent meta-analyses of proton MRS studies using different magnetic field strengths (ranging from 1.5 Tesla (1.5T) to 7T) reported lower glutamate levels in the medial PFC in schizophrenia (Merritt et al., 2021; Smucny et al., 2021). The recent convergence on evidence of lower glutamate levels in the medial PFC in schizophrenia could reflect the higher number of

quality studies in recent years (Smucny et al., 2021). The development in MRI technology, particularly the introduction of ultra-high field strength of 7T, offers enhanced spectral resolution of glutamate (and GABA) from related metabolites (Godlewska et al., 2017). Indeed, a smaller meta-analysis that only included 7T studies also identified lower glutamate levels in the medial PFC of schizophrenia (Sydnor & Roalf, 2020). However, it is important to note that these findings in the medial PFC might not extend to the DLPFC (Kaminski et al., 2021; Smucny et al., 2021). More studies are necessary to fully elucidate the nature of the disease effect and to dissociate this effect from other confounders, such as antipsychotic dosing and aging effects (Merritt et al., 2021).

In vivo measurements of cortical GABA using proton MRS have yielded conflicting results in the prefrontal cortex more broadly in participants with schizophrenia. Two reviews of GABA levels using proton MRS in schizophrenia failed to find clear evidence of differences in GABA levels in the prefrontal cortex (Taylor & Tso, 2015; Egerton et al., 2017). To date, the only 7T MRS study of GABA levels conducted in the prefrontal cortex in schizophrenia reported lower levels of GABA (Marsman et al., 2014), consistent with 7T findings of lower GABA in the occipital cortex of those with schizophrenia (Thakkar et al., 2017). Thus, more studies at high magnetic field strength might reveal evidence consistent with lower levels of GABA in the prefrontal cortex of individuals with schizophrenia.

Even at higher levels of spectral resolution, MRS studies are limited to assessing total tissue levels of GABA and glutamate, which includes pools of these molecules involved in metabolism and synaptic transmission. Thus, the relationship between these studies and GABAergic neurotransmission in schizophrenia remains unclear. One strategy for overcoming this limitation comes from the advent of novel chemical ligands for use in positron emission transmission (PET) imaging studies. For example, measuring the binding of a PET radioligand, [^{11}C] flumazenil,

which binds to the benzodiazepine site of GABAA receptors, can selectively measure shifts in extracellular GABA levels, as higher GABA levels in the synapse enhance the affinity of $GABA_A$ receptors for binding the radiotracer at this site (Frankle et al., 2012). Antipsychotic-naïve patients with schizophrenia showed a significantly lower tissue distribution volume of [^{11}C] flumazenil compared to unaffected comparison subjects, and this effect was significant in the dorsolateral PFC (Frankle et al., 2015). These strategies *in vivo* suggest that levels of glutamate and GABA signaling in the prefrontal cortex of persons with schizophrenia might be lower and offer substantial promise for the development of biomarkers in schizophrenia (Schoonover et al., 2020).

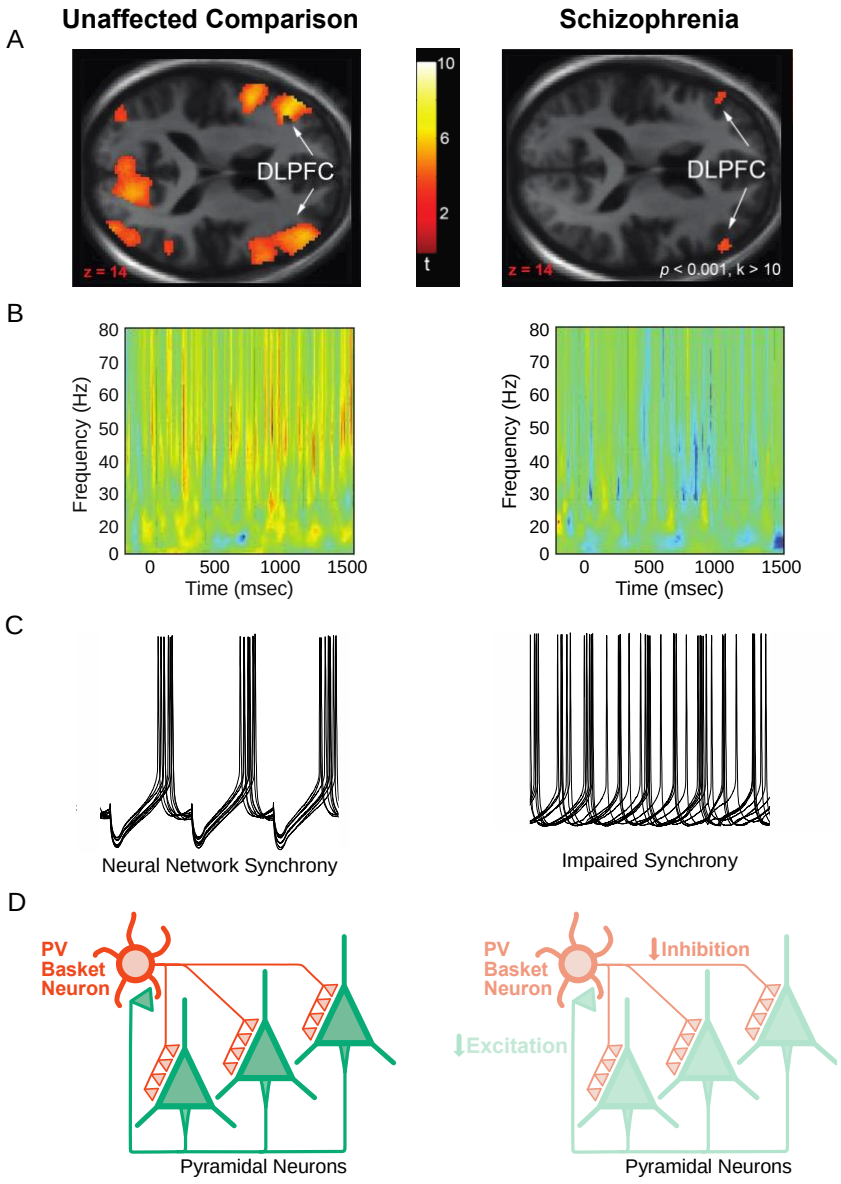

Figure 2. DLPFC alterations during working memory in schizophrenia at multiple levels of resolution.
A) DLPFC activation associated with cognitive control during the AX Continuous Performance Task in unaffected comparison individuals (left) and those with schizophrenia (right). Data taken from a previously published sample (Smucny et al., 2020). **B)** Frequency-time plots of scalp EEG recordings of prefrontal oscillatory activity during the delay period of the Preparing to Overcome Prepotency Task. Warmer colors indicate higher oscillatory power and cooler colors indicate lower power. Note that power in the gamma band (30-80 Hz) is substantially greater in healthy individuals compared to people with schizophrenia. Adapted from (Cho et al., 2006). **C)** Schematic representation of neural network synchrony (coordinated intracellular membrane recordings from pyramidal neurons) at gamma frequency in the healthy state and the hypothesized loss of this synchrony in schizophrenia. Adapted from (Gonzalez-Burgos & Lewis, 2008). **D)** Diagram of local neural circuit in cortical layer 3. In the healthy state, inhibition from PV basket neurons synchronizes the activity of groups of pyramidal neurons at gamma frequency, but lower levels of both excitation and inhibition could contribute to impaired synchrony in schizophrenia, as depicted in **C.** Figure adapted from (Smucny et al., 2022).

1.6 POSTMORTEM STUDIES OF THE DLPFC IN SCHIZOPHRENIA PROVIDE LAMINAR AND CELLULAR RESOLUTION OF ALTERATIONS IN THE DLPFC MICROCIRCUIT

As described above, the above methods offer invaluable insight into the role that the DLPFC and certain elements of its circuitry have in mediating working memory function and how these elements might be disrupted in people with schizophrenia. However, at the present moment, the only mechanism for the interrogation of these alterations at a cellular level is through the study of the postmortem human brain. The brain is a tremendously complex system of circuits and cells and pooling together of the alterations in these cells obscure knowledge about the underlying cellular dysfunction in the disorder. As one example, we conducted a secondary data analysis of multiple mRNAs related to excitatory and inhibitory neurotransmission obtained through postmortem studies in schizophrenia. Here, each of the studies were conducted at multiple levels of anatomic resolution: first, in total gray matter homogenates where the entirety of the DLPFC gray matter was homogenized and measured, second in layer-specific homogenates isolated to layer 3, and third in cell-specific homogenates conducted in layer 3 pyramidal neurons and layer 3 parvalbumin neurons. This analysis revealed that the same transcripts exhibited markedly different disease effects at these all three levels of resolution in a manner not explained by difference in cohorts of individuals with schizophrenia nor methodologies employed to study these transcripts (Dienel et al., 2020). While novel methods employed in humans are able to probe the DLPFC with laminar resolution (Finn et al., 2019), there are no currently available *in vivo* approaches that permit interrogation of cell-specific alterations in the disorder. Here, I review some of the major findings from postmortem studies of the DLPFC in schizophrenia and different cell

types appear to be altered in the disorder, with special attention to the layer 3 microcircuit that studies in non-human primates have specifically implicated in working memory.

1.6.1 Layer 3 pyramidal neuron alterations in the DLPFC of schizophrenia

At this moment, MRS studies of glutamate levels in schizophrenia are unable to determine the sources of those altered levels at either laminar or cellular levels of resolution. Given evidence of different roles that pyramidal neurons in different cortical layers could have in working memory, alterations that are specific to this circuitry in the superficial layers likely contribute to the neural substrate of altered working memory function in schizophrenia.

Consistent with this conjecture, postmortem studies of the DLPFC in individuals with schizophrenia have found smaller somal volumes of pyramidal neurons in layer 3 (Pierri et al., 2001; Rajkowska et al., 1998). Somal volumes are correlated with the size and branching complexity of the dendritic arbor, and, accordingly, the length and branching complexity of the dendritic tree of pyramidal neurons in layer 3 of the DLPFC have been shown to be lower in schizophrenia (Glantz & Lewis, 2000). In addition, schizophrenia is associated with fewer dendritic spines that stud the dendritic tree of pyramidal neurons (Glantz & Lewis, 2000; Garey et al., 1998; Konopaske et al., 2014). This deficit appear most pronounced on layer 3 pyramidal neurons in the DLPFC and is less marked on layer 3 pyramidal neurons in the visual cortex (Glantz & Lewis, 2000) or on pyramidal neurons in layers 5 and 6 (Kolluri et al., 2005) of the DLPFC. The combination of fewer dendritic spines and shorter dendritic branches suggests that the total number of spines, and putatively the number of excitatory inputs, onto layer 3 pyramidal neurons in the DLPFC is markedly lower in schizophrenia.

These morphological alterations in layer 3 pyramidal neurons have been suggested to stem from disturbances in signaling pathways that regulate the actin dynamics essential for dendritic arbor and spine formation and maintenance (Dienel et al., 2022). In schizophrenia, genetic risk factors implicate gene products involved in regulating actin dynamic signaling pathways (Trubetskoy et al., 2022). In postmortem samples of layer 3 pyramidal neurons, individuals with schizophrenia exhibit lower levels of critical molecules that regulate actin, including the Rho GTPase CDC42 (Datta et al., 2015), which regulates actin polymerization, and Arp2/3 (Datta et al., 2017), a major final common pathway for spine actin remodeling (Kim et al., 2013).

A markedly lower complement of excitatory inputs would be predicted to result in hypoactivity of these neurons, and, accordingly, DLPFC layer 3 pyramidal neurons in schizophrenia also exhibit marked downregulation of levels of multiple transcripts that are either activity-dependent (Kimoto et al., 2015) or that regulate mitochondrial function and energy production (Glausier et al., 2020a; Arion et al., 2015). The latter finding has been interpreted as a reflection that layer 3 pyramidal neurons have a lower demand for energy production due to hypoactivity secondary to weaker excitatory drive, rather than a primary impairment in mitochondria in schizophrenia, for the following reasons (Dienel et al., 2022): 1) genetic studies have not implicated nuclear genes regulating mitochondrial function as risk factors for schizophrenia (Fromer et al., 2014; Purcell et al., 2014; Trubetskoy et al., 2022); 2) our cell type-specific studies in SZ comparing the transcriptome alterations in pyramidal and PV neurons reveal larger alterations in mitochondrial gene transcript levels in layer 3 pyramidal neurons (Glausier et al., 2020a; Arion et al., 2015) than in PV basket cells (Enwright Iii et al., 2018); and 3) genetic manipulations that impair mitochondrial function in PV neurons were associated with greater excitatory inputs onto PV neurons and greater gamma band power , the opposite of the findings in

schizophrenia (Dienel et al., 2022). Together, these findings converge on the notion that layer 3 pyramidal neurons are hypoactive in schizophrenia (**Figure 3A**).

1.6.2 Alterations in DLPFC GABA signaling in schizophrenia

Although the resultant hypoactivity of the DLPFC might emerge from overactive inhibitory neurotransmission in the DLPFC in schizophrenia, the abundance of postmortem studies that estimate the capacity for GABA neurotransmission, consistent with the interpretation of *in vivo* studies in the disorder (Starc et al., 2017), have summarily supported the alternative: that GABA neurotransmission is weaker in the DLPFC of individuals with schizophrenia. While GABA itself is rapidly degraded after death and cannot be studied in postmortem studies of schizophrenia, the strength of GABA neurotransmission is proportional to the availability of GABA in the presynaptic terminal. In schizophrenia, levels of the mRNA for one of the two enzymes responsible for GABA synthesis, the 67 kilodalton isoform of glutamic acid decarboxylase 67 (GAD67), encoded by the *GAD1* gene, has been revealed to be lower in total tissue homogenates of the DLPFC of individuals with schizophrenia in multiple studies (Kimoto et al., 2014; Vawter et al., 2002; Akbarian et al., 1995; Volk et al., 2000; Woo et al., 2008). Similarly, levels of GAD67 protein are lower in the DLPFC of individuals with schizophrenia (Curley et al., 2011; Guidotti et al., 2000). At the cellular level, the density of neurons with detectable GAD67 mRNA is 25-35% lower across cortical layers 2-5, while the remaining GAD67-expressing neurons seem to have levels that are similar to the matched unaffected comparison individuals. These findings suggest that different subsets of GABA neurons in the DLPFC of individuals with schizophrenia might be differentially affected in schizophrenia in terms of their capacity to synthesize GABA, yet it has remained unclear which GABA neuron subtypes exhibit lower levels of GAD67 mRNA in

schizophrenia (**4.0**). The other major isoform of GAD (GAD65), encoded by the *GAD2* gene, exhibits a less obvious pattern of alteration in the DLPFC of individuals with schizophrenia (Glausier et al., 2015).

1.6.2.1 PV neurons exhibit multiple alterations in the DLPFC of schizophrenia

In the DLPFC of schizophrenia, PV neurons exhibit lower GAD67 mRNA levels such that ~50% of PV-positive neurons lack detectable GAD67 mRNA (Hashimoto et al., 2003). Furthermore, PV levels per PV neuron are also lower in the DLPFC, and this deficit was clearly evident in layers 3-4, but not in layer 2 (Hashimoto et al., 2003; Chung et al., 2016b).

Whether lower levels of PV mRNA reflect lower PV mRNA levels per neuron or a deficit in PV neuron density in schizophrenia has been a matter of debate in the field of postmortem brain research in schizophrenia (**3.0**) (Krystal et al., 2003). First, counts of Nissl-labeled cells suggested that the density of small, round, interneuron-like Nissl-labeled cells were lower in the DLPFC of those with schizophrenia (Benes et al., 1991). Later, a lower density of PV-immunoreactive neurons was found in some (Beasley & Reynolds, 1997; Reynolds & Beasley, 2001) but not all (Woo et al., 1997; Tooney & Chahl, 2004) studies of schizophrenia. The only study to date to simultaneously quantify PV mRNA levels per neuron and quantify the density of neurons exhibiting specific labeling for PV mRNA reported lower PV levels per neuron and no difference in the density of neurons (Hashimoto et al., 2003). However, the effect size for a deficit in PV neuron density was large even if this difference did not reach statistical significance (Cohen's d = 0.79). In fact, one meta-analysis of PV neuron alterations in the DLPFC of schizophrenia revealed by postmortem studies concluded that there was a deficit in PV neuron density without lower gene expression per neuron (Kaar et al., 2019).

However, multiple studies (Chung et al., 2016a; Enwright et al., 2016) from our group reported no difference in the density of PV-immunoreactive neuron density, and one study reported that the basis for this conclusion was contingent on the level of microscopic resolution used, even in the same tissue sections (Enwright et al., 2016). These findings supported the idea that PV neurons were not "lost" in schizophrenia; rather, a disease-related deficit in PV mRNA and protein expression rendered the most affected neurons difficult to visualize by microscopy.

At the protein level, PV basket cells are clearly altered in the DLPFC of persons with schizophrenia. PV basket cells exhibit both isoforms of GAD, while PV chandelier cells only exhibit GAD67 mRNA and protein (Fish et al., 2011; Fish et al., 2018). The axon terminals of PV basket cells (i.e., those that contain GAD65) exhibit lower levels of GAD67 protein (Fish et al., 2021; Rocco et al., 2016a) and PV (Glausier et al., 2014), while PV chandelier cells cartridges appear to have unaltered levels of GAD67 protein (Rocco et al., 2016a). While levels of GAD67 might not be lower in PV chandelier cell inputs, levels of the GABA membrane transporter (GAT1) appear to be lower in persons with schizophrenia (Woo et al., 1998; Pierri et al., 1999), while levels for the α2 $GABA_A$ receptor subunit postsynaptic to chandelier cell inputs appears to be higher (Volk et al., 2002). The combination of pre- and postsynaptic changes would appear to strengthen GABA neurotransmission at PV chandelier cell inputs in schizophrenia, although how these alterations could contribute to working memory alterations in schizophrenia remain unclear.

1.6.2.2 SST neurons are clearly altered in schizophrenia

In addition to PV neurons, SST neurons are also plainly altered in the DLPFC of individuals with schizophrenia. The initial findings of lower SST peptide in the brains of individuals with schizophrenia (Nemeroff et al., 1983; Gabriel et al., 1996) has been more consistently demonstrated at the level of mRNA in schizophrenia (Hashimoto et al., 2008a; Morris

et al., 2008; Fung et al., 2010; Volk et al., 2016; Tsubomoto et al., 2019). However, beyond abundant evidence of lower SST mRNA in the disorder, knowledge about the nature of SST neuron alterations in schizophrenia remain unclear. For example, the apparent density of SST-expressing neurons in schizophrenia is 30% lower in the DLPFC, which could reflect markedly lower SST levels per neuron such that some are rendered undetectable or fewer neurons in the disorder (Morris et al., 2008) (Error! Reference source not found.). Second, although SST and GAD67 l evels are correlated in schizophrenia (Morris et al., 2008), GAD67 levels have not been directly examined within SST neurons in schizophrenia, and the thus the nature of their involvement in impaired GABA signaling in the DLPFC in the disorder remains unclear (Error! Reference source n ot found.**)**.

1.6.2.3 CR/VIP neuron alterations in schizophrenia are poorly understood

Levels of CR mRNA do not appear to be altered in the DLPFC of people with schizophrenia (Hashimoto et al., 2003; Fung et al., 2010) and may not exhibit the same alterations as other interneuron subtypes. In addition to unaffected levels of CR mRNA, levels of CR protein and the density of CR-immunoreactive axon terminals are similarly unaltered in schizophrenia. However, VIP mRNA levels, which are frequently co-expressed in these cells, appears to be lower in schizophrenia (Tsubomoto et al., 2019; Fung et al., 2010). Moreover, no study to date has directly examined levels of GAD67 within CR/VIP cells in schizophrenia **(4.0**).

Together, while much is known about how these subtypes of GABA neurons (**Figure 3B**) are altered in schizophrenia, clearly fundamental questions remain about the nature and cell type-specificity of those alterations, especially with regard to SST neuron alterations. Aside from strongly supported evidence of lower SST in the disorder, no other cell type-specific alterations in this subtype are clearly identified.

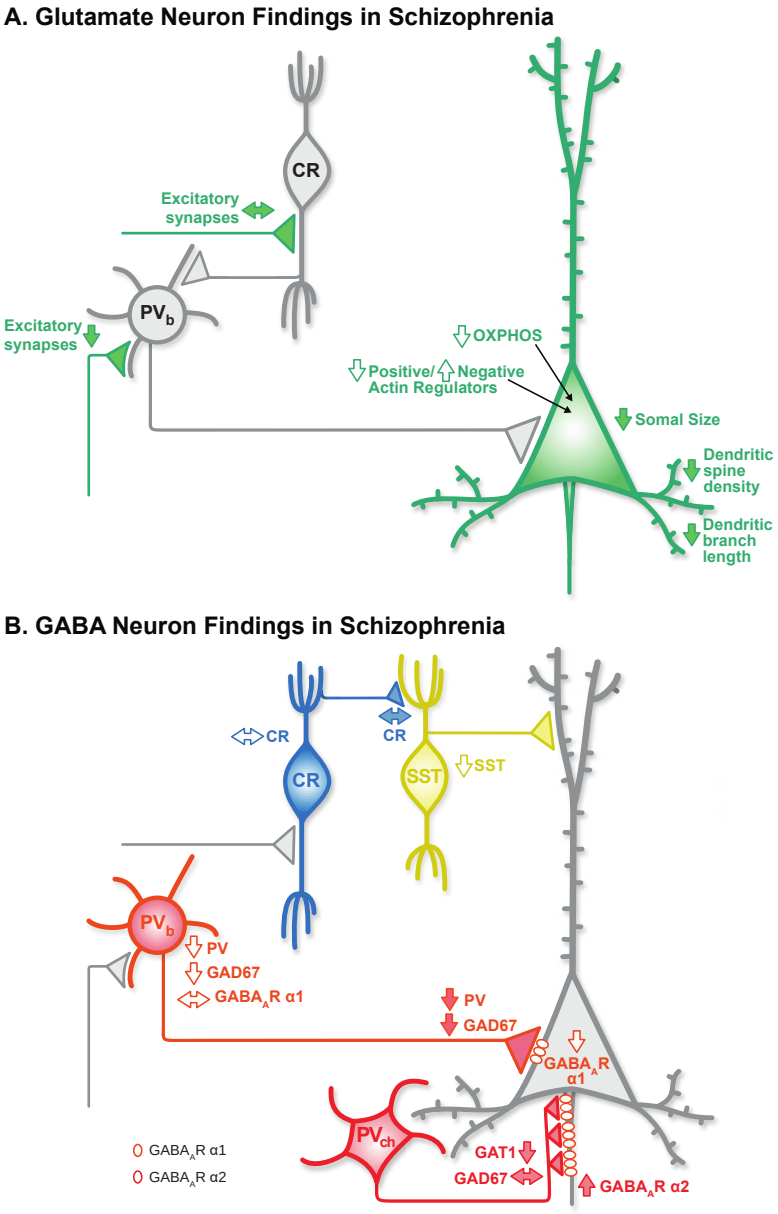

Figure 3. Schematic summary of alterations in superficial DLPFC microcircuit in schizophrenia.

A) Alterations in glutamate-containing pyramidal neurons (green) in schizophrenia. Here, we specifically focus on the alterations observed in layer 3 pyramidal neurons from postmortem studies of schizophrenia. Layer 3 pyramidal neurons in schizophrenia exhibit lower gene expression levels of positive regulators and higher gene expression levels of negative regulators of actin filaments that are critical for structural features of pyramidal neurons, and these alterations are thought to contribute to smaller somal volumes, shorter basilar dendrites and lower dendritic spine density of layer 3 pyramidal neurons in schizophrenia. The deficit in total dendritic spines likely represents fewer glutamatergic inputs onto layer 3 pyramidal neurons from other layer 3 pyramidal neurons and glutamatergic neurons in other brain regions. As a result, layer 3 pyramidal neurons are thought to be hypoactive which results in the activity-related downregulation of transcripts involved in mitochondrial energy production and oxidative phosphorylation (OXPHOS). The density of glutamatergic excitatory inputs is also lower on parvalbumin basket cells (PVb) but not on calretinin (CR) interneurons. **B)** The perisomatic inhibition of pyramidal neurons by PVb cells (red) is lower due to (1) lower levels of GAD67 mRNA and protein, and therefore less GABA synthesis; (2) higher levels of μ opioid receptor expression that both reduces PVb cell activity and suppresses GABA release; and (3) less mRNA for, and presumably fewer, postsynaptic $GABA_A\alpha1$ receptors in pyramidal neurons. Levels of the GABA membrane transporter 1 (GAT1) are lower in the axon terminals of PV-expressing chandelier (PVch) cells, whereas levels postsynaptic $GABA_A$ α2-containing receptors are higher in pyramidal neuron axon initial segments. However, levels of GAD67 protein in PVch cells are not altered in schizophrenia. Somatostatin (SST)-containing cells (yellow) express lower mRNA levels of SST. Finally, calretinin (CR)-containing cells (blue) are thought to be unaffected in schizophrenia as CR mRNA and protein levels are not altered. It should be noted that GAD67 levels have not yet been directly examined in SST or CR cells in schizophrenia. Open arrows indicate mRNAs; filled arrows indicate proteins. Adapted from (Dienel & Lewis, 2017).

1.7 GOALS OF THIS DISSERTATION

Prefrontal SST-expressing GABA neurons are strongly implicated in working memory, through animals models which demonstrate that their activity is necessary for working memory in rodents and computational models of the primate DLPFC during working memory (Froudist-Walsh et al., 2021; Wang et al., 2004). These models specifically point to a role of dendritic inhibition from SST neurons in distractor resistance during working memory. Neuropsychological testing of individuals with schizophrenia suggests that the ability to resist distracting stimuli during working memory in schizophrenia is also impaired. Therefore, the previously reported regional enrichment for SST mRNA in the DLPFC relative to other cortical regions, especially primary sensory areas such as the primary visual cortex (V1), supports the imputation that an enrichment of these neurons in the DLPFC represents part of the neural substrate for the resilience of the DLPFC to distractors (while other cortical regions reliably encode distracting stimuli). Moreover, a schizophrenia-associated deficit in SST mRNA expression supports the notion that alterations to this neuron in the disorder represent part of the neural substrate for impaired distractor filtering.

A key theme and goal of this dissertation is to address the *basis* for differences in transcript levels across cortical regions and in the DLPFC in the context of schizophrenia. Differences in SST mRNA levels reported at the level of total tissue homogenate might reflect differences in the relative proportion of neurons expressing a given transcripts, differences in transcript levels per neuron, or both. The prior studies that provide the background support for the hypotheses described above lacked the laminar and cellular resolution necessary to address these questions. In this dissertation, I test the following hypotheses: are higher levels of SST in the DLPFC relative to V1 in the primate neocortex due to differences in SST levels per SST neuron or the relative proportion of neurons that express SST (**2.0**)? Second, do lower levels of SST mRNA in the DLPFC of

persons with schizophrenia reflect lower gene expression per neuron or fewer SST neurons (**3.0**)? Third, do SST neurons exhibit evidence of a diminished capacity to synthesize GABA, indexed by lower levels of a key GABA synthesizing enzyme, GAD67 (**4.0**)? While this dissertation is framed around SST neurons, all the experiments described in this dissertation work utilize other GABA neurons as comparators for the findings reported in SST neurons.

2.0 DISTINCT LAMINAR AND CELLULAR PATTERNS OF SOMATOSTATIN TRANSCRIPT LEVELS IN MONKEY PREFRONTAL AND VISUAL CORTICES

Adapted from: Dienel SJ, Ciesielski AJ, Bazmi HH, Profozich EA, Fish KN, Lewis DA. Distinct Laminar and Cellular Patterns of GABA Neuron Transcript Expression in Monkey Prefrontal and Visual Cortices. *Cerebral Cortex* 31(5): 2345–2363.

2.1 INTRODUCTION

Cortical interneurons, which utilize the inhibitory neurotransmitter γ-aminobutyric acid (GABA), regulate cortical network activity by shaping the excitatory inputs received by pyramidal neurons and the excitatory outputs they generate (Markram et al., 2004; Kepecs & Fishell, 2014; Tremblay et al., 2016). GABA neurons have been subtyped based on their physiologic, morphologic, and/or molecular properties (Ascoli et al., 2008; DeFelipe et al., 2013). Classification schemes based on uniquely expressed gene products have defined four major groups of GABA neurons in the primate neocortex: those expressing the calcium-binding protein parvalbumin (PV), the neuropeptides somatostatin (SST) or vasoactive intestinal peptide (VIP), or the cannabinoid receptor 1 (CB1R) (DeFelipe, 1993; Condé et al., 1994; Gabbott & Bacon, 1996; DeFelipe, 1997; del Rio & DeFelipe, 1997; Eggan & Lewis, 2007). Some of these cell types frequently, but not exclusively, also express other calcium-binding proteins such as calbindin (CB) and calretinin (CR) (Condé et al., 1994; del Río & DeFelipe, 1996; DeFelipe, 1997) or other neuropeptides such as cholecystokinin (CCK) (Oeth & Lewis, 1990). For example, most SST

neurons in superficial layers also express CB (González-Albo et al., 2001), CR and VIP are frequently co-expressed (Gabbott et al., 1997; Meskenaite, 1997), and many CB1R-containing neurons also express CCK (Eggan et al., 2010).

Studies in humans suggest that expression levels of GABA neuron subtype-specific gene products differ across the cortical mantle, with pronounced differences between higher-order association regions (e.g., dorsolateral prefrontal cortex, DLPFC) and primary sensory areas (e.g., primary visual cortex, V1) (Hashimoto et al., 2008b; Hawrylycz et al., 2012; Tsubomoto et al., 2019). For example, in humans, PV mRNA levels are ~4 fold higher in V1 relative to DLPFC, whereas SST mRNA levels are ~2 fold higher in DLPFC relative to V1 (Hashimoto et al., 2008b; Tsubomoto et al., 2019). However, these studies examined total gray matter tissue homogenates and could not determine the contribution of individual cortical layers to the differences between regions.

Studies across cortical layers in monkeys and humans indicate that the relative densities of GABA neurons tend to be higher in layers 2 and 4, as demonstrated by counts of neurons immunoreactive for GABA (Hendry et al., 1987)or labeled for glutamic acid decarboxylase 67 (GAD67) mRNA (Akbarian et al., 1995; Volk et al., 2000) the enzyme responsible for most GABA synthesis in the cortex (Asada et al., 1997). Moreover, the cell bodies of GABA neuron subtypes are differentially enriched in layers 2 and 4. For example, in the primate DLPFC, the density of SST/CB (Lewis et al., 1986; Gabbott & Bacon, 1996), VIP/CR (Condé et al., 1994) and CB1R/CCK (Eggan et al., 2010) neurons is highest in layer 2, whereas the density of PV neurons is highest in layer 4 (Condé et al., 1994; Hof et al., 1999). However, these studies were limited to counts of labeled neurons and could not determine the contribution of gene expression per neuron to the observed regional differences in GABA-related transcript levels.

To determine the laminar and cellular bases for the marked differences in GABA-related transcript levels between monkey DLPFC and V1, we conducted two studies. First, we quantified levels of transcripts that distinguish among subtypes of GABA neurons, or that index pre- and post-synaptic GABA neurotransmission, in tissue homogenates restricted to layers 2 and 4 of macaque monkey DLPFC and V1. We selectively studied layers 2 and 4 given the enrichment of GABA-immunoreactive (Hendry et al., 1987), GAT1 mRNA-positive (Volk et al., 2001) and GAD67 mRNA-positive neurons (Volk et al., 2000) in these layers and prior reports that distinct GABA subtypes are differentially enriched in these layers (Condé et al., 1994; Gabbott & Bacon, 1996). Second, we used multiplex fluorescent *in situ* hybridization to quantify relative neuronal densities and transcript levels per neuron in the same regions and layers. We found that regional and laminar differences in GABA-related transcripts reflect differences in the complement of GABA neuron subtypes and/or in subtype-specific expression levels per neuron.

2.2 METHODS

2.2.1 Animals and tissue preparation

Three cohorts (total n = 15) of adolescent or young adult rhesus monkeys (*Macaca mulatta)* were used (**Table 1**). All animals were trained to perform working memory tasks under a water restriction protocol, described elsewhere (Verrico et al., 2011), and served solely as vehicle controls in those studies. The seven animals in Cohort 1 were deeply anesthetized with ketamine and pentobarbital and perfused transcardially with ice-cold artificial cerebrospinal fluid as previously described (Gonzalez-Burgos et al., 2008). The eight animals in Cohorts 2 and 3 were

deeply anesthetized with ketamine and pentobarbital without transcardial perfusion. In all animals, the brain was extracted intact, the right hemisphere was blocked, and the blocks were flash-frozen in isopentane and stored at -80°C until the time of the experiment. All housing and experimental procedures were conducted in accordance with guidelines set by the US Department of Agriculture and the National Institutes of Health Guide for the Care and Use of Laboratory Animals and with the approval of the University of Pittsburgh's Institutional Animal Care and Use Committee.

Table 1. Characteristics of monkeys used in these studies.

Cohort	Subject	Age (months)	Sex	Perfusion Status	Weight (kg)	Storage Time (months)
1	MJ219	41	M	+	4.7	96
	MJ401	41	M	+	7.4	94
	MJ508	41	M	+	4.1	94
	MJ324	42	M	+	8.5	94
	MJ407	42	M	+	4.6	93
	MJ607	42	M	+	4.4	92
	MJ523	44	M	+	4	90
2	RH341	60	M	−	8.2	37
	RH340	61	F	−	8.1	37
	RH343	61	F	−	6	37
	RH335	62	F	−	7	38
	RH338	62	M	−	10	38
	RH345	63	M	−	9.6	37
3	RH303	65	F	−	5.2	106
	RH301	101	M	−	11	106

2.2.2 Laser microdissection procedure

Cryostat sections (12 μm) were cut from coronal blocks of the right prefrontal cortex containing the principal sulcus and from sagittal blocks of the right occipital cortex containing the

calcarine sulcus (**Figure 4A-C**). Sections were thaw-mounted onto glass polyethylene naphthalate membrane slides that had been UV treated at 254 nm for 30 minutes, dried briefly, and stored at −80°C. On the day of laser microdissection, slides were immersed in an ethanol-acetic acid fixation solution and stained for thionin, as previously described (Dienel et al., 2017). Using a 5x microscope objective, cortical regions were confirmed by cytoarchitectonic criteria (Walker, 1940; Lund, 1973) and layers were identified based on the characteristic differences in packing density and size of Nissl-stained cells (**Figure 4D, E**). In coronal sections containing the principal sulcus, DLPFC was defined based on defining features of area 9 and 46 (Walker, 1940) and included the zone extending from the medial border of area 9 (i.e., the fundus of the cingulate sulcus) through the lateral border of area 46 (i.e., the ventral bank of the principal sulcus) (**Figure 4D**). In sagittal sections containing the calcarine sulcus, V1 was defined based on the cytoarchitectonic criteria for area 17 (Lund, 1973), and tissue samples containing layer 2 or layer 4 (including all sublayers) were captured (**Figure 4E**). In each region, tissue samples were collected across 3 adjacent cryostat sections to obtain a total cross-sectional tissue area of ~5 x 10^6 μm^2 in each layer from each animal. Samples were lysed in RLT Plus Buffer (QIAGEN) with β-mercaptoethanol, frozen, and RNA was extracted and purified using the RNeasy Plus Micro Kit (QIAGEN). All four samples (DLPFC layer 2 and layer 4 and V1 layer 2 and layer 4) from a single animal were collected during the same day by a single investigator (S.J.D or A.J.C) to minimize technical variance.

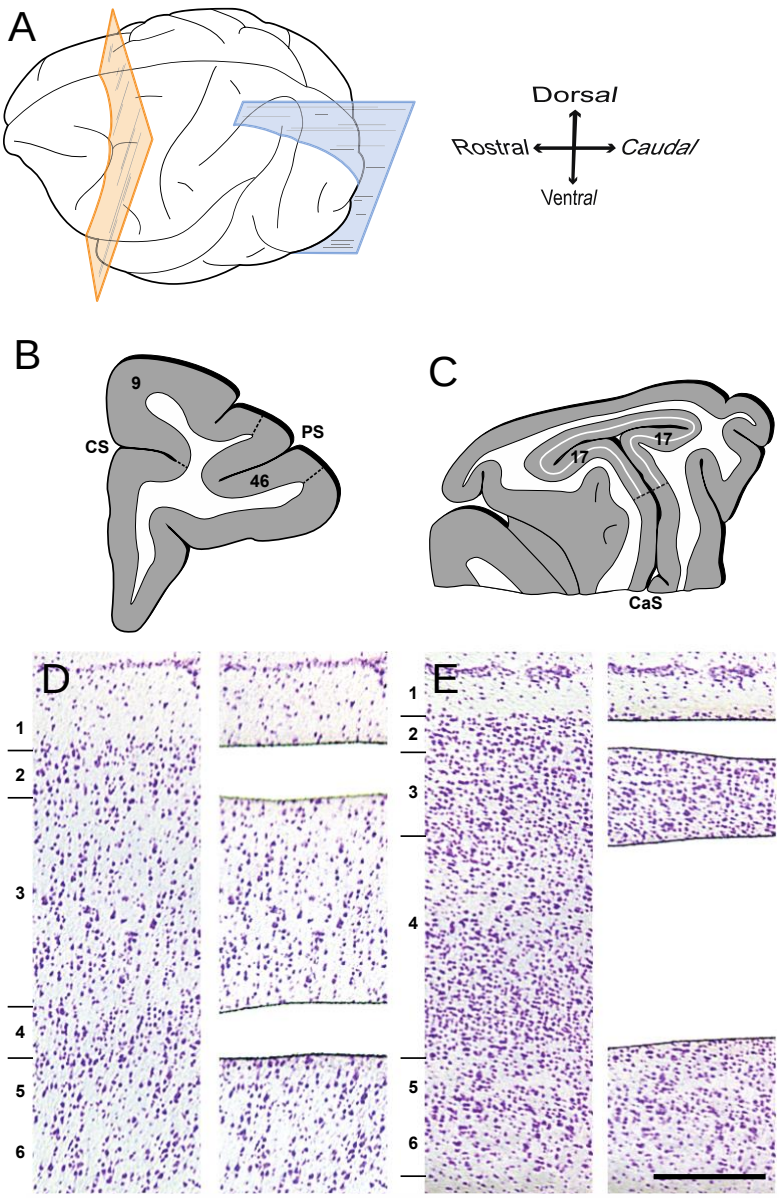

Figure 4. Cortical regions and layers in macaque monkeys.
A) Schematic of the macaque monkey brain. Orange and blue colored planes indicate locations of tissue blocks from the **B)** DLPFC and **C)** V1, respectively. Dashed lines indicate approximate locations of areas 9/46 and 17 identified by cytoarchitectonic criteria. Tissue sections were stained for Nissl substance, and layers 2 and 4 from **D)** DLPFC and **E)** V1 were laser microdissected and prepared for qPCR analysis. Numbers indicate cortical layers. PS = principal sulcus, CS = cingulate sulcus, CaS = calcarine sulcus. Scale bar (400µm) applies to panels D and E.

2.2.3 Quantitative polymerase chain reaction (qPCR)

Total RNA was converted to complementary DNA using the SuperScript™ IV VILO™ Master Mix (ThermoFisher Scientific, Waltham, MA, USA). Given the within-animal design of the study, all four cortical samples for each animal were represented in quadruplicate for each transcript on a single 384 well qPCR plate. Because of this design, which controls for any potential batch effects within animal, only 16 transcripts could be quantified. We designed forward and reverse primers to target the transcripts of the following 13 GABA-related markers (**Table 2**): those known to be primarily expressed in unique GABA neuron subtypes (SST, CB, VIP, CR, CB1R, CCK, and PV) and those related to GABA neurotransmission, including GABA synthesis (GAD67 and GAD65), vesicular packaging (vesicular GABA transporter, vGAT), reuptake (GABA membrane transporter 1, GAT1), and postsynaptic receptor subunits of the $GABA_A$ receptor (GABRA1 and GABRA2), which tend to be differentially enriched at specific postsynaptic sites (Nusser et al., 1996). The same approach was used for 3 housekeeping genes: β-actin (ACTB), cyclophilin A (PPIA), and glyceraldehyde 3-phosphate dehydrogenase (GAPDH). All primers showed 90-100% efficiency and each amplified product resulted in a single and specific amplicon. Levels of each transcript were assessed using Power SYBR Green fluorescence and the ViiA™7 Real Time PCR System to determine the cycle threshold (CT). The expression level of each transcript was calculated by subtracting the geometric mean of the three normalizers from the CT values of the gene of interest (difference in CT, or dCT). Normalizers are thought to account for variation in amounts of RNA due to a variety of factors, including differences in cell packing density. Based on the greater cell packing density in V1 relative to DLPFC in primates (Rockel et al., 1980; Carlo & Stevens, 2013; Collins et al., 2016), the expression of these housekeeping genes would be expected to be greater in V1 relative to DLPFC.

Consistent with our prediction, a repeated measures ANOVA demonstrated that the geometric mean of the normalizer genes was significantly higher in V1 than DLPFC ($F_{1,14} = 8.32$, $p = 0.012$). Because the dCT represents the $\log_2$-transformed expression ratio of each target transcript to the mean of the normalizer genes, the relative expression levels of the target transcripts are reported as the more intuitive expression ratio, or the 2^{-dCT}.

2.2.4 Multiplex Fluorescent in situ Hybridization

In the study utilizing multiplex fluorescent *in situ* hybridization, tissue sections from Cohort 2 animals (3 males and 3 females; **Table 1**) were used. Cryostat sections (20 μm) were cut from the same fresh-frozen coronal blocks of the right DLPFC and sagittal blocks of the right V1, and thaw-mounted on SuperFrost slides (ThermoFisher). Slides were stored at -80°C until labeling. Probes were designed by Advanced Cell Diagnostics, Inc (Hayward, CA, USA) to detect mRNAs of the *Macaca mulatta* genes for somatostatin (*SST*), parvalbumin (*PVALB*), and GAD67 (*GAD1*) (**Table 2**). Tissue sections were processed using the RNAscope® fluorescent multiplex assay according to the manufacturer's protocol (Wang et al., 2012). Briefly, after removal from -80°C, tissue sections were immediately immersed in ice-cold 4% paraformaldehyde for 15 minutes, dehydrated through a series of ethanol washes (50%, 70%, 100% and repeated with fresh 100% ethanol for 5 minutes each at room temperature) and treated with protease IV (ACDbio) for 30 minutes at room temperature. Probes were then hybridized to their target mRNAs for 2 hours at 40°C. After a series of amplification steps at 40°C (Amp 1 for 30 minutes, Amp 2 for 15 minutes, and Amp 3 for 30 minutes), GAD67, PV, and SST mRNAs were visualized by Alexa 488, Atto 550, and Atto 647N fluorophores, respectively, via oligonucleotide binding to specific channels (C1, C2, and C3) using Amp 4C for 15 minutes at 40°C. After counterstaining with DAPI, slides

were stored at 4°C until imaging. One section per region was used, and all tissue sections from each animal (n = 12 sections, 2 regions per 6 animals) were labeled together in the same batch.

2.2.5 Microscopy

Images were collected on a custom wide-field epifluorescence Olympus (Center Valley, PA, USA) IX83 inverted microscope equipped with a Spectra III light engine (Lumencor, Beaverton, OR, USA), a high-precision XYZ motorized stage with linear XYZ encoders (Prior Scientific, Rockland, MA, USA), an ORCA-Flash 4.0 sCMOS camera (Hamamatsu Photonics, Hamamatsu City, Japan), and custom dichroic mirrors and excitation/emission filters for simultaneous imaging of 6 channels (excitation wavelengths 350-, 405-, 568-, 647-, 750-nanometers). The microscope and ancillary equipment were controlled using SlideBook 6.0 (Intelligent Imaging Innovations, Inc., Denver, CO, USA). Images were captured using a 60x 1.42 N.A. oil immersion Plan Apochromat objective (Olympus). To select the imaging sites, a low-magnification image was taken, and a sampling grid composed of 240 μm x 240 μm squares was placed over the entirety of the gray matter for each section. Imaging sites were selected based on the laminar boundaries determined by the DAPI counterstain alone; thus, the experimenter (S.J.D) was blind to the labeling of the dependent measures of interest during imaging site selection. For V1, layer 4 included all sublayers, consistent with the studies performed using laser microdissection. 3D image stacks (17 2D images successively captured at intervals separated by 0.25 μm in the z-dimension) sized at 2048 x 2048 pixels (~220 x 220 μm; pixel size = 0.107 μm/pixel) were acquired to capture total tissue thickness. In each case, the z-axis was 4.25 μm. Throughout an image stack, fluorescent channels (DAPI, 488, 568, 647) were sequentially captured. Because macaques of this age group tend to accumulate lipofuscin, a lysosomal

degradation product, in cortical brain tissue (Brizzee et al., 1974), lipofuscin was imaged in a custom lipofuscin channel (ex: 405, em: 705) as previously described (Rocco et al., 2016b). Exposure times were established before beginning the experiment to optimize the dynamic range of the fluorescent grains, and exposure times and laser power were kept constant throughout the experiment: 405 nm at 100 milliseconds (ms), 488 nm at 1000 ms, 568 nm at 800 ms, and 647 nm at 300 ms, custom lipofuscin channel at 500 ms; all solid-state light source intensities were maintained at 10%. To minimize within-animal experimental variance, the sampling order of region (DLPFC vs V1) and layer (layer 2 vs layer 4) were systematically randomized and all regions and layers from a single animal were imaged in a day. For each animal, 30 sampling sites were obtained per layer per region, resulting in an equivalent sampling size of ~6.6 mm^2 per area.

2.2.6 Image Processing

Each fluorescent channel was processed using a 3D Gaussian blurred subtraction filter in MATLAB by calculating a difference of Gaussians using sigma values of 0.7 and 2. Within SlideBook, an average z-projection algorithm was used to generate a 2D representation of the 3D image stack. The lipofuscin channel was subtracted from each fluorescent channel using SlideBook channel subtraction algorithm. The resulting 2D projection image was exported as a quantitative 16-bit depth tiff files and imported into HALO (IndicaLabs, Albuquerque, NM, USA) for nucleus segmentation and grain counting.

Mask thresholding was optimized to capture fluorescent grains based on the following parameters: contrast threshold = 0.01, minimum intensity = 0.015, spot size = 0.09 – 2 µm, copy intensity = 1, segmentation aggressiveness = 1. These parameters were held constant for all analyses across regions and layers. Two analyses were performed: the first automatically

segmented DAPI-labeled nuclei and counted grains located over each nucleus and within the surrounding 2 μm perimeter. Optimal parameters for nucleus segmentation were selected to minimize contamination by glial nuclei, which tend to be smaller than neuronal nuclei (Vincent et al., 1989; Peters et al., 1994; Garcia-Cabezas et al., 2016), and exclude nuclear objects located at the edge of the tissue section (nuclei settings: nuclear contrast threshold = 0.5, minimum nuclear intensity = 0.04, segmentation aggressiveness = 0.5, nuclear size range = 30 – 250 μm^2, minimum roundness = 0.65, cytoplasm set to 2 μm perimeter). Because we were unable to include a glial cell marker, we cannot exclude a small contribution of glial nuclei to our data. Second, an analysis was performed to count grains in each image, regardless of their relationship to DAPI-labeled nuclei, using the same settings for counting grains. To determine the background grain density, the total grains associated with nuclei were subtracted from the full-field grain density, resulting in a value that represented the grain density per μm^2 for grains not associated with any nucleus. This background value was calculated as an average among all 60 imaging sites for a given animal and region, providing a within-slide control for random fluctuations in background grain density.

To detect nuclei that were positive for a given marker, a threshold based on grain density, rather than absolute grain counts per nucleus, was used to minimize false positive cell counts. Using this approach, PV+ or SST+ cells were defined as a nucleus that contained 2X greater than background levels for either of these transcripts and for GAD67 mRNA. A GAD67-Only cell was defined as one containing 2X the background density for GAD67 with PV and SST mRNA levels <2X their respective background levels. Based on these definitions, the 4.0-7.5% of PV and SST mRNA-containing nuclei across all samples that lacked GAD67 grains were considered false positives and excluded from analysis.

2.2.7 Experimental Design and Statistical Analyses

For the qPCR study, data were obtained from DLPFC layer 2, DLPFC layer 4, V1 layer 2, and V1 layer 4 samples for all 15 monkeys. To determine the differences in transcript levels between layers and across regions by qPCR, linear models were conducted using region, layer, and region-by-layer interaction as fixed factors, and ANOVA tables were computed based on the linear models. Because 13 transcripts were studied, we corrected for multiple comparisons using Bonferroni's procedure and set the significance level at $\alpha = 0.0038$ (0.05/13). Within each cohort, animals were very similar in age and tissue storage time, but these measures (and whether the animal was perfused with artificial cerebrospinal fluid) differed across cohorts (**Table 1**); thus, we included cohort as a covariate term in all linear models. Similarly, we included sex as a separate covariate. The inclusion of cohort and sex as covariates did not reach the set level of statistical significance for any transcript with the exception of GAD65, which showed higher expression in males than females across DLPFC and V1 layers 2 and 4 ($F_{(1,53)}=11.7$, $p=0.0012$). Because each animal has 4 different cortical samples, mixed models were also performed using animal as a random factor. However, in nearly every case, the Akaike information criteria (AIC) (Akaike, 1974) was smaller for the simpler linear model without animal as a random factor, indicating that the inclusion of the random factor did not meaningfully improve the model fit. Therefore, the most parsimonious model utilizing region, layer, and region-by-layer interaction terms was used and the results from this model are reported.

For the multiplex fluorescent *in situ* hybridization study, the same 4 laminar locations (DLPFC layer 2, DLPFC layer 4, V1 layer 2, V1 layer 4) were imaged in each of 6 monkeys. Linear models were employed using either percent of positive cells for each marker (relative to total nuclei count in that location) or mRNA grain density per neuron as dependent variables, and

region, layer, and region-by-layer interaction as independent variables. ANOVA tables were generated from these linear models. The cohort was balanced for sex, and the inclusion of sex as a separate independent variable in the model did not significantly explain the variance in any dependent measure in any case. Similarly, mixed models were also conducted including animal as a random factor, and the AIC indicated that the simpler linear model was a better fit for the data in nearly every case. Therefore, the most parsimonious model of including region, layer, and region-by-layer interaction was used for each dependent measure. Cohen's D effect sizes were employed to give an estimation of the normative differences between regions and layers.

All analyses were conducted in R using 'car' (Fox & Weisberg, 2019), 'tidyverse' (Wickham et al., 2017), and 'lme4' (Bates et al., 2015) packages. Figures were generated in R using 'ggplot2' (Wickham, 2016) and 'ggbeeswarm' (Clarke & Sherrill-Mix, 2017) packages. 'TukeyHSD' function in base R was used to compute posthoc comparisons.

All values provided in the text and figures are mean ± standard deviation.

2.3 RESULTS

2.3.1 Regional and Laminar Patterns of GABA-related Transcript Levels

Plots of the levels of GABA-related transcripts revealed three patterns across layers 2 and 4 of the DLPFC and V1 (**Figs 2 – 4**). Thus, the results are presented according to these patterns.

Pattern 1: Higher Transcript Levels in DLPFC than V1 and in Layer 2 than Layer 4. The most common pattern, exhibited by most transcripts expressed in specific subtypes of GABA neurons, was defined by higher transcript levels in DLPFC relative to V1 and layer 2 relative to

layer 4. Transcripts which are frequently co-expressed in the same neurons (e.g., SST and CB; CB1R and CCK; VIP and CR) tended to show a similar regional and laminar pattern. The most striking example of this shared expression pattern was for SST (**Figure 5A**) and CB (**Figure 5B**) mRNAs. Both these transcripts showed a significant effect of region (higher in DLPFC than V1) and layer (higher in layer 2 than layer 4). CB mRNA also showed a significant region-by-layer interaction, suggesting that the magnitude of the laminar difference was greater in the DLPFC (laminar effect size = 2.7) than V1 (laminar effect size = 1.6). Both CB1R (**Figure 5C**) and CCK (**Figure 5D**) mRNAs showed similar significant effects of region and layer, although without significant region-by-layer interactions. Finally, VIP (**Figure 5E**) and CR (**Figure 5F**) mRNAs also demonstrated this pattern, with significantly higher levels in DLPFC than V1 and in layer 2 than layer 4. A region-by-layer interaction was observed for CR mRNA, with the difference between layers 2 and 4 greater in V1 (laminar effect size = 6.5) than in DLPFC (laminar effect size = 4.1).

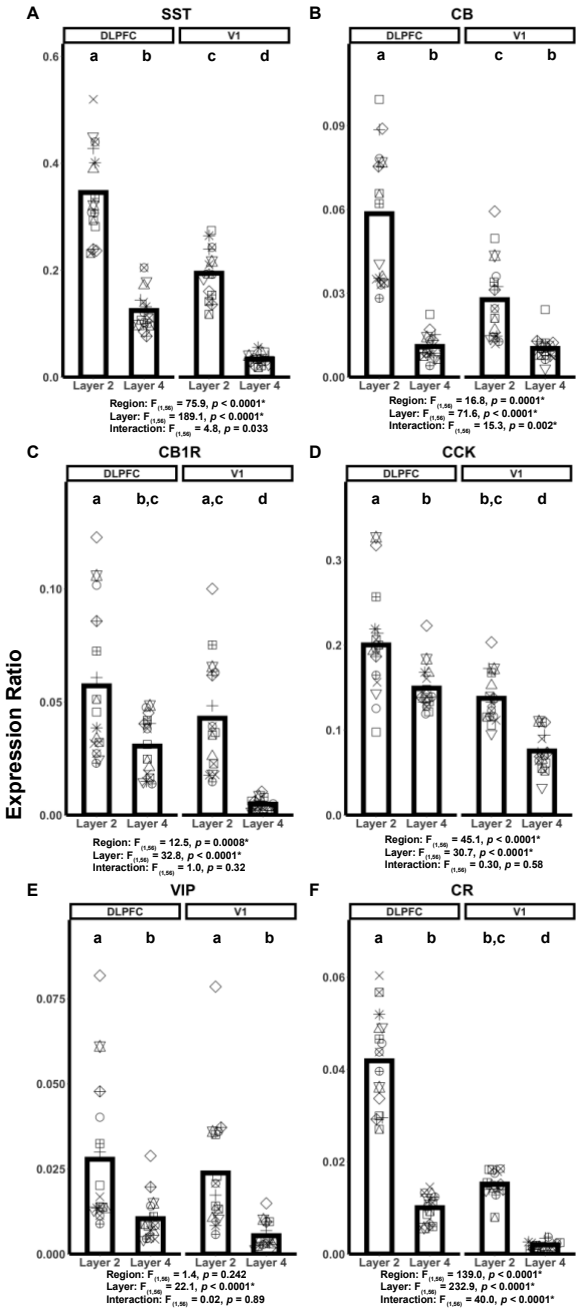

Figure 5. Transcripts that tend to be co-expressed in specific subsets of GABA neurons exhibit Pattern 1, with higher mRNA levels in DLPFC relative to V1 and in layer 2 relative to layer 4.

Both **A)** SST and **B)** CB mRNAs and **C)** CB1R and **D)** CCK mRNAs show similar regional and laminar patterns of expression. Although **E**) VIP and **F**) CR mRNAs are frequently co-expressed in the primate neocortex, the laminar effect size was larger for CR than VIP in both DLPFC and V1. Within each graph, bars not sharing the same lower-case letter are significantly different by Tukey's HSD (p<0.05).

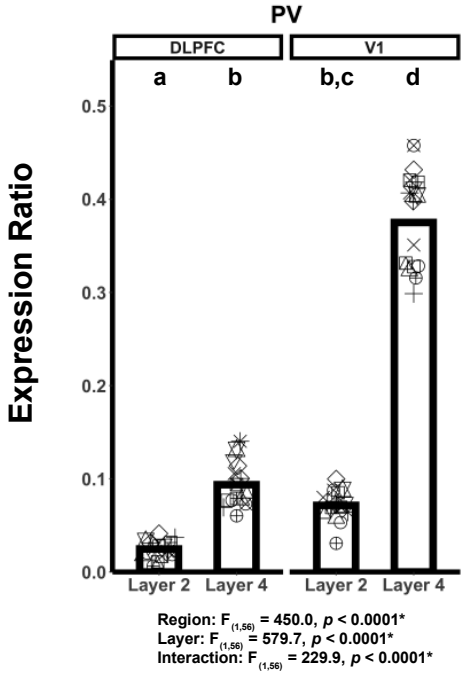

Figure 6. PV mRNA exhibited Pattern 2 of expression, with higher levels in V1 and layer 4 relative to DLPFC and layer 2.
Bars not sharing the same lower-case letter are significantly different by Tukey's HSD (p<0.05).

Pattern 2: Higher Transcript Levels in V1 than DLPFC and in Layer 4 than in Layer 2.

PV mRNA showed a distinctly different pattern from the other markers of GABA neuron subtypes, with higher levels in V1 than in DLPFC and in layer 4 than in layer 2. The effects of region, layer, and their interaction were significant (**Figure 6**). The difference between layers 4 and 2 was more pronounced in V1 (laminar effect size = 8.0) than in DLPFC (laminar effect size = 3.7)

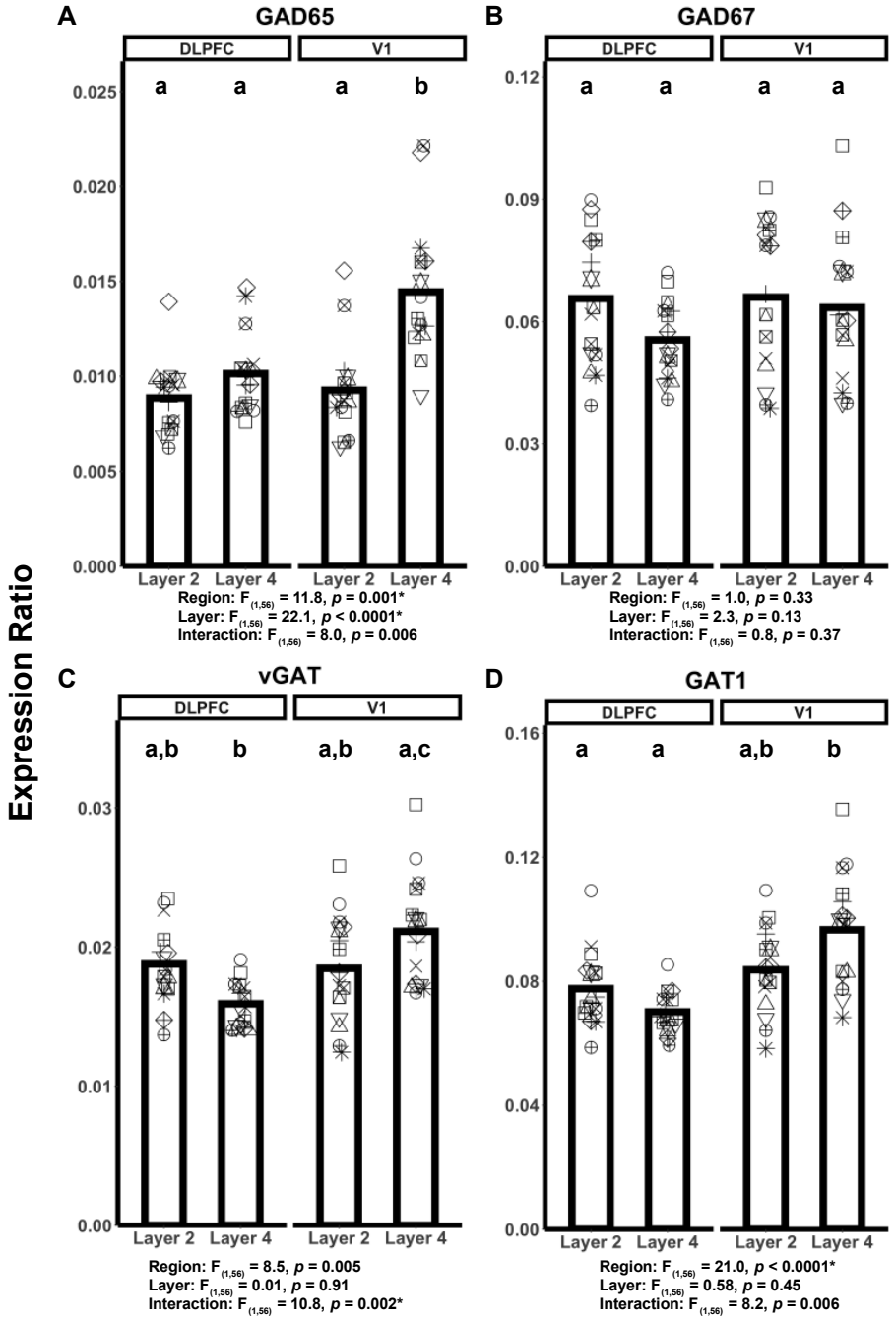

Figure 7. Regional and laminar expression levels for markers of GABA neurotransmission illustrate Pattern 3. A) GAD65, **B)** GAD67, **C)** vGAT, and **D)** GAT1 showed more modest regional and laminar patterns of expression than GABA neuron subtype-specific transcripts. Within each graph, bars not sharing the same lower-case letter are significantly different by Tukey's HSD (p<0.05).

Pattern 3: Modest Region or Laminar Differences in Transcript Levels. In contrast to the findings above, transcripts regulating GABA synthesis, release or reuptake exhibited only modest or no differences in expression across regions and layers. Levels of GAD65, vGAT, and GAT1 (but not GAD67) mRNAs (**Figure 7**) showed significant effects for region, with levels higher in V1 than DLPFC. Only GAD65 (**Figure 7A**) showed a significant effect of layer with levels higher in layer 4 than in layer 2, resembling (but much less striking than) the pattern exhibited by PV mRNA. Although many of the differences between regions and layers did not reach the stringent cutoff for statistical significance, expression levels of GAD65, vGAT, and GAT1 were higher in layer 4 of V1 relative to all other layers examined.

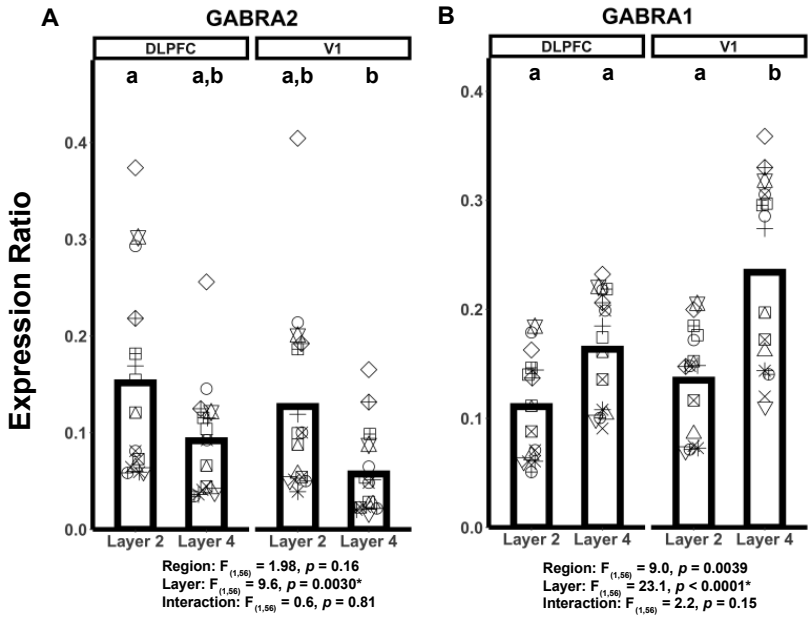

Figure 8. Regional and laminar expression levels for postsynaptic GABAA receptor subunits exhibit Patterns 1 and 2.

A) GABRA2 demonstrated Pattern 1 expression seen with most markers of GABA neuron subtypes, with higher expression in DLPFC and layer 2 relative to V1 and layer 4, respectively. **B**) GABRA1 showed the opposite Pattern 2, with higher expression in V1 and layer 4 relative to DLPFC and layer 2, respectively. Within each graph, bars not sharing the same lower-case letter are significantly different by Tukey's HSD ($p<0.05$).

$GABA_A$ Receptor Subunits Confirm Patterns 1 and 2: Expression levels of postsynaptic markers of GABA neurotransmission, GABRA2 and GABRA1 mRNAs, were similar to Patterns 1 and 2, respectively. That is, levels of GABRA2 mRNA (**Figure 8A**) were higher in DLPFC than V1 and in layer 2 than layer 4 (although the regional difference did not achieve statistical significance), whereas levels of GABRA1 mRNA (**Figure 8B**) were higher in V1 than DLPFC and in layer 4 than in layer 2.

Consistency of Laminar and Regional Effects within Animals. The group level patterns for each of these transcripts were highly consistent within individual animals. These highly conserved effects were demonstrated by an analysis of the within-animal rank for each of the four region/layer samples. For example, SST mRNA (**Figure 9A**) levels were always highest in DLPFC layer 2 (rank 1), followed by V1 layer 2 (rank 2), DLPFC layer 4 (rank 3), and V1 layer 4 (rank 4). PV mRNA levels (**Figure 9B**) were consistently highest in V1 layer 4 (rank 1); except for three animals, DLPFC layer 4 was ranked second and V1 layer 2 ranked third; and for all animals, DLPFC layer 2 ranked fourth. Other transcripts exhibiting patterns similar to PV or SST mRNAs also largely showed very consistent within-animal rank order by region and layer. In contrast to the consistent patterns across animals of these transcripts, neither GAD67 mRNA (**Figure 9C**) nor GAD65, vGAT, nor GAT1 mRNAs showed a consistent within-animal ranking patterns by region or layer.

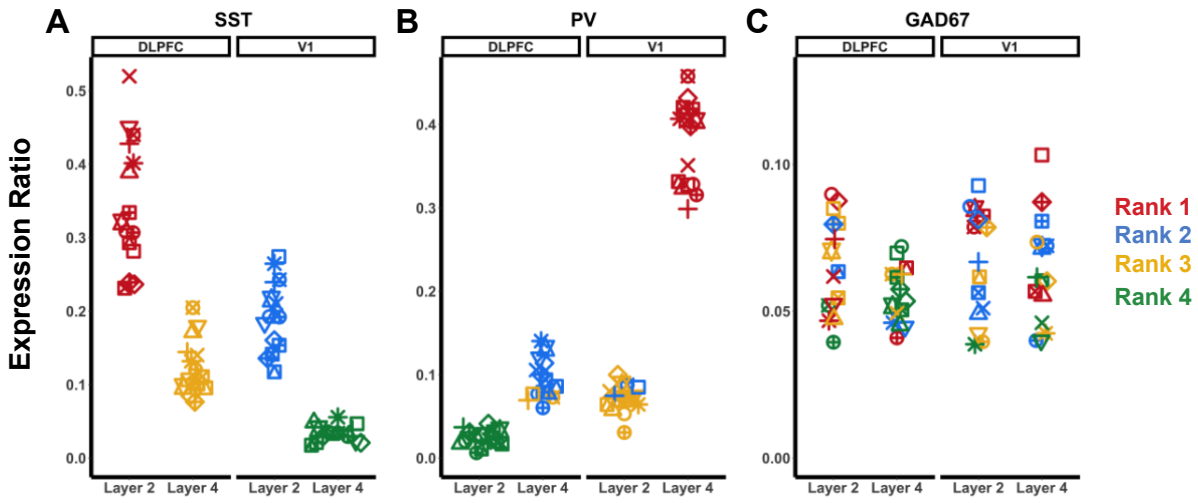

Figure 9. Expression patterns of each transcript were highly consistent across individual animals.
Values for each animal are shown as different shapes and the within-animal rank order of expression levels for each transcript are indicated by colors. In every animal, **A**) SST showed the highest expression in DLPFC layer 2, followed by V1 layer 2, DLPFC layer 4, and V1 layer 4. **B)** In nearly every case, PV showed the opposite pattern: higher expression in V1 layer 4, followed by DLPFC layer 4, V1 layer 2, and DLPFC layer 2. **C)** In contrast, GAD67 did not show consistent rank orders of expression levels within animals by region or layer.

2.3.2 Cellular Patterns of GABA-related Transcript Levels

Fluorescent in Situ Hybridization for SST, PV, and GAD67 mRNA Probes. To determine the cellular basis for the regional and laminar patterns of GABA-related gene products described above, multiplex fluorescent *in situ* hybridization was conducted for SST, PV and GAD67 mRNAs as exemplars of the three patterns observed by qPCR. High magnification images (**Figure 10**) demonstrated the specificity of each probe: PV or SST mRNAs were colocalized in the same nucleus with GAD67 mRNA, whereas PV and SST mRNAs were never colocalized. As expected, in both layer of both regions, some cells contained only GAD67 mRNA. Low magnification

images (**Figure 11**) revealed regional and laminar patterns of labeled cells for each mRNA consistent with the 3 patterns found by qPCR.

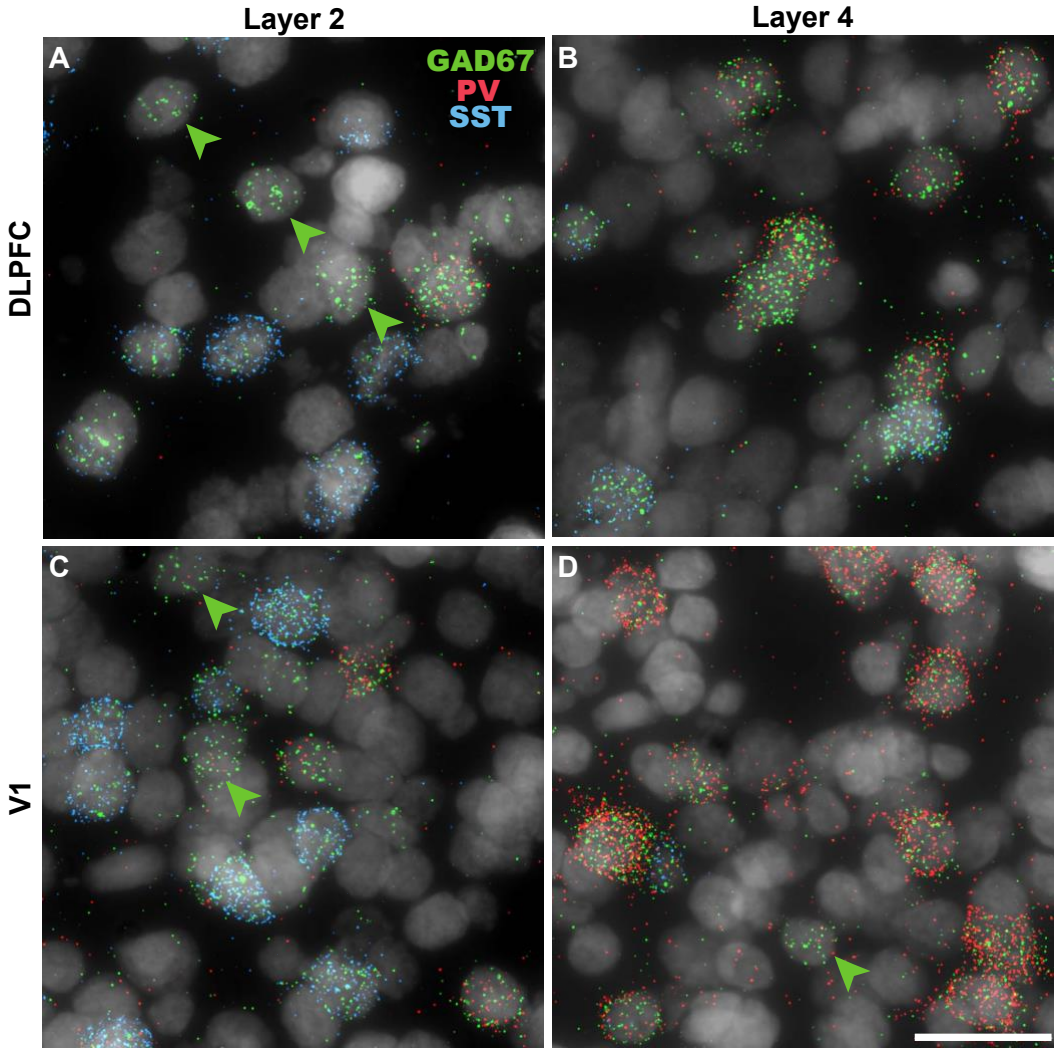

Figure 10. Representative high magnification images using multiplex fluorescent in situ hybridization. Green grains indicate GAD67 mRNA, red grains indicate PV mRNA, and blue grains indicate SST mRNA. Green arrowheads indicate GAD67+ Only neurons, red/green arrowheads indicate PV+ GABA neurons (also expressing GAD67 mRNA), and blue/green arrowheads indicate SST+ GABA neurons (also expressing GAD67 mRNA). In **A**) layer 2 of DLPFC, SST+ and GAD67+ Only neurons predominate, whereas **B**) layer 4 of DLPFC is populated mostly by PV neurons. In **C**) layer 2 of V1, SST neurons predominate and **D**) layer 4 of V1 is heavily populated by PV neurons expressing high levels of PV mRNA. Scale bar (30 µm) in **D**) applies to all panels, and color associated with each transcript shown in **A)** applies to all panels.

Density and Proportion of All Positive Nuclei. The density of all DAPI-labeled nuclei was highest in V1 layer 4 (726.3±37.4 nuclei/mm^2), followed by V1 layer 2 (663.0±45.0 nuclei/mm^2), DLPFC layer 4 (448.6±47.0 nuclei/mm^2), and DLPFC layer 2 (365.2±37.9 nuclei/mm^2). In addition, combining values across layers for each region revealed a greater density of nuclei in V1 (1,389.4±70.3 nuclei/mm^2) than in DLPFC (813.8 ± 83.6 nuclei/mm^2), consistent with prior findings of a greater cell packing density in V1 relative to other cortical areas (Rockel et al., 1980; Hendry et al., 1987; Collins et al., 2016). Similarly, the density of GAD67 mRNA-positive neurons was greater in V1 than in DLPFC (**Table 2**), but the proportion of GAD67 mRNA-positive neurons relative to all DAPI-labeled nuclei was lower in V1 (15.0 ± 3.3%) compared to DLPFC (24.0 ± 4.1%), consistent with prior measures of GABA-immunoreactive neurons in these regions (Hendry et al., 1987).

To account for these differences in cell packing density, we report the relative proportion of all DAPI-labeled nuclei that express 1) both SST and GAD67 mRNAs (SST+ nuclei), 2) both PV and GAD67 mRNAs (PV+ nuclei), and 3) GAD67 but not PV or SST mRNAs (GAD67+ Only nuclei). Relative neuron density measures were consistent across all six animals (**Table 2**).

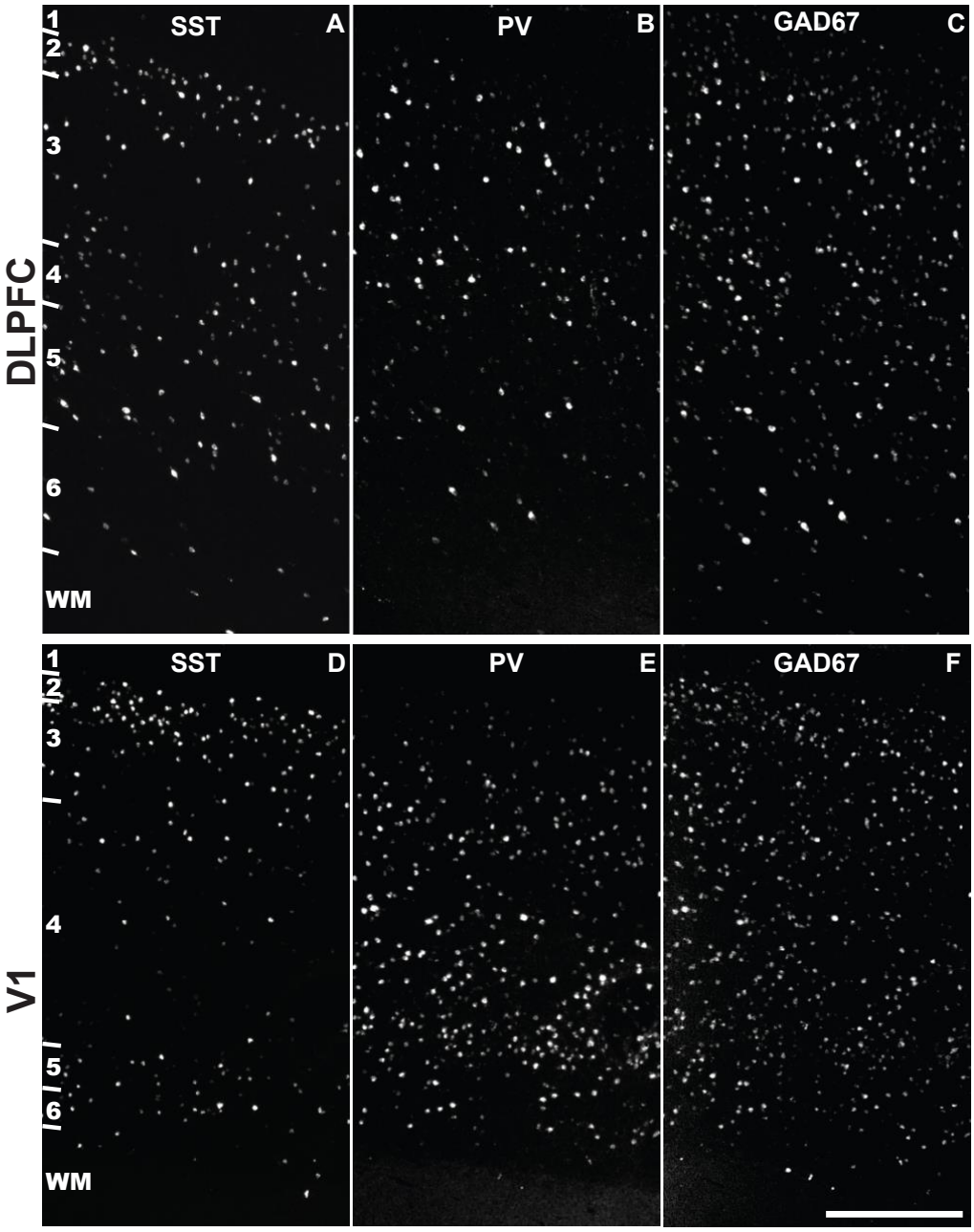

Figure 11. Representative low magnification images of multiplex fluorescently labeled *in situ* sections.
A) SST neurons in the DLPFC are present across cortical layers and in the superficial white matter but are relatively enriched in layers 2 and 5, whereas **B**) PV neurons in the DLPFC are present predominately in layer 4 and deep layer 3. **C**) GAD67 neurons are present in all cortical layers. **D**) SST neurons in V1 are largely confined to a dense band in layer 2. **E**) PV neurons in V1 are abundant and are present in high densities throughout layer 4. **F**) GAD67 neurons, as in the DLPFC, are present across all cortical layers in V1. Numbers indicate cortical layers, WM = white matter. Scale bar (500 μm) in **F**) applies to all panels.

Table 2. Density (positive neurons/mm^2) and relative proportion of total nuclei expressing a given marker listed in parentheses.

Total GABA nuclei (All GAD67+ nuclei)

	DLPFC Layer 2		DLPFC Layer 4		V1 Layer 2		V1 Layer 4	
RH335	80.2	(26.9%)	72.6	(19.8%)	124.4	(21.3%)	97.3	(14.5%)
RH338	91.2	(26.5%)	80.2	(18.5%)	126.1	(18.9%)	83.9	(11.5%)
RH340	116.4	(30.6%)	101.5	(22.6%)	142.1	(19.7%)	79.7	(11.3%)
RH341	106.7	(27.6%)	104.2	(20.9%)	102.0	(14.8%)	98.3	(13.3%)
RH343	109.1	(28.4%)	90.6	(19.9%)	103.3	(15.9%)	92.9	(12.8%)
RH345	103.0	(25.8%)	98.9	(20.3%)	97.3	(14.5%)	92.6	(11.8%)
Mean	**101.1**	**(27.6%)**	**91.3**	**(20.3%)**	**115.9**	**(17.5%)**	**90.8**	**(12.5%)**
Regional Mean		**96.2**	**(24.0%)**			**103.3**	**(15.0%)**	

SST+

	DLPFC Layer 2		DLPFC Layer 4		V1 Layer 2		V1 Layer 4	
RH335	27.9	(9.4%)	24.1	(6.6%)	50.5	(8.6%)	12.4	(1.8%)
RH338	29.5	(8.6%)	20.6	(4.7%)	51.4	(7.7%)	9.8	(1.3%)
RH340	38.5	(10.1%)	31.4	(7.0%)	67.7	(9.4%)	11.2	(1.6%)
RH341	34.1	(8.8%)	29.4	(5.9%)	44.7	(6.5%)	13.5	(1.8%)
RH343	36.2	(9.4%)	24.1	(5.3%)	41.4	(6.4%)	12.1	(1.7%)
RH345	34.2	(8.6%)	25.2	(5.2%)	41.4	(6.2%)	8.5	(1.1%)
Mean	**33.4**	**(9.1%)**	**25.8**	**(5.8%)**	**49.5**	**(7.5%)**	**11.3**	**(1.6%)**
Regional Mean		**29.6**	**(7.5%)**			**30.4**	**(4.5%)**	

PV+

	DLPFC Layer 2		DLPFC Layer 4		V1 Layer 2		V1 Layer 4	
RH335	13.3	(4.5%)	29.5	(8.1%)	22.9	(3.9%)	69.4	(10.3%)
RH338	10.8	(3.1%)	34.1	(7.9%)	21.4	(3.2%)	56.7	(7.8%)
RH340	15.5	(4.1%)	38.8	(8.6%)	27.1	(3.8%)	54.7	(7.8%)
RH341	11.2	(2.9%)	37.6	(7.5%)	21.1	(3.1%)	62.6	(8.4%)
RH343	16.5	(4.3%)	34.1	(7.5%)	23.9	(3.7%)	61.8	(8.5%)
RH345	13.8	(3.5%)	32.6	(6.7%)	18	(2.7%)	59.4	(7.6%)
Mean	**13.5**	**(3.7%)**	**34.4**	**(7.7%)**	**22.4**	**(3.4%)**	**60.8**	**(8.4%)**
Regional Mean		**24.0**	**(5.7%)**			**41.6**	**(5.9%)**	

GAD67+ Only

	DLPFC Layer 2		DLPFC Layer 4		V1 Layer 2		V1 Layer 4	
RH335	38.9	(13.1%)	18.9	(5.2%)	51.1	(8.7%)	15.5	(2.3%)
RH338	50.9	(14.8%)	25.5	(5.9%)	53.3	(8.0%)	17.4	(2.4%)
RH340	62.4	(16.4%)	31.4	(7.0%)	47.3	(6.6%)	13.8	(2.0%)
RH341	61.4	(15.9%)	37.3	(7.5%)	36.2	(5.3%)	22.3	(3.0%)
RH343	56.4	(14.7%)	32.4	(7.1%)	38.0	(5.8%)	18.9	(2.6%)
RH345	55.0	(13.8%)	41.2	(8.4%)	37.9	(5.7%)	24.7	(3.2%)
Mean	**54.2**	**(14.8%)**	**31.1**	**(6.8%)**	**44.0**	**(6.7%)**	**18.8**	**(2.6%)**
Regional Mean		**42.6**	**(10.8%)**			**31.4**	**(4.6%)**	

Measures of SST+ Neurons. The proportion of DAPI-labeled nuclei that were SST+ neurons was higher in DLPFC than V1 and in layer 2 than layer 4, consistent with Pattern 1 observed by qPCR (**Figure 12A**). Additionally, the region-by-layer interaction term was significant, indicating that the laminar difference in the proportion of SST+ DAPI-labeled nuclei was larger in V1 (effect size = 6.2) than DLPFC (effect size = 4.5). Average SST mRNA grain density per positive neuron did not differ between regions, but the density of SST mRNA grains per neuron was higher in layer 2 than layer 4 in both regions (**Figure 12B**). This combination of findings suggests that the higher levels of SST mRNA in DLPFC than V1 observed by qPCR (**Figure 5A**) primarily reflect a regional difference in the proportion of neurons that express SST mRNA, whereas the higher levels of SST mRNA in layer 2 versus layer 4 are driven by both a higher proportion of neurons that express SST mRNA and higher levels of SST mRNA expression per neuron in layer 2.

Measures of PV+ Neurons. The proportion of DAPI-labeled nuclei that were PV+ neurons did not differ between DLPFC and V1 (**Figure 12C**). However, due to the greater density of DAPI-labeled nuclei in V1, PV+ neuron density was greater in V1, consistent with the higher levels of PV mRNA found by qPCR (**Figure 6**). In both regions, the relative proportion of PV+ neurons was greater in layer 4 than layer 2 (**Figure 12C**). The mean density of PV mRNA grains per PV+ neuron was significantly higher in V1 than DLPFC and in layer 4 than layer 2 (**Figure 12D**), consistent with Pattern 2 observed by qPCR. Thus, the regional differences in PV mRNA levels observed by qPCR (**Figure 6**) appear to primarily reflect greater PV expression per neuron in V1 than DLPFC, whereas the laminar differences within each region are driven by both a higher proportion of neurons that express PV mRNA and higher levels of PV mRNA expression per neuron in layer 4.

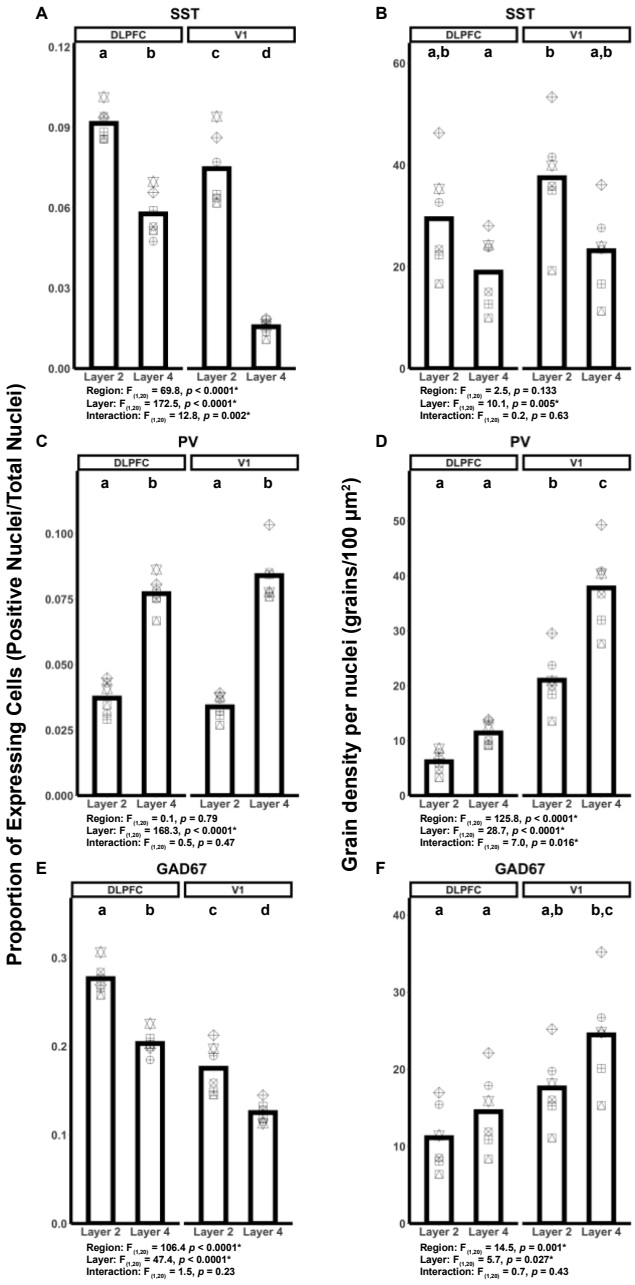

Figure 12. Proportion of nuclei expressing a given transcript and the grain density of each transcript per positive nuclei.

Bars show the mean of six monkeys with individual animal data plotted as unique symbols. Panels **A**), **C**), and **E**) show the proportion of DAPI-labeled nuclei positive for SST, PV, or GAD67 mRNAs, respectively. Panels **B**), **D**), and **E**) show the average grain density per positive nucleus for SST, PV, or GAD67 mRNAs, respectively. Within each graph, bars not sharing the same lower-case letter are significantly different by Tukey's HSD (p<0.05). Note that panels **E**) and **F**) show data for all GAD67+ neurons regardless of subtype.

Measures of GAD67+ Neurons. The proportion of DAPI-labeled nuclei that were GAD67+ (regardless of subtype) was higher in DLPFC and layer 2 relative to V1 and layer 4, respectively (**Figure 12E**), with no region-by-layer interaction detected. In contrast, average GAD67 grain density per neuron showed the opposite pattern: grain density per neuron was higher in V1 and layer 4 relative to DLPFC and layer 2, respectively (**Figure 12F**). Thus, the lack of differences across regions and layers in GAD67 mRNA expression observed by qPCR (**Figure 7B**) appears to reflect these opposite patterns in the regional/laminar proportions of GAD67-expressing cells and of GAD67 mRNA expression per neuron.

GAD67 mRNA Grains per GABA Neuron Subtype. Finally, in order to assess which GABA neuron subtype(s) contributes to differences in GAD67 grain density per neuron, we compared GAD67 grain density per neuron for SST+, PV+, and GAD67+ Only neurons across layers 2 and 4 of DLPFC and V1 (**Figure 13**). For all three classes of GABA neurons, GAD67 grain density per neuron was higher in V1 relative to DLPFC, with only modest differences between layers. Within both regions, mean GAD67 grain density was highest in PV+ neurons, intermediate in SST+ neurons and lowest in GAD67+ Only neurons.

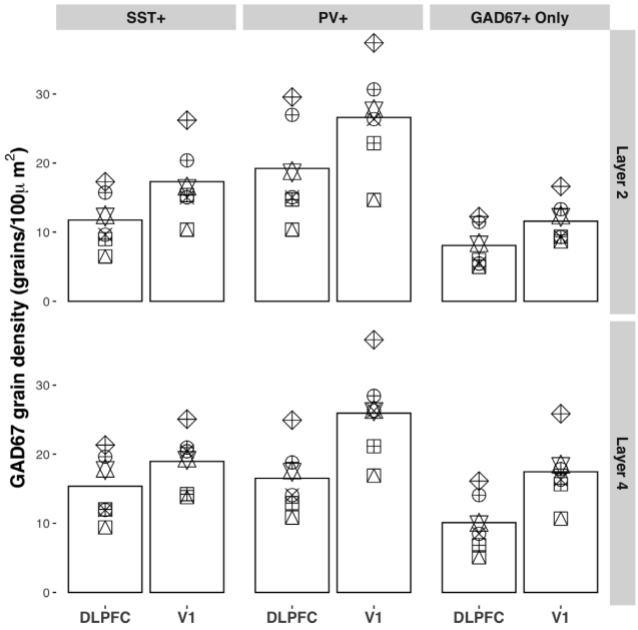

Figure 13. Grain density of GAD67 mRNA among GABA neuron subtypes.
Grain density of GAD67 mRNA among GABA neuron subtypes. Bars show the mean of 6 monkeys with individual animal mean data plotted as unique symbols. Among all 3 GABA neuron subtypes, the expression of GAD67 per neuron was greater in V1 than DLPFC, with modest differences observed between layers. PV neurons tended to show the highest GAD67 expression per neuron, with the effect most noticeable in V1.

2.4 DISCUSSION

Here, we identified three distinct expression patterns of GABA-related transcripts across layers 2 and 4 of macaque monkey DLPFC and V1. At the cellular level, these patterns reflect transcript-specific differences in the relative proportion of GABA neurons that express a given transcript and/or in the cellular level of expression of that transcript. Together, these findings illustrate that understanding the basis for regional differences in levels of GABA-related transcripts (Hashimoto et al., 2008b; Bernard et al., 2012; Hawrylycz et al., 2012; Tsubomoto et al., 2019) requires studies with both laminar- and cell type-specific levels of resolution. Our

findings also provide insights into how laminar, cellular, and molecular differences in GABA neurons might contribute to regional differences in information processing.

All GABA-related transcripts studied exhibited one of three expression patterns across layers 2 and 4 of DLPFC and V1. The majority of transcripts expressed in distinct GABA neuron populations, including SST, CB, CB1R, CCK, VIP, and CR mRNAs, had Pattern 1: higher expression in DLPFC and layer 2 relative to V1 and layer 4, respectively. In contrast, PV mRNA showed the opposite Pattern 2: higher expression in V1 and layer 4 relative to DLPFC and layer 2, respectively. These two patterns were also shared by transcripts that mediate postsynaptic GABA neurotransmission but are not selectively expressed in GABA neurons: GABRA2 mRNA followed Pattern 1, whereas GABRA1 mRNA followed Pattern 2. Interpreting the results of the postsynaptic GABRA subunits further requires knowledge of the relative expression levels of these markers in each GABA neuron subtype. Relative to markers of specific subtypes of GABA neurons, presynaptic markers of GABA neurotransmission showed only modest or no regional and laminar differences (Pattern 3). This pattern may reflect the fact that these transcripts are expressed by all subtypes of GABA neurons; therefore, the signal from any particular cell type is not apparent.

2.4.1 Cellular Basis for Regional and Laminar GABA-related Transcript Patterns

These three distinct patterns appear to be due regional and laminar differences in the relative number of, and/or levels of gene expression in, specific cell types. For example, the regional difference for SST mRNA appeared to reflect primarily a greater proportion of SST-expressing nuclei in DLPFC relative to V1. Although the total density of DAPI-labeled nuclei might include some contamination by non-neuronal (glial) nuclei, this contamination would likely

be similar across cortical regions and layers, and thus would not affect differences in the relative proportions of DAPI-labeled nuclei that are SST+. Because SST neurons are thought to gate excitatory inputs to pyramidal neurons (Horn & Nicoll, 2018), a greater representation of SST neurons may provide additional inhibitory control in cortical areas, such as the DLPFC, that integrate numerous inputs. In primate DLPFC and V1, SST-containing GABA neurons principally inhibit the distal dendrites of pyramidal neurons (de Lima & Morrison, 1989; Melchitzky & Lewis, 2008), including those residing in layer 3 (**Figure 14A**). Layer 3 pyramidal neurons have larger and more complex dendritic arbors and a higher density of dendritic spines in DLPFC than V1. Thus, a greater proportion of neurons that are SST+ in the DLPFC likely contributes to greater inhibitory control over numerous inputs to DLPFC pyramidal neurons. Similarly, levels of VIP and CR mRNAs followed the same pattern as SST mRNA across regions and layers. As VIP/CR neurons are thought to primarily target SST neurons (Wang, 2020), similar regional and laminar patterns of SST and VIP/CR neurons would provide for a conserved capacity to disinhibit pyramidal neurons.

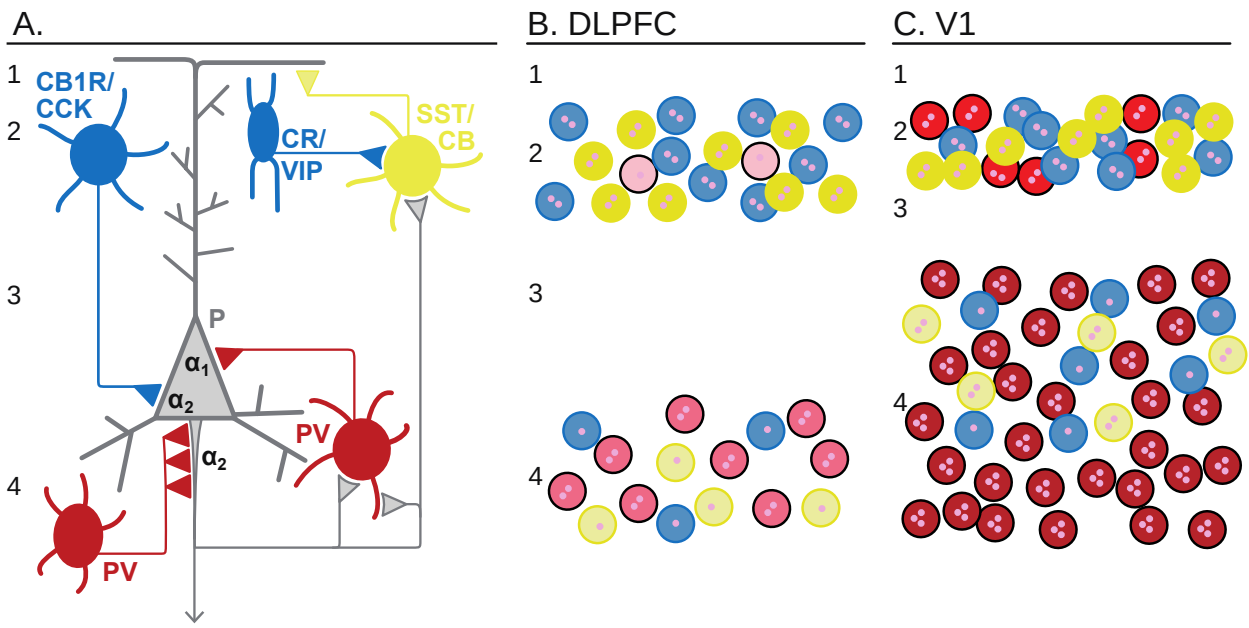

Figure 14. Relative representation of GABA neuron subtypes and levels of gene expression per neuron in layers 2 and 4 of the primate DLPFC and V1.

A) Canonical microcircuit of excitatory layer 3 pyramidal neurons (P) and the main subtypes of GABA neurons that influence their activity. Somatostatin (SST)/calbindin (CB)-containing neurons predominately reside in layer 2 and principally target the distal dendrites of pyramidal neurons. Calretinin (CR)/vasoactive intestinal peptide (VIP) neurons are also located predominately in layer 2 and primarily provide inhibition onto other GABA neurons, disinhibiting pyramidal neurons. Basket cells expressing cholecystokinin (CCK) and cannabinoid 1 receptor (CB1R) target the perisomatic region of pyramidal neurons, at sites enriched in $GABA_A$ receptors containing the α2 subunit. PV neurons are predominately located in layer 4 and target either the perisomatic region (where the postsynaptic surface is enriched in $GABA_A$ receptors containing the α1 subunit) or the axon initial segment (at sites enriched in $GABA_A$ α2 receptor subunits) of pyramidal neurons. Not shown are pyramidal neurons in layers 2 and 4 which are also likely influenced by the activity of GABA neurons in their own layer. For simplicity, PV and CB1R neurons are shown only innervating the cell body, although there are other cell types targeted by these cells. **B)** DLPFC appears to be distinguished by a relatively higher complement in layer 2 of SST neurons (yellow circles), as well as CR/VIP and CB1R/CCK neurons (blue circles). **C)** V1, in contrast, is distinguished by a relatively higher complement in layer 4 of PV neurons (red circles). In **B)** and **C)**, blue and red shading intensity indicates the relative expression levels of SST and PV mRNAs, respectively, and number of pink dots illustrate the relative levels of GAD67 mRNA per neuron.

In contrast to our finding that the relative proportion of SST neurons differs across regions, the laminar difference in SST mRNA levels reflected both a greater proportion of SST-expressing

neurons and higher SST mRNA levels per neuron in layer 2 than layer 4 in both DLPFC and V1. Because SST is a signaling neuropeptide that is both co-released with GABA and can independently inhibit cortical circuits (Viollet et al., 2008; Riedemann & Sutor, 2019; Song et al., 2020), higher levels of SST mRNA in layer 2 suggest these neurons exhibit greater inhibitory control over their targets relative to those in layer 4. In layer 2 of the rodent neocortex, SST neurons principally target and inhibit pyramidal neurons, whereas those in layer 4 appear to principally target PV neurons and thus disinhibit pyramidal neurons (Xu et al., 2013). Although care must be taken in extrapolating findings in the rodent neocortex to the present findings in monkeys, our findings suggest that by virtue of their greater density and greater expression of SST, the inhibitory capacity of layer 2 SST neurons is likely to exceed the disinhibitory capacity of layer 4 SST neurons over layer 3 pyramidal neurons.

In contrast to SST mRNA, higher levels of PV mRNA in V1 primarily reflect higher levels of PV mRNA per neuron without regional differences in the proportion of PV mRNA+ neurons. Fast-spiking PV neurons principally target the perisomatic region of pyramidal neurons (Williams et al., 1992; Freund & Katona, 2007), including those in layer 3 (**Figure 14A**), providing rapid feedback inhibition necessary for synchronizing the activity of large groups of pyramidal neurons (Buzsaki & Wang, 2012). This orchestration of network activity depends on the ability of PV neurons to release GABA in discrete time intervals (Volman et al., 2011). The precise timing of inhibition from PV neurons is achieved, in part, by the rapid depression of PV synapses during high frequency stimulation (Pouille & Scanziani, 2001). However, during repetitive firing, the accumulation of calcium in the intracellular space can lead to both the asynchronous release of GABA from PV neurons (Manseau et al., 2010) and to PV synapses becoming facilitating, rather than depressing (Caillard et al., 2000). This calcium accumulation is buffered by the calcium-

binding capacity of PV (Lee et al., 2000), preserving the synchronous release of GABA and synaptic depression at PV inputs. Thus, the higher levels of PV mRNA (and presumably, the cognate protein) per neuron, in V1 relative to DLPFC might buffer against the rapid accumulation of calcium in the context of the greater excitability, and presumably higher activity, of layer 3 pyramidal neurons in V1 (Amatrudo et al., 2012). The resulting effective coupling of activity in the local pyramidal neuron-PV neuron circuit (**Figure 14A**) likely contributes to the integration of PV neurons into stimulus-specific ensembles of pyramidal neurons in V1 (Runyan et al., 2010; Khan et al., 2018).

In DLPFC and V1, due to both a greater density of PV-expressing neurons and greater PV mRNA expression per neuron, PV mRNA levels were higher in layer 4 than layer 2. The ratios of GAD65/GAD67 (**Figure 7A and 4B**) and GABRA1/GABRA2 (**Figure 8A and 5B**) mRNAs were also higher in layer 4 than layer 2. Although we cannot be certain of the cellular origins of these ratios, their similarities with PV mRNA suggest that GABA neurotransmission from PV neurons is characterized by 1) relatively higher levels of GAD65, enhancing the ability of PV neurons to synthesize GABA under conditions of repetitive firing (Patel et al., 2006a); and 2) fast synaptic inhibition mediated by the faster decay kinetics of $GABA_A$ receptors enriched in $\alpha 1$ versus $\alpha 2$ subunits (Farrant & Nusser, 2005), enhancing rapid perisomatic inhibition and synchronization of pyramidal neurons at high frequencies (Gonzalez-Burgos et al., 2015; Farrant & Nusser, 2005).

2.4.2 Functional Implications of Distinct Complements of GABA Neuron Subtypes in DLPFC and V1

The few systematic studies of inhibitory interneurons across cortical regions generally support the notion that the PV/SST neuron ratio is highest in primary sensory areas (such as V1)

and lowest in association areas (such as DLPFC) in both rodents (Kim et al., 2017) and primates (Torres-Gomez et al., 2020). However, important species differences exist between rodents and primates with regard to the molecular markers that distinguish interneuron subtypes. For example, the primate neocortex apparently lacks SST neurons that co-express CR, whereas approximately 30% of SST neurons in the rodent neocortex co-express CR (Xu et al., 2006). Moreover, CB and CR do not appear to colocalize in primate cortex (Condé et al., 1994) but do in rodent cortex (Park et al., 2002). Such differences may reflect distinct developmental trajectory of these neurons between species (Petanjek et al., 2009; Clowry, 2015). Therefore, our present findings of distinctive patterns of GABA neurons in primate neocortex have important implications for understanding both normal information processing in the primate and human brain and how alterations to GABA neurons in neuropsychiatric diseases may disrupt that information processing.

In the primate neocortex, layer 2 primarily receives corticocortical inputs whereas layer 4 also receives thalamocortical inputs in both DLPFC and V1. Given that the weighting of SST-mediated inhibition is greater in 2, these neurons are positioned to gate the numerous sources of corticocortical inputs to this layer. Consistent with this notion, SST-mediated inhibition is also greatest in an association region (DLPFC) thought to receive and integrate numerous inputs from other cortical regions (Barbas & Rempel-Clower, 1997). In contrast, PV-mediated inhibition appears to be preferentially enriched in layer 4, the site of the majority of thalamocortical inputs in DLPFC and V1 (Giguere & Goldman-Rakic, 1988; Lund, 1988). Although the nature of the relationship between PV-mediated inhibition and thalamocortical inputs requires further investigations, based on findings that thalamocortical inputs target both excitatory pyramidal neurons and inhibitory PV+ neurons (Freund et al., 1989; DeFelipe & Jones, 1991; Melchitzky et al., 1999; Cruikshank et al., 2007), the PV-enrichment in layer 4 and in V1 might be critically

positioned to regulate feedforward inhibition of thalamocortical circuits (Kruglikov & Rudy, 2008).

Across primate neocortical regions, intrinsic differences in timescales exist along a cortical hierarchy, such that primary sensory areas (e.g., V1) exhibit brief, transient responses to input, whereas association areas (e.g., DLPFC) exhibit longer responses to and integrate inputs over time (Murray et al., 2014a; Chaudhuri et al., 2015). These regional differences in timescales likely reflect the constituent components of the microcircuits in each region, such as differences in the intrinsic properties of pyramidal neurons across the cortical hierarchy (Elston, 2002; Amatrudo et al., 2012; Gonzalez-Burgos et al., 2019). The relative greater representation of SST neurons in the DLPFC and of PV neurons in V1 (**Figure 14B, C**) found in the present study and in prior reports (Kim et al., 2017; Torres-Gomez et al., 2020) suggests that regional specificity in the complement of GABA neuron subtypes likely also contributes to the variation in timescales across regions. For example, SST-mediated inhibitory currents are initially weakly depressing and later facilitating (Ma et al., 2012), subsequently leading to a longer time frame of inhibition over dendritic inputs and longer timescales as observed in the DLPFC. In contrast, PV-mediated inhibitory currents are rapidly depressing, leading to a much shorter time frame of inhibition (Pouille & Scanziani, 2001; Cardin, 2018) and a shorter timescales as observed in V1. Thus, regional differences in the complement of either perisomatic (PV)-targeting or dendritic (SST)-targeting GABA neuron subtypes likely contribute to the heterogeneity in timescales across cortical regions, timescales which likely underlie region-specific types of information processing.

The present findings, which demonstrate laminar and cellular bases for regional differences in the intrinsic properties of neural circuits in the primate neocortex, might also provide insight into the nature of cortical interneuron alterations in various psychiatric disorders (Luscher et al.,

2011; Robertson et al., 2016; Dienel & Lewis, 2019). For example, schizophrenia is associated with deficits in total gray matter levels of PV mRNA in both DLPFC and V1 (Tsubomoto et al., 2019). In both regions, this finding appears to be due to lower PV mRNA levels per neuron, rather than fewer neurons, in the illness (Woo et al., 1997; Chung et al., 2016a; Enwright et al., 2016). Because PV mRNA levels per neuron are higher in V1 than DLPFC, schizophrenia-associated deficits in PV mRNA levels might be expected to be greater in V1 than DLPFC. Consistent with this idea, the average deficit in PV mRNA levels in V1 is approximately twice the deficit observed in DLPFC in the same subjects with schizophrenia (Tsubomoto et al., 2019). Although both PV and SST neurons appear to be affected across cortical regions in schizophrenia, the functional impact of these alterations likely differs based on the layer and region in which they occur. Our findings of regional, laminar, and cellular differences in GABA neuron transcripts in the present study can similarly inform the design and interpretation of other studies of GABA neuron subtypes in psychiatric disorders.

3.0 THE NATURE OF PREFRONTAL CORTICAL SOMATOSTATIN TRANSCRIPT ALTERATIONS IN SCHIZOPHRENIA: MARKEDLY LOWER GENE EXPRESSION WITHOUT MISSING NEURONS

Adapted from: Dienel SJ, Fish KN, and Lewis DA. The Nature of Prefrontal Cortical GABA Alterations in Schizophrenia: Markedly Lower Somatostatin and Parvalbumin Gene Expression without Missing Neurons. *submitted.*

3.1 INTRODUCTION

Alterations in markers of cortical gamma-aminobutyric acid (GABA) signaling are among the most widely replicated findings in postmortem brain studies of schizophrenia (Dienel & Lewis, 2019; de Jonge et al., 2017). In the dorsolateral prefrontal cortex (DLPFC), consistent findings of lower levels of gene products related to GABA neuron signaling converge on the notion that inhibitory neurotransmission signaling is weaker in people with schizophrenia (Dienel & Lewis, 2019). Lower tissue levels of GABA-related transcripts could be a consequence of lower levels of these transcripts per neuron, fewer neurons that contain these transcripts, or both. Discriminating among these possibilities has major implications both for understanding the pathogenesis of GABA neuron dysfunction in schizophrenia and for developing novel treatment strategies. For example, the possibility of missing neurons in the DLPFC of schizophrenia, due to either incomplete neural migration or excessive neuronal death (Duchatel et al., 2019b; Akbarian et al., 1996; Kaar et al., 2019), has motivated interest in transplantation of embryonic GABA neurons as

a therapeutic strategy (Inan et al., 2013; Southwell et al., 2014). In contrast, the alternative view that cortical GABA neurons are present but functionally altered in schizophrenia has motivated efforts to develop therapeutics that augment the function of the affected GABA neuron subtypes (Lewis & Sweet, 2009; Xu & Wong, 2018).

All published studies to date, whether using markers of all GABA neurons or of specific subsets of GABA neurons, have not been able to definitively determine whether lower levels of GABA-related transcripts reflect deficits in neuron number or gene expression per neuron. Indeed, the first study of the mRNA encoding the 67-kiloDalton isoform of glutamic acid decarboxylase (GAD67) mRNA, a principal GABA synthesizing enzyme in the cortex, illustrates this challenge. The authors found markedly fewer neurons that were detectable by single label *in situ* hybridization for GAD67 mRNA in the DLPFC of people with schizophrenia (Akbarian et al., 1995), findings that were interpreted as lower expression per neuron given that the density of all Nissl-stained neurons was not altered in the same individuals (Akbarian et al., 1995). However, other investigators reported that the density of small Nissl-stained neurons, presumably GABA neurons, was lower in the DLPFC of people with schizophrenia (Benes et al., 1991).

Studies of the subset of GABA neurons that contain the calcium-binding protein parvalbumin (PV) have produced similar interpretive challenges. Although lower levels of PV mRNA in schizophrenia have been confirmed in multiple studies of DLPFC tissue homogenates (Volk et al., 2016; Hashimoto et al., 2008a; Fung et al., 2010; Tsubomoto et al., 2019; Joshi et al., 2015; Morris et al., 2008), the nature of this deficit remains a matter of debate (Kaar et al., 2019; Dienel & Lewis, 2019). Studies that measured PV mRNA at a cellular level of resolution reported lower levels of PV mRNA per neuron without a deficit in PV mRNA-positive neuron density (Hashimoto et al., 2003; Bitanihirwe & Woo, 2014), whereas some (Reynolds & Beasley, 2001;

Sakai et al., 2008; Beasley & Reynolds, 1997), but not all (Tooney & Chahl, 2004; Woo et al., 1997; Chung et al., 2016a; Enwright et al., 2016), protein-based studies reported a lower density of PV-immunoreactive neurons in schizophrenia. Interpretive uncertainty also exists for studies of somatostatin (SST), a neuropeptide present in a different subpopulation of cortical GABA neurons. SST mRNA levels are markedly lower in DLPFC tissue homogenates from people with schizophrenia (Volk et al., 2016; Fung et al., 2010; Fung et al., 2014; Tsubomoto et al., 2019), and the only single-label *in situ* study reported both fewer SST mRNA-positive neurons and lower SST mRNA levels per positive neuron in schizophrenia (Morris et al., 2008).

One possible explanation for these apparently disparate findings is that the levels of the identifying gene products, SST and PV, are lower in many of these GABA neurons in schizophrenia, with the levels falling below the level of detection for the methods employed in some neurons (Stan & Lewis, 2012). In particular, using SST or PV, the levels of which are markedly lower in schizophrenia, as the sole label to identify the neurons of interest, and then quantifying the relative densities of neurons containing each label, conflates the independent and dependent variables and clouds interpretive clarity. Indeed, all prior studies that used single label methods could not dissociate the presence of PV or SST neurons from the detectability of the identifying transcripts. Thus, counting neurons based on the detectability of a transcript in the presence of lower tissue levels of that transcript means that some neurons could be "missed" even if they are not "missing."

Here, we sought to address the challenge of determining whether lower tissue levels of SST and PV mRNAs in schizophrenia are due to lower levels of these transcripts per neuron, fewer neurons that contain these transcripts, or both. To do so, we developed a new multiplex fluorescent *in situ* hybridization strategy to label four mRNA targets simultaneously with cellular resolution.

This approach, which has not previously been used in postmortem human brain studies, permits the independent determination of transcript levels per neuron and neuron density without conflating the two measures. Specifically, proxy markers (i.e., transcripts that are expressed in SST and PV neurons but whose expression in the DLPFC is not altered in schizophrenia were used to independently identify SST and PV neurons and then levels of SST and PV in those neurons were quantified. We focused our analysis on layers 2 and 4 of the human DLPFC as these layers exhibit the highest density of GABA neurons (Akbarian et al., 1995; Volk et al., 2000; Hornung & De Tribolet, 1994) and are differentially enriched for SST and PV neurons, respectively (Hashimoto et al., 2003; Morris et al., 2008; Dienel et al., 2021). Given that the only stereological analysis of total neuron number found a normal complement of neurons in the frontal lobe of people with schizophrenia (Thune et al., 2001), we predicted that levels of SST and PV mRNAs per neuron are lower without a difference in neuron density in schizophrenia.

3.2 METHODS

3.2.1 Human postmortem brain tissue specimens

Brain specimens (n = 60) were obtained during routine autopsies conducted at the Allegheny County Office of the Medical Examiner (Pittsburgh, PA, USA, n = 57) or the Davidson County Medical Examiner's Office (Nashville, TN, USA, n =3) after consent was obtained from the next-of-kin. An independent team of clinicians made consensus, lifetime DSM-IV diagnoses for each subject using the results of an extensive psychological autopsy, including structured interviews with family members and review of medical records, as well as toxicological and

neuropathological reports (Glausier et al., 2020b). Unaffected comparison individuals had no known history of psychiatric or neurological disorders except for in remission psychiatric diagnoses in one subject specified (see footnotes in **Appendix Table 1**). The listed race and biological sex of the decedents (**Table 3; Appendix Table 1**) reflect the concurrence of information available in the autopsy report and next-of-kin interviews. All procedures were approved by the University of Pittsburgh Committee for Oversight of Research and Clinical Training Involving Decedents and Institutional Review Board for Biomedical Research.

Table 3. Summary Demographic and Tissue Characteristics of Brain Tissue Specimens used in Chapter 3.0.

Measure	Unaffected Comparison	Schizophrenia	Statistics
N	30	30	N/A
Sex	22M/8F	22M/8F	N/A
Race	25W/5B	23W/7B	χ^2=0.42, p=0.52
Age (years)	51.5 ± 14.3	50.1 ± 13.8	$t_{1,58}$=0.40; p=0.70
Body Mass Index	28.6 ± 6.1	28.3 ± 8.2	$t_{1,56}$=0.15; p=0.88
Postmortem interval (hours)	19.0 ± 5.7	19.0 ± 8.6	$t_{1,58}$=0.04; p=0.97
Brain pH	6.7 ± 0.2	6.5 ± 0.3	$t_{1,58}$=2.6; p=0.01
RIN	8.2 ± 0.6	8.0 ± 0.7	$t_{1,58}$=1.2; p=0.22
Tissue storage time (months)	202.9 ± 47.0	206.7 ± 56.1	$t_{1,58}$=0.29; p=0.78

Values shown are mean ± standard deviation

As the goal of the present study was to understand the nature of the SST and PV mRNA deficits in gray matter homogenates, we selected postmortem samples of individuals with schizophrenia from a study of SST and PV transcript levels in DLPFC total gray matter homogenates (Volk et al., 2016) which had lower levels of both SST and PV mRNAs relative to

their matched comparison subjects. In the resulting 30 pair cohort, subjects with schizophrenia had mean deficits of 50.1% in SST mRNA and 36.7% in PV mRNA levels. In the prior and present study, a matched pair design in which each schizophrenia subject was matched to one unaffected comparison subject perfectly for sex and as closely as possible for age (**Appendix Table 1**), was employed to reduce biological variance between groups and to control for experimental variance at every stage of the experiment. Mean age, postmortem interval (PMI), RNA integrity number (RIN) and storage time at –80ºC did not differ between subject groups, nor did race distribution (**Table 3**). Although brain pH significantly differed between groups, the mean difference was 0.2 pH units and of uncertain biological significance.

3.2.2 Fluorescent in situ hybridization tissue labeling

For each subject, fresh-frozen coronal tissue blocks containing right DLPFC area 9 were mounted in a cryostat and sections 20 μm in thickness were cut, thaw-mounted onto SuperFrost slides (ThermoFisher), and stored at -80°C until tissue labeling. mRNA probes were designed by Advanced Cell Diagnostics, Inc (Hayward, CA, USA) to detect mRNAs encoding somatostatin (*SST*), parvalbumin (PV; *PVALB*), SRY-box transcription factor 6 (*SOX6*), and the vesicular GABA transporter (VGAT; *SLC32A1*) (**Appendix Table 3**). VGAT was used as a GABA neuron marker as it is expressed by all GABA neurons but no other cell types, and levels of VGAT mRNA are unaltered or only modestly lower in the DLPFC of people with schizophrenia (Fung et al., 2011; Hoftman et al., 2015). SOX6 (Azim et al., 2009; Batista-Brito et al., 2009), which is selectively expressed in SST and PV neurons due to their shared embryonic origin in the medial ganglionic eminence and which continues to be robustly expressed in the adult primate neocortex

(Ma et al., 2013), was used to distinguish SST and PV neurons from other GABA neurons. See **Appendix C** for details about probe fluorophore assignments and mRNA labeling protocols.

3.2.3 Sampling

Images were collected on a custom widefield Olympus IX83 inverted microscope (Center Valley, PA, USA) equipped with a 6-line (350-, 405-, 488-, 568-, 647-, 750-nm) Spectra III light engine (Lumencor). The present study focused sampling on layers 2 and 4 for imaging as these layers are known to be differentially enriched for SST and PV neurons, respectively (DeFelipe, 1993; Morris et al., 2008; Hashimoto et al., 2003; Dienel et al., 2021). Each imaging site was collected as a 3D image stack (2D images successively captured at intervals separated by 0.25 μm in the z-dimension). Autofluorescence from lipofuscin was imaged in a separate channel, as previously described (Fish et al., 2018; Rocco et al., 2016a). See **Appendix C** for details on imaging parameters.

3.2.4 Image processing

For segmenting fluorescent grains, a Gaussian filter was applied for each channel (except DAPI) by calculating a difference of Gaussians using sigma values of 0.7 and 2 in MATLAB, and an average z-projection algorithm was used to generate a 2D representation of the 3D image stack. Lipofuscin was subtracted from the image (see **Appendix C** for details). DAPI-labeled nuclei were segmented using a deep learning algorithm, and fluorescent grains were counted within a cellular region of interest constituting the segmented nucleus and a 2 μm perimeter around the nucleus using CellProfiler 4.2.0 (Stirling et al., 2021). Cells were classified based on the specific

expression of a given transcript above background levels, and relative expression per cell was quantified as the average grain density per cell (grains/μm^2). See **Appendix C** for details on cell segmentation and classification.

3.2.5 Statistical Analysis

Diagnostic differences in two dependent measures, the relative density of positive cells and grain density per cell, were evaluated for each cell type using linear mixed models (Kuznetsova et al., 2017). These models included main effects of diagnosis, layer, and diagnosis-by-layer interaction. Covariates included age, sex, PMI, pH, and RIN, with human subject included as a random factor. Storage time was not included as a covariate because it has been shown in prior studies to not influence SST or PV mRNA expression (Hoftman et al., 2015; Volk et al., 2016). Within each layer, post-hoc testing was conducted using estimated marginal means derived from the mixed model (Lenth, 2022). We report an overall F-test for the main effects of diagnosis, layer, and an interaction for each measure, and we report posthoc t-tests for within-layer diagnosis effects derived from the main models. Statistical significance was set at $\alpha = 0.05$. Group differences for grain density per neuron were compared using the average grain density per neuron (grains/μm^2) in each layer per subject. Likewise, analyses for neuron density were conducted on values of neurons/mm^2 in each layer per subject. All statistical analyses and figure generation were conducted in R (R Core Team, 2018; Kassambara, 2021 ; Wickham et al., 2017; Morey & Rouder, 2018; Kuznetsova et al., 2017; Lenth, 2022). All values listed in the text are mean ± standard deviation.

Effect sizes were computed for each dependent measure within a layer, with negative values indicating a lower value in the schizophrenia group relative to the unaffected comparison

group. Bayes' Factors were used to evaluate the strength of the evidence in favor of either the alternative or null statistical hypotheses (Keysers et al., 2020). Bayes' factors values are reported relative to the alternate hypothesis notation, designated as BF_{10}. We use Jeffrey's interpretation of BF values (Jeffreys, 1961): BF_{10} values of 3-10 are considered substantial evidence in favor of the alternative hypothesis, 10-100 are considered strong evidence, and >100 are considered decisive evidence; BF_{10} values of 0.10-0.33 are considered substantial evidence in favor of the null hypothesis, 0.01-0.10 are considered strong evidence, and <0.01 are considered decisive evidence. See **Appendix C** for analyses of comorbid factors in schizophrenia subjects.

3.3 RESULTS

3.3.1 Laminar distribution of GABA Neurons in DLPFC of unaffected comparison subjects

Fluorescent *in situ* hybridization revealed robust labeling of all four mRNA targets. Most VGAT/SOX6-dual expressing neurons were either SST or PV mRNA-positive (**Figure 15; Appendix Figure 1**). Conversely, almost all SST and PV neurons expressed both VGAT and SOX6 mRNAs, and, as expected, VGAT neurons without SOX6 expressed neither SST nor PV (**Figure 15A**). For the SZ subject in Pair 2 (**Appendix Table 1**) labeling of all four target mRNAs was poor; data from this pair was removed from the analysis.

In the unaffected comparison subjects, the density of VGAT/SOX6-dual expressing neurons was very similar in both layer 2 (61.9 ± 15.5 neurons/mm^2) and layer 4 (59.9 ± 9.9 neurons/mm^2). The density of VGAT neurons without SOX6 was greater in layer 2 (56.6 ± 13.9 neurons/mm^2) than layer 4 (28.0 ± 6.8 neurons/mm^2), consistent with prior findings that caudal ganglionic eminence-derived interneurons are enriched in the superficial layers of the primate neocortex (DeFelipe, 1993). Among VGAT/SOX6-positive cells, the density of those expressing SST was greater in layer 2 (36.0 ± 11.5 neurons/mm^2) than 4 (22.2 ± 5.7 neurons/mm^2), whereas the density of cells expressing PV was greater in layer 4 (31.7 ± 7.0 neurons/mm^2) than 2 (13.4 ± 6.1 neurons/mm^2), replicating prior studies of the differential laminar distribution of SST and PV neurons (Morris et al., 2008; Hashimoto et al., 2003; Dienel et al., 2021).

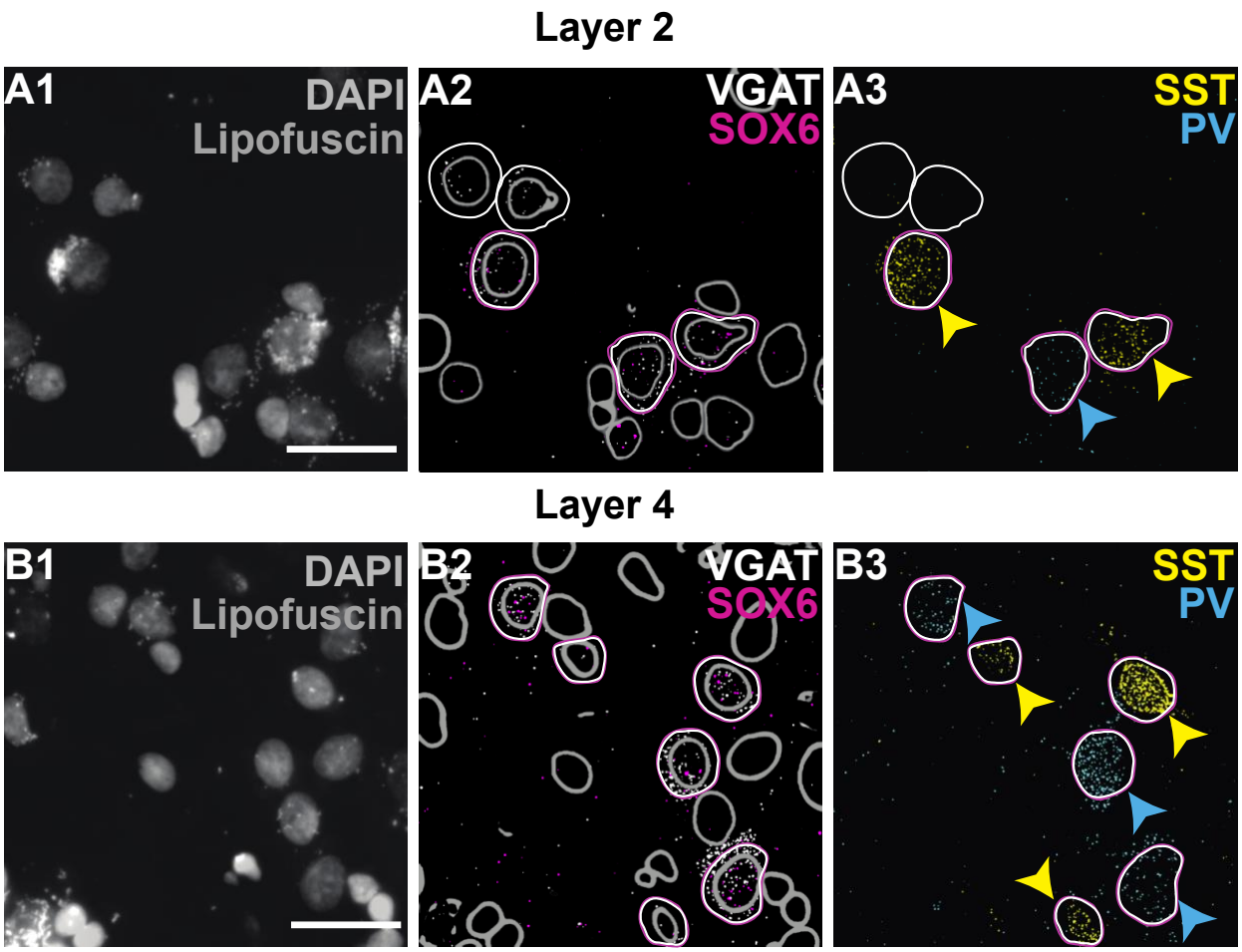

Figure 15. Representative high magnification (60x objective) images of multiplex fluorescent *in situ* hybridization.

Images shown are from a single unaffected comparison individual (HU1792), and both layer 2 (top row) and layer 4 (bottom row) are shown. Each row illustrates represent a single multichannel fluorescent image, and within each row colors represent separate fluorophores. **A1)** and **B1)** DAPI counterstain of neuronal cell nuclei (dark gray). Lipofuscin granules (lighter gray) are evident as clusters over neuronal nuclei and surrounding cytoplasm (not labeled). **A2)** and **B2)** Segmented nuclei are indicated by gray outlines. Nuclei expressing both VGAT and SOX6 mRNAs are highlighted with magenta and white boundaries that demarcate the perinuclear area in which fluorescent mRNA grains were counted. Nuclei with only a white perinuclear boundary are VGAT nuclei that lack SOX6 mRNA. **A3)** and **B3)** VGAT/SOX6-expressing nuclei that contain SST (yellow arrows) or PV (blue arrows) mRNA. Scale bars in A1 and B1 equal 30 μm and apply to all panels in the same row.

3.3.2 Markedly lower levels of SST and PV mRNA per neuron without a deficit in neuron density in schizophrenia

In SST neurons, levels of SST mRNA per neuron were markedly lower in individuals with schizophrenia relative to unaffected individuals ($F_{1,51}$ = 40.7, $p < 0.0001$) in both layers 2 (d = –1.5; t-ratio = 5.3, $p < 0.0001$) and 4 (d = –1.6; t-ratio = 6.7, $p < 0.0001$) (**Figure 16A**). SST mRNA levels per neuron were lower in the schizophrenia subject in 24/29 and 26/29 subject pairs in layers 2 and 4, respectively (**Figure 16B**); in general, in SZ subjects the distribution of SST levels per neuron appeared to be left shifted in both layers (**Appendix Figure 2A**). In contrast, the relative density of SST neurons did not differ between subject groups ($F_{1,51}$ = 0.001, $p = 0.97$) in either layer 2 or 4 (**Figure 16C, 16D**). Bayes' Factor substantially supported the evidence of no group difference in SST neuron density in either layer (both $BF_{10} < 0.27$). In addition, SST levels per neuron averaged across both layers were positively correlated ($r = 0.86$, $p < 0.0001$; **Appendix Figure 3A**) with SST transcript levels measured previously by qPCR in total tissue homogenates in these same subjects (Volk et al., 2016), whereas the density of SST neurons was not ($r = 0.23$, $p = 0.09$; **Appendix Figure 3B**); these comparisons further support the hypothesis that lower tissue levels of SST mRNA in schizophrenia reflect solely lower SST mRNA levels per neuron.

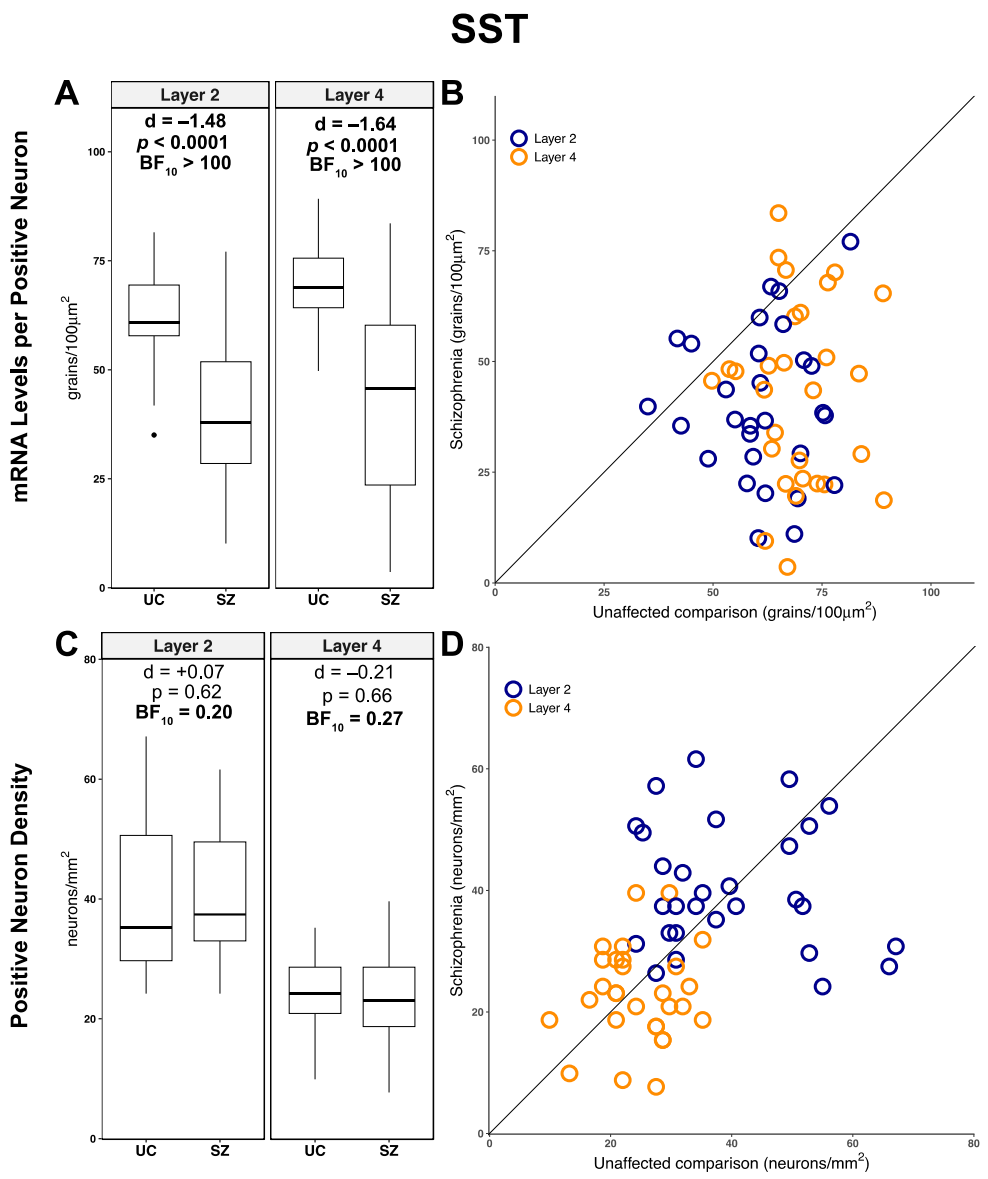

Figure 16. SST mRNA levels per SST neuron and relative density of SST neurons in schizophrenia.
SST neurons were defined as any nucleus that contained SST, VGAT, and SOX6 mRNAs. **A)** Boxplots of the median, quartile, and 95% range of unaffected comparison (UC) and schizophrenia (SZ) for SST mRNA expression per SST neuron. Within the boxplots, values for Cohen's d, the posthoc between group comparison p-value, and the Bayes' Factor (BF) in favor of the alternate hypothesis are shown; bolded effect sizes and p-values indicate large and statistically significant effects. **B)** SST levels per SST neuron shown as unity plots. In these plots, individual points represent a matched subject pair; the x-axis shows the value for the unaffected comparison individual and the y-axis shows the value for the individual with schizophrenia. Points below the unity line indicate a lower value in the individual with schizophrenia relative to their matched unaffected comparison individual. SST mRNA levels per neuron were lower in the SZ individual in 24/29 and 26/29 subject pairs in layers 2 and 4, respectively. **C)** Boxplots of the median, quartile, and 95% range of UC and SZ for the relative density of SST neurons in each layer. The bolded BF value indicates substantial evidence in favor of the null hypothesis. **D)** Unity plot of the individual subject data for the relative density of SST neurons in each layer. In all panels, data are shown for 29 subject pairs.

In PV neurons, levels of PV mRNA were markedly lower in schizophrenia ($F_{1,51}$ = 14.0, p = 0.0005). The diagnosis-by-layer interaction was also significant ($F_{1,56}$ = 18.7, p < 0.0001), reflecting the fact that PV levels were lower in layer 4 (d = –1.1), but not in layer 2 (d = –0.23), in schizophrenia relative to unaffected individuals (**Figure 17A**). In layer 4, cellular levels of PV mRNA were lower in the schizophrenia subject in 24/29 of the pairs (**Figure 17B**) and the distribution of PV levels per neuron appeared to be left-shifted in schizophrenia (**Appendix Figure 2B**). The relative density of PV neurons did not differ between subject groups ($F_{1,51}$ = 0.05, p = 0.83) in either layer 2 or 4 (**Figure 17C, 17D**), and Bayes' Factor substantially supported the evidence of no group difference in both layers (both BF_{10} < 0.27). In addition, PV levels per neuron in layer 4 were highly correlated (r = 0.55, p < 0.0001; **Appendix Figure 3C**) with PV transcript levels measured previously by qPCR in total tissue homogenates in these same subjects (Volk et al., 2016), whereas the density of PV neurons was not (r < 0.01, p > 0.99; **Appendix Figure 3D**); these comparisons further support the hypothesis that lower tissue levels of PV mRNA In schizophrenia reflect solely lower PV mRNA levels per neuron in layer 4.

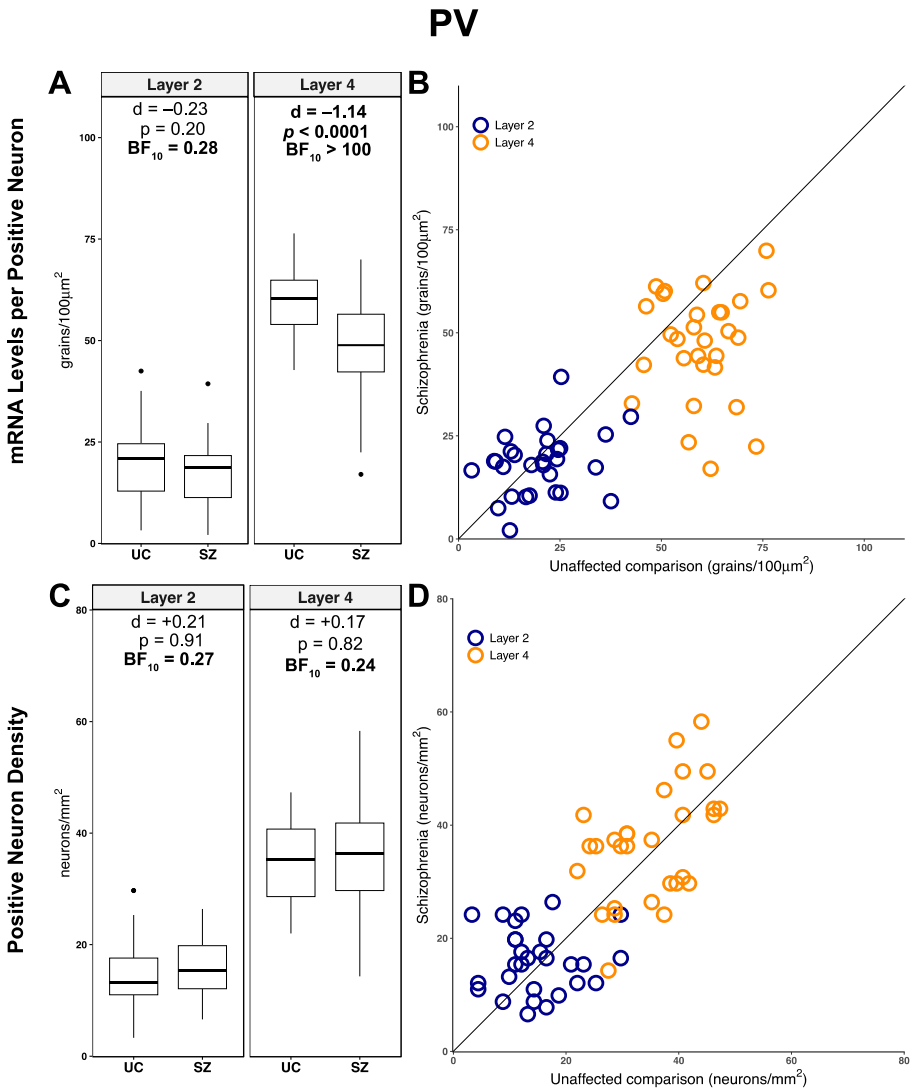

Figure 17. PV mRNA levels per PV neuron and relative density of PV neurons in schizophrenia.
PV neurons were defined as any nucleus that contained PV, VGAT, and SOX6 mRNAs. **A)** Boxplots of the median, quartile, and 95% range of unaffected comparison (UC) and schizophrenia (SZ) for PV mRNA expression per PV neuron. Within the boxplots, values for Cohen's d, the posthoc between group comparison p-value, and the Bayes' Factor (BF) in favor of the alternate hypothesis are shown; bolded values indicate large and statistically significant effects for PV levels per PV neuron in layer 4, while the bolded BF value indicates substantial evidence for the null hypothesis for PV levels per PV neuron in layer 4. **B)** PV levels per PV neuron shown as individual subject data as unity plots. In these plots, individual points represent a subject pair, and the x-axis shows the value for the unaffected comparison individual and y-axis shows the value for the individual with schizophrenia. Colors indicate the layer for which the data are shown. Points below the line indicate a lower value in the individual with schizophrenia relative to their matched unaffected comparison individual. For PV mRNA levels per neuron, PV mRNA levels were lower in the SZ individual in 24/29 subject pairs in layer 4. **C)** Boxplots of the median, quartile, and 95% range of UC and SZ subjects for the relative density of PV neurons in each layer. The bolded BF values in panel C indicate substantial evidence in favor of the null hypothesis. **D)** Unity plot of the individual subject data for the relative density of PV neurons in each layer. In all graphs, data are shown for 29 subject pairs in each layer.

3.3.3 Unaltered density of VGAT/SOX6 neurons in layer 2 or 4 of the DLPFC in schizophrenia

To assess the robustness of the finding that the densities of SST and PV neurons were not altered in schizophrenia, we also quantified the density of VGAT/SOX6 co-expressing neurons in both layers, independent of the presence of SST or PV mRNAs. The density of VGAT/SOX6 neurons did not differ between subject groups ($F_{1,51} = 3.1$, $p = 0.08$) in either layer 2 (t-ratio = –1.8, $p = 0.08$) or 4 (t-ratio = –1.0, $p = 0.32$) (**Figure 18A, B**). In addition, consistent with prior findings (Hoftman et al., 2015; Volk et al., 2012) that VGAT and SOX6 mRNA levels in total DLPFC gray matter are not significantly altered or only modestly altered in schizophrenia, we did not find evidence of lower VGAT ($F_{1,51} = 2.0$, $p = 0.17$) or SOX6 ($F_{1,51} = 2.1$, $p = 0.15$) per VGAT/SOX6 neuron in schizophrenia in either layer (**Appendix Figure 4**).

3.3.4 Influence of comorbid factors on SST and PV levels per neuron in schizophrenia

Levels of SST mRNA per neuron in either layer 2 or 4, or levels of PV mRNA per neuron in layer 4, in schizophrenia subjects did not appear to differ on the basis of death by suicide, a diagnosis of schizoaffective disorder, comorbid substance or alcohol use disorder at time of death, or nicotine, antipsychotic, antidepressant, or benzodiazepine/antiepileptic use at time of death (**Appendix Figures 5 and 6**).

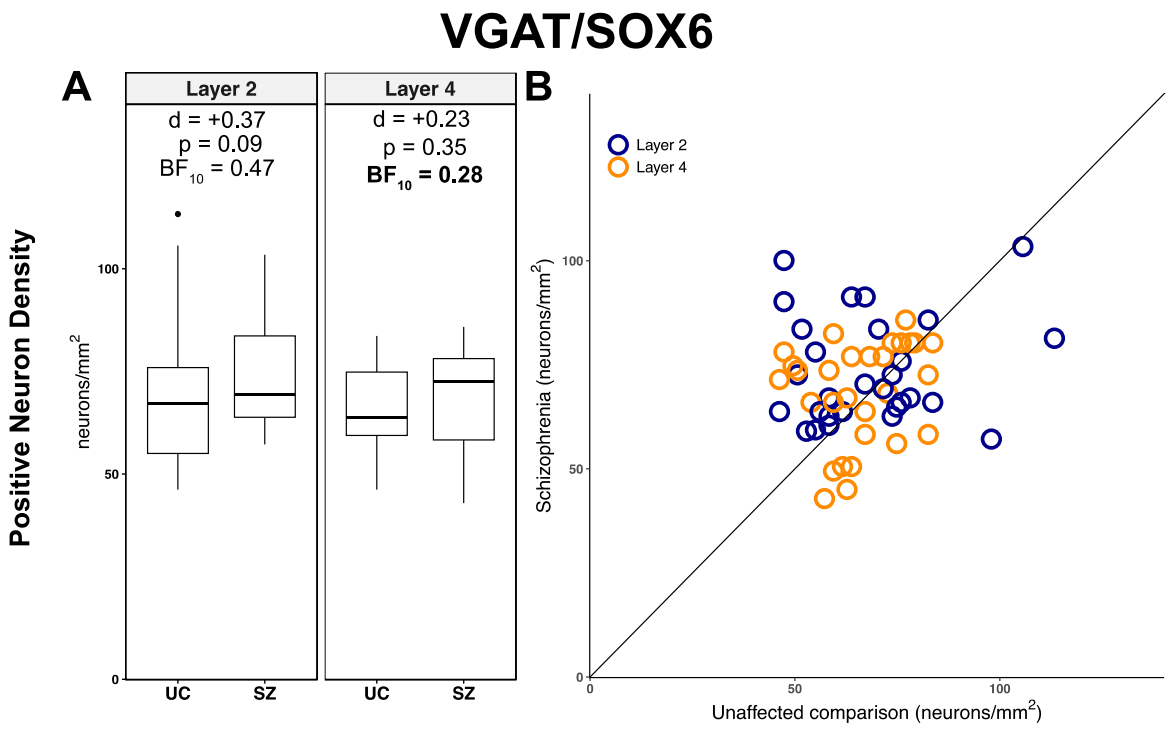

Figure 18. Relative densities of all VGAT/SOX6 neurons independent of the presence of absence of SST or PV mRNAs.

(A) Boxplots of the median, quartile, and 95% range of unaffected comparison (UC) and schizophrenia (SZ) for the relative density of VGAT/SOX6 neurons. Within the boxplots, values for Cohen's d, the posthoc between group comparison p-value, and the Bayes' Factor (BF) in favor of the alternate hypothesis are shown. (B) The relative density of VGAT/SOX6 neurons shown as individual subject data as unity plots. In these plots, individual points represent a subject pair, and the x-axis shows the value for the unaffected comparison individual and y-axis shows the value for the individual with schizophrenia. Points below the line indicate a lower value in the individual with schizophrenia relative to their matched unaffected comparison individual. In all graphs, data are shown for 29 subject pairs in each layer.

3.4 DISCUSSION

Deficits in DLPFC tissue levels of SST and PV mRNA levels have been reported in multiple cohorts of subjects with schizophrenia by several research groups using different quantitative methods (Volk et al., 2016; Fung et al., 2010; Hashimoto et al., 2008a; Morris et al., 2008; Choi et al., 2008; Fromer et al., 2016; Pérez-Santiago et al., 2012). However, the nature of those deficits has been unclear, with some reviews suggesting that schizophrenia is associated with fewer GABA neurons (Reynolds, 2021; Kaar et al., 2019) and others suggesting that GABA neurons are functionally altered but not fewer in number in the illness (de Jonge et al., 2017; Sohal, 2022). Critically, the prior studies on which these interpretations are based lacked the technical capacity to distinguish unequivocally between these alternative views. Here, using a new multi-label technique that overcomes the technical limitations of prior studies, we found strong evidence that schizophrenia is associated with lower SST and PV mRNA levels per neuron in the DLPFC without a difference in the relative density of either GABA neuron subtype. Thus, the basis for lower tissue levels of SST and PV mRNAs in schizophrenia is lower gene expression per neuron and not fewer neurons. As discussed below, these findings have major implications for understanding the pathogenesis of GABA neuron alterations in schizophrenia and for the design of therapeutic interventions targeting these alterations.

3.4.1 Novel multiplex in situ hybridization approaches illuminate the basis for SST and PV expression deficits in schizophrenia

Prior studies of SST and PV mRNA (or PV protein) in postmortem studies of schizophrenia at the cellular resolution have produced mixed findings as to whether the density of these neurons

is lower in the disorder. These mixed findings likely reflect multiple technical limitations of these prior studies. The few studies which have examined SST or PV mRNAs with cellular resolution have reported lower levels of SST and PV mRNA per neuron (Morris et al., 2008; Hashimoto et al., 2003), suggesting that this deficit was due to lower gene expression per neuron. However, the latter study also reported fewer SST mRNA-positive neurons (Morris et al., 2008). Studies of PV neuron density in the DLPFC of subjects with schizophrenia have produced mixed results (Reynolds & Beasley, 2001; Sakai et al., 2008; Beasley & Reynolds, 1997; Chung et al., 2016a; Enwright et al., 2016). Importantly, in all published studies to date of SST or PV neuron density in schizophrenia, lower gene expression per neuron could render some SST or PV neurons undetectable using the single-label methods employed.

The approach used in the current study has several advances over the prior methods, providing a clearer picture of the nature of SST and PV mRNA deficits in schizophrenia. First, relative to earlier radiolabeled *in situ* hybridization assays, fluorescent *in situ* hybridization assays have both markedly higher sensitivity and specificity and lower background grain density (Erben & Buonanno, 2019; Wang et al., 2012). For example, using single label *in situ* hybridization for SST mRNA in schizophrenia, we previously reported a lower density of SST mRNA-positive neurons (Morris et al., 2008); however, the high background labeling of mRNA grains in that study rendered low-expressing neurons difficult to detect. The findings of the present study clarify that neurons with low SST expression are still present in schizophrenia.

In addition to a normal complement of SST neurons in schizophrenia, we also found that the density of PV mRNA-expressing neurons was not altered in the illness. Thus, prior studies reporting lower densities of PV-immunoreactive neurons in schizophrenia (Kaar et al., 2019) may have been confounded by a limited ability to detect those neurons given the techniques employed.

For example, in the same tissue sections from schizophrenia and unaffected comparison individuals, a deficit in PV neuron density which appeared to be present at lower magnification was clearly not present at higher magnification (Enwright et al., 2016). Similarly, prior studies which reported a deficit in PV-immunoreactive neuron density in paraffin-embedded sections (Beasley et al., 2002) were likely confounded by the reduced immunoreactivity associated with that approach (Stan & Lewis, 2012), an interpretation supported by findings of no schizophrenia-associated deficits in PV-immunoreactive neuron density in studies using immunohistochemical methods with more robust antigen detection (Woo et al., 1997; Enwright et al., 2016; Chung et al., 2016a).

Second, even with methodological advances that improve sensitivity for detecting labeled neurons, approaches that rely on visualizing SST or PV alone still conflate the presence of the neuron with the expression level of the index transcript. Here, simultaneously labeling for both SST and PV in concert with their colocalization with independent proxy markers of these neurons (VGAT and SOX6) has rigorously demonstrated that the densities of SST and PV neurons are not altered in schizophrenia. This interpretation is particularly robust given that we used a cohort of subjects with pronounced deficits in SST and PV mRNA levels in DLPFC total gray matter (Volk et al., 2016) in order to maximize the likelihood of detecting a deficit in SST or PV neuron density in schizophrenia if one existed.

Finally, proper interpretation of null results requires more evidence than is available from p-values generated by frequentist statistical tests (Keysers et al., 2020). Bayes' Factors (Kass & Raftery, 1995) provide a quantitative metric for evaluating the strength of the null hypothesis over the alternative. Here, for all findings of neuron density, the statistical null hypothesis was at least 3 times more likely than the alternative, providing substantial evidence for no difference in neuron

density between subject groups. In contrast, the evidence for the findings of lower SST or PV mRNA per neuron can be considered decisive.

Together, the methods employed here provide multiple advances over prior methods to strongly support the conclusion that SST and PV mRNA expression is lower, but that SST and PV neurons are not missing, in the DLPFC of individuals with schizophrenia. We note that the present study only indexes neuron density, not absolute neuron number, which can only be assessed using stereological methods, but the only such study to date found no difference in total neuron number in the frontal lobe of people with schizophrenia (Thune et al., 2001).

3.4.2 Implications for understanding the etiology of GABA neuron dysfunction in schizophrenia

Our finding of a normal complement of SST and PV neurons in DLPFC layers 2 and 4 strongly argues that neither excessive death nor aberrant migration of these GABA neurons is operative in the disease process of schizophrenia. The presence of lower expression levels of both SST and PV mRNAs in schizophrenia is more likely to reflect upstream alterations in in the cortical circuit shared by SST and PV neurons. The expression of both SST (Hou & Yu, 2013; Papadopoulos et al., 1993; Marty, 2000; Marty & Onténiente, 1997; Benevento et al., 1995) and PV (Donato et al., 2013; Carder et al., 1996) transcripts appear to be influenced by neuronal activity, suggesting that deficient excitatory drive to these neurons in schizophrenia could account for lower SST and PV mRNA levels. In monkey DLPFC, ~50% of local axon collaterals from layer 3 pyramidal neurons innervate GABA neurons (Melchitzky et al., 2001), with most of these synapses targeting PV neurons in layer 4 and most likely SST neurons in layer 2 (Melchitzky & Lewis, 2003). In schizophrenia, convergent lines of evidence suggest that layer 3 pyramidal

neurons are hypoactive in the DLPFC (Arion et al., 2015; Kimoto et al., 2015; Glausier et al., 2020a), suggesting that weaker excitatory drive from layer 3 pyramidal neurons might contribute to the activity-dependent downregulation of SST and PV mRNAs.

Alternatively, these alterations in SST and PV neurons might emerge in early development in individuals who are diagnosed with schizophrenia later in life. Early environmental insults, such as maternal immune activation, have been reported to alter the properties both SST (Duchatel et al., 2019a) and PV (Canetta et al., 2016) neurons in rodent models, including lower expression levels of both transcripts. Finally, altered gene expression in SST and PV neurons could reflect independent, cell type-specific, alterations in schizophrenia. For example, altered alternative splicing of ErbB4 in PV neurons could lead to fewer excitatory synapses onto these cells and lower PV expression (Chung et al., 2016a; Chung et al., 2016b); consistent with this idea, ErbB4 splicing shifts are correlated with PV levels in schizophrenia (Chung et al., 2016b). Alterations to N-methyl-D-aspartate receptors (NMDARs) have been posited to principally affect SST neurons (reviewed in (Krystal et al., 2017)) and not PV neurons (Gonzalez-Burgos & Lewis, 2012), suggesting that hypofunction of NMDARs in SST neurons might contribute to lower activation of these cells and subsequent downregulation of activity-dependent SST expression.

3.4.3 Implications for therapeutic strategies targeting cognitive dysfunction in schizophrenia

If deficient inhibitory signaling from DLPFC SST and PV neurons represents part of the neural substrate for cognitive dysfunction in schizophrenia (Smucny et al., 2022), augmenting the excitability of these neurons could enhance inhibitory capacity and restore cognitive functions in the disorder. Our present findings of a normal complement of SST and PV neurons suggests that

these neurons are viable targets for novel pro-cognitive therapeutic interventions (Rudolph & Knoflach, 2011; Ballard et al., 2009; Gill & Grace, 2014; Fee et al., 2021). Some preclinical models provide support for this strategy. For example, a recent study found that positive allosteric modulators acting at mGluR1 receptors preferentially target SST (over PV) neurons and enhances performance on certain working memory tasks in rodents (Maksymetz et al., 2021). Alternatively, if SST and PV neuron alterations are a consequence of diminished excitatory drive from layer 3 pyramidal neurons (Melchitzky & Lewis, 2003), then augmentation of pyramidal neuron function, and in turn more robustly engaging inhibitory neurotransmission from SST and PV neurons, could restore normal circuitry activity in the DLPFC of individuals with schizophrenia.

3.4.4 Conclusions

Our study elucidates the nature of SST and PV neuron mRNA deficits in schizophrenia by finding robust evidence for lower gene expression per neuron of both transcripts without a deficit in neuron density in the DLPFC. These findings have important implications both for understanding the pathogenesis of GABA neuron dysfunction and for informing novel strategies for therapeutic interventions for cognitive dysfunction in schizophrenia. Future studies might illuminate other alterations in SST and PV neurons in schizophrenia that could serve as new therapeutic targets specific to either or both cell populations; the methodological strategies used in the current study offer a road map for the conduct of such cell type-specific investigations.

4.0 ALTERED LEVELS OF GLUTAMIC ACID DECARBOXYLASE 67 IN PREFRONTAL CORTICAL SOMATOSTATIN NEURONS IN SCHIZOPHRENIA

Adapted from: Alterations in GAD67 Transcript Levels in Dendritic-Targeting Somatostatin and Calretinin Neurons in the Prefrontal Cortex of Schizophrenia (*in preparation)* and Diagnostic and Laminar Differences in GAD67 and GAD65 Transcript Levels in the Dorsolateral Prefrontal Cortex (*in preparation*)

4.1 INTRODUCTION

The neural substrate for cognitive dysfunction in schizophrenia, including deficits in working memory performance (Forbes et al., 2009), appears to include altered GABA signaling in the dorsolateral prefrontal cortex (DLPFC) (Smucny et al., 2022). For example, in humans, working memory performance is correlated with DLPFC GABA levels as measured by spectroscopy (Chen et al., 2014; Yoon et al., 2016; Michels et al., 2012), and in monkeys, disruptions of GABA signaling in the DLPFC impairs working memory performance (Sawaguchi et al., 1989; Rao et al., 2000). In postmortem studies of schizophrenia, substantial evidence suggests that signaling from certain GABA neurons the DLPFC is weaker (Smucny et al., 2022). Thus, altered GABA neurotransmission in the DLPFC might contribute to the neural substrate for working memory deficits reported in the disorder.

Levels of the mRNA for the 67 kilodalton isoform of glutamic acid decarboxylase (GAD67; encoded by the *GAD1* gene) have been consistently reported to be lower in the DLPFC

of individuals with schizophrenia relative to unaffected comparison individuals (Volk et al., 2000; Volk et al., 2016; Akbarian et al., 1995; Straub et al., 2007; Torrey et al., 2005; Woo et al., 2008; Hyde et al., 2011). In addition, GAD67 mRNA levels in schizophrenia appear to be lower in both layers 2 - superficial 3 and layers deep 3- 4 (Akbarian et al., 1995; Volk et al., 2000), laminar zones containing the highest densities of GAD67-expressing neurons in the human and non-human primate DLPFC (Akbarian et al., 1995; Volk et al., 2000; Dienel et al., 2021). These two laminar zones are enriched for different subpopulations of GABA neurons, suggesting that different subpopulations of GABA neurons might exhibit lower levels of GAD67 in schizophrenia. For example, the middle layers (layers deep 3 -4) are enriched in parvalbumin (PV)-expressing basket cells relative to other cortical layers in the human and non-human primate DLPFC (Hashimoto et al., 2003; Dienel et al., 2021), and these neurons have been shown to the GAD67 mRNA deficit in schizophrenia (Enwright Iii et al., 2018; Hashimoto et al., 2003). Consistent with these findings, GAD67 protein levels have been reported in the axon terminals of PV basket cells (Fish et al., 2021; Curley et al., 2011). Together, these findings strongly indicate PV basket cells are one source of lower GAD67 levels in schizophrenia.

However, PV basket cells are relatively sparse in layers 2 - superficial 3, suggesting that other GABA neuron subtypes contribute to the GAD67 deficit in these layers in schizophrenia. This laminar zone tends to be enriched for GABA neurons that express either the neuropeptide somatostatin (SST) or the calcium-binding protein, calretinin (CR) (Condé et al., 1994; Dienel et al., 2021; Gabbott & Bacon, 1996; DeFelipe, 1997). Multiple studies have found that SST mRNA, but not CR mRNA, is lower in the DLPFC of individuals with schizophrenia (Hoftman et al., 2015; Hashimoto et al., 2003; Chung et al., 2016b; Hashimoto et al., 2008a), suggesting that SST neurons might also exhibit lower levels of GAD67 in schizophrenia. Moreover, levels of CR and GAD67

mRNAs do not appear to be correlated in schizophrenia (Hashimoto et al., 2003). To date though, no study has directly examined GAD67 levels within SST (or CR) neurons in the DLPFC of schizophrenia.

Consequently, we conducted two studies with different levels of anatomic resolution in postmortem brain tissue from individuals with schizophrenia and matched unaffected comparison individuals. First, laser microdissection was used to capture samples of layers 2 - superficial 3 from the DLPFC of schizophrenia and unaffected comparison individuals. In these samples, we used qPCR to quantify SST and GAD67 mRNA levels, with the prediction that both would be lower in schizophrenia and that these measures would be correlated across subjects. In the second study using a subset of schizophrenia and matched unaffected comparison individuals, we used multiplex FISH to quantify GAD67 levels within SST and CR neurons in the same laminar zone. Because levels of SST mRNA, but not CR mRNA, are lower in schizophrenia, we predicted that GAD67 mRNA deficits would be specific to SST neurons.

4.2 METHODS

4.2.1 Postmortem Brain Tissue Specimens

Brain tissue specimens (n = 84) were obtained during routine autopsies conducted at the Office of the Allegheny County of the Medical Examiner (Pittsburgh, PA, USA, n = 77) or the Davidson County Medical Examiner's Office (Nashville, TN, USA, n = 7) after consent was obtained from the next-of-kin. An independent team of clinicians made consensus, lifetime DSM-IV diagnoses for each subject using the results of an extensive psychological autopsy, including

structured interviews with family members as well as review of medical records and toxicological and neuropathological reports (Glausier et al., 2020b). Unaffected comparison individuals had no known history of psychiatric or neurological disorders except for minor or in remission psychiatric diagnoses in 6 individuals (for details, see footnotes in **Appendix Table 2**). The listed race and biological sex of the decedents (**Table 4; Appendix Table 2**) reflect the concurrence of information available in the autopsy report and next-of-kin interviews. All procedures were approved by the University of Pittsburgh Committee for Oversight of Research and Clinical Training Involving Decedents and Institutional Review Board for Biomedical Research.

4.2.2 Laser microdissection

Cryostat sections (12 μm) were cut from coronal blocks of the right DLPFC that contained Brodmann area 9. Sections were thaw-mounted onto glass polyethylene naphthalate membrane slides that had been UV treated at 254 nm for 30 minutes, dried briefly, and stored at –80°C. On the day of laser microdissection, slides were immersed in an ethanol-acetic acid fixation solution and stained for thionin, as previously described (Dienel et al., 2021).

Table 4. Summary Demographic and Tissue Characteristics of Brain Tissue Specimens used in Chapter 4.0.

	qPCR Cohort			FISH (RNAscope) Cohort		
Characteristic	UC	SZ	*p*-value[1]	UC	SZ	*p*-value[1]
n	43	41		24	24	
Age, years, mean (SD)	47.6 (13.8)	46.4 (12.2)		46.5 (9.7)	47.0 (11.3)	0.9
Sex, n (%)			>0.9			NA
Female	18 (42%)	17 (41%)		12 (50%)	12 (50%)	
Male	25 (58%)	24 (59%)		12 (50%)	12 (50%)	
Race, n (%)			0.1			0.1
Black	5 (12%)	12 (29%)		1 (4.2%)	6 (25%)	
White	38 (88%)	29 (71%)		23 (96%)	18 (75%)	
PMI, hours, mean (SD)	19.3 (5.7)	19.6 (7.3)	0.8	19.0 (6.3)	20.7 (7.3)	0.4
RIN, mean (SD)	8.1 (0.6)	8.0 (0.6)	0.7	8.2 (0.6)	8.1 (0.6)	0.5
brain pH, mean (SD)	6.7 (0.2)	6.5 (0.3)	0.08	6.6 (0.2)	6.6 (0.3)	>0.9
Tissue storage time at –80°C, months, mean (SD)	173.0 (55.3)	181.8 (64.1)	0.5	180.2 (55.6)	194.8 (64.0)	0.4

[1]t-test; Pearson's Chi-squared test

Abbreviations: UC = unaffected comparison, SZ = schizophrenia, PMI = postmortem interval, RIN = RNA integrity number, qPCR = quantitative polymerase chain reaction, FISH = fluorescent *in situ* hybridization

Using a 5x microscope objective, portions of the tissue section that were cut perpendicular to the pial surface were identified. The boundary between layers 1 and 2 was identified and a box that extended 400 μm from this boundary into the most superficial aspect of layer 3 was drawn. For each subject, tissue from two such boxes (total cross-sectional tissue area of ~$5x10^6$ μm^2) was captured by laser microdissection into tubes and the tissue lysed in RLT Plus Buffer (QIAGEN) with β-mercaptoethanol and frozen. RNA was extracted and purified using the RNeasy Plus Micro Kit (QIAGEN). Investigators performing laser microdissection, RNA extraction, and qPCR were blind to subject diagnostic group. These experiments were conducted as part of a larger project incorporating individuals diagnosed with bipolar disorder or major depressive disorder (**Appendix D**), and, as much as possible, subjects were processed together in groups of four (one from each of the four diagnostic groups), with the collection order further balanced across diagnostic groups.

4.2.3 Quantitative PCR Analysis

Total RNA was converted to complementary DNA using the qScript cDNA SuperMix (Quanta Biosciences, Gaithersburg, MD, USA). To reduce technical variance, as much as possible, each plate included samples from individuals in both diagnostic groups on a 384-well quantitative PCR (qPCR) plate in quadruplicate. Forward and reverse primers were designed for each transcript, and all primers showed 90-100% efficiency and each amplified product resulted in a single and specific amplicon. Levels of each transcript were assessed using Power SYBR Green fluorescence and the ViiA™7 Real Time PCR System to determine the cycle threshold (CT). The level of each transcript was normalized to the geometric mean of the 3 housekeeping, or normalizer, genes (beta actin, cyclophilin-A, and GAPDH). The level of each transcript was calculated by subtracting the mean of the three normalizers from the CT values of the gene of

interest (difference in CT, or dCT). Because the dCT represents the log2-transformed expression ratio of each target transcript to the mean of the normalizer genes, the relative expression levels of the target transcripts are reported as the more intuitive expression ratio, or the 2-dCT.

4.2.4 Multiplex fluorescent in situ hybridization

As described in Results (**4.3**), GAD67 and SST mRNA levels in the superficial laminar zone determined by qPCR significantly covaried by brain pH and RIN, and SST levels also significantly covaried by age. To reduce the likelihood that the outcome in the multiplex FISH experiment would be influenced by group differences in pH or RIN, we utilized a subset of the sex- and age-matched schizophrenia and unaffected comparison subject pairs that also had small within-pair differences for pH and RIN. In the resulting 24 pair cohort, the group means, and standard deviations were nearly identical for both pH and RIN (**Table 4**).

For each subject, a fresh-frozen coronal tissue block containing right DLPFC area 9 was mounted in a cryostat, and sections were cut at 20 µm thickness onto SuperFrost slides (ThermoFisher), thaw-mounted, and stored at –80ºC until tissue labeling. mRNA probes were designed by Advanced Cell Diagnostics, Inc (Hayward, CA, USA) to detect mRNAs encoding vesicular GABA transporter (VGAT, *SLC32A1* gene), calretinin (CR, *CALB2* gene), somatostatin (*SST* gene), and GAD67 (*GAD1* gene). VGAT was used as an independent proxy marker for all GABA neurons, and cells were separated into SST or CR subtypes. We used VGAT, rather than GAD67, as an independent proxy for GABA neurons, because VGAT mRNA levels do not appear to be altered in schizophrenia (**3.0**; (Hoftman et al., 2015; Hoftman et al., 2018; Fung et al., 2011)).

Commercially available fluorescent *in situ* hybridization assays from ACDbio are available in two kits using different strategies to label mRNA. V2 kits conjugate a horseradish-peroxidase

(HRP) enzyme to the mRNA targets of interest, which enzymatically deposits fluorophore at the target site *in situ* (Schmidt et al., 1997). This approach results in an abundance of signal at the location of the bound mRNA probe, increasing the likelihood of successfully detecting low-expressing mRNA targets. In contrast, V1 kits directly conjugate the fluorophore to the mRNA target via oligonucleotide binding. This strategy optimizes the ability to distinguish fluorescent grains by preventing the oversaturation of signal. In the present study, we developed a novel integration of these two strategies to label VGAT mRNA with a V2 kit and to label SST, CR, and GAD67 mRNAs using a V1 kit, therefore simultaneously optimizing our ability to detect all GABA neurons (via VGAT) and quantify levels of the relevant transcripts within every VGAT-positive cell.

After removal from –80ºC, slides with mounted sections were immediately immersed in ice-cold 4% paraformaldehyde for 15 minutes, dehydrated through a series of ethanol washes (50%, 70%, 100%, and repeated 100% ethanol for 5 minutes each), followed by pretreatment with protease IV (ACDbio) for 30 minutes at room temperature and H_2O_2 for 10 minutes at room temperature. Slides were then incubated with the VGAT probe, diluted 1:50 in blank probe diluent and incubated for 2 hours at 40ºC. After amplification steps, slides were incubated in horseradish peroxidase enzymes specific to the VGAT channel (HRP-C4) for 15 minutes at 40ºC. Following the addition of HRP molecules, slides were incubated with tyramide signal amplification reagents conjugated to digoxigenin (TSA-DIG; Akoya Biosciences, diluted 1:1000 in 1x Plus Amplification Diluent) for 15 minutes at 40ºC. After blocking the enzymatic activity of the HRP molecules, the V1 protocol was initiated by incubation of probes targeting *GAD1*, *CALB2*, and *SST* mRNAs for 2 hours at 40ºC. After subsequent amplification steps using V1 kits, fluorophores were assigned to each target mRNA as follows: Alexa 488 (CR), Atto 550 (GAD67), Atto 650 (SST). After the

final amplification step was completed, Opal 780, an anti-DIG antibody conjugated to a near-infrared fluorophore, was diluted in PBS (1:200) and applied to sections for 15 minutes at 40ºC. Slides were counterstained for DAPI, which was applied to each section for 30 seconds and subsequently rinsed in PBS. Tissue sections from a given pair were always processed together and the order for each step of the labeling process was randomized by diagnosis. The project was processed in four batches, with six subject pairs within each batch.

4.2.5 Microscopy

Slide scans were collected on Olympus VS200 SlideView slide scanner (Center Valley, PA, USA) equipped with a 9-channel X-CITE NOVEM light engine and a Hamamatsu ORCA-flash 4.0 camera. All equipment was controlled using the VS200 software suite. Using the slide scanning microscope, the entirety of the section was captured using a 20x objective. Areas where the tissue section was cut perpendicular to the pial surface were identified for subsequent high-magnification imaging. For each section, three boxes (1.0 mm wide) containing layers 2-superficial 3 were outlined as described above for laser microdissection, using the DAPI counterstain to identify the boundary between layers 1 and 2.

Using a high resolution 60x 1.42 N.A oil immersion objective (Olympus), each box was captured as a 3D image stack (successive 2D images spaced 0.6 µm apart in the z-dimension, equivalent to the depth of field for this objective). Six fluorescent channels, including DAPI, CR, SST, GAD67, VGAT, and lipofuscin autofluorescence, were captured at set exposure times that were optimized to prevent saturation of fluorescent signal intensity and were held constant throughout the project.

4.2.6 Image processing

Offline, images were imported into CellSens software and deconvolved using the constrained iterative deconvolution algorithm (3 iterations). After deconvolution, a representative average z-projection image was created for subsequent analysis. Using QuPath (Bankhead et al., 2017), the DAPI-counterstained nuclei were automatically segmented using the StarDist (Schmidt et al., 2018) algorithm. The cellular region-of-interest (ROI) was defined as a 2 µm perimeter surrounding each DAPI nucleus unless overlapping with another nucleus. Nuclei with a cross sectional area smaller than 30 µm, which likely represent either small glial nuclei or the edges of nuclei whose centers are located in a separate plane, were excluded from the analysis *a priori*. Fluorescent grains were counted within a cellular ROI that excluded signal that overlapped with lipofuscin (**Figure 19**). Fluorescent grains were segmented based on intensity of an individual grain and subsequently size gated using the subcellular detection function within QuPath. Clusters of signal were included, and the number of grains within a given cluster was estimated by the size of the clustered object and the approximate size of a given grain. The appropriate fluorescence threshold for grain inclusion was determined empirically for each channel and independently for each of the four batches. The same parameters were used to quantify the background grain density, defined as grains per μm^2 that was not attributable to a cellular ROI or lipofuscin signal. As before (**3.0**), we set a relatively high threshold of 7x the background density for a cell to be considered to specifically express VGAT mRNA. Among VGAT-expressing cells, we set a slightly lower threshold of 4x the background grain density for specifically expressing either SST or CR, as the likelihood of false-positives is smaller given the requirement for the localization of both VGAT and SST or CR mRNA transcripts. Thus, we quantified GAD67 levels within three populations of VGAT-expressing cells: VGAT/SST (SST cells), VGAT/CR (CR cells) and VGAT cells without

SST or CR (VGAT-Only cells). Final estimates of transcript levels, indexed by fluorescent grain density per neuron (grains/μm^2), reflect the number of grains within a cellular ROI after subtracting the background grain density.

4.2.7 Statistical Analysis

Analysis of transcript levels from the qPCR study was performed using linear models, including the log-transformed transcript level (to stabilize the variance) as the dependent variable, diagnosis as a fixed effect, and age, sex, PMI, brain pH, and RIN as covariates. Tissue storage time at –80ºC did not differ across diagnostic groups and has been previously demonstrated to not influence mRNA levels of many of the transcripts studied here; therefore, storage time was not included as a covariate (Morris et al., 2008; Hoftman et al., 2015). *F* tests were computed from linear models to assess the overall diagnosis effect. The same models were employed for the study using fluorescent *in situ* hybridization with the inclusion of batch as a covariate. Figure generation and analyses were conducted in R (R Core Team, 2018) using the 'lme4' (Bates et al., 2015), 'lmerTest' (Kuznetsova et al., 2017), 'tidyverse' (Wickham et al., 2017), and 'rstatix' (Kassambara, 2021) packages.

To provide an estimate of the deficits in SST and GAD67 mRNAs in the schizophrenia relative to the unaffected comparison group while controlling for significant covariates (i.e., age, RIN, and brain pH), we computed a 'w-score' that indexes the deviation of SST levels in schizophrenia compared to what would be predicted from a linear model of the unaffected comparison individuals. To achieve this, we computed 'w-scores', estimates of the deviation of a value for a given individual with schizophrenia based on predicted values of a linear model generated from the unaffected comparison population's age, brain pH, and RIN.

In certain comparisons, especially in instances where we sought to quantify the strength of the evidence in favor of the statistical null hypothesis, Bayes' factors (Keysers et al., 2020) were computed using the BayesFactor package in R (Morey & Rouder, 2018). A Bayes' Factor is a ratio of the likelihood of one particular hypothesis relative to the likelihood of the other hypothesis and provides a quantitative measure of evidence in favor of the alternative or null hypothesis. In the model used to compute the BF value, the true standardized difference is assumed to be 0 under the null hypothesis and to follow the Cauchy distribution under the alternative. The prior is described by a Cauchy distribution with a width parameter of 0.707, corresponding to a probability of 80% that the effect size lies between -2 and 2. Here, we use the standard designation of BF_{10} to denote evidence in favor of the alternative hypothesis, or H_1. We use Jeffrey's interpretation of BF values (Jeffreys, 1961): BF_{10} values of 3-10 are considered substantial evidence in favor of the alternative hypothesis, 10-100 are considered strong evidence, and >100 are considered decisive evidence; BF_{10} values of 0.10-0.33 are considered substantial evidence in favor of the null hypothesis, 0.01-0.10 are considered strong evidence, and <0.01 are considered decisive evidence.

To provide an estimate of the disease effect (Kraemer, 2019), Cohen's d effect sizes were calculated in R (Torchiano, 2020; Cohen, 1988) for each subject group in a given comparison. Based on (Coe, 2002), we designated any effect size > 0.60 as 'large' and note these values specifically in the text.

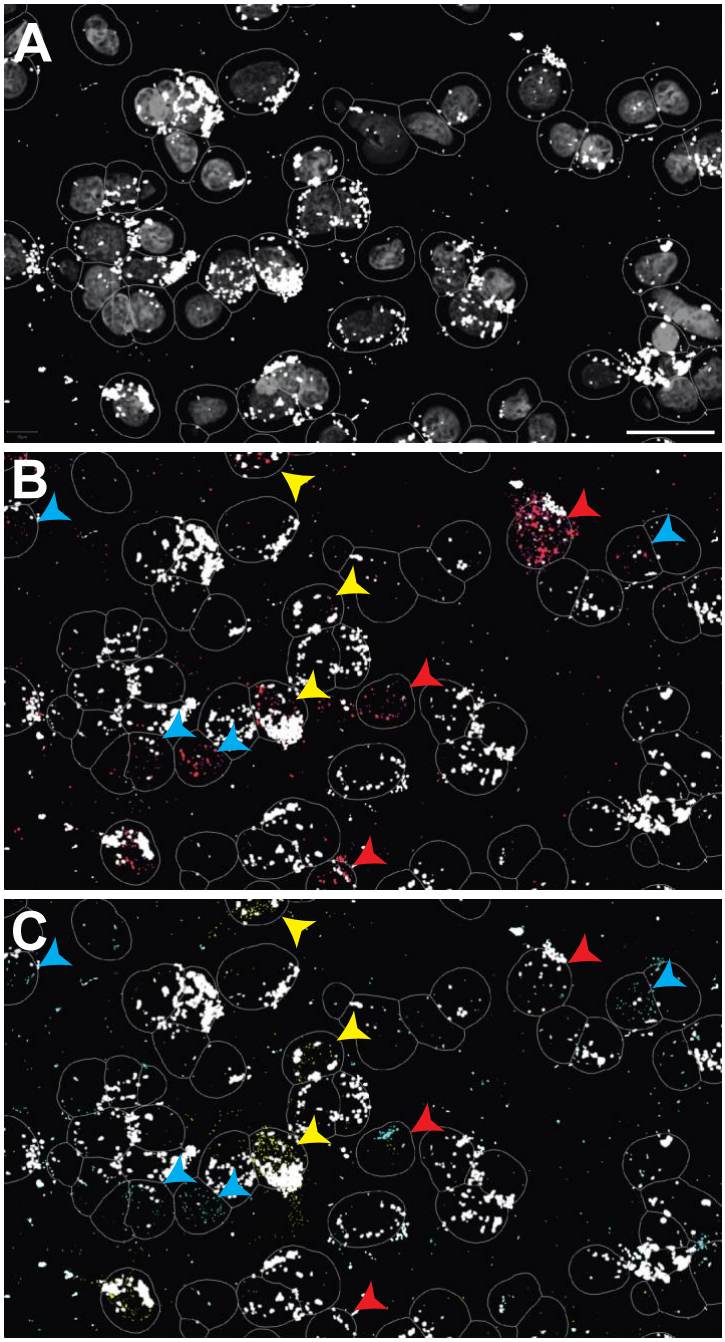

Figure 19. Representative stitched high magnification (60x objective) of multiplex FISH.
(above) Together, **A-C** represent a single multiplex fluorescent images, with only two channels shown per panel.**A)** DAPI-counterstained image showing nuclei (gray) and the cellular ROI demarcated automatically. Lipofuscin signal is shown in white, and the lipofuscin granules are traced by the cellar ROI and excluded. B) VGAT (red) and GAD1 (magenta) signal showing high colocalization in the same cells. **C)** SST (yellow) and CR (blue) Arrowheads indicate the cellular identity: SST (yellow), CR (blue), or VGAT-Only (red). Scale bar in **A** = 20 µm.

The potential influence of certain comorbid variables, such as concurrent alcohol or substance use disorder, death by suicide, or prescription drug use at time of death (grouped into three categories: benzodiazepines or antiepileptic drugs (AEDs), antidepressants, and antipsychotics) on each transcript of interest was assessed by conducting *F* tests using the level of a given transcript as the dependent measure, presence of a given comorbid feature as the independent measure, and age, sex, PMI, pH, and RIN as covariates within the schizophrenia group. The Benjamini-Hochberg procedure was used to correct for a false discovery rate of 5% for multiple comparisons across comorbid factors.

4.3 RESULTS

4.3.1 SST and GAD67 mRNA levels in the layer 2-superficial 3 in schizophrenia

In individuals with schizophrenia, there were pronounced deficits in SST mRNA in laminar isolates of layer 2-superficial 3 of the DLPFC ($F_{1,77}$ = 9.1, $p < 0.0001$, Cohen's $d = 0.67$; **Figure 20A**). Significant covariates included age ($F_{1,77} = 4.6$, $p = 0.035$), brain pH ($F_{1,77} = 7.1$, $p = 0.009$), and RIN ($F_{1,77} = 6.2$, $p = 0.01$). Likewise, levels of GAD67 mRNA were also markedly lower in this same laminar zone ($F_{1,77}$ = 9.1, $p = 0.003$, Cohen's $d = 0.72$; **Figure 20B**), and significant covariates included brain pH ($F_{1,77} = 10.4$, $p = 0.001$) and RIN ($F_{1,77} = 5.9$, $p = 0.01$). Levels of SST and GAD67 mRNAs were highly correlated in both the unaffected and schizophrenia groups, although the strength of the correlation was stronger in the schizophrenia group (**Figure 20C**). These findings indicate that deficits in SST and GAD67 mRNAs are evident in layer 2-superficial 3 in a large cohort of individuals with schizophrenia.

To assess the within-individual deficits in SST and GAD67 in schizophrenia, we computed 'w-scores', estimates of the deviation of a value for a given individual with schizophrenia based on predicted values of a linear model generated from the unaffected comparison population's age, brain pH, and RIN. Using this approach, 31/41 and 30/41 of individuals with schizophrenia exhibited a negative w-score for SST and GAD67 mRNAs, respectively, indicating that more than 70% of persons with schizophrenia have lower levels of SST and GAD67 mRNAs than those predicted from the unaffected comparison population. Across individuals with schizophrenia, w-scores for SST and GAD67 mRNAs were highly correlated ($r = 0.65$, $p < 0.001$; **Figure 20D**).

4.3.2 GAD67 mRNA levels in SST and CR neurons in schizophrenia

While these findings strongly suggest that SST neurons might exhibit lower levels of GAD67, studies at the level of laminar homogenates did not permit assessments of the cell type-specificity of findings. Therefore, we conducted a second study using a subset of subject pairs matched to sex and as closely as possible for age, pH and RIN. This strategy resulted in a 24 pair cohort that did not differ in average age (UC: 46.5 ± 9.7 years, SZ: 47.0 ± 11.3 years; $p = 0.9$), pH (UC: 6.6 ± 0.2, SZ: 6.6 ± 0.3, $p > 0.9$), or RIN (UC: 8.2 ± 0.5, SZ: 8.1 ± 0.6, $p > 0.5$). This subset of individuals had a disease effect size similar to, albeit slightly larger, for both SST (Cohen's $d = 0.88$; **Figure 21A**) and GAD67 (Cohen's $d = 0.89$; **Figure 21B**) that the full cohort used for the qPCR study.

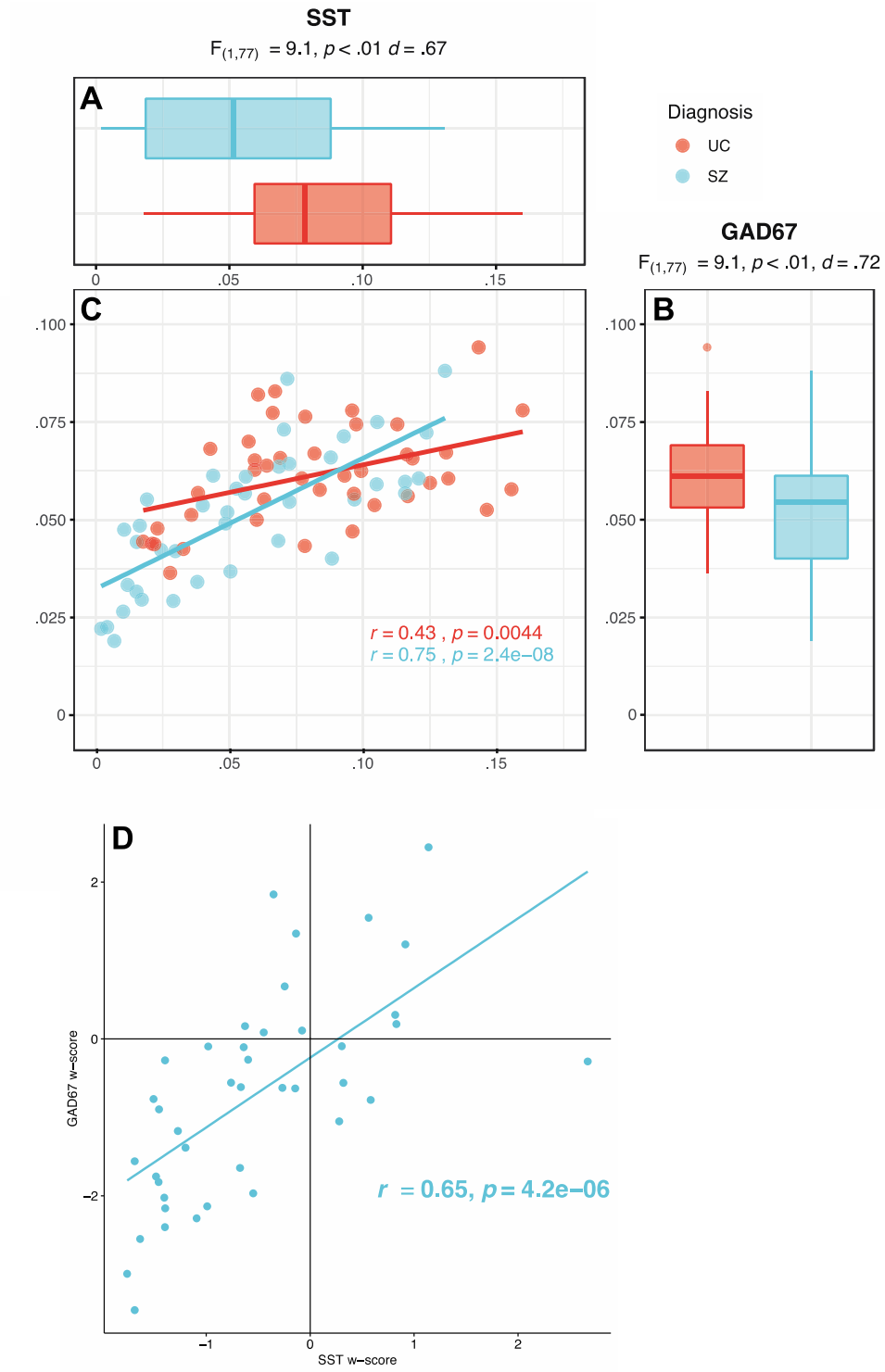

Figure 20. Deficits in SST and GAD67 mRNA in layer 2-3 of the DLPFC in schizophrenia.
Boxplot showing the median, quartiles, and 95% range for the schizophrenia (SZ) and unaffected comparison (UC) groups for **A)** SST and **B)** GAD67 mRNA levels. **C)** Correlation for each diagnostic group, with Pearson's r displayed. **D)** Correlation of w-scores between SST (x-axis) and GA67 (y-axis) among the individuals with SZ.

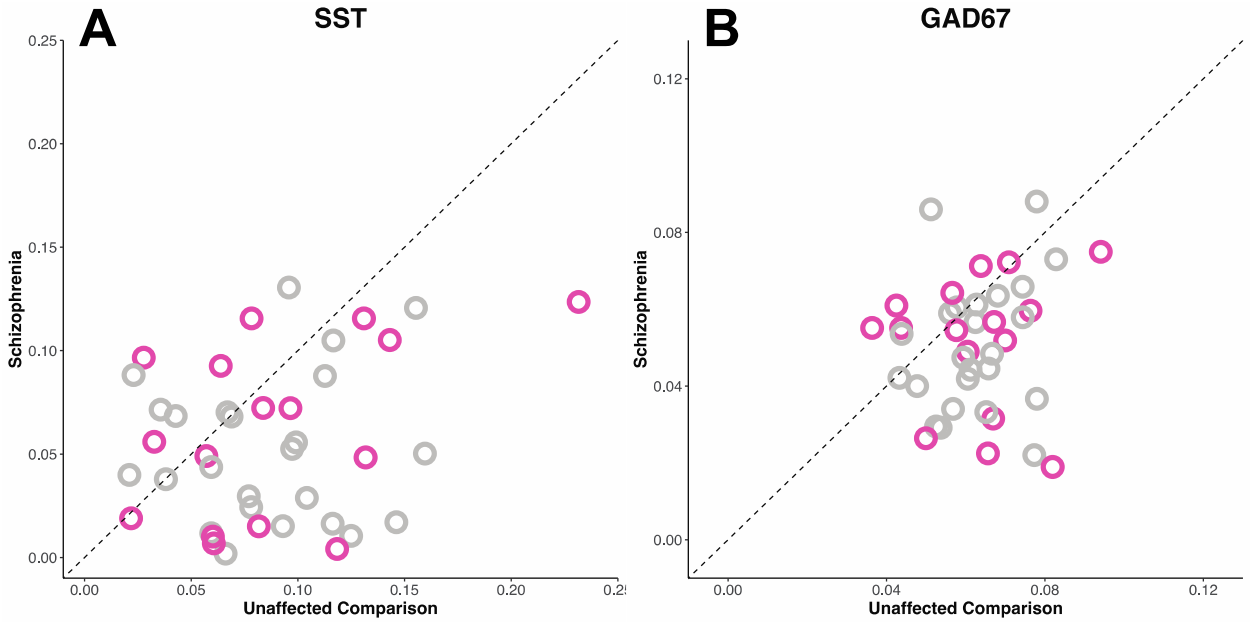

Figure 21. Unity plots of pairing scheme for schizophrenia.
A) Unity plots for SST. Each point represents a schizophrenia and unaffected comparison individual pairing based on age and sex. Pink highlighted points are the subject pairs used in the subsuquent FISH study. **B)** Same as **A)** for GAD67 mRNA in the same pairs.

To directly assess levels of GAD67 in SST neurons, multiplex fluorescent *in situ* hybridization was conducted for VGAT (a marker of all GABA neurons), SST, and GAD67 mRNAs. Because GABA neurons containing CR mRNA are also prominent in layers 2-superficial 3, we also measured GAD67 mRNA within CR neurons in the same tissue sections. In the unaffected comparison population, this approach yielded approximately equal proportions of VGAT+ cells that expressed SST, CR, or neither transcript. Consistent with prior studies in rat (Kubota, 1994) and primate neocortex (González-Albo et al., 2001; Krienen et al., 2020) (but not mouse cortex (Xu et al., 2006; Tremblay et al., 2016)), we found that less than 2% of VGAT+ cells contained by SST and CR mRNAs; these cells were excluded from subsequent analyses. Additionally, one pair (Pair 13) failed to show evidence of VGAT labeling, and both subjects in this pair were excluded from the analysis.

In SST neurons, GAD67 mRNA levels were markedly lower in schizophrenia ($F_{1,36}$ = 6.6, p = 0.01; Cohen's d = 0.77; **Figure 22**). Significant covariates for GAD67 levels in SST neurons included batch ($F_{3,36}$ = 25.5, p < 0.001) and age ($F_{1,36}$ = 5.3, p = 0.027). Similarly, CR neurons also exhibited lower levels of GAD67 mRNA, albeit with a smaller disease effect size relative to the deficit in SST neurons ($F_{1,36}$ = 4.2, p = 0.048; Cohen's d = 0.51 **Figure 22**). Significant covariates included batch ($F_{3,36}$ = 11.5, p < 0.001) and age ($F_{1,36}$ = 13.7, p < 0.001). Finally, VGAT-expressing cells without SST or CR, also exhibited lower levels of GAD67 mRNA with a diagnosis effect size comparable to that seen in CR neurons but did not achieve statistical significance ($F_{1,36}$ = 3.1, p = 0.087; Cohen's d = 0.56; **Figure 22**). Significant covariates included batch ($F_{3,36}$ = 12.4, p < 0.001) and age ($F_{1,36}$ = 10.5, p < 0.001). Interestingly, the Bayes' Factor suggests substantial evidence for a difference in GAD67 levels in schizophrenia within SST neurons (BF_{10} = 4.2), while the evidence for GAD67 deficits in CR and VGAT-Only neurons was anecdotal (BF_{10} = 1.2 and BF_{10} = 1.0, respectively). Taken together, schizophrenia appears to be associated with lower GAD67 levels in multiple GABA neuron subpopulations in layer 2-superficial 3, although the disease effect on GAD67 appears to be most robust within SST neurons.

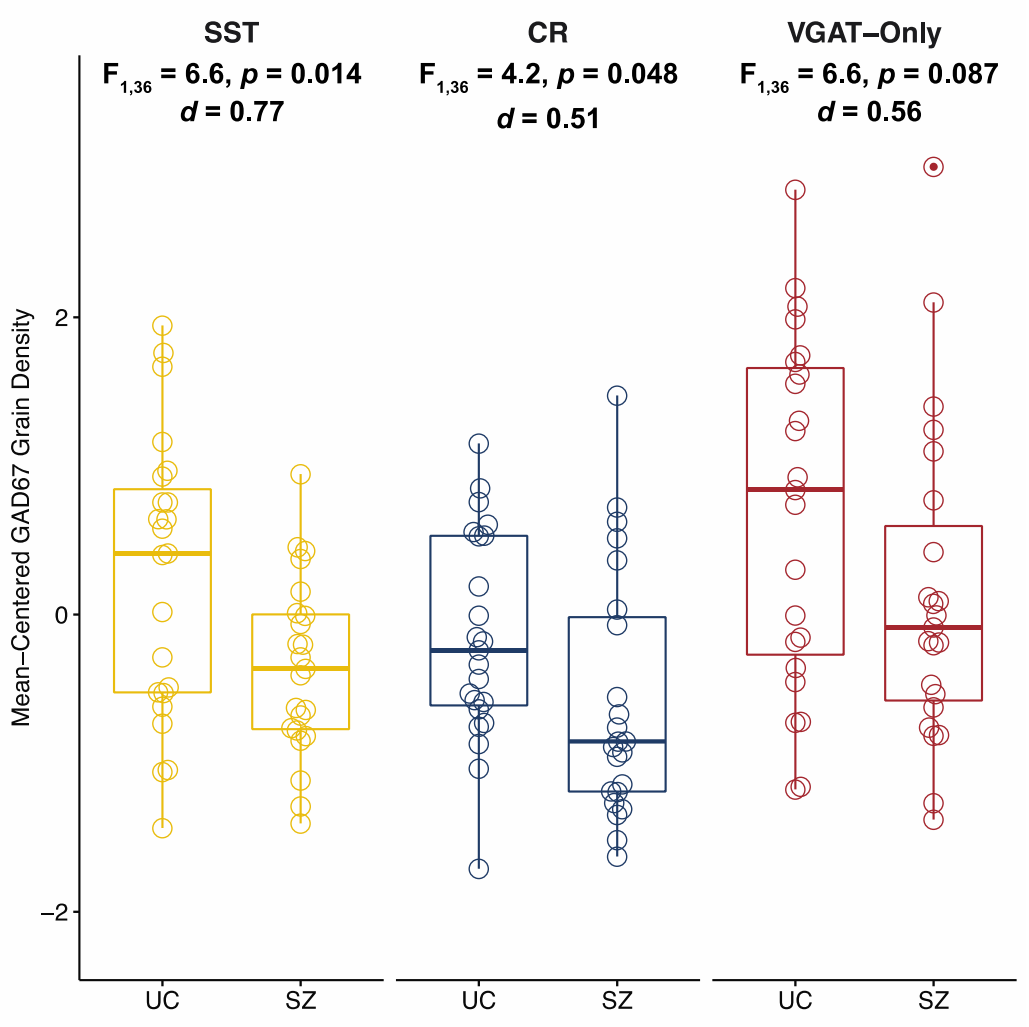

Figure 22. Boxplots of GAD67 levels per GABA subtype in schizophrenia.
Because of the batch effect observed, the y-axis repesents the mean-centered GAD67 value within a batch. Effect sizes (Cohen's *d* are shown at the top for each cell type, represented by color. UC = unaffected comparison, SZ = schizophrenia.

4.3.3 Relative proportions and levels of SST and CR per neuron in schizophrenia

Consistent with prior reports, in the unaffected comparison group, 20.7% of all neurons were labeled for VGAT mRNA (**Figure 23A**). Among VGAT-expressing cells, our classification scheme resulted in 31.8% defined as SST-expressing, 32.3% as CR-expressing, and 36.0% as

VGAT-expressing without either SST or CR (**Figure 23B**). These proportions were strikingly similar in schizophrenia (**Figure 23B**).

We had previously shown (**3.0**) that the deficits in SST mRNA in layer 2 in schizophrenia reflect lower mRNA levels per neuron and not fewer neurons. Here, in a largely nonoverlapping group of individuals with schizophrenia, we found that SST levels per SST neuron are lower ($F_{1,36}$ = 5.4, p = 0.026; Cohen's *d* = 0.72; **Figure 24A**) without a deficit in the relative density of SST neurons in this laminar zone ($F_{1,36}$ = 0.33, *p* = 0.57; **Figure 23C**). Here, the Bayes' factor indicated substantial evidence of no difference in SST neuron density between groups (BF_{10} = 0.34). Significant covariates for SST mRNA levels per neuron included batch ($F_{1,36}$ = 7.4, *p* < 0.001) and age ($F_{1,36}$ = 18.8, *p* < 0.001), whereas pH was not statistically significant ($F_{1,36}$ = 3.7, *p* = 0.06).

Unlike SST mRNA, levels of CR mRNA per CR neuron were not lower in schizophrenia ($F_{1,36}$ = 2.1, *p* = 0.16; **Figure 24B**), nor was there significant differences between groups in the density of CR-expressing cells in schizophrenia ($F_{1,36}$ = 0.03, p = 0.87; **Figure 23C**), with the Bayes' factor indicating substantial evidence of no difference in CR neuron density between groups (BF_{10} = 0.29). Finally, the density of VGAT-Only cells in schizophrenia was significantly different in persons with schizophrenia ($F_{1,36}$ = 4.4, *p* = 0.044), with a marginally higher density of this neuron population. Here, the Bayes' Factor only indicated anecdotal support (BF_{10} = 0.43). Together, these findings support the prior findings that schizophrenia is associated with altered levels of GABA-related transcripts per neuron in the DLPFC without a deficit in neuron density and suggests that the distribution of GABA neuron subtypes is comparable in the disorder.

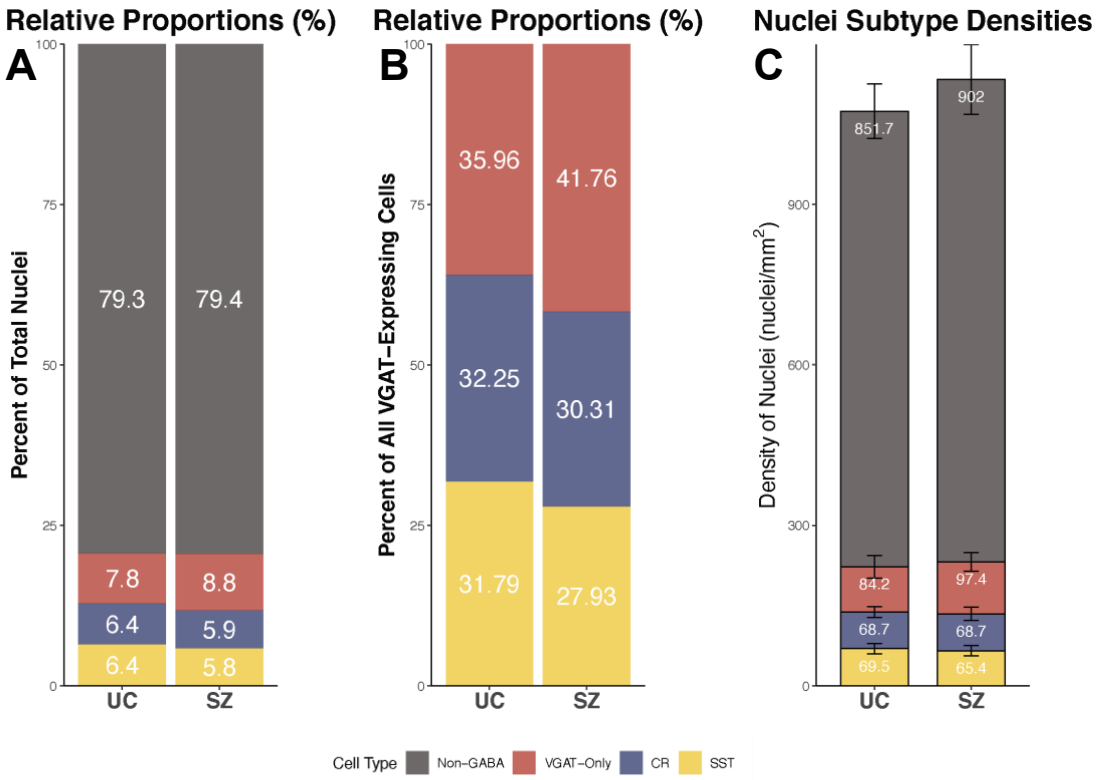

Figure 23. Relative proportions and densities of GABA neuron subtypes in unaffected and schizophrenia. **A)** The average proportion of each cell type (non-GABA, gray), VGAT-only (red), CR (blue), or SST (yellow) across all subjects. Numbers shown are percentages in each diagnostic group. **B)** Relative proproportion of among GABA subtypes in both diagnostic groups. **C)** The density of each cellular subtype between diagnostic groups. Error bars shown are 95% confidence interval.

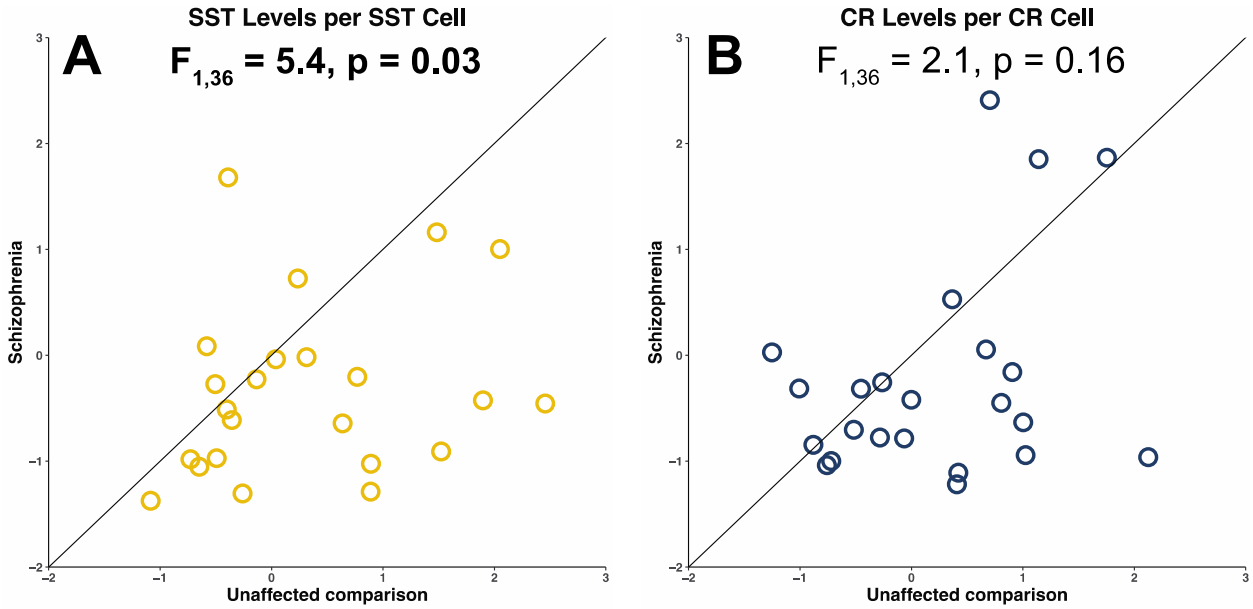

Figure 24. Unity plots for SST and CR levels per respective neuron in schizophrenia.
Levels of **A)** SST or **B)** CR per respective neuron subtype. Unity plots show each pair as an individual point and the line of unity. Points above the line indicate a higher value in schizophrenia relative to their matched unaffected comparison individual.

4.3.4 Relationship of SST or CR deficits and GAD67 deficits in schizophrenia

Here, we found deficits in SST, but not CR, mRNA levels per neuron, and lower GAD67 mRNA levels in both cell types, with a stronger disease effect in SST cells. Within SST cells in individuals with schizophrenia, the deficits in SST and GAD67 mRNAs (indexed by their respective w-scores) were highly correlated (r = 0.7, $p < 0.0001$; **Figure 25A**). In contrast, within CR cells in individuals with schizophrenia, the correlations between CR and GAD67 were weaker and not statistically significant (r = 0.34, $p = 0.11$; **Figure 25B**). Finally, the deficits in GAD67 mRNA in SST cells were highly correlated with the deficits in GAD67 in CR cells (r = 0.8, $p < 0.0001$; **Figure 25C**).

4.3.5 Relationship of SST and GAD67 measured by PCR and *in situ* hybridization

Here, we had two transcripts (SST and GAD67) that were measured in both studies in the same tissue specimens by different methods. We compared the within-subject correlation of SST and GAD67 mRNAs measured by both approaches (qPCR and FISH) in both subject groups. To make the appropriate comparison across methods, GAD67 or SST levels per neuron, scaled to account for batch effects, were multiplied by the relative density of all VGAT-expressing or VGAT/SST-expressing cells, respectively. For both SST (**Figure 26A-C**) and GAD67 (**Figure 26D-F**), the disease effect size was comparable in size as assessed by the two methods, and, across all subjects, values were highly correlated with each other.

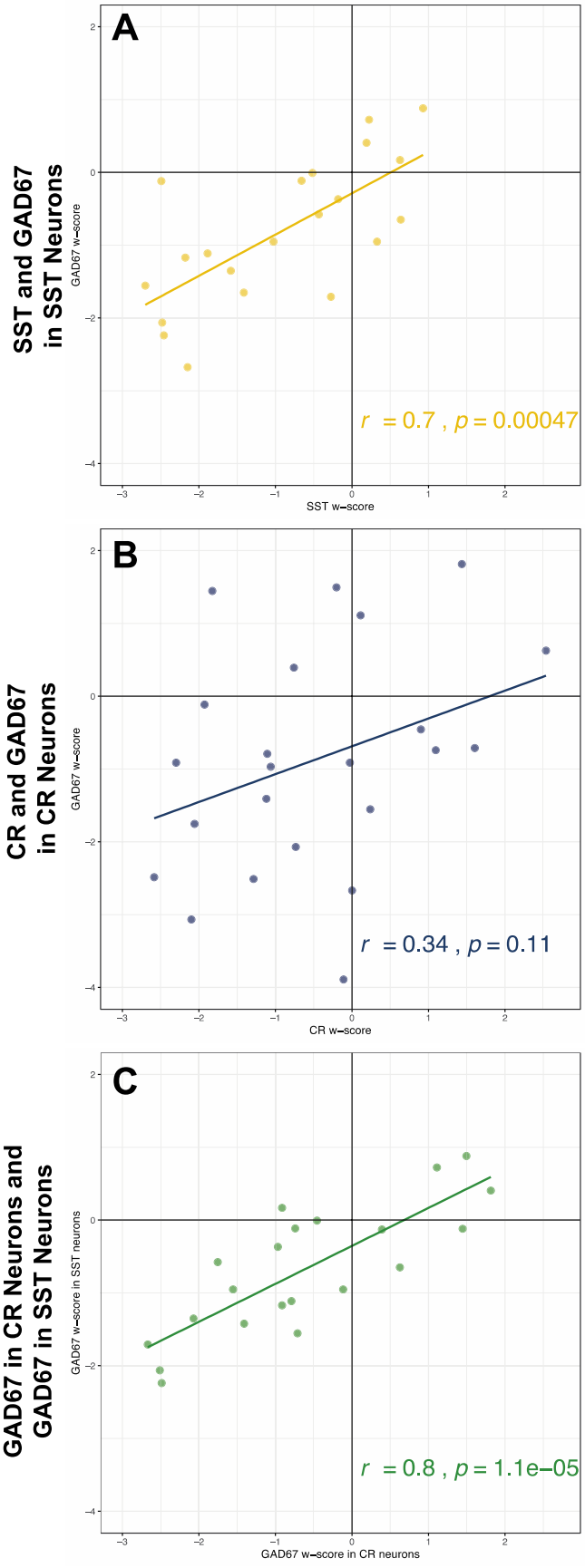

Figure 25. Correlations of w-scores for individuals with schizophrenia for SST, CR, and GAD67.

A) Correlations of GAD67 and SST levels within SST cells across 23 individuals with schizophrenia. B) Correlations of GAD67 and CR levels within CR neurons in schizophrenia. C) Correlations of GAD67 in SST vs GAD67 in CR cells in schizophrenia. In all panels, Pearson's correlation coefficient is shown.

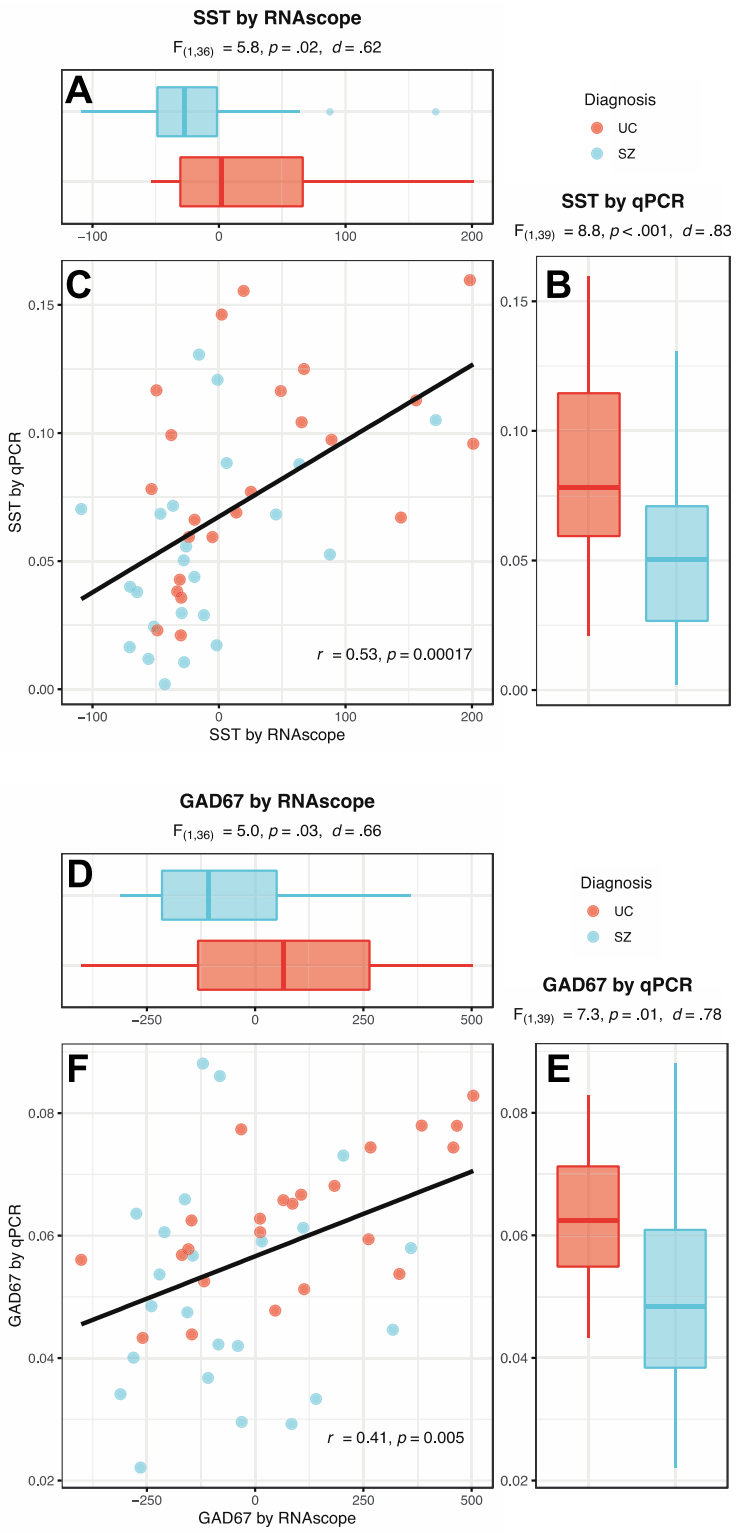

Figure 25. Relationship of SST between two approaches for quantifying mRNA.

A) Boxplots of the median, quartiles, and 95% range for values of SST measured by FISH. B) Same as A) but for SST measured in the same subjects by qPCR. C) Correlations among unaffected comparison (UC) and schizophrenia (SZ) individuals for SST measured in the same subjects by different methods. D-F) Same as A-C but for GAD67 levels measured by the two methods.

4.4 DISCUSSION

To date, the published studies that examined GAD67 mRNA levels in a laminar-specific manner in schizophrenia were both conducted in cohort sizes of 10 schizophrenia and unaffected comparison pairs (Volk et al., 2000; Akbarian et al., 1995). Here, in the largest cohort to date that has examined GABA transcripts in a laminar-specific fashion, we found lower levels of GAD67 mRNA in schizophrenia in layer 2-superficial 3. Additionally, the same subjects exhibited a deficit in SST levels in this laminar zone, and these measures were correlated within subject.

While correlations of transcripts in homogenates of layer 2-superficial 3 suggest that SST neurons might exhibit lower GAD67, such studies cannot address the question of whether the transcript deficits are present in the same neurons. Because schizophrenia is associated with a normal complement of SST neurons that are detectable by SST mRNA (**3.0**), it is possible to interrogate other cell type-specific alterations within this neuronal population. The present study addresses a longstanding question about what other GABA neurons, aside from PV basket cells, exhibit deficits in GAD67 mRNA in schizophrenia. In addition, we found that CR neurons and VGAT-Only neurons also exhibit lower levels of GAD67 mRNA in schizophrenia, albeit with smaller effect sizes compared to that seen in SST neurons. Given the diverse roles of different GABA neuron populations in cortical circuits, our findings have important implications for understanding the circuit dysfunction in the DLPFC in schizophrenia that likely contribute to cognitive dysfunction.

4.4.1 Methodological advances permit cell type-specific interrogation into GAD67 levels in multiple cell types in schizophrenia

The diversity of GABA neurons in the neocortex and the distinct roles that each subtype might play in working memory (Kamigaki, 2019) suggest that depending on which population(s) of neurons have an impaired capacity to synthesize GABA in schizophrenia, the functional consequences for the activity of the circuit could be substantially different. However, only one study to date has examined GAD67 mRNA levels in a cell type-specific manner in schizophrenia (Hashimoto et al., 2003), and this study, which focused on PV neurons, was unable to quantify levels of GAD67 per neuron and could only report on the presence of absence of GAD67 signal in PV neurons. Multiplex fluorescence *in situ* hybridization provides the means necessary to quantify levels of a transcripts like GAD67 with cellular levels of resolution in different cell types.

Another advantage of multiplex approaches is the capacity to quantify GAD67 in multiple GABA neuron subtypes simultaneously. While we principally sought to examine GAD67 within SST neurons, the possibility of multiplexing allowed us to also examine another prevalent GABA neuron subtype in this laminar zone, CR-expressing cells, as well as GABA neurons that do not contain either SST or CR. Although we found that GAD67 deficits were lower across all three cell types, the effect size was largest for SST neurons, and within-cell, these measures were highly correlated with SST levels. These findings suggest that some of the upstream factors that might contribute to lower SST in SST cells could also lead to lower GAD67 in these neurons.

4.4.2 Deficits in GAD67 mRNA in schizophrenia appear to exhibit some cell type-specificity

Prior studies of GAD67 mRNA quantified by *in situ* hybridization reported that the density of neurons with detectable GAD67 mRNA was ~30% lower across cortical layers, and this deficit was evident in layer 2. In contrast, there was no difference in GAD67 mRNA levels per neurons in the neurons that were detectable (Volk et al., 2000). This finding led to the hypothesis that only certain subsets of GABA neurons exhibit deficits in GAD67 mRNA. While it was apparent that one subtype, the PV basket cell, exhibited deficits in GAD67 (Hashimoto et al., 2003), knowledge about what other subtypes might have contributed to the deficit (and which might be unaffected) remained unclear. Here, we find evidence of lower GAD67 mRNA in multiple GABA subpopulations, albeit with differing effect sizes. Additionally, although the differences in GAD67 mRNA in CR neurons was statistically significant with a medium effect size, the Bayes' factor supporting evidence of a difference was anecdotal. One possible interpretation of these findings is that CR (and VGAT-only) cells constitute a highly heterogenous population of GABA neurons, and that further divisions of these cell populations into distinct subtypes would reveal a subset of CR or VGAT-only neurons that exhibit lower GAD67 and separate unaffected populations.

A key species difference between rodent and primate is the enrichment in CR neurons relative to PV neurons in primates (Krienen et al., 2020; Condé et al., 1994; Gabbott & Bacon, 1996). Given recent transcriptomic findings of GABA neuron diversity, it has been suggested that rather than just a primate-specific expansion of CR-positive neurons developmentally (Džaja et al., 2014; Hladnik et al., 2014), more CR-positive neurons in primates might be associated with broader CR mRNA expression in multiple GABA populations (Krienen et al., 2020). In sum, it seems clear that both CR and VGAT-only populations defined here are broad categories and measuring GAD67 in the entire population of CR or VGAT-only cells might aggregate affected

and unaffected populations of GABA neurons in schizophrenia. Future studies should be conducted that meaningfully subdivide the population of CR and VGAT-Only cells here and assess GAD67 mRNA deficits in those populations. For example, at least two subtypes appear to exist in the primate neocortex: CR neurons that do and do not express the neuropeptide cholecystokinin (Krienen et al., 2020).

4.4.3 Etiology of GAD67 deficits in multiple GABA neuron subtypes in DLPFC of schizophrenia

What could explain shared GAD67 deficits in multiple subtypes of GABA neurons that are 1) derived from different embryonic origins (Ma et al., 2013; Wonders & Anderson, 2006; Letinic et al., 2002); 2) exhibit distinct synaptic connectivity in DLPFC circuitry (Campagnola et al., 2022); and 3) differ in their sources of synaptic inputs from cortical and subcortical regions (Bloem et al., 2014; Froudist-Walsh et al., 2021)? Given these distinctions, a plausible mechanism for lower GAD67 mRNA could be an upstream schizophrenia-associated genetic or epigenetic alterations at the *GAD1* gene or its promoter sequences (Mitchell et al., 2015). In support of this view, some studies suggest that allelic variation in the *GAD1* gene or variation in the 5' flanking region of the gene, which likely includes promoter sequences, confer greater risk for schizophrenia in family-based samples (Straub et al., 2007; Addington et al., 2005). Allelic variation at these loci is also associated with other features of persons with schizophrenia, including cortical gray matter volume deficits (Addington et al., 2005) and cognitive dysfunction (Straub et al., 2007). While these allelic variations might be evident in certain familial instances of schizophrenia, this genetic architecture is not well supported by recent genome-wide association studies (Trubetskoy et al., 2022).

In contrast, genome-wide association studies frequently identify schizophrenia risk in genes that are highly expressed in the pyramidal cell population (Trubetskoy et al., 2022; Skene et al., 2018), and GAD67 expression levels are clearly regulated by neuronal activity (Benson et al., 1994; Lau & Murthy, 2012). Thus, an alternative possibility is that alterations in GAD67 mRNA levels reflect upstream deficits in downregulated excitatory drive in multiple GABA neuron subtypes (Dienel & Lewis, 2019). Consistent with this, layer 3 pyramidal neurons, which are strongly suggested to be hypoactive in schizophrenia, appear to provide a large complement of excitatory input onto SST neurons in the primate DLPFC in layer 2 (Melchitzky & Lewis, 2003). In addition, SST mRNA, at least in cell culture, appears to be associated with activity levels (Sánchez-Muñoz et al., 2010), so impaired excitation of these neurons by layer 3 pyramidal cells could contribute to coordinated downregulation of both SST and GAD67. The data presented here lends some support for this notion, given the strong correlation of the deficits in SST and GAD67 within individuals with schizophrenia (**Figure 20A**).

In contrast to SST cells in the primate DLPFC, CR neurons do not appear to receive many excitatory inputs from local layer 3 pyramidal neurons (Melchitzky & Lewis, 2003). However, CR neurons, relative to other GABA neurons at least, might receive the majority of excitatory inputs coming from other cortical regions (Naskar et al., 2021), including other DLPFC regions. For example, in primates, excitatory inputs from DLPFC area 46 into DLPFC area 9 more frequently form synapses onto CR neurons compared to other GABA neurons (Medalla & Barbas, 2009). Thus, if pyramidal neurons in DLPFC area 46 are also hypoactive, then deficient excitatory drive from cross-areal intra-DLPFC connections could contribute to lower GAD67.

4.4.4 Functional consequences of deficient GABA signaling onto excitatory and inhibitory dendrites

Lower levels of GAD67 transcript in different GABA neuron populations suggests that the inhibition these neurons provide to their postsynaptic targets is diminished. Broadly (although certainly not exclusively), SST neurons in the superficial layers preferentially make synapses onto the dendrites of excitatory cells, while CR neurons in this layer preferentially make synapses onto the dendrites of other GABA neurons (Melchitzky & Lewis, 2008). Although more work is necessary to understand the distinct role that each of these DLPFC GABA neurons have in mediating working memory, the available data based on computational models of this connectivity suggest that dendritic inhibition onto excitatory cells by SST-containing neurons is crucial for rendering the DLPFC circuit resilient to the effect of intervening distractors during cognitive tasks such as working memory.

Because SST neurons appear to be active even in quiescent circuits (Urban-Ciecko & Barth, 2016), disinhibition of excitatory dendrites, through CR-mediated inhibition onto SST cells, might be necessary for the bottom-up transfer of information about memoranda to be maintained during working memory to be encoded into the DLPFC circuitry (Wang et al., 2004). Thus, while perhaps not directly a recipient of excitatory synapses in the local DLPFC circuit, these neurons could exhibit similar tuning curves as excitatory cells within the same cortical column and diminished inhibitory control over SST neurons could contribute to encoding deficits during working memory in schizophrenia (Kang et al., 2018) .

4.4.5 Conclusions, Limitations, and Future Directions

In conclusion, we found lower levels of GAD67 in SST and CR neurons, as well as VGAT-only neurons in layer 2-superficial 3 of the DLPFC in persons with schizophrenia. Within the same subjects, the strongest disease effect size in GAD67 mRNA levels was localized to SST neurons. Consistent with prior studies, alterations in GABA neurons in schizophrenia principally seem to reflect functional alterations, and not a deficiency in the number of DLPFC GABA neurons.

Here, we had *a priori* knowledge of GAD67 and SST mRNA levels by PCR prior to conducting the study using FISH. On the one hand, the concordance of SST and GAD67 mRNA levels quantified by two different methods in the same subjects offers evidence of the rigor and reliability of the finding in schizophrenia. On the other hand, although the cohort of individuals selected for follow-up study was not based on *a priori* knowledge of GAD67 and SST levels, it was biased towards showing a larger disease-related effect size compared to the larger cohort. Thus, to obtain a more robust estimate of the disease effect size for GAD67 in multiple GABA neuron subtypes in schizophrenia, we plan to conduct the same study in a new postmortem cohort of 23 individuals with schizophrenia and age- and sex- matched unaffected comparison individuals that have not previously been studied by any research group.

Finally, there are still limitations on the number of transcripts that can be simultaneously identified spatially, so the ability to index disease-related alterations in GAD67 mRNA in subgroups of CR or the VGAT-only population identified here is limited. Future studies should seek to identify the important and larger subgroups of CR neurons, or the population of VGAT-only cells identified here. Such studies would further inform our knowledge of how these alterations arise in schizophrenia and the functional consequences of these alterations in the context of working memory and other cognitive functions.

5.0 GENERAL DISCUSSION

In this thesis, I have presented data from our lab showing that the basis for regional differences in SST expression between monkey DLPFC and V1 primarily reflect differences in the relative proportions of SST neurons between regions, rather than differences in gene expression per neuron between regions. In contrast, the schizophrenia-associated deficits in SST gene expression in the DLPFC principally reflect lower gene expression per neuron and not fewer neurons. Demonstration of a normal complement of SST neurons in the DLPFC in schizophrenia and a methodology that allows for investigation of those neurons in schizophrenia permits other cell type-investigations into their alterations, and the third chapter demonstrated that SST neurons also exhibit lower levels of a principal GABA synthesizing enzyme, GAD67. Together, these findings suggest that the SST enrichment in associational rather than primary sensory cortical regions might contribute to the key types of information processing that take place in the DLPFC and the functional alterations to the ability of these neurons to inhibit other cells in schizophrenia might disrupt these kinds of information processing and lead to impairments in working memory.

5.1 TECHNICAL CONSIDERATIONS FOR THE INVESTIGATION OF GABA NEURONS AND THEIR ALTERATIONS IN SCHIZOPHRENIA

As more studies begin to interrogate the alterations in schizophrenia at the level of different cell types, understanding how we define those cells will become crucial so that we do not reach wrong conclusions about the nature of the alterations in people with the disorder. One example

from this dissertation work has been a prevalent viewpoint in the literature that PV neurons are deficient in number in the DLPFC of individuals with schizophrenia, perhaps most clearly stated in a recent meta-analysis of postmortem findings of PV interneurons in schizophrenia (Kaar et al., 2019). This meta-analysis concludes that there is robust evidence for deficient PV neuron number in the DLPFC of schizophrenia without a reduction in PV levels per neuron. These conclusions have inspired a deluge of animal models for schizophrenia that introduce manipulations resulting in fewer PV neurons in the cortex (Lodge et al., 2009; Stansfield et al., 2015). When the identifying marker of a neuron is also the disease- or manipulation-dependent variable, then there must be other markers to indicate the identity of that neuron in the face of an abnormal phenotype.

One practical application of this point is looking towards the advent of new single-cell and single-nucleus RNA sequencing approaches, used very successfully to illuminate the rich cellular diversity of neurons in a regional and species specific manner (Krienen et al., 2020; Welch et al., 2019; Butler et al., 2018). These approaches, applied to the postmortem brains of individuals with schizophrenia, offers significant promise towards elucidating cell type-specific alterations in the disorder (Price et al., 2021). At the same time, the clustering approaches used to unbiasedly sort cells into certain subgroups dependent heavily, at least for GABA neurons, on markers that are dramatically altered in people with schizophrenia. For example, *GAD1* (GAD67) is one of the most robust distinguishers between GABA and non-GABA neurons. Similarly, subgroups of PV, SST, and VIP neurons are clustered based on the expression of those transcripts, all of which are altered in schizophrenia. Without other markers to rely on as proxies of what the phenotype of a given neuron *should be* were it not for the presence of schizophrenia, erroneous conclusions about what subtypes are affected in the disorder might be reached. Rather than unsupervised classification approaches in both subject groups, one strategy might be to employ robust transfer learning

strategies that presume an underlying latent space of similar cellular phenotypes across diagnostic states (Peng et al., 2021). For a simplistic example, knowledge that SST and PV neurons across diagnostic states share phenotypic expression of both VGAT and SOX6 could reliably identify the most affected populations of these neurons that might be mislabeled in a strategy that depends on their expression of either SST or PV mRNA.

5.1.1 Rigor and reproducibility in this thesis dissertation

Issues of rigor and reproducibility have been widely publicized and received a great deal of attention in recent years, and the field of psychiatric neuroscience is far from exempt from these concerns. One of the major goals of this dissertation work was to demonstrate examples of how experimental design can incorporate both independent replication of certain prior findings while offering new levels of insight and furtherance of knowledge about neocortical GABA neurons and their alterations in schizophrenia. In Chapter 2, we studied a large number of monkeys to better understand the normative distribution of GABA neuron transcript with regional, laminar, and cellular specificity. In this chapter, the patterns we found were strikingly consistent across animals, with nearly every animal exhibiting the same rank-ordered levels of transcripts such as SST and PV. Moreover, this study replicates, at the level of mRNA, prior protein studies that examine GABA neuron densities in various regions of the primate neocortex. Additionally, the studies conducted using FISH replicate the results obtained by qPCR, demonstrating replicability of the core finding by multiple modalities. Finally, the findings of normative distributions of GABA neurons in the primate neocortex have been confirmed by other studies using different methods. For example, recent single cell RNAseq studies across regions of the monkey neocortex confirm the findings from this study and prior studies (Hendry et al., 1987) that while there are more

GABA-containing neurons in primate DLPFC, they constitute a smaller overall proportion of all neurons in this region (Krienen et al., 2020).

The experiments in chapter 3 were designed to robustly test the hypothesis that SST neurons exhibit lower mRNA levels per neuron without a deficit in neuron density in the DLPFC of persons with schizophrenia, while providing independent confirmation in a larger cohort that the levels of PV mRNA per neuron are lower (Hashimoto et al., 2003) without a deficit in the density of PV neurons. Moreover, this study confirmed that PV levels per PV neuron are not lower for those located in layer 2, consistent with prior studies with laminar resolution in schizophrenia (Chung et al., 2016b; Hashimoto et al., 2003). Finally, this study affirmed findings at the total gray matter level of analysis that VGAT (Fung et al., 2011) and SOX6 (Volk et al., 2012) mRNA levels are not markedly different in persons with schizophrenia. Thus, multiple levels of analysis confirm the same finding in the context of schizophrenia.

In chapter 4, the experiments were designed to address whether SST neurons, in addition to having lower levels of SST mRNA, also exhibit deficits in GAD67 mRNA. Technical replication was accomplished by utilizing both qPCR and FISH in the same tissue specimens from the same cortical area, showing strong agreement between both methods within a given individual. Further, the results in this experiment re-affirmed the findings in chapter 3 that there is no deficit in SST neuron (or VGAT-positive neurons generally) density in schizophrenia in a largely non-overlapping cohort of individuals with schizophrenia. Finally, similar to prior reports (Chung et al., 2016b; Hashimoto et al., 2003), we failed to find evidence of alteration in CR mRNA in the schizophrenia group, while finding some evidence of lower GAD67 mRNA levels within these neurons.

Taken together, the experiments described in this thesis represent both technical replicability using different methods (especially qPCR and FISH), and biological replication by demonstrating consistent findings across multiple cohorts of individuals with schizophrenia. Future experimental design that both confirms the veracity of prior findings while offering novel insights has multiple benefits for scientific endeavors: if the prior finding is demonstrated to be replicable and robust, then the confirmation of those results supplies epistemological confidence in the novel finding. Conversely, if the prior finding is not robust, then this experimental strategy serves to prevent poorly substantiated historical findings from gaining a foothold in the minds of experimenters.

5.2 POSTMORTEM STUDIES OF SST NEURON ALTERATIONS INFORM ETIOLOGIC ORIGINS OF THOSE ALTERATIONS

The postmortem brain is indispensable for a clear understanding of the basis for neuropsychiatric disorders, such as schizophrenia, that is not yet available through other modes of inquiry. For example, animal models are crucial for understanding mechanisms and the functional consequences of the hypothesized altered neuronal function that is present in disorders like schizophrenia but cannot speak to the cellular alterations that are actually evident in the brains of individuals with schizophrenia. Likewise, *in vivo* studies of schizophrenia are the only manner in which to link altered brain function to behavior or to observe change over time during different epochs of schizophrenia but are unable to characterize these alterations at the level of cells and circuits that underlie those alterations. Finally, genome-wide association studies operationally define the ‘upstream’ causal factors that contribute to the emergence of the disorder but cannot

independently demonstrate how that genetic diversity contributes to altered cellular function or explain how these genes cause the complex alterations in persons diagnosed with schizophrenia. Postmortem studies of the brains of those diagnosed with schizophrenia reveal, at the level of individual cells and circuits, the neural alterations that contribute to altered *in vivo* imaging. Likewise, knowledge of the cellular basis for altered *in vivo* findings could provide a bridge between novel therapeutic interventions and reliable biomarkers to index the efficacy of those interventions (Schoonover et al., 2020).

At the same time, there are a set of limitations that need to be taken into consideration when reporting alterations in gene expression levels identifying in schizophrenia through postmortem studies. First, postmortem studies are limited as to only capturing a single snapshot in a persons' life and is not able to account for the full range of dynamic gene and/or protein expression that's possible across time (Lewis, 2002). Moreover, findings of certain morphological, molecular, or biochemical alterations in the postmortem brain of people with schizophrenia cannot explain how those findings arise or what factors are operative to achieve that state. With that stated caveat, I suggest that reasonable inferences about the etiology of those alterations are possible through understanding of both the nature of the alterations in schizophrenia and the pattern of those alterations across brain regions, across cortical layers, different cell types, and diagnostic categories for different psychiatric disorders. To exemplify this process, I examine the findings of the preceding dissertation chapters, contextualize them to knowledge about other postmortem alterations in schizophrenia, and offer conjectures about how the constellation of those alterations might arise in the disorder.

5.2.1 Are SST alterations reported in schizophrenia a confound of postmortem studies?

Two major challenges have long shielded SST neurons from investigation in the context of schizophrenia historically. When the majority of postmortem studies were conducted by immunohistochemistry, it was found that the SST peptide that certain well-characterized antibodies targeted was highly sensitive to the effects of postmortem decay (Hayes et al., 1991). The SST peptide was first described as a tetradecapeptide (SST-14) released from the axon terminals of GABA neurons and co-released with GABA after being packaged into dense core vesicles. Later, an N-terminal extended peptide was identified (SST-28). Different antibodies were able to target each of these peptide forms, and in general, it was found that SST-28 was well-localized to the perinuclear cell body, while SST-14 was prevalent in both cell bodies and axon terminals. Additionally, an N-terminal dodecapeptide named SST-$28_{(1-12)}$ was identified through different antibodies targeted to the C-terminus of that peptide that does not recognize SST-28. SST-$28_{(1-12)}$ is thought to be a byproduct of the conversion of SST-28 into SST-14. During the first 120 minutes of a postmortem delay, it was shown that protein levels of SST-28 rapidly decline, and levels of SST-14 and SST-$28_{(1-12)}$ concurrently increase. These findings were interpreted that SST-28 cleaves into SST-14 and SST-$28_{(1-12)}$ during the postmortem delay (Hayes et al., 1991). Thus, while not specifically confounding studies of the postmortem brains of those with schizophrenia, the ability to visualize these neurons at the level of protein in the postmortem brain was limited. This example highlights a key limitation for interrogating the alterations in this neuron type in the postmortem brain of those with schizophrenia and raises questions about what other factors involved in postmortem studies might confound the interpretation of SST neurons in postmortem studies of schizophrenia.

In addition to the challenges of studying SST protein, prior studies found fewer neurons detectable by SST mRNA ((Morris et al., 2008), and see **3.1**), which either suggested that a subset of affected neurons were deficient in number in schizophrenia or that the most affected subtype were difficult to visualize. Fewer SST neurons detectable by SST mRNA, or so it was posited, rendered knowledge about other cell type-specific alterations to this population in schizophrenia challenging. In this dissertation, we attempted to resolve this concern by utilizing proxy markers for SST neurons that did not depend on the presence or absence of SST signaling itself. In those experiments, a normal complement of SST mRNA-expressing neurons suggested that the sensitivity of the assay and microscopic methods rendered these neurons difficult to see by less sensitive approaches. However, it was clear from findings in chapter 4 that lower SST levels per neuron were strongly associated with brain pH and RIN levels, raising the specter that lower SST mRNA levels, like the cognate protein, might be sensitive to some factors that are only relevant in the context of studies in postmortem human brain and not related to the disease process of schizophrenia.

Brain pH in particular, in most cohort studies of schizophrenia that our group has conducted, appears to be lower at a group level in schizophrenia relative to unaffected comparison individuals, and some suggest this is part of the pathophysiology of schizophrenia (Park et al., 2021) and other psychiatric disorders (Hagihara et al., 2018). Brain pH is a complex value because it is principally used as an indicator of the quality of brain tissue used for subsequent studies (Lipska et al., 2006; Kingsbury et al., 1995; Monoranu et al., 2009). Thus, one plausible interpretation is that lower SST in persons with schizophrenia reflect differences in brain pH, rather than the disease process of schizophrenia. If levels of SST are directly influenced by brain pH, then findings of lower levels of SST mRNA in schizophrenia might actually reflect differences in

brain tissue integrity or acidity in individuals living with the disorder (perhaps as a consequence of medication confounds (Halim et al., 2008)).

A few findings shown here from other data on SST levels from our group do not support this claim. First, in the second study in chapter 4, we utilized a subset of subjects matched on brain pH and RIN. This subset of subjects exhibited a disease effect on SST that was larger than the entire cohort and exhibited no group differences in brain pH. Second, brain pH levels were not a significant covariate in the tissue cohort used in chapter 3 ($F_{1,51} = 0.22$, $p = 0.64$).

Finally, to fully assess the influence of brain pH and other covariates on SST levels in different subject cohorts in schizophrenia, I took advantage of other data from our lab where SST mRNA was measured by qPCR or by RNAseq in total gray matter samples of DLPFC. Cohort descriptions are described in the original manuscripts. In the first cohort, total gray matter SST levels were measured by PCR in 62 pairs of schizophrenia and unaffected comparison individuals (Volk et al., 2016), and a subset of these individuals were selected for the data in chapter 3. In 57 of those pairs, RNAseq values for SST levels were also available, providing a way to index how these covariates differ by technical variance. In the third cohort, SST mRNA levels were quantified by PCR in 40 schizophrenia and matched unaffected comparison individuals (Chung et al., 2018)—a cohort closely resembling that used in chapter 4. In each of these datasets, while age and diagnosis were clearly significant predictors and explained a significant proportion of the variance of SST levels, pH never emerged as a significant covariate. Taken together, SST levels are clearly lower in schizophrenia in a manner that reflects a process other than simply lower brain pH in the disorder.

Table 5. Regression table across studies of SST mRNA, the significant predictor variables in each (bolded), and the proportion of variance explained.

	Ch 3 Cohort			**Ch 4 Cohort**			**Ch 4 Cohort**		
Cohort Size	29 UC/29 SZ			43 UC/41 SZ			23 UC/23 SZ		
Method	FISH			qPCR			FISH		
Layer	L2/3s			L2/3s			L2/3s		
R^2	0.451			0.290			0.500		
	Estimate	p-value	Proportion Explained	Estimate	p-value	Proportion Explained	Estimate	p-value	Proportion Explained
Sex	-1.053	0.805	0.1%	-0.1526	0.392	1.7%	-0.2389	0.400	1.9%
Age	-0.169	0.218	2.1%	**-0.0164**	**0.016**	**5.0%**	**-0.0413**	**0.000**	**18.5%**
PMI	-0.501	0.109	3.8%	-0.0224	0.110	3.7%	0.0005	0.981	1.5%
pH	-5.55	0.439	1.0%	0.4575	0.173	3.2%	**1.2543**	**0.025**	**9.9%**
RIN	2.50	0.428	2.5%	0.2814	0.061	6.1%	0.2901	0.166	7.2%
Diagnosis	**-22.3**	**0.000**	**35.7%**	**-0.5185**	**-0.004**	**9.4%**	**-0.4374**	**0.008**	**10.7%**
	Volk et al, 2016			**Fromer et al, 2014**			**Cohort 2 (40 pairs, PCR)**		
Cohort Size	62 UC/62 SZ			57 UC/57 SZ			40 UC/40 SZ		
Method	qPCR			RNAseq			qPCR		
Layer	Total Gray Matter			Total Gray Matter			Total Gray Matter		
R^2	0.469			0.172			0.391		
	Estimate	p-value	Proportion Explained	Estimate	p-value	Proportion Explained	Estimate	p-value	Proportion Explained
Sex	-0.0054	0.337	0.4%	-0.1697	0.470	0.4%	0.0002	0.968	0.0%
Age	**-0.0013**	**0.000**	**22.2%**	**-0.0242**	**0.001**	**8.0%**	**-0.0010**	**0.000**	**26.7%**
PMI	-0.0008	**0.037**	**3.1%**	-0.0044	0.765	0.4%	-0.0003	0.346	0.8%
pH	0.0105	0.235	2.5%	-0.2915	0.413	0.2%	0.0141	0.119	2.0%
RIN	0.0008	0.850	0.5%	0.1370	0.446	0.5%	0.0020	0.614	1.6%
Diagnosis	**-0.0304**	**0.000**	**18.3%**	**-0.6543**	**0.002**	**7.7%**	**-0.0126**	**0.006**	**7.8%**

5.2.2 Homeostatic synaptic plasticity mechanisms contributing to altered cortical SST levels revealed through model systems

Having shown that tissue factors likely do not account for significant difference in SST mRNA levels in schizophrenia, it is worth looking to animal and cell culture models to examine what upstream factors might contribute to lower SST in the disorder. While this section highlights many factors, it is important to note that virtually none of these possibilities are mutually exclusive, and multiple mechanisms might be operative in schizophrenia.

One factor that has the clearest evidence of a cause-and-effect relationship on SST mRNA levels are upstream signaling through brain-derived neurotrophic factor (BDNF). BDNF is synthesized in excitatory neurons (not SST neurons) and activates other neurons through activity of its cognate receptor, tropomyosin receptor kinase B (TrkB, *NTRK2* gene). Within SST neurons, TrkB activation and the subsequent signaling through tyrosine kinase pathways appears necessary to sustain SST mRNA levels. Genetically engineered mice deficient in BDNF exhibit lower levels of both SST and neuropeptide Y (NPY) mRNA, another neuropeptide co-expressed in many SST neurons. The deficit in SST mRNA levels is evident regardless of the timing of the gene knockout (Glorioso et al., 2006), and these deficits are also evident in mice lacking the TrkB receptor (Morris et al., 2008). In the postmortem brain of individuals with schizophrenia, lower BDNF and TrkB mRNA levels are evident in the DLPFC (Hashimoto et al., 2005; Hashimoto et al., 2008a; Weickert et al., 2003), and there is an association between the alterations in BDNF and SST/NPY levels in schizophrenia (Mellios et al., 2009; Morris et al., 2008).

Alternatively, but not mutually exclusively, deficiencies in excitatory drive onto SST neurons in schizophrenia could contribute to lower levels of SST and GAD67 in these cells. Thus,

rather than acting through neurotrophic signaling, alterations to the glutamatergic afferents onto SST neurons might contribute to the coordinated downregulation of both SST and GAD67 in the same cells. While it has yet to be empirically demonstrated that SST neurons in the primate DLPFC receive a major source of excitatory inputs from layer 3 pyramidal neurons, these neurons appear to receive the majority of excitatory inputs that are made onto GABA neurons in the superficial layer (Melchitzky & Lewis, 2003).

Certain postsynaptic mechanisms of excitatory inputs onto SST neurons could further contribute to diminished excitatory drive onto these cells. Since the first observations that phencyclidine (Javitt & Zukin, 1991) or subanesthetic doses of ketamine (Krystal et al., 1994), both acting largely (but not exclusively) as noncompetitive NMDA receptor antagonists, recapitulated certain cognitive and psychotic features of schizophrenia, NMDA receptor hypofunction is thought to contribute to the pathophysiology of schizophrenia (Krystal et al., 2003; Coyle, 2012). Relative to PV neurons, SST neurons appear to be more sensitive to the effects of NMDA receptor antagonists (Lu et al., 2007; Wang & Gao, 2009), and a recent report found that ketamine administration directly suppressed the activity of SST neurons (Ali et al., 2020).

It is unclear whether this downregulation of SST activity in the face of NMDA receptor antagonism reflects intrinsic activity of SST or a presynaptic homeostatic compensation. For example, weaker excitatory drive via NMDA receptors on pyramidal neuron dendrites might evoke certain cellular mechanisms that downregulate the strength of inhibition received at those dendrites by SST cells. There is some evidence of this mechanism operative at least in rodent hippocampus: pyramidal neuron-specific biolistic transfection of a CRISPR/Cas9 system targeted to the obligatory subunit of NMDA receptors caused a downregulation of inhibitory currents mediated by SST neurons in hippocampal slices (Horn & Nicoll, 2018). In this manner, the alterations in

SST neurons could represent an example of homeostatic synaptic plasticity that serve to balance levels of excitatory and inhibition in cortical circuits generally, and within dendrites specifically (Chiu et al., 2019).

5.2.3 Regional, laminar, and cellular specificity of SST alterations in schizophrenia

Much of the dissertation has focused on the alterations in GABA neurons in the DLPFC, especially within the superficial layers, of people with schizophrenia given the crucial role of this circuit in mediating working memory and distractor filtering. However, SST neurons are not exclusive to this laminar zone or cortical region, and nor are all SST neurons evident and identification of alterations in these neurons in other locations could inform how those alterations arise.

In the DLPFC, transcriptionally and functionally distinct subtypes of SST neurons are present in the subcortical white matter. Approximately 40% of SST neurons in this laminar zone are a transcriptionally unique subtype of SST neuron that expresses extremely high levels of mRNA for other neuropeptides, including NPY and TAC1 (also known as substance P). These GABA-containing neurons are also distinct from other GABA neurons (indeed, other SST neurons) in that they form corticocortical projections. In addition, these neurons appear to have a crucial role in neurovascular coupling (Ruff, 2021). This might be mediated through the robust expression of nitric oxide synthase 1 (NOS1; also functionally synonymous with labeling of nicotinamide adenine dinucleotide phosphate (NADPH)-diaphorase described historically (Hope et al., 1991)) and the receptor for the tachykinin 1 (TACR1; also known as substance P receptor). Transcriptomic studies reveal that these neurons are the near-exclusive expressor of a c-type lectin, chondrolectin (CHODL); therefore, I refer to this unique SST subtype as CHODL cells henceforth.

One prior study suggested that in contrast to the cortical gray matter layers, SST mRNA levels were not statistically significantly lower in the subcortical white matter (Morris et al., 2008). In contrast, some studies reported a higher density of SST neurons (Yang et al., 2011) and NADPH-diaphorase reactive neurons (Akbarian et al., 1993; Akbarian et al., 1996) in the subcortical DLPFC white matter in schizophrenia, perhaps indicative of abnormal neuronal migration (Connor et al., 2010; Duchatel et al., 2019b).

To test whether SST levels were lower in this laminar zone, at the same time that we used laser microdissection to isolate layer 2-superficial 3 (**4.0**), we also used microdissection to isolate the subcortical white matter from the same tissue samples (see **Appendix D** for details). We hypothesized that this laminar zone would be unaffected in schizophrenia, possibly reflecting a combination of higher SST neuron density and lower SST levels per neuron. In contrast, in this cohort, we found a deficit in SST expression in this laminar zone that was similar to the magnitude of the disease effect in the superficial gray matter levels. While apparently in conflict with the prior study (Morris et al., 2008), the disease effect size here (Cohen's d = 0.62) was remarkably similar to the effect size reported in that previous study (Cohen's d = 0.60; (Morris et al., 2008)). This suggests that SST neurons, regardless of their laminar location in the DLPFC, might be affected in a similar manner in schizophrenia.

Consistent with the idea that all SST neurons might be affected regardless of layer or region, studies that have examined other neocortical regions, such as V1, association visual cortex (V2), posterior parietal cortex, motor cortex, and anterior cingulate cortex (Hashimoto et al., 2008b; Tsubomoto et al., 2019), consistently show lower SST mRNA levels in schizophrenia. In addition, some subcortical regions, including the hippocampus and amygdala, exhibit alterations in SST neurons in those with schizophrenia (Pantazopoulos et al., 2017; Lanz et al., 2019; Konradi

et al., 2011). This, coupled with the pan-laminar deficit in SST mRNA within the DLPFC, converges on the idea that SST neurons are vulnerable regardless of their regional or laminar location or cellular identity.

However, some other findings challenge this idea. One microarray study examining GABA-related transcripts in the DLPFC, hippocampus, and associative striatum (especially the dorsal aspect of the caudate and putamen), found that SST levels were lower in the DLPFC and hippocampus, but not the striatum (Lanz et al., 2019). In contrast to their sparsity in the DLPFC, CHODL-SST are the near-exclusive subtype of SST neuron in the striatum (Tepper & Koós, 2017; Tepper et al., 2018), raising the possibility that this neuron subtype, which constitutes only ~40% of the SST neuron population in the subcortical white matter, might not exhibit lower levels of SST in schizophrenia.

To test this hypothesis, we are currently conducting an investigation of CHODL-SST cells in the subcortical white matter of the DLPFC and striatum. As a first step, we confirmed that in this cohort of schizophrenia and matched unaffected comparison individuals, there were deficits in the intensity of SST mRNA labeling in the subcortical white matter of the DLPFC (Cohen's $d = 0.52$), but not in the dorsal head of the caudate (Cohen's $d = 0.04$) (**Figure 27A**). We are currently conducting a cell type-specific comparison of SST levels in CHODL-SST cells in both regions, with the hypothesis that CHODL-SST cells exhibit normal levels of SST in schizophrenia, based on preliminary findings of CHODL-SST cells in schizophrenia (**Figure 27B**).

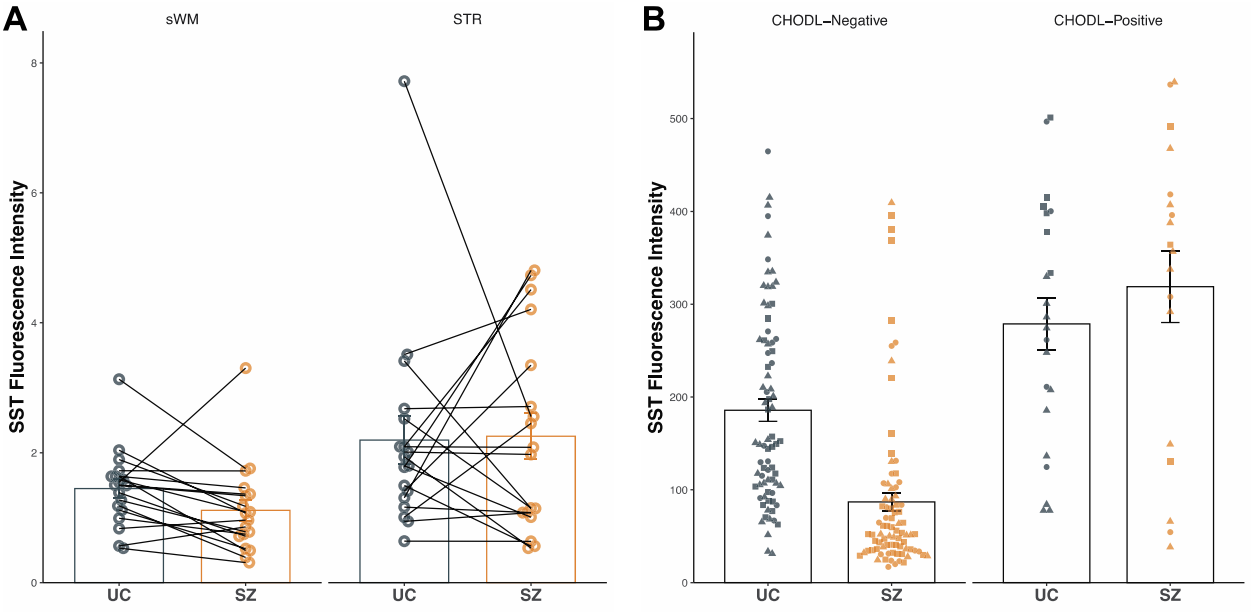

Figure 26. Potential regional and cell-type specificity of the SST alterations in schizophrenia.
A) Regional differences in SST fluorescence intensity from SST mRNA in DLPFC superficial white matter (sWM) and in the dorsal head of the caudate (striatum; STR). Bars indicate the mean, and points show individual subjects. Lines connect the 18 matched pairs of schizophrenia (SZ) and unaffected comparison (UC) individuals. **B)** Results of a single-cell specific study in 3 pairs of SZ and UC individuals for CHODL-negative (left) and CHODL-positive (right) SST cells. Each point represents a cell, and the shape indicates the human subject pair.

5.2.4 Are SST neuron alterations a consequence of living with a neuropsychiatric disorder?

SST neurons appear to be altered in multiple neuropsychiatric disorders (Lin & Sibille, 2013), including (but not limited to) major depression, Alzheimer's disease, Parkinson's disease, post-traumatic stress disorder (Girgenti et al., 2021), bipolar disorder, and alcohol use disorders (Brockway & Crowley, 2020; Lin & Sibille, 2015). This has led to a hypothesis that the vulnerability of SST neurons in all these disorders could index an upstream causal factor that is common across disorders, such as stress. Consistent with this idea, chronic unpredictable stress rodent models result in lower levels of SST mRNA, as well as other neuropeptides (Banasr et al., 2017; Oh et al., 2019). Some other studies comparing across diagnostic categories find that SST and other neuropeptides, including NPY and TAC1, might be altered in the DLPFC in bipolar and

major depression, especially in cases where those individuals exhibited psychotic features (Choi et al., 2008).

In one study (**Appendix D**), we compared the SST and related neuropeptide alterations in the superficial gray matter (superficial zone) and subcortical white matter (deep zone) identified in schizophrenia to individuals diagnosed with bipolar disorder or major depressive disorder. Interestingly, we found a deficit in SST mRNA levels in the superficial zone in major depression that was comparable to the deficit in schizophrenia, there was no deficit in the deep laminar zone in major depression. In bipolar disorder, there was no apparent deficit in SST mRNA in either laminar zone (**Appendix D**). These patterns held true for certain other neuropeptides (NPY and TAC1) as well. In sum, schizophrenia is associated with lower levels of neuropeptides in both superficial and deep laminar zones, while the deficit in major depression is identified only in the superficial zone. The laminar-specific deficit in major depression, coupled with the lack of a significant alteration in bipolar disorder in the superficial or deep laminar zone, argues that neuropsychiatric conditions or their associated features (i.e., stress or substance use disorders) are not simply a blunderbuss on SST expression levels in the brain. Future studies should focus on further dissecting the different factors that might cause alterations in SST neurons in regionally, laminarly, and cellular-specific fashions.

5.2.5 Vulnerability of somatostatin neurons in normal and pathologic aging

In contrast to the small effect of pH or RIN on SST levels, the data from this dissertation consistently reveals age as a significant negative predictor of SST mRNA levels. The findings here are consistent with prior studies in human (Fung et al., 2010; Hoftman et al., 2015; Mohan et al., 2018; Morris et al., 2008) and monkey (Hayashi et al., 1997). Given the dependence of SST

neurons on neurotrophic support via BDNF signaling described above, the age-dependent decline in BDNF could result in lower SST mRNA levels with normal aging.

Alternatively, SST neurons might exhibit some intrinsic vulnerability to certain processes in normal aging (Tomoda et al., 2022). One of the most striking incidental findings from this dissertation work was the extraordinary accumulation of lipofuscin granules within SST neurons that was not as pronounced in other neurons (**Figure 28**). Lipofuscin is a nondegradable byproduct of lysosomal degradation pathways, constituting of oxidized protein (30-58%) and lipid (19-51%) clusters with some metal ions like copper and iron (Terman & Brunk, 2004; Jolly et al., 2002), and accumulates with aging in postmitotic cells (Jung et al., 2007), including neurons (Peters et al., 1994; Benavides et al., 2002). In fact, this age-dependent accumulation is so consistent that in other species, it has been used to reliably estimate the age of certain crustations (Maxwell et al., 2007; Sheehy et al., 1994). Indeed, the relationship between lipofuscin accumulation and aging across all neurons in the studies here was nearly perfectly correlated (**Figure 28B**).

Lysosomal degradation processes, including those that result in lipofuscin accumulation, have been posited to play a critical role in neurodegenerative disorders, especially Alzheimer's disease (Dowson, 1982; Kao et al., 2017). Lipofuscin is posited to not only be a passive byproduct that accumulates with aging but rather an active part of the processes that contribute to neurodegeneration (Moreno-García et al., 2018). SST neurons have long-been known to be altered in Alzheimer's disease : SST immunoreactivity (Davies et al., 1980; Beal et al., 1986; Beal et al., 1985) and mRNA levels (Dournaud et al., 1994) are lower in Alzheimer's disease. SST neurons show morphological alterations consistent with neurodegeneration in Alzheimer's disease (Roberts et al., 1985). Further, neuronal tangles, a pathologic hallmark of Alzheimer's disease, is associated with SST immunoreactivity (Roberts et al., 1985; Armstrong et al., 1985; Morrison et

al., 1985). More recently, a study using single-cell RNAseq in the DLPFC from those with Alzheimer's disease found a heightened vulnerability of SST neurons in the disorder (Consens et al., 2022). Thus, there seems to be a strong link between the vulnerability of SST neurons in aging and the emergence of Alzheimer's disease, perhaps related to the abnormal accumulation of lipofuscin in these neurons.

In addition to its role as a signaling neuropeptide, SST appears to regulate the aggregation of amyloid beta (Aβ), another pathologic hallmark of Alzheimer's disease. SST itself might prevent the accumulation of Aβ in these neurons, either through direct binding to Aβ itself and subsequent inhibition of Aβ aggregation (Puig et al., 2020; Wang et al., 2017) or indirectly through upregulation of Aβ degradation by neprilysin (Iwata et al., 2001; Saito et al., 2005; Rofo et al., 2021). The latter mechanism has been posited to be a crucial role in sporadic Alzheimer's disease, given the negative relationship between age and SST levels (Hama & Saido, 2005).

A few intriguing hypotheses emerge from these findings. One is that if DLPFC SST neurons do mediate distractor resistance, then their presumed progressive dysfunction during aging could contribute to age-dependent diminishment of working memory capacity due to impaired distractor resistance (McNab et al., 2015). Another possibility is that accelerated lipofuscin accumulation in these cells leads to lower levels of SST and abnormal Aβ accumulation that seeds the pathology observed in Alzheimer's disease. Of course, establishing this causal linkage of events requires rigorous examination in model systems, coupled with findings in the postmortem brain (see **5.5**).

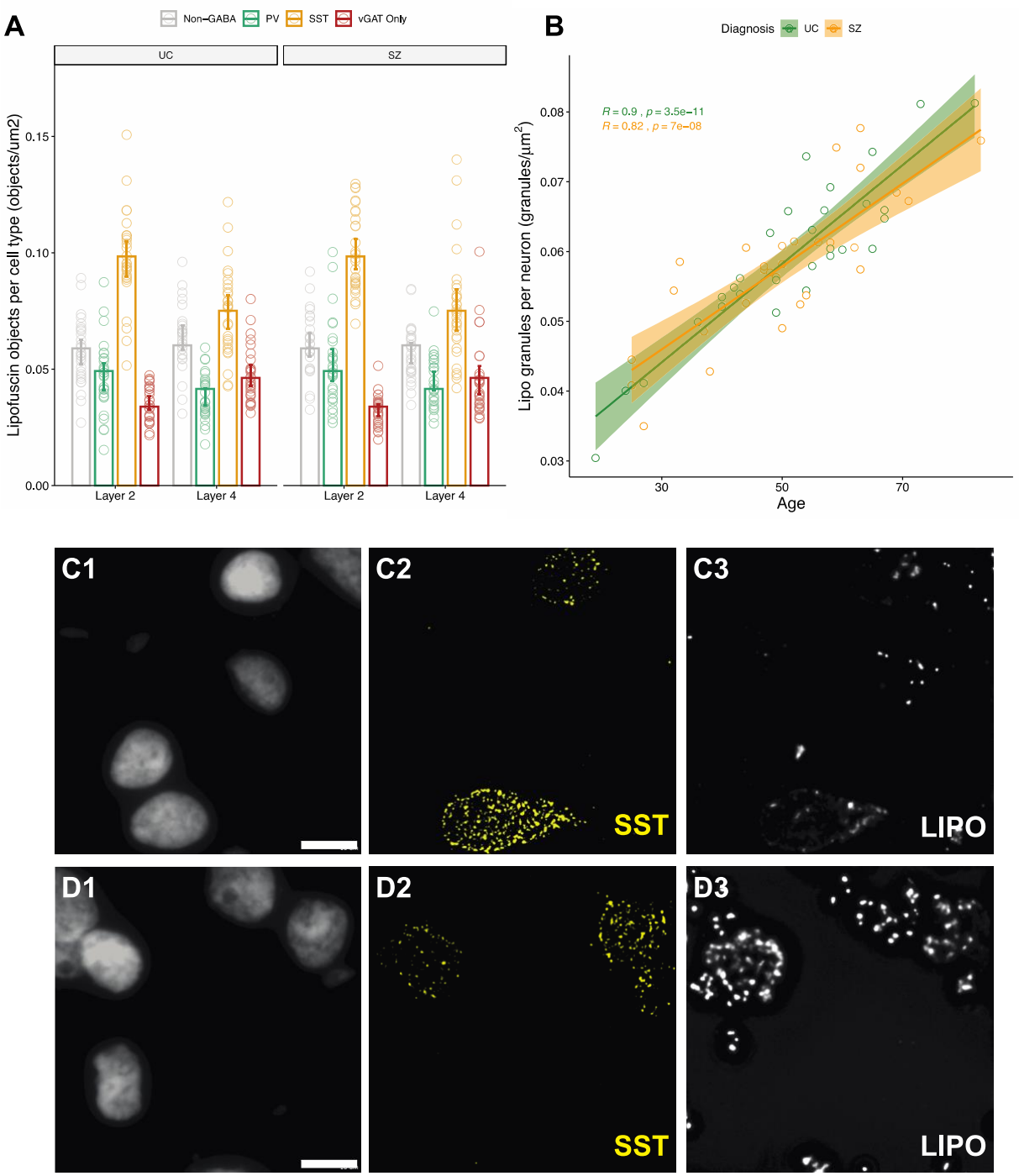

Figure 27. Markedly higher levels of lipofuscin in SST neurons relative to other neuron subtypes.

A) SST neurons exhibit markedly higher levels of lipofuscin relative to other cell types, although the were no differences between diagnostic groups (UC, left, SZ, right). With regard to lipofuscin per neuron, the effect of layer ($F_{1,386} = 11.4$, p. = 0.0008) and cell type ($F_{3,398} = 263.9$, $p < 0.00001$) were both significant, while diagnosis was not. **B)** As predicted, lipofuscin levels per neuron (y-axis) are highly correlated with age in this cohort in both diagnostic groups. **C)** and **D)** Representative images showing lipofuscin accumulation in SST neurons in **(C1-3)** a 24 year old female (HU1099) and in **(D1-3)** a 67 year old female (HU818). Note the accumulation of lipofuscin with aging and the decline in SST signal. Scale bar in C1 and D1 = 10 µm.

5.3 FUNCTIONAL IMPLICATIONS OF ALTERED SOMATOSTATIN NEURONS IN THE DLPFC OF SCHIZOPHRENIA

In this dissertation, I have posited that alterations in SST neuron function in the DLPFC could contribute to cognitive dysfunction, specifically in the context of working memory. For the majority of this dissertation, the interpretation of 'SST neuron' function has revolved around those that appear to preferentially target pyramidal neuron dendrites and provide an inhibitory gate to the excitatory inputs received there. It is important to caveat here that this is not the exclusive type of synaptic connection that SST neurons can make; they also appear to form synaptic connections onto VIP-expressing cells and PV-expressing cells (Campagnola et al., 2022). In rodent cortex, SST cells in layer 4 preferentially target PV neurons over pyramidal cells (Xu et al., 2013). Moreover, the subtype of subcortical white matter SST neuron appears to project their axons over long distance, and it remains unclear what the preferred postsynaptic target is (Tomioka & Rockland, 2007). With those caveats, I constrain the subsequent discussion of functional consequences by inferring the consequences of alterations to SST neuron that synapse onto pyramidal neuron dendrites in layer 2-superficial 3 in the context of the working memory circuit, while briefly commenting on the implications for neurovascular coupling.

5.3.1 Alterations to dendritic integration of inputs in pyramidal neurons in the DLPFC of schizophrenia

As stated in the General Introduction (**1.4.4**), dendritic inhibition clearly has a critical role in controlling the activity of cortical circuits, and possibly refining the tuning curves of excitatory cells. One possibility is that weaker GABA-mediated inhibition from SST neurons contributes to

broader tuning curves in excitatory cells in the DLPFC circuitry in schizophrenia (Starc et al., 2017; Murray et al., 2014b). Functionally, this could result in pyramidal ensembles that are poorly tuned to the specific memoranda to be kept online in working memory

Dendritic inhibition also has a crucial role in the control of calcium spikes in pyramidal neuron dendrites. Classically, calcium signaling in dendrites is thought to be a key player in short and long-term synaptic plasticity. Recently though, and in a manner that appears exclusive to human neocortical layer 2/3 cortical pyramidal neurons, dendritic calcium signaling also results in action potentials generated within the dendrite. These action potentials render certain logical operations (i.e., XOR, not only than AND/OR) to be computed efficiently in a manner not dependent on multilayered networks by suppressing the amplitude of the calcium-mediated action potential when the input strength is above a certain optimal strength (Gidon et al., 2020). Importantly, these dendritic action potentials critically depend on inhibition at dendrites, as inhibition repolarizes the dendritic subregion also targeted by excitatory synapses to recover dendritic action potential amplitude (Gidon et al., 2020). This notion is consistent with the idea that inhibition may also counterintuitively enhance the excitability of the dendrite (Chiu et al., 2013).

Finally, GABAergic inhibition by SST neurons onto dendritic spines might support the stability of those spines over development. For example, GABA signaling onto dendrites has a similar role to glutamate (Kwon & Sabatini, 2011) in the promotion of dendritic spine formation: manipulation of GABA release from SST neurons results in concurrent up- or down-regulation of dendritic spines in development through $GABA_A$ receptors and control of calcium signaling in the dendrites (Oh et al., 2016). One possibility is that dendritic inhibition, mediated through $GABA_A$ receptors, carefully controls calcium signaling in dendrites to both mediate synaptic plasticity in

the form of dendritic spine growth (Marlin & Carter, 2014; Higley, 2014) and prevent excessive calcium signaling which might contribute to degradation cascades contributing to spine deficits (Arnsten et al., 2020). In fact, SST released from SST terminals might have a unique role in controlling dendritic calcium signaling, as described in the next section. Thus, while the available data suggests that pyramidal neuron alterations are upstream to SST alterations in schizophrenia, deficit inhibitory drive from SST neurons onto pyramidal neuron dendrites in the disorder could conversely contribute to pathologic calcium signaling in dendritic spines and subsequent decay of spines.

5.3.1.1 What is the role of SST as a signaling neuropeptide?

Much of this dissertation has focused on SST as a shorthand for a particular subtype of GABA neuron, expressing SST, with certain functional, physiological, and connectivity properties. However, consistent findings of lower SST in the disorder raise important questions about the functional consequences of diminished release of SST as a signaling neuropeptide. As alluded to above, there has been some early evidence that SST itself controls calcium signaling in neurons (Inoue & Yoshii, 1992; Meriney et al., 1994). However, the specific role of SST as a signaling neuropeptide has remained somewhat elusive. Early studies in cell culture report dose-dependent effects of SST on neuronal firing: lower concentrations of SST tended to favor neuronal depolarization, while higher concentrations of SST tend to depress the activity of neurons (Delfs & Dichter, 1983). While this might reflect postsynaptic mechanisms through SST receptors, SST also appears to act on presynaptic SST receptors on excitatory terminals to suppress excitatory output from pyramidal neurons (Boehm & Betz, 1997). In the rodent visual cortex, this connectivity profile was found to improve the visual discrimination *in vivo* by inhibiting excitatory drive onto PV neurons (Song et al., 2020). In the context of schizophrenia, I predict that lower

SST levels contribute to the disrupted homeostatic calcium signaling in dendrites, in concert with diminished GABA signaling from those neurons. Together, these alterations could disrupt the tuning of pyramidal neurons in the DLPFC either directly through their actions on pyramidal neurons or indirectly by altered the excitatory synapses onto PV neurons.

5.3.2 Implications of SST neuron alterations for neurovascular coupling

SST neurons have been clearly implicated in the process known as neurovascular coupling (Cauli et al., 2004; Cauli & Hamel, 2010). This process couples neuronal activity to dilation of local arterioles and increased cerebral blood flow to brain areas that are highly active. A certain transcriptional subtype of SST neuron, namely CHODL-SST neurons, exhibit markedly high levels of nitric oxide synthase 1 (NOS1) (Dawson et al., 1991; Bredt et al., 1991; Yan et al., 1996; Smiley et al., 2000). Moreover, these neurons form close appositions to blood vessels nearby (Vaucher et al., 2000; Ruff, 2021). Upstream signals for the release of nitric oxide onto could come from other neurons in the cerebral cortex that express tachykinin 1 (TAC1), including PV basket cells (Jones et al., 1988) which also have a direct role in the regulation of arteriole dilation (Jansen et al., 1991) and SST neurons, including CHODL-SST cells (unpublished observations). Given the rich expression of TAC1 receptor on CHODL-SST cells, the activity-dependent activation of PV neurons might cause the release of TAC1, which acts in a paracrine manner to stimulate CHODL-SST cells and subsequent release of nitric oxide onto local vasculature (Vruwink et al., 2001). In the context of schizophrenia, lower DLPFC activation during working memory likely reflects deficient neuronal activity and thus less ‘demand,’ but how that demand is translated into altered local cerebral blood flow is less clear. One possibility is that deficient neuronal activity contributes to the activity-dependent downregulation of TAC1 (Hendry et al., 1988; Benson et al., 1994),

leading to lower activation of CHODL-SST neurons that are enriched in the TAC1 receptor and less dilation of arterioles through NO release. In addition, alterations in levels of NOS1 or NPY (which causes vasoconstriction (Cauli et al., 2004)) could alter the coupling of neuronal activity to increases in cerebral blood flow. Elucidation of the alterations in this SST subtype in the context of schizophrenia remains an ongoing study.

5.4 THERAPEUTIC IMPLICATIONS FOR TARGETING SOMATOSTATIN NEURON DYSFUNCTION IN SCHIZOPHRENIA

If the alterations to DLPFC SST neurons in schizophrenia underlie some aspect of working memory disturbances in schizophrenia, then targeting these neurons through novel therapeutic interventions might provide amelioration of the cognitive disturbances in the disorder. The work in this dissertation has shown that SST neurons are present, not absent, in the DLPFC of those with schizophrenia. The presence of a normal complement of SST neurons in schizophrenia motivates new therapeutic strategies that target these neurons and ameliorate their dysfunction, with the goal of restoring the distractor-resistant circuit in the DLPFC. Importantly, because there are no SST neurons to 'replace,' the current findings argue for therapeutic strategies aside from cell-based transplantation approaches (Southwell et al., 2014). Here, I posit three alternative strategies of how therapeutic approaches could contribute to enhanced efficacy of SST neuron signaling in the context of schizophrenia.

One strategy is to enhance the efficacy of presynaptic glutamate release onto SST neurons, and some preclinical models provide support for this strategy. Augmentation of metabotropic glutamate receptor 1 (mGluR1) preferentially enhances the activity of SST neurons in rodent

models, and a mGluR1 positive allostatic modulator restored the cognitive deficits introduced by MK-801, an NMDA receptor antagonist, in rodents (Maksymetz et al., 2021).

Alternatively, if the activity of SST neurons in schizophrenia reflects homeostatic compensatory mechanisms in response to weaker excitation of dendrites, then upregulation of the activity at the site of the dendrite could restore the strength of SST neuron inhibition. As an intriguing new avenue of research in this area involves the use of psychedelics like psilocybin to restore dendritic spine deficits introduced by chronic stress (Shao et al., 2021). The structural alterations in spines are rapid and enduring in rodents, but it is unclear what the impact on SST-mediated inhibition is in this model. The complex role that drugs like ketamine and psilocybin have in cortical circuits requires more research to understand possible region- and cell-type specific consequences (Savalia et al., 2021).

SST neurons classically form synapses onto postsynaptic $GABA_A$ receptors enriched in the α5 subunit (Cao et al., 2020; Ali & Thomson, 2008; Schulz et al., 2018), and agonists acting at $GABA_A$-α5 containing have garnered a great deal of interest for their potential pro-cognitive benefits in preclinical models (Jacob, 2019; Gill & Grace, 2014; Gill et al., 2011). GABAA-α5 receptors might play critical roles in restoring the homeostasis of dendrites, as their administration restores atrophy in the dendritic arbor in aging and stress paradigms (Fee et al., 2021; Prevot et al., 2021; Prevot et al., 2020). Given the early developmental role that GABA has in inducing spine formation (Oh et al., 2016), it is possible that strengthening of these GABAergic synapses might restore the dendritic dysfunction observed in schizophrenia (Glausier & Lewis, 2013).

Finally, SST analogues, the most common of which is octreotide, have been used clinically for the treatment of disorders of excessive growth hormone release and other endocrine disorders. However, these drugs do not seem feasible for the treatment of brain disorders, including

schizophrenia, given their poor passage through the blood-brain barrier, although some novel approaches are seeking to remedy this problem to improve the availability of SST analogues to enter the brain (Song et al., 2021). The functional consequences of such a strategy are unclear, but side effects relating to endocrine function seem likely based on the role of SST in the hypothalamus.

5.5 CONCLUSIONS & FUTURE DIRECTIONS

In conclusion, the findings of this dissertation work contribute to a body of knowledge advancing knowledge about GABA neuron disruption in the context of schizophrenia. This knowledge elucidates different hypotheses for the emergence of those disruptions in schizophrenia and how we might develop more specific therapeutics to target those disruptions.

5.5.1 Further elucidation of mechanisms that render SST mRNA levels lower in schizophrenia

Here, I have posited the idea that deficits in SST and GAD67 mRNA within SST neurons are a reflection of upstream alterations in pyramidal neurons. While both transcripts are clearly activity-dependent (Hou & Yu, 2013; Benson et al., 1994), evidence of this cause-and-effect relationship within cortical circuits is lacking. To address this, I propose to examine SST and GAD67 mRNA levels in a variety of animal models with downregulated pyramidal neuron activity. For example, ARP2/3 knockout mice (Kim et al., 2013) introduce spine deficits in cortical pyramidal neurons in embryo, likely introducing early alterations in excitatory drive that could

lead to lower levels of SST mRNA. Indeed, in the medial PFC of these mice, SST mRNA levels are lower (**Table 6**), in support of the model that genetically mediated deficits in dendritic spines in schizophrenia contribute to alterations in SST neurons.

In addition, it has been previously shown that embryonic or adult gene deficits in BDNF production result in lower levels of SST and NPY in these mice (Glorioso et al., 2006; Hashimoto et al., 2005). However, these prior studies were not able to assess whether the timing of the knockout interacted with the distinct subtypes of affected SST neurons. I hypothesize that embryonic, and not adult, deficits in BDNF result in deficits in SST expression specifically in the CHODL-SST subtype. In support of this hypothesis, a survey of prior labeled *in situ* slides for SST and NPY mRNA in these mice showed that SST levels are lower in the gray matter of the medial PFC, but not in the corpus callosum or striatum, where CHODL-SST neurons are enriched. Affirmative findings would offer insight into laminar differences in SST alterations observed in schizophrenia compared to major depressive disorder (**Appendix D**).

Consistent with this idea, manipulations in pyramidal neuron function should take place at multiple developmental stages. To accomplish this, current studies are investigating the alterations to SST and GAD67 within SST neurons in the context of viral-mediated downregulation of pyramidal neuron activity through overexpression of Kir2.1 (Xue et al., 2014). Kir2.1 under control of the CamKIIA promoter renders pyramidal neurons hypoactive by introducing potassium channels that bring the membrane potential closer to –90 mV. In one monkey, we found robust labeling of the transfected gene, mouse Kir2.1 (Kcnj2) mRNA within pyramidal and not SST neurons. At the site of injections, however, levels of SST mRNA were lower compared to the non-injection sites (**Table 6**). Future experiments should be conducted that control for the injection

manipulation by injection of a Kir2.1 channel with a mutation in the pore that renders this channel nonconducting.

Finally, the association of lipofuscin accumulation, age, and downregulation of SST mRNA with aging raise the interesting possibility that higher lipofuscin accumulation contributes to the deficits in SST mRNA. To address this causal link, progranulin-deficient mice accumulate lipofuscin much faster than wild-type animals (Ahmed et al., 2010; Evers et al., 2017; Kao et al., 2017). In these animals, I propose to examine the age-dependent decline in SST mRNA levels, with the hypothesis that this decline is accelerated in the progranulin deficient animals (Table

Table 6. Proposed experimental systems to elucidate upstream causes of lower SST.

Experimental System	Species	Timing	SST mRNA Alteration
ARP2/3 Knockout	*Mus musculus*	Embryo	mPFC: –19.9% | M1: +4.0%
BDNF Knockout	*Mus musculus*	Embryo	mPFC: –46.3% | CC: –44.9% | STR: – 36.3%
BDNF Knockout	*Mus musculus*	Adult	mPFC: –31.6% | CC: –14.5% | STR: –5.4%
Kir2.1 Viral Overexpression in Pyramidal neurons	*Rhesus macaque*	Adult	Injection Site: –26.8%
Progranulin Deficiency	*Mus musculus*	Embryo	?

Abbreviations: mPFC, medial prefrontal cortex; M1, motor cortex; CC, corpus callosum; STR, striatum. Percentages reflect initial findings from pilot studies in these systems.

5.5.2 Somatostatin from the cradle to the grave: examining age-dependent trajectories in SST neuron function

One of the outstanding questions raised from this dissertation work regards the timing of GABA neuron alterations in schizophrenia. We have posited that alterations in GABA neurons are a consequence of temporally and causally upstream alterations in pyramidal neurons (Dienel et al., 2022). One possibility is that genetic risk for schizophrenia enriched in excitatory cells early in development interferes with the normal maturation of SST neurons (Pan et al., 2019; Wong et al., 2018a). However, finding of a normal complement of SST neurons in the present study argues against a frank migratory deficit, as observed in some of those animal models (Wong et al., 2018a).

Alternatively, these alterations could emerge later in embryogenesis, given the early maturational profile of SST expression in embryo (Fitzpatrick-McElligott et al., 1991; Hayashi & Oshima, 1986; Yamashita et al., 1989; Wahle, 1993; Chun & Shatz, 1989). This early maturation of SST neurons appears to be critical for the developmental of cortical layers (Tuncdemir et al., 2016). Thus, maternal immune activation might contribute to a deficit in the proper maturation of SST neurons, although the mechanisms of that interaction remain unclear (Duchatel et al., 2019a; Duchatel et al., 2016) and may not capture the nature of the alteration observed in schizophrenia. Thus, I propose to examine SST neurons in the context of an animal model of maternal immune activation to assess whether this recapitulates the disease alterations or is reflective of a disease process that might not be operative in schizophrenia.

Moreover, fundamental questions about the postnatal developmental trajectory of SST neurons remains unclear. The available data suggests that individuals have the highest levels of SST at birth, and those levels decline steadily throughout life (Fung et al., 2010; Hoftman et al., 2015). However, other factors of the developmental profile of SST neurons in the DLPFC are

unclear and could have implications for the working memory over the course of adolescence. For example, humans (Olesen et al., 2007) and monkeys (Zhou et al., 2016) appear to improve in their ability to resist distracting stimuli during adolescence. Therefore, I hypothesize that levels of GAD67 increase specifically in the SST neuron population over the course of adolescent development, and that this increased capacity to provide GABA inhibition onto dendrites by SST cells contributes to the age-associated improvement in distractor resistance.

If the model we propose is explanatory (Dienel et al., 2022), then individuals in the earliest stages of the disease course of schizophrenia should show deficits in SST levels than what would be expected for this age. There is some weak evidence supporting this idea, given the alterations in even young individuals with schizophrenia shown in Chapter 3. However, only a few individuals fell into this category. In a future experiment, I would be interested in utilizing a cohort of younger (ages 20-35) individuals diagnosed with schizophrenia to assess whether the alterations in SST neurons are present at this early stage of the disorder. In our brain bank, there are at least 15 individuals with schizophrenia who fit into this age group.

Finally, given the vulnerability of SST neurons in a panoply of neuropsychiatric conditions and aging, I am interested in dissecting the relationship between these factors. I think an important first step towards this goal would be to characterize the nature of SST alterations in multiple disorders in the aged population, comparing individuals with Alzheimer's disease, early Braak stage individuals, late life mood disorders (Sweet et al., 2004), elder individuals with schizophrenia, and neuropsychiatrically unaffected individuals. Characterizing the nature of the SST alterations across these conditions could suggest interesting hypotheses about how each disorder could individually lead to lower SST through distinct disease pathways. In a first step towards supporting that hypothesis, diagnosis-specific alterations across SST in different laminar

locations and different subtypes could generate new ideas about how different upstream factors might lead to a similar outcome in each disorder (i.e., lower SST).

5.5.3 Conclusions

In conclusion, results of this dissertation work have demonstrated that SST neuron enrichment in the DLPFC reflects differences in the proportion of SST neurons in that region, and not differences in SST expression levels per neuron. Conversely, the SST mRNA deficit observed in schizophrenia is due to lower levels of SST mRNA per neuron and not fewer neurons. Finally, inhibition from SST neurons is very likely weaker in schizophrenia, given lower levels of the principal GABA synthesizing enzyme, GAD67, in these cells. Together, our findings illuminate that the DLPFC enrichment in SST neurons, and the alterations to that cell type in schizophrenia, likely underlie the normative distractor-resistant circuit in the DLPFC and the heightened sensitivity to distractors in people with schizophrenia. These cognitive functions likely have generalizable outcomes that reflect functional outcomes in schizophrenia. Given the normal complement of SST neurons in schizophrenia, therapeutic strategies that restore the function of these neurons offer hope for the introduction of a novel pro-cognitive therapeutics that might finally ameliorate the cognitive burden in the disorder and improve the lives of those with it.

APPENDIX A DEMOGRAPHIC, POSTMORTEM, AND CLINICAL CHARACTERISTICS OF HUMAN BRAIN TISSUE SPECIMENS USED IN THIS DISSERTATION

Appendix Table 1. Demographic and tissue characteristics of human postmortem subjects used in Chapter 3.0.

Unaffected Comparison Subjects

Pair	Case	Sex	Race	Age (yr)	BMI	PMI (hr)	pH[a]	RIN	Tissue Storage Time (mo)[b]	Medications ATOD[c]	Tobacco ATOD	Manner of Death	Cause of Death
1	1406	M	B	27	34.9	14.6	6.3	8.3	162.2	N	Y	Natural	Peritonitis
2	700	M	W	42	U	26.1	7.1	8.7	282.1	N	U	Natural	Cardiovascular Disease
3	988	M	W	82	29.6	22.5	6.7	8.4	273.9	O	N	Accidental	Blunt Force Trauma
4	806	M	W	57	28.0	23.8	7.0	7.8	278.0	O	N	Natural	Pulmonary Embolism
5	852	M	W	54	34.4	8.2	6.8	9.1	224.8	N	Y	Natural	Cardiac Tamponade
6	987^	F	W	65	26.5	21.6	6.7	9.1	249.3	O	N	Natural	Cardiovascular Disease
7	727	M	B	19	25.6	7.0	7.0	9.2	224.8	N	N	Accidental	Blunt Force Trauma
8	1374	M	W	43	41.0	21.7	6.6	7.2	258.0	O	Y	Natural	Cardiovascular Disease
9	818	F	W	67	37.8	23.5	7.1	8.4	248.1	O	N	Accidental	Anaphylaxis
10	857	M	W	48	21.7	16.2	6.7	8.9	273.0	N	Y	Natural	Cardiovascular Disease
11	739	M	W	40	19.2	15.8	6.7	8.4	209.1	N	Y	Natural	Cardiovascular Disease
12	10003	M	W	49	29.2	21.2	6.5	8.4	174.1	N	N	Accidental	Blunt Force Trauma
13	1122	M	W	55	29.2	15.4	6.5	8.9	205.5	O	Y	Natural	Cardiac Tamponade
14	1336	M	W	65	27.8	18.4	6.7	8.0	184.6	O	Y	Natural	Cardiac Tamponade
15	1092	F	B	40	39.3	16.6	6.7	8.0	226.9	O	N	Natural	Mitral Valve Prolapse
16	1284	M	W	55	25.2	6.4	6.8	8.7	198.0	N	Y	Natural	Cardiovascular Disease
17	970	M	W	42	28.6	25.9	6.4	7.2	190.1	N	Y	Natural	Cardiovascular Disease
18	1268	M	B	49	27.1	19.9	6.9	7.9	176.6	O	N	Natural	Cardiovascular Disease
19	1247	F	W	58	35.9	22.7	6.2	8.4	208.1	O	N	Natural	Cardiovascular Disease
20	1159	M	W	51	38.5	16.7	6.5	7.6	202.0	O	N	Natural	Cardiovascular Disease
21	1326	M	W	58	32.1	16.4	6.7	8.0	176.2	O	N	Natural	Cardiovascular Disease
22	1466	F	B	64	27.1	20.0	6.7	8.8	241.2	O	N	Accidental	Blunt Force Trauma
23	902	M	W	60	25.2	23.6	6.6	7.7	169.4	N	Y	Natural	Cardiovascular Disease
24	1792	F	W	36	21.0	28.1	6.4	7.5	186.9	O	Y	Natural	Pulmonary Embolism
25	1270	F	W	73	24.6	19.7	6.7	7.7	151.8	O	N	Accidental	Blunt Force Trauma
26	1583	M	W	58	23.2	19.1	6.7	8.2	94.0	N	Y	Accidental	Blunt Force Trauma
27	1384	M	W	67	26.5	21.9	6.6	7.0	186.6	O	Y	Natural	Cardiovascular Disease
28	1558	M	W	54	20.6	24.4	6.8	7.7	129.4	O	N	Natural	Cardiovascular Disease
29	1324	M	W	43	30.9	22.3	6.8	7.3	167.3	N	N	Natural	Aortic Dissection
30	1099	F	W	24	18.2	9.1	6.5	8.6	134.2	O	Y	Natural	Cardiomyopathy
	Mean			**51.5**	**28.6**	**19.0**	**6.7**	**8.2**	**202.9**				
	Standard Deviation			**14.3**	**6.1**	**5.7**	**0.2**	**0.6**	**47.0**				

Schizophrenia Subjects

Pair	Case	DSM-IV Schizophrenia Diagnosis ATOD	Duration of Schizophrenia Diagnosis (yr)	DSM-IV Co-Morbid Substance Use Diagnosis ATOD	Sex	Race	Age (yr)	BMI	PMI (hr)	pH[a]	RIN	Tissue Storage Time (mo)[b]	Medications ATOD[c]	Tobacco ATOD	Manner of Death	Cause of Death
1	547	Schizoaffective Disorder	9	None	M	B	27	U	16.5	6.9	7.4	301.0	B C D L O P	U	Accidental	Heat Stroke
2	539	Schizoaffective Disorder	31	None	M	W	50	26.4	40.9	6.9	8.1	306.6	C D O P	Y	Undetermined	Combined Drug Overdose
3	621	Undifferentiated Schizophrenia	55	None	M	W	83	22.6	15.6	7.2	8.7	254.8	O	U	Accidental	Asphyxiation
4	665	Paranoid Schizophrenia	32	Alcohol Dependence	M	B	59	26.3	28.0	7.0	9.2	302.2	D O P	Y	Natural	Intestinal Hemorrhage
5	781	Schizoaffective Disorder	15	None	M	B	52	21.1	8.0	6.7	7.7	288.4	D O P	Y	Accidental	Peritonitis
6	802	Schizoaffective Disorder	43	Alcohol Dependence	F	W	63	25.2	28.9	7.0	9.2	264.2	C O P	Y	Natural	Cardiovascular Disease
7	829	Schizoaffective Disorder	5	Alcohol Dependence	M	W	25	24.2	5.0	6.8	9.3	260.1	B C	Y	Suicide	Salicylate Overdose
8	904	Schizoaffective Disorder	8	None	M	W	33	38.4	28.0	6.3	7.1	238.0	C O P	Y	Natural	Pneumonia
9	917	Undifferentiated Schizophrenia	50	None	F	W	71	25.5	23.8	7.1	7.0	234.6	O P	Y	Natural	Cardiovascular Disease
10	930	Disorganized Schizophrenia	28	None	M	W	47	34.6	15.3	6.3	8.2	234.0	C O	Y	Natural	Cardiovascular Disease
11	933	Disorganized Schizophrenia	22	None	M	W	44	45.6	8.3	6.1	8.1	200.5	C D O P	N	Natural	Myocarditis
12	1088	Undifferentiated Schizophrenia	24	Alcohol Dependence;	M	W	49	27.1	21.5	6.4	8.1	200.7	D O P	Y	Accidental	Combined Drug Overdose
13	1105	Schizoaffective Disorder	5	None	M	W	53	30.3	7.9	6.1	8.9	207.6	P	Y	Natural	Cardiovascular Disease
14	1173	Disorganized Schizophrenia	33	None	M	W	62	22.9	22.9	6.3	7.7	198.9	O P	Y	Natural	Cardiovascular Disease
15	1178	Schizoaffective Disorder	11	None	F	B	37	31.7	18.9	6.1	8.4	194.1	B P	Y	Natural	Pulmonary Embolism
16	1188	Undifferentiated Schizophrenia	33	None	M	W	58	17.3	7.7	6.1	8.4	209.5	C O P	Y	Natural	Cardiovascular Disease
17	1222	Undifferentiated Schizophrenia	16	Alcohol Abuse	M	W	32	31.8	30.8	6.4	7.5	190.9	D P	N	Suicide	Combined Drug Overdose
18	1230	Undifferentiated Schizophrenia	28	None	M	W	50	31.9	16.9	6.4	8.2	190.2	D O P	Y	Suicide	Doxepin Overdose
19	1240	Undifferentiated Schizophrenia	25	None	F	B	50	44.6	22.9	6.2	7.7	189.4	O P	Y	Natural	Cardiovascular Disease
20	1296	Undifferentiated Schizophrenia	35	None	M	W	48	16.7	7.8	6.3	7.3	182.3	D O P	Y	Natural	Pneumonia
21	1314	Undifferentiated Schizophrenia	33	None	M	W	50	22.1	11.0	6.6	7.2	178.8	C D O P	N	Natural	Cardiovascular Disease
22	1341	Schizoaffective Disorder	30	Opioid Dependence	F	W	44	19.1	24.5	6.5	8.8	171.5	B O P	N	Accidental	Penetrating Force Trauma
23	1361	Schizoaffective Disorder	47	None	M	W	63	26.7	23.2	6.4	7.7	241.2	C O P	Y	Natural	Cardiomyopathy
24	1506	Schizoaffective Disorder	29	Alcohol Dependence	F	W	47	48.7	14.1	6.6	7.5	192.5	D O P	Y	Accidental	Combined Drug Overdose
25	1579	Schizoaffective Disorder	44	Alcohol Dependence;	F	W	69	22.9	16.1	6.6	7.7	173.4	B O P	Y	Natural	Cardiovascular Disease
26	1686	Paranoid Schizophrenia	36	None	M	B	56	28.5	14.1	6.2	8.3	144.8	B D O P	Y	Natural	Cardiovascular Disease
27	1712	Schizoaffective Disorder	45	Sedative or Hypnotic or	M	W	63	33.1	15.1	6.1	7.1	130.0	C D O P	N	Natural	Cardiovascular Disease
28	1734	Undifferentiated Schizophrenia	32	Cannabis Dependence	M	W	54	22.8	28.6	6.1	7.7	112.7	O P	Y	Natural	Pneumonia
29	10020	Paranoid Schizophrenia	20	Alcohol Abuse; Other/Unknown	M	W	38	19.8	28.8	6.5	7.4	106.3	C D P	Y	Suicide	Salicylate Overdose
30	10023	Disorganized Schizophrenia	10	None	F	B	25	32.8	20.1	6.5	7.4	102.6	B D P	N	Suicide	Drowning
	Mean		**27.8**				**50.1**	**28.3**	**19.0**	**6.5**	**8.0**	**206.7**				
	Standard Deviation		**13.7**				**13.8**	**8.2**	**8.6**	**0.3**	**0.7**	**56.1**				

Footnotes:

[a]Reported value is the mean of prefrontal and cerebellar or occipital pH values. Case 818 is the exception, with only the prefrontal pH value reported.

[b]Stored at -80C

[c]Medications at time of death: B, benzodiazepines; C, anticonvulsants; D, antidepressants; L, lithium; N, no medications; O, other medication(s); P, antipsychotic; U, unknown

^987: Posttraumatic Stress Disorder in remission for 39 years

Abbreviations yr, years; PMI, postmortem interval (hours); RIN, RNA integrity number; mo, months; ATOD, at time of death; F, female; M, male; B, black; W, white; Y, yes; N, no; U, unknown

Appendix Table 2. Demographic and tissue characteristics of human postmortem subjects used in Chapter 4.0.

Unaffected Comparison Subjects													Schizophrenia Subjects													
Case	Sex	Race	Age (yr)	BMI	PMI (hr)	pH[a]	RIN	Tissue Storage Time (mo)[b]	Medications ATOD[c]	Tobacco ATOD	Manner of Death	Cause of Death	Case	DSM-IV Schizophrenia Diagnosis ATOD	Duration of Schizophrenia Diagnosis (yr)	DSM-IV Co-Morbid Substance Use Diagnosis ATOD	Sex	Race	Age (yr)	BMI	PMI (hr)	pH[a]	RIN	Tissue Storage Time (mo)[b]	Medications ATOD[c]	Tobacco ATOD	Manner of Death	Cause of Death
686	F	W	52	27.3	22.6	7.1	8.5	278	O	Y	Natural	Cardiovascular Disease	517	Disorganized Schizophrenia	20	Alcohol Dependence	F	W	48	20.4	3.7	6.7	9.3	302.7	P	Y	Natural	Intracerebral Hemorrhage
789	M	W	22	23.4	20.1	6.9	7.8	260.7	N	N	Accidental	Asphyxiation	537	Schizoaffective Disorder	8	None	F	W	37	U	14.5	6.8	8.6	300.3	N	U	Suicide	Asphyxiation
795	M	W	68	28.7	11.8	6.7	8.2	259.2	N	N	Natural	Ruptured Aortic Aneurysm	587	Undifferentiated Schizophrenia	20	None	F	B	38	38.3	16.9	7	9	292.1	B L O P	Y	Natural	Cardiovascular Disease
838	M	W	58	24.5	16.5	7.1	8.5	249.9	O	N	Natural	Cardiovascular Disease	656	Schizoaffective Disorder	30	Alcohol Dependence	F	B	47	20.1	19.8	7.2	9.2	282.2	O P	Y	Suicide	Gunshot Wound
840^	F	W	41	26.1	15.4	6.7	9.1	249.5	N	Y	Natural	Cardiovascular Disease	781	Schizoaffective Disorder	15	None	M	B	52	21.1	8	6.7	7.7	262.2	D O P	Y	Accidental	Peritonitis
841	M	W	70	26.6	21.2	7.3	7.2	249.4	N	N	Natural	Cardiomyopathy	787	Schizoaffective Disorder	3	Cannabis Abuse	M	B	27	34.7	19.1	6.9	8.4	261	O P	N	Suicide	Gunshot Wound
855	M	B	62	23.3	11.4	7	8.4	246.1	O	N	Natural	Cardiomyopathy	802	Schizoaffective Disorder	43	Alcohol Dependence	F	W	63	25.2	28.9	7	9.2	258	C O P	Y	Natural	Cardiovascular Disease
988	M	W	82	29.6	22.5	6.7	8.4	222.8	O	N	Accidental	Blunt Force Trauma	843	Disorganized Schizophrenia	16	None	F	W	41	22.6	17.1	7.1	9.4	249	P	Y	Suicide	Blunt Force Trauma
1031	M	W	53	34.8	23.2	7	8.9	215.6	N	N	Natural	Cardiovascular Disease	917	Undifferentiated Schizophrenia	50	None	F	W	71	25.5	23.8	7.1	7	235.9	O P	Y	Natural	Cardiovascular Disease
1047	M	W	43	29.4	13.8	6.6	9	213.6	O	N	Natural	Cardiovascular Disease	930	Disorganized Schizophrenia	28	None	M	W	47	34.6	15.3	6.3	8.2	232.5	C O	Y	Natural	Cardiovascular Disease
1081^	F	W	57	26.9	14.9	6.8	9	208.2	B O	N	Natural	Chronic Obstructive Pulmonary Disease	1088	Undifferentiated Schizophrenia	24	Alcohol Dependence; Cannabis Abuse	M	W	49	27.1	21.5	6.4	8.1	207.5	D O P	Y	Accidental	Combined Drug Overdose
1086	M	W	51	25.5	24.2	6.7	9.3	207.7	N	Y	Natural	Cardiovascular Disease	1178	Schizoaffective Disorder	11	None	F	B	37	31.7	18.9	6.1	8.4	198.5	B P	Y	Natural	Pulmonary Embolism
1092	F	B	40	39.3	16.6	6.7	8	207.1	O	N	Natural	Mitral Valve Prolapse	1188	Undifferentiated Schizophrenia	33	None	M	W	58	17.3	7.7	6.1	8.4	196.8	C O P	Y	Natural	Cardiovascular Disease
1153	M	W	55	34.2	28	6.4	8	200.5	N	N	Natural	Cardiovascular Disease	1189	Schizoaffective Disorder	4	None	F	W	47	37.8	14.4	6.3	8.3	196.6	B C D O P	Y	Suicide	Combined Drug Overdose
1196^	F	W	36	23.3	14.5	6.4	8.2	195.8	O	N	Accidental	Asphyxiation	1211	Schizoaffective Disorder	12	None	F	W	41	32.4	20.1	6.3	7.8	194.2	D O P	Y	Natural	Cardiovascular Disease
1247	F	W	58	35.9	22.7	6.2	8.4	188.1	O	N	Natural	Cardiovascular Disease	1222	Undifferentiated Schizophrenia	16	Alcohol Abuse	M	W	32	31.8	30.8	6.4	7.5	192	D P	N	Suicide	Combined Drug Overdose
1282	F	W	39	30.6	24.5	6.8	7.5	182.7	N	N	Natural	Cardiovascular Disease	1240	Undifferentiated Schizophrenia	25	None	F	B	50	44.6	22.9	6.2	7.7	188.8	O P	Y	Natural	Cardiovascular Disease
1293	F	W	65	19.7	18.5	6.5	7	180.8	N	N	Accidental	Blunt Force Trauma	1256	Undifferentiated Schizophrenia	6	None	M	W	34	22.2	27.4	6.3	7.9	186.6	P	N	Suicide	Asphyxiation
1298	M	W	48	36.4	24.5	6.6	7.9	179.7	N	N	Natural	Cardiovascular Disease	1263	Undifferentiated Schizophrenia	41	None	M	W	62	17.9	22.7	6.7	8.5	185.7	D P	Y	Accidental	Asphyxiation
1324	M	W	43	30.9	22.3	6.8	7.3	174.5	N	N	Natural	Aortic Dissection	1314	Undifferentiated Schizophrenia	33	None	M	W	50	22.1	11	6.6	7.2	176.8	C D O P	N	Natural	Cardiovascular Disease
1355	F	W	74	29	24.9	6.6	7	169.9	O	N	Natural	Subarachnoid Hemorrhage	1341	Schizoaffective Disorder	30	Opioid Dependence	F	W	44	19.1	24.5	6.5	8.8	171.3	B O P	N	Accidental	Penetrating Force Trauma
1371	M	B	33	20.9	13	6.2	8.5	167.9	O	N	Natural	Myocarditis	1367	Schizoaffective Disorder	24	Alcohol Dependence; Cocaine Dependence	M	W	47	34.3	28.9	6.5	7.2	168.9	N	N	Accidental	Combined Drug Overdose
1374	M	W	43	41	21.7	6.6	7.2	167.4	O	Y	Natural	Cardiovascular Disease	1420	Schizoaffective Disorder	29	None	M	W	47	32.3	23.4	6.8	8.2	157.7	D P	Y	Suicide	Blunt Force Trauma
1391	F	W	51	28.3	7.8	6.5	7.1	163.5	O	Y	Natural	Cardiovascular Disease	1453	Paranoid Schizophrenia	32	Alcohol Dependence	M	W	62	23.3	11.1	6.4	8.2	152	B D O P	Y	Accidental	Blunt Force Trauma
1394	M	W	45	23.3	17.3	6.5	7.3	162.5	N	N	Natural	Cardiovascular Disease	1454	Paranoid Schizophrenia	33	None	M	W	59	32.4	24.1	6.1	7.6	151.1	D O P	Y	Accidental	Blunt Force Trauma
1403^	F	W	45	22.5	12.3	6.5	8.2	160.9	O	Y	Natural	Cardiovascular Disease	1506	Schizoaffective Disorder	29	Alcohol Dependence	F	W	47	48.7	14.1	6.6	7.5	142.8	D O P	Y	Accidental	Combined Drug Overdose
1429	M	B	44	36	23.9	6.8	7.5	156.1	O	N	Natural	Cardiomyopathy	1542	Paranoid Schizophrenia	40	None	M	W	65	29.8	17.4	6.5	7.8	134.2	B D O P	Y	Undetermined	Combined Drug Overdose

1444	M	W	46	30.4	22	6.4	8.4	153.7	N	N	Natural	Pulmonary Embolism	1579	Schizoaffective Disorder	44	Alcohol Dependence; Sedative or Hypnotic or	F	W	69	22.9	16.1	6.6	7.7	127.9	B O P	Y	Natural	Cardiovascular Disease
1482	M	W	25	35.6	20.2	6.5	9.1	147.5	N	N	Natural	Cardiovascular Disease	1629	Schizoaffective Disorder	24	None	M	B	53	24	14.6	6.4	8.1	120.9	O P	Y	Natural	Sepsis
1489	M	W	25	18.7	16.9	6.3	8.3	146.7	O	N	Natural	Hypoglycemia	1691	Paranoid Schizophrenia	29	Opioid Dependence	M	W	51	34.4	31.9	6.5	7.7	109	B L O P	Y	Accidental	Combined Drug Overdose
1598	M	W	50	29.4	23.8	6.8	7.8	125.2	N	N	Natural	Cardiovascular Disease	1706	Schizoaffective Disorder	41	None	M	B	60	31.7	28.1	6.6	8.4	105.5	O P	Y	Undetermined	Sepsis
1605	F	W	21	26.8	23.9	6.8	8.2	123.7	O	N	Natural	Cardiovascular Disease	1734	Undifferentiated Schizophrenia	32	Cannabis Dependence	M	W	54	22.8	28.6	6.1	7.7	100.5	O P	Y	Natural	Pneumonia
1637	M	W	46	32.9	16.6	6.9	8.2	119.6	N	N	Natural	Cardiovascular Disease	1807	Schizoaffective Disorder	28	Alcohol Dependence	M	B	36	34.3	14.1	7	8.6	89.5	D O P	Y	Suicide	Blunt Force Trauma
1694	F	W	67	25.3	8.5	6.7	8.9	108.6	O	N	Natural	Myocarditis	10020	Paranoid Schizophrenia	20	Alcohol Abuse; Other/Unknown Substance	M	W	38	19.8	28.8	6.5	7.4	188.2	C D P	Y	Suicide	Salicylate Overdose
1719	M	W	48	47.9	25.5	6.4	7.9	102.7	B O	N	Natural	Pulmonary Embolism	10023	Disorganized Schizophrenia	10	None	F	B	25	32.8	20.1	6.5	7.4	187.4	B D P	N	Suicide	Drowning
1770	M	W	52	30	28.3	6.8	8.2	96.5	N	N	Accidental	Asphyxiation	10024	Paranoid Schizophrenia	17	None	M	B	37	25.8	6	6.1	7.5	186.9	O	N	Natural	Cardiovascular Disease
1783^	F	W	23	29.6	15.9	6.7	8.5	93.4	O	Y	Accidental	Blunt Force Trauma	10025	Disorganized Schizophrenia	30	None	M	B	52	22.5	27.1	6.6	7.8	186.7	N	Y	Natural	Cardiovascular Disease
1789	F	W	53	34.2	13.7	6.8	8.5	92.4	N	Y	Natural	Cardiovascular Disease	10026	Undifferentiated Schizophrenia	24	None	F	W	46	20.8	23.8	6.6	7.6	186.5	D O P	Y	Suicide	Thermal Injuries
1792	F	W	36	21	28.1	6.4	7.5	92	O	Y	Natural	Pulmonary Embolism	13045	Schizoaffective Disorder	22	Opioid Dependence; Sedative or Hypnotic or	F	W	29	23.2	8.3	6.3	7.9	77.4	C D O P	Y	Undetermined	Undetermined
10003	M	W	49	29.2	21.2	6.5	8.4	196	N	N	Accidental	Blunt Force Trauma	13097	Paranoid Schizophrenia	5	Alcohol Abuse; Cannabis Dependence	M	W	25	20.5	24.3	6.6	7.7	68.7	D P	Y	Suicide	Doxepin Overdose
10019^	F	B	41	38.2	19.3	6.6	7.6	189.3	O	N	Natural	Cardiomyopathy	13316	Paranoid Schizophrenia	U	Cocaine Abuse; Opioid Abuse	M	W	24	30.8	25	6.3	7	40	C D O P	U	Accidental	Combined Drug Overdose
13082	M	W	41	39.3	27.4	6.4	7.4	71.3	O	N	Natural	Cardiovascular Disease																
13149	F	W	46	26	7.6	6.3	7.9	61.6	N	N	Natural	Cardiovascular Disease																

Footnotes:

[a]Reported value is the mean of prefrontal and cerebellar or occipital pH values

[b]Stored at -80C

[c]Medications at time of death: B, benzodiazepines; C, anticonvulsants; D, antidepressants; L, lithium; N, no medications; O, other medication(s); P, antipsychotic; U, unknown

* In remission ATOD

^ 840- Adjustment Disorder, Current; Alcohol Abuse, In Remission 20 years

^1081- Alcohol Abuse, In Remission 20 years

^1196- Alcohol Intoxication, Current

^1403- Adjustment Disorder, In Remission 0.7 years

^1783- Premenstrual Dysphoric Disorder

^10019- Conduct Disorder, In Remission 24 years; Alcohol Abuse, In Remission 6 years; Cannabis and Cocaine Abuse, In Remission 8 years

Abbreviations:

yr, years; BMI, body mass index; PMI, postmortem interval (hours); RIN, RNA integrity number; mo, months; ATOD, at time of death; F, female; M, male; B, black; W, white; Y, yes; N, no; U, unknown

APPENDIX B SUPPLEMENTAL INFORMATION FOR CHAPTER 2.0

DISTINCT LAMINAR AND CELLULAR PATTERNS OF SOMATOSTATIN TRANSCRIPT EXPRESSION IN MONKEY PREFRONTAL AND VISUAL CORTICES

Appendix Table 3. Primer sets and FISH probe design used in Chapter 2.0.

Gene	Species	Accession #	Forward Primer (F) Reverse Primer (R)	Efficiency
Beta Actin	*Macaca mulatta*	NM_001033084	(F1) gatgtggatcagcaagca (R1) agaaagggtgtaacgcaacta	100%
Cyclophillin	*Macaca mulatta*	NM_001032809	(F2) gcagacaaggttccaaag (R2) gaagtcaccaccctgacac	100%
Glyceraldehyde-3-phosphate dehydrogenase (GAPDH)	*Macaca mulatta*	XM_001105471.1	(F8) tgccccaccaactgcttagc (R8) agtgatggcgtggactgtg	97%
Glutamic acid decarboxylase 1 (GAD67)	*Macaca mulatta*	XM_001082995.2	(F2) aggaagcaccgccataaa (R2) cagcacacccatcatcttgt	97%
Glutamic acid decarboxylase 2 (GAD65)	*Macaca mulatta*	XM_001101800	(F4) cccaaagcggatgtcaacta (R1) atcttgcagaaacgccaaag	99%
SLC32A1 solute carrier family 32 (GABA vesciular transporter member 1, vGAT)	*Macaca mulatta*	XM_001089139	(F3) aaggccgtgtccaagttc (R3) tgcccgcgatagacagta	97%
SLC6A1 solute carrier family 6 member 1 (GABA member transporter 1, GAT1)	*Macaca mulatta*	XM_001088606	(F5) gatcggcctctctaacatcac (R5) aaagaacacgaggaacagcag	98%
Calbindin 2 (calretinin, CR)	*Macaca mulatta*	XM_002802566	(F3) atgagctggatgcccttt (R3) cgctctttctgtagttggtgag	98%
Vasoactive intestinal peptide (VIP)	*Macaca mulatta*	NM_001260752.1	(F1) gacaactatacccgccttagaaa (R1) ttctccctcactgctcctct	98%
Calbindin 1 (CB)	*Macaca mulatta*	XM_015145675.1	(F1) gatgctgacggaagtggtt (R1) gataactccaatccagccttct	100%
Somatostatin (SST)	*Macaca mulatta*	NM_001194239	(F2) gctgctctctgaacccaac (R2) ctctgcaactcaagcctcatt	98%
Cholecystokinin (CCK)	*Macaca mulatta*	XM_002802837.2	(F3) aagctccttctggacgaatg (R4) tgtagtcccggtcacttatcct	97%
Cannabinoid 1 Receptor (CB1R)	*Macaca mulatta*	NM_001032825.1	(F3) tatgctctgcctgctgaact (R3) gtcgcaggtccttactcctc	97%
Parvalbumin (PV)	*Macaca mulatta*	XM_001085875.1	(F1) gctattgactccttcgac (R1) atgaatcccagctcatcc	101%
GABAA Receptor a1 subunit (GABRA1)	*Macaca mulatta*	XM_001086287	(F2) caagtgtccttctggctcaa (R2) gatgcttagcgttgtcatgg	98%
GABAA Receptor a2 subunit (GABRA2)	*Macaca mulatta*	XM_001100133.1	(F3) tctccccaaagtggcttatg (R3) cccatcctcttttggtgaag	97%

***In situ* Hybridization Probes**

Gene	Species	Accession #	Target Region	Channel
Glutamic acid decarboxylase 1 (GAD67)	*Macaca mulatta*	XM_015110351.1	558 - 1716	C1
Parvalbumin (PV)	*Macaca mulatta*	XM_015150253.1	3 - 593	C2
Somatostatin (SST)	*Macaca mulatta*	NM_001194239.1	2-614	C3

APPENDIX C SUPPLEMENTAL INFORMATION FOR CHAPTER 3.0

THE NATURE OF PREFRONTAL CORTICAL SOMATOSTATIN TRANSCRIPT ALTERATIONS IN SCHIZOPHRENIA

APPENDIX C.1 SUPPLEMENTAL TABLES

Appendix Table 4. Reagents used in Chapter 3.0.

Reagent	Vendor	Reference/Catalog	Lot
Hs-SOX6 - C1	ACDbio	524791	20058B
Hs-SLC32A1 - C2	ACDbio	415681 - C2	20059C
Hs-SST - C3	ACDbio	310591 - C3	20059C
Hs-PVALB - C4	ACDbio	422181 - C4	20059C
RNAscope v2 kit	ACDbio	323110	2007958
RNAscope Ancillary Kit	ACDbio	323120	2007469
H_2O_2	ACDbio	322335	2008735
1X Plus Amplification Diluent	Akoya Biosciences	FP1498	191213005
Opal 520	Akoya Biosciences	OP001001	20194101
Opal 570	Akoya Biosciences	OP-001003	20193901
TSA Cy5	Akoya Biosciences	FP1171	2620021
Opal 780	Akoya Biosciences	OP-001008	20194201
TSA DIG	Akoya Biosciences	OP-001007	20200102
Prolong Diamond Antifade Mountant	ThermoFisher	P36970	2168848A

APPENDIX C.2 SUPPLEMENTAL METHODS

Appendix C.2.1 Fluorescent *in situ* Hybridization Tissue Labeling

For each subject, fresh-frozen coronal tissue blocks containing right DLPFC area 9 were mounted in a cryostat. Areas where the cortex had been blocked perpendicular to the pial surface were demarcated using a scalpel and cut at 20 µm thickness onto SuperFrost slides

(ThermoFisher), thaw-mounted, and stored at -80°C until tissue labeling. mRNA probes were designed by Advanced Cell Diagnostics, Inc (Hayward, CA, USA) to detect mRNAs encoding somatostatin (*SST* gene), parvalbumin (PV; *PVALB* gene), SOX6, and the vesicular GABA transporter (VGAT; *SLC32A1* gene) (**Appendix Table 4**). VGAT was used as a GABA neuron marker as it is expressed by all GABA neurons and levels of VGAT mRNA are unaltered or only modestly lower in the DLPFC of people with schizophrenia (Fung et al., 2011; Hoftman et al., 2015). SOX6 (SRY-box transcription factor 6) (Azim et al., 2009; Batista-Brito et al., 2009) was used to distinguish SST and PV neurons from other GABA neurons. SOX6 is selectively expressed in SST and PV neurons due to their common embryonic origin in the medial ganglionic eminence (MGE) and continues to be robustly expressed in the adult primate neocortex (Ma et al., 2013). SOX6 was favored in this experiment over other markers of MGE-derived interneurons, such as Nkx2.1, the expression of which is rapidly downregulated postnatally (Ma et al., 2013), or Lhx6, the expression of which is lower in the DLPFC in people with schizophrenia (Volk et al., 2012; Volk et al., 2014).

Based on the study design, we employed an assay that would allow for the simultaneous fluorescent imaging of four mRNA targets together with a DAPI counterstain to label nuclei. Fluorescent in situ hybridization assays (RNAscope®, ACDbio, Hayward, CA, USA) version 2 (v2) kits were used to achieve four-target labeling simultaneously. Here, we use Opal fluorophores (Akoya Biosciences) in conjunction with the RNAscope v2 assay (Opal 520 – PV; Opal 570 – SST; TSA Cy 5 – VGAT). We selected our fourth fluorophore to be compatible with our existing light engine and filter sets without the need for spectral unmixing, employing the novel use of a two-step near-infrared fluorophore (Opal 780; Akoya Biosciences) to label SOX6.

Tissue sections were processed using the RNAscope® fluorescent multiplex assay v2 kits according to the manufacturer's protocol. Briefly, after removal from –80°C, tissue sections were immediately immersed in ice-cold 4% paraformaldehyde and fixed for 15 minutes, dehydrated through a series of ethanol washes (50%, 70%, 100%, and repeated 100% ethanol for 5 minutes each), followed by H2O2 pretreatment to quench endogenous peroxidases and reduce off-target labelling. Target probes were then hybridized to their target mRNAs for 2 hours at 40°C. After a series of amplification steps included in the assay (Amp 1-v2 for 30 minutes at 40°C, Amp 2-v2 for 30 minutes at 40°C, Amp 3-v2 for 15 minutes at 40°C), fluorophores were assigned to each target mRNA in a stepwise manner. First, horseradish-peroxidase enzymes specific to a target channel (HRP C1-C4) were applied to tissue sections for 15 minutes at 40°C. Following the addition of HRP molecules, working solutions of Opal fluorophores diluted in 1x Plus Amplification Diluent (Akoya Biosciences) were sequentially applied to tissue sections to fluorescently target each mRNA in the following concentrations: Opal 520–1:600 (PV), Opal 570–1:750 (SST), TSA Cy5–1:600 (VGAT), and TSA-DIG–1:600 (SOX6). After each fluorophore was added, the HRP reaction was quenched using the provided HRP blocker in the V2 kit for 15 minutes at 40ºC. This process was repeated for all four targets. Opal 780, an anti-DIG antibody conjugated to the near infrared fluorophore, was diluted in PBS (1:200) and applied to the tissue section for 15 minutes at 40ºC after the last HRP block was completed, as this antibody is exquisitely sensitive to the effects of active HRP molecules.

Appendix C.2.2 Microscopy

Images were collected on a custom wide-field epifluorescence Olympus IX83 inverted microscope (Center Valley, PA, USA) equipped with a 6-line (350-, 405-, 488-, 568-, 647-, 750-

nm) Spectra III light engine (Lumencor), a high-precision XY motorized stage (Prior Scientific) with linear XYZ encoders, and a Hamamatsu ORCA-Flash 4.0 sCMOS camera. The microscope and ancillary equipment were controlled using SlideBook 6.0 (Intelligent Imaging Innovations, Inc., Denver, CO, USA) and images were captured using a 60x 1.42 N.A. SC oil immersion objective (Olympus).

We focus here on layers 2 and 4 for imaging as these layers are known to be differentially enriched for SST and PV neurons, respectively (DeFelipe, 1993; Morris et al., 2008; Hashimoto et al., 2003; Dienel et al., 2021). Layer 2 was defined as 10-20% of the pia-white matter distance and layer 4 was defined as 40-50% of the pia-white matter distance, as previously described (Fish et al., 2018). Imaging sites were selected by taking a low magnification image (4x) of the tissue using the DAPI counterstain. A sampling grid was placed over the tissue that included the entire gray matter section, and grids sized 110 µm x 110 µm (1024 x 1024-pixel imaging site; pixel size = 0.1075 µm/pixel) were placed 30 µm apart to avoid representation of the same cell in different sampling sites. Imaging sites that were located within the laminar zones defined above were selected for capture at 60x magnification.

Each imaging site was collected as a 3D image stack (2D images successively captured at intervals separated by 0.25 µm in the z-dimension). Our initial pilot results suggested that ~14 z-planes successfully captured the full range of in-focus mRNA grain information. In total, six channels were captured. Five channels were dedicated to imaging DAPI, PV, SST, VGAT, and SOX6 (DAPI (ex 359nm, em 461nm), FITC (ex 495nm, em 519 nm), TRITC (ex 552 nm, em 578 nm), Cy5 (ex 649 nm, em 666 nm) Cy7 (ex 753nm, em 775 nm), respectively). The 6th channel (custom 495 ex/666 em filter combination, as previously described (Fish et al., 2018; Rocco et al., 2016a)) was used to image lipofuscin, an intracellular lysosomal protein that accumulates with age

in human brain tissue (Benavides et al., 2002) and fluoresces across the visible spectrum. Exposure times were established before the beginning of the experiment to avoid saturation of pixels for the given mRNA fluorescent grain channels. These exposure times and laser power were kept constant throughout the experiment (DAPI (100ms at 10% power), FITC (250 ms at 20% power), TRITC (250 ms at 20% power), Cy5 (600 ms at 20% power), Cy7 (500 ms at 10% power), lipofuscin (500 ms at 10% power)). Slides were coded such that the single investigator (S.J.D) was blind to diagnostic group. All subject pairs were imaged within the same 24-hour period, to minimize technical variance within a pair. For each subject, 75 sampling sites were selected to be imaged in each layer, resulting in an equivalent sampling size of 0.9075 mm2 per layer per subject.

Appendix C.2.3 Image Processing

Each fluorescent channel for grains was processed using a 3D Gaussian subtraction filter in MATLAB by calculating a difference of Gaussians using sigma values of 0.7 and 2. Within SlideBook, an average z-projection algorithm was used to generate a 2D representation of the 3D image stack. To avoid inadvertently counting lipofuscin objects as grain objects, the signal in the lipofuscin channel was subtracted from grain channels of interest using channel math within SlideBook, with the exception of SOX6 (780) as the lipofuscin signal in the near-infrared channel was weak or nonexistent. To automatically and accurately segment DAPI-labelled nuclei, DAPI channel images were segmented on a pre-trained deep learning u-net in Python 3.8.5 using tensorflow packages and a keras backend (https://github.com/VolkerH/unet-nuclei). The Python script generated an RGB image which masked the DAPI nuclei, the borders of those nuclei, and the background. Within CellProfiler 4.2.0, the masked DAPI images were imported, and primary objects were designated as the pre-masked DAPI nuclei. To capture transcripts in the perinuclear

cytoplasm, ‘cellular’ objects were created by expanding the perimeter of the DAPI-labeled nuclei by 2 μm until reaching the expanded perimeter of another DAPI-labeled nucleus. Grain channels were masked and size gated, and relative levels of mRNA per cell were quantified by the average grain density per cell (grains/μm2). Granules of lipofuscin per cell were quantified in a similar manner but were not size-gated.

Appendix C.2.4 Definition of Nuclei and Cells

To determine the density of grains not associated with a nucleus, grains were masked over the entirety of the image. Background grain density was determined by subtracting the grains overlapping with a DAPI-mask from the total grains over the entire image and dividing by the total image minus that total area of all DAPI nuclei. The background grain density was calculated for each subject within a given layer, providing a within-subject control for random fluctuations in background grain density or intensity. Grain density measures per cell were corrected by subtracting the background grain density quantified in the neuropil.

Assignment of nuclei that specifically expressed a given transcript was determined based on the density of grains within the boundaries of a masked nucleus. VGAT and SOX6 signals were highly localized to the nucleus, resulting in minimal background grain density (Figure 1). We used a relatively high threshold for designating a nucleus as VGAT+ or SOX6+, setting the threshold to 7X the background grain density for a given cell to minimize potential false positives, based on previous in situ studies showing high sensitivity and specificity for nuclei with this threshold (Morris et al., 2008). Because the likelihood of a false-positive identification for SST mRNA-positive and PV mRNA-positive cells was lower given the requirement of both VGAT and SOX6 specific labeling, 4X background grain density was utilized for SST and PV mRNA-positive

cells and quantified over the 'cellular' object, defined as the area including a 2 μm perimeter around each nucleus, to include cytoplasmic SST and PV mRNA signal. The requirement for multiple mRNA markers co-expressed in the same nuclei minimizes the likelihood of false positives and makes it more likely that a true difference in neuron density could be detected if one existed. Using these criteria, relatively few nuclei (<1.0% of all nuclei across subjects) were designated as dual PV and SST positive (**Appendix Figure 1**); these cells were excluded from the final analysis.

Small nuclei, which might be either a glial nucleus or a fragment of a larger nucleus in a different plane of the z-axis, with a cross-sectional area less than 40 μm^2 were eliminated from the analysis. We also excluded nuclei that were located at the border of the image or not fully within the frame of view by excluding nuclei whose XY centers were located within 12 μm of the edge. This boundary was set based on the radius (center) of the largest cross-sectional area of a VGAT+ nucleus in the current study, found to be 469 μm^2.

Appendix C.2.5 Statistical Analysis for Comorbid Factors in Schizophrenia

To assess the influence of certain comorbid factors in SST and PV levels per neuron in schizophrenia, ANCOVAs were conducted using the same covariate factors as in the main analyses, the addition of diagnosis as a covariate, and the comorbid factor in each instance as the main effect. The comorbid factors Analyses were conducted separately in each layer. P-values shown in the figure are corrected using the Benjamini-Hochberg procedure for multiple comparisons across comorbid factors, controlling for a 5% false discovery rate (Kassambara, 2021; Benjamini & Hochberg, 1995). Comorbid analyses were only conducted in instances where there was a significant diagnosis effect observed in the main analysis.

APPENDIX C.3 SUPPLEMENTAL FIGURES FOR CHAPTER 3.0

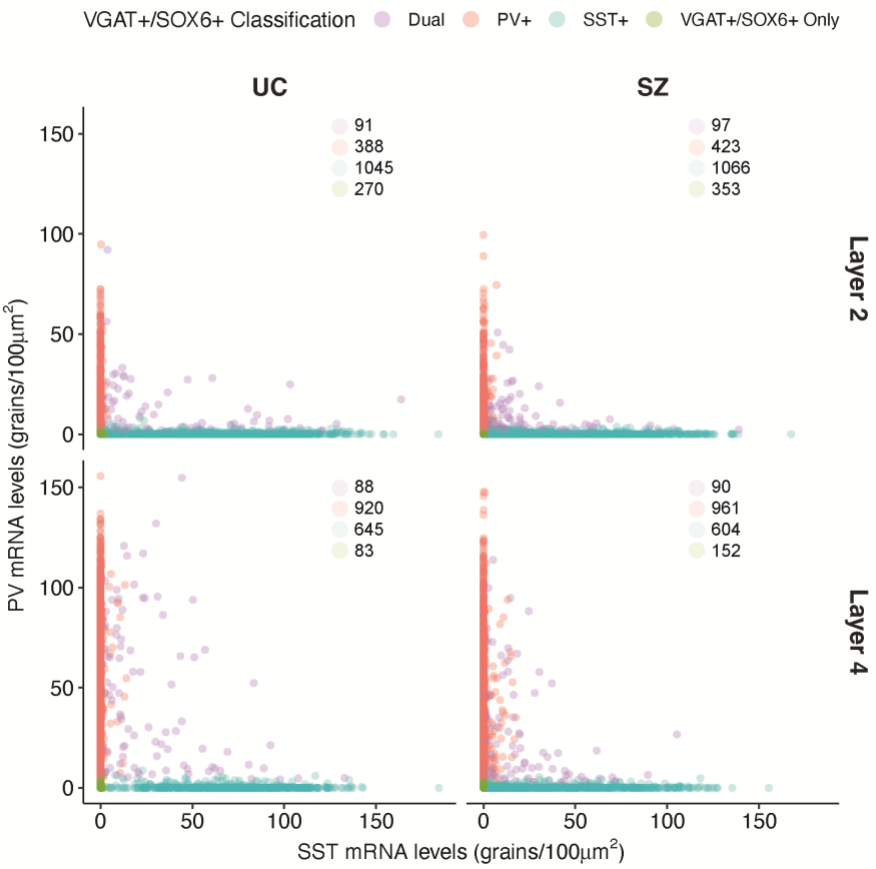

Appendix Figure 1. Classification of each VGAT+/SOX6+ cell based on the expression of SST (x-axis) and PV (y-axis) mRNA levels.

On the left are the values for the unaffected comparison (UC) individuals and on the right are the values for the schizophrenia (SZ) individuals in layers 2 (top panels) and 4 (bottom panels). Color indicates the classification of each VGAT+/SOX6+ cell as an SST+ or PV+ neuron, a VGAT+/SOX6+/SST+/PV+ (labeled dual positive here and were ultimately excluded from the analysis), and VGAT+/SOX6+ neurons without either SST or PV signal. The number of neurons classified into each group is shown at the top right of each panel across all unaffected (n = 29) and schizophrenia (n = 29) individuals.

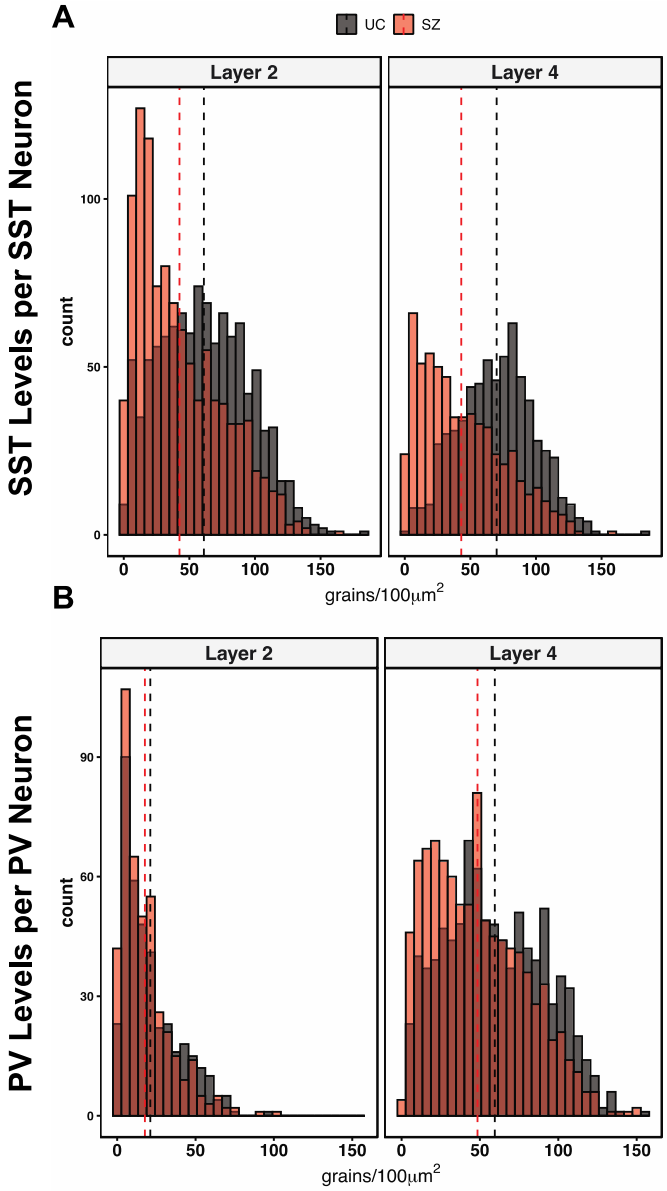

Appendix Figure 2. Histograms for individual cell data across layers.
(A) SST levels per SST+ neuron in both layers 2 and 4 in unaffected comparison (UC) and schizophrenia (SZ). Counts are the number of cells in each category, and colors indicate the diagnostic group. **(B)** PV levels per PV+ neuron in both layers 2 and 4 in UC and SZ individuals.

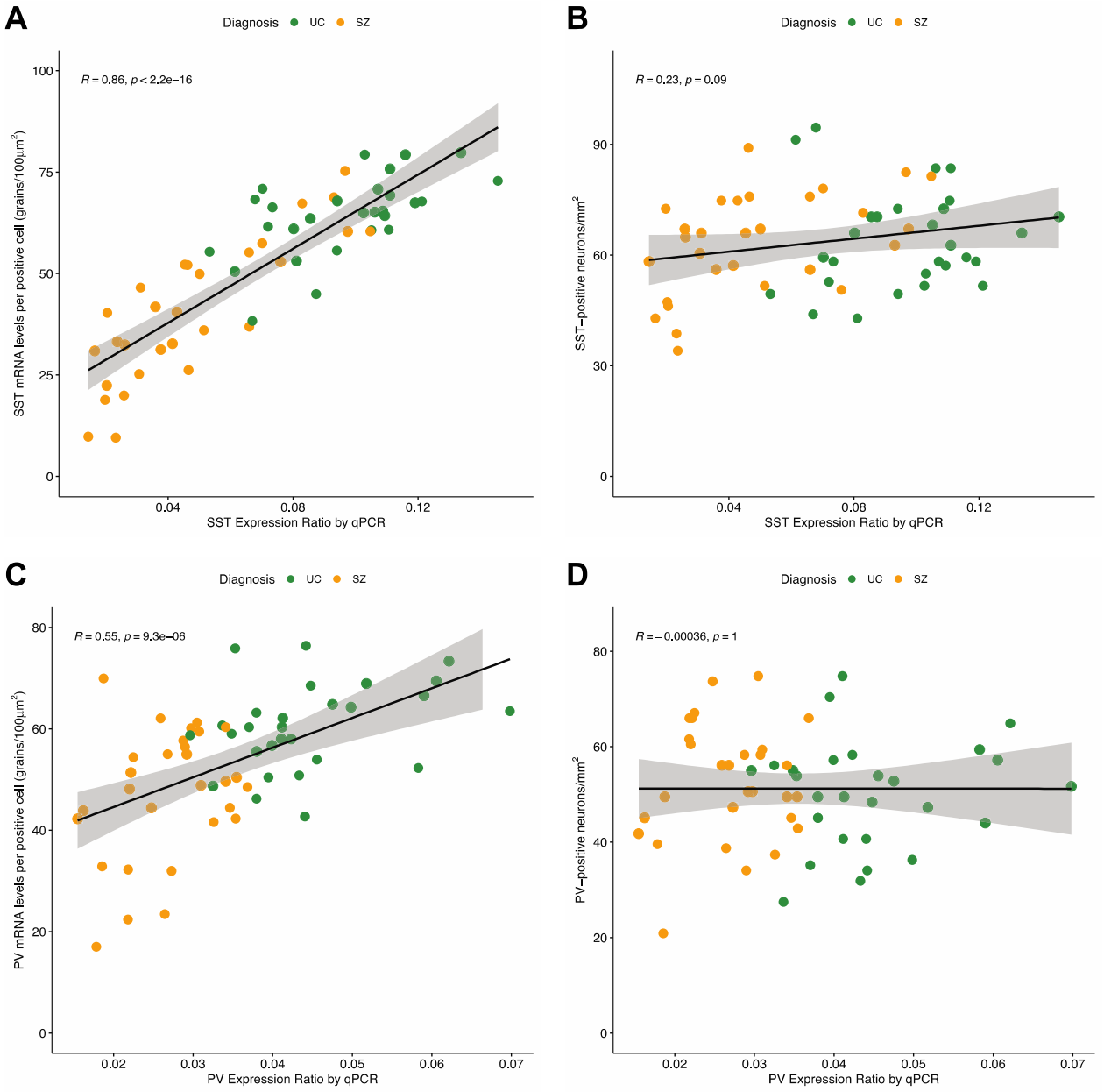

Appendix Figure 3. Correlation of SST and PV measures of grain density per neuron and the density of neurons in the current study with the previous expression ratios obtained by qPCR.

(A) Correlation of SST mRNA per SST+ neuron, indexed by grain density per SST+ neuron averaged across layers 2 and 4 (y-axis) and the expression ratio of SST in the DLPFC total gray matter by qPCR. Each point is an individual subject, and the colors indicate the diagnosis. **(B)** Correlation of the neuron density of SST+ neurons averaged between layers 2 and 4 (y-axis) and the expression ratio of SST in the DLPFC total gray matter by qPCR (x-axis). **(C)** Correlation of PV mRNA per PV+ neuron in layer 4 (y-axis) and PV expression ratio in total gray matter (x-axis). **(D)** Correlation of the neuron density of PV+ neurons averaged between layers 2 and 4 (y-axis) and the expression ratio of SST in the total gray matter (x-axis). Pearson correlation coefficients in all panels are shown for the entire cohort.

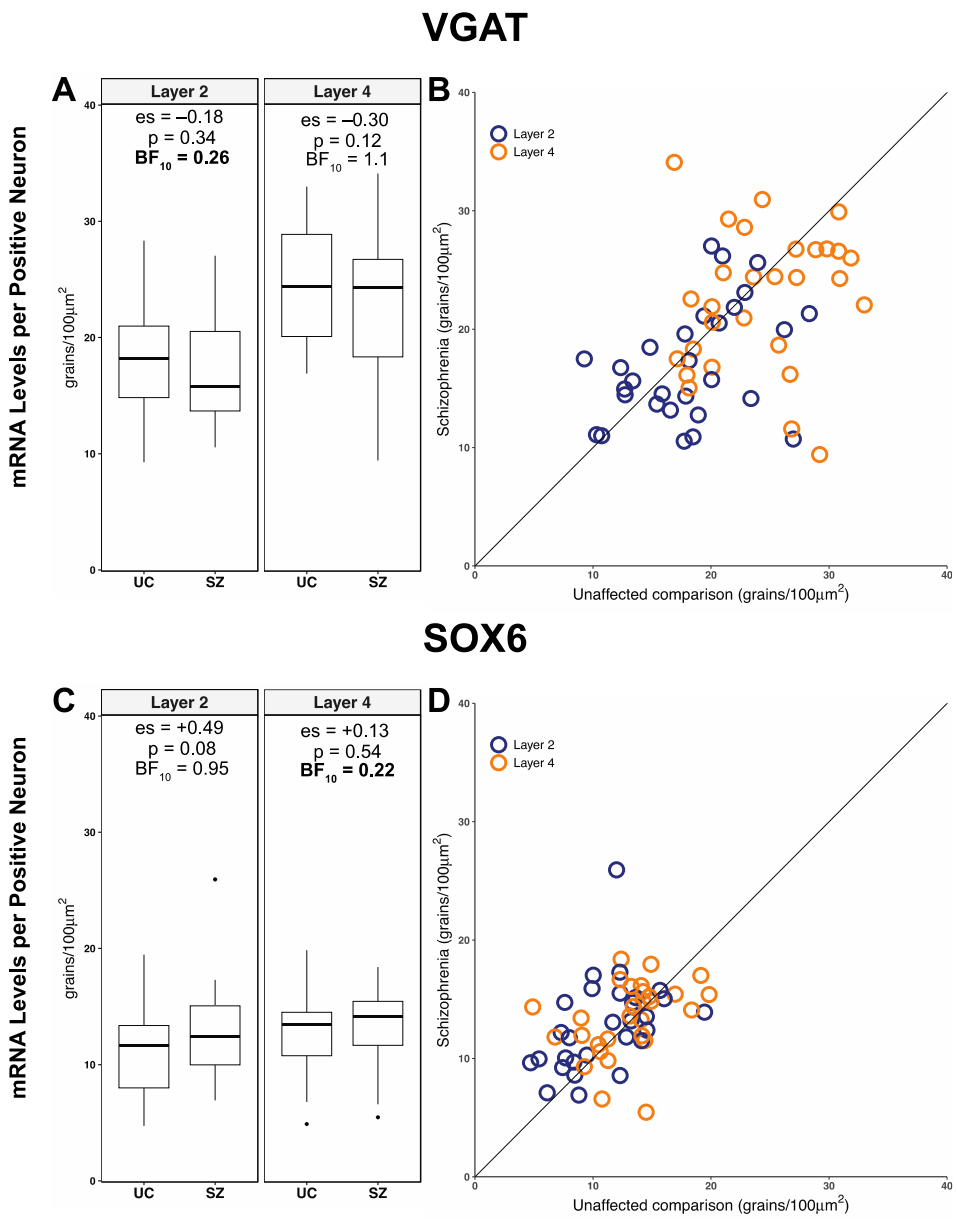

Appendix Figure 4. Levels of VGAT and SOX6 per VGAT+/SOX6+ neuron in layers 2 and 4 of the DLPFC in unaffected comparison (UC) and schizophrenia (SZ).

(A) Boxplots of the median, quartile, and 95% range of unaffected comparison (UC) and schizophrenia (SZ) for VGAT mRNA expression per VGAT+/SOX6+ neuron. Within the boxplots, values for effect size (es), the posthoc between-group comparison p-value, and the Bayes' Factor (BF10) in favor of the alternate hypothesis are shown. Bolded BF value indicates strong evidence for the null hypothesis. **(B)** VGAT levels per VGAT+/SOX6+ neuron shown as individual subject data as unity plots. In these plots, individual points represent a subject pair, and the x-axis shows the value for the unaffected individual and y-axis shows the value for the individual with schizophrenia. Colors indicate the layer for which the data are shown. Points below the line indicate a lower value in the individual with schizophrenia relative to their matched unaffected comparison individual. **(C)** Boxplots of the median, quartile, and 95% range of UC and SZ for SOX6 mRNA expression per VGAT+/SOX6+ neuron. **(D)** Unity plot of the individual subject data for levels of SOX6 per VGAT+/SOX6+ neuron. In all graphs, data are shown for 29 subject pairs in each layer.

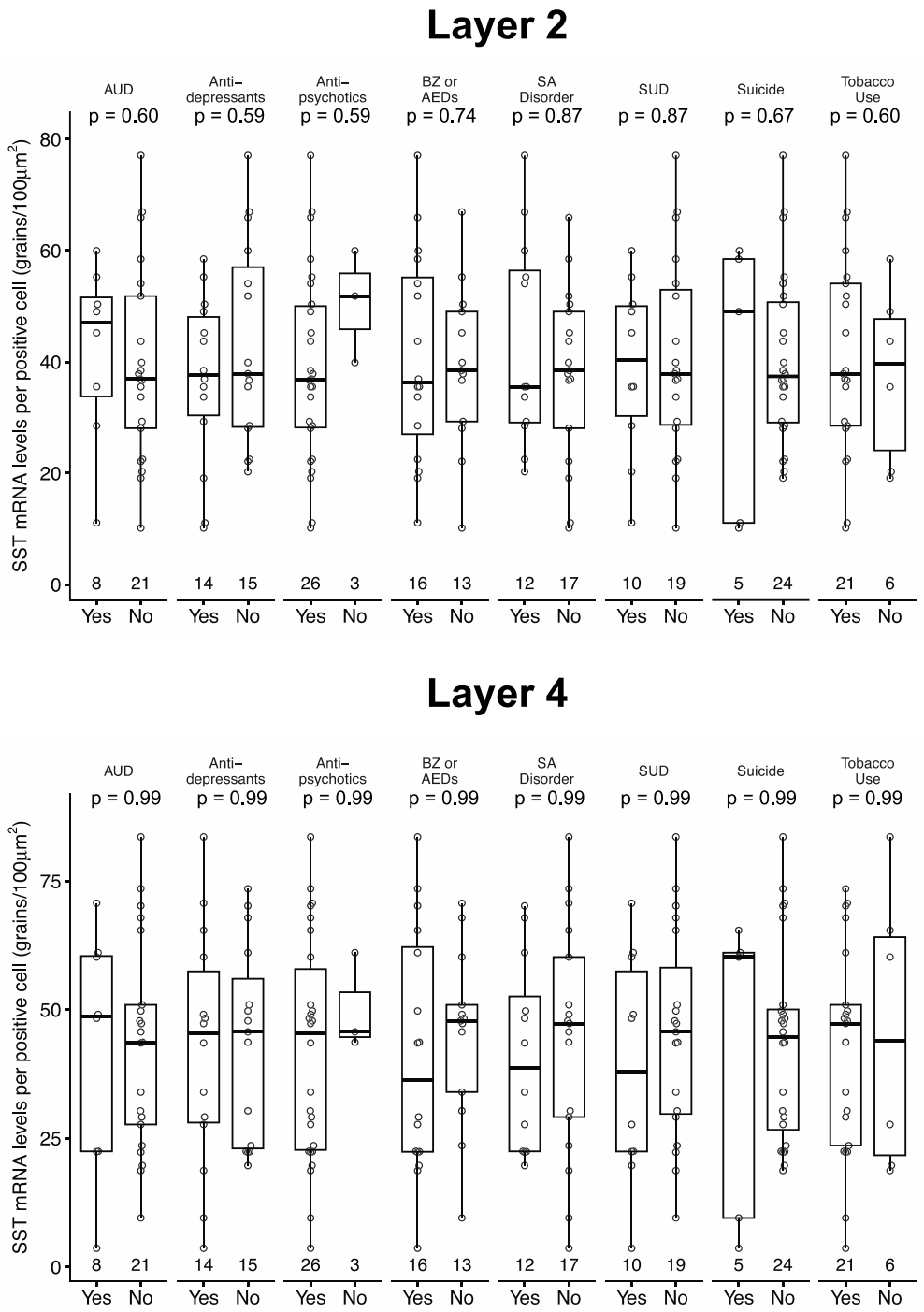

Appendix Figure 5. Comparison of certain comorbid factors on SST levels per positive neuron in layer 2 (top panel) and 4 (bottom panel) in individuals with schizophrenia.

P-values shown are corrected for multiple comparisons using false discovery rate of 0.05 across comorbid factors. Values at the bottom indicate the number of schizophrenia subjects with or without a certain comorbid feature. Two individuals with SZ had unknown tobacco use at time of death. Each point represents an individual SZ subject, and boxplots show the median, quartile, and 95% range. AUD = alcohol use disorder, BZ = benzodiazepines, AEDs = antiepileptic drugs, SA = schizoaffective, SUD = substance use disorder (including opioids, cocaine, and sedatives/hallucinogens).

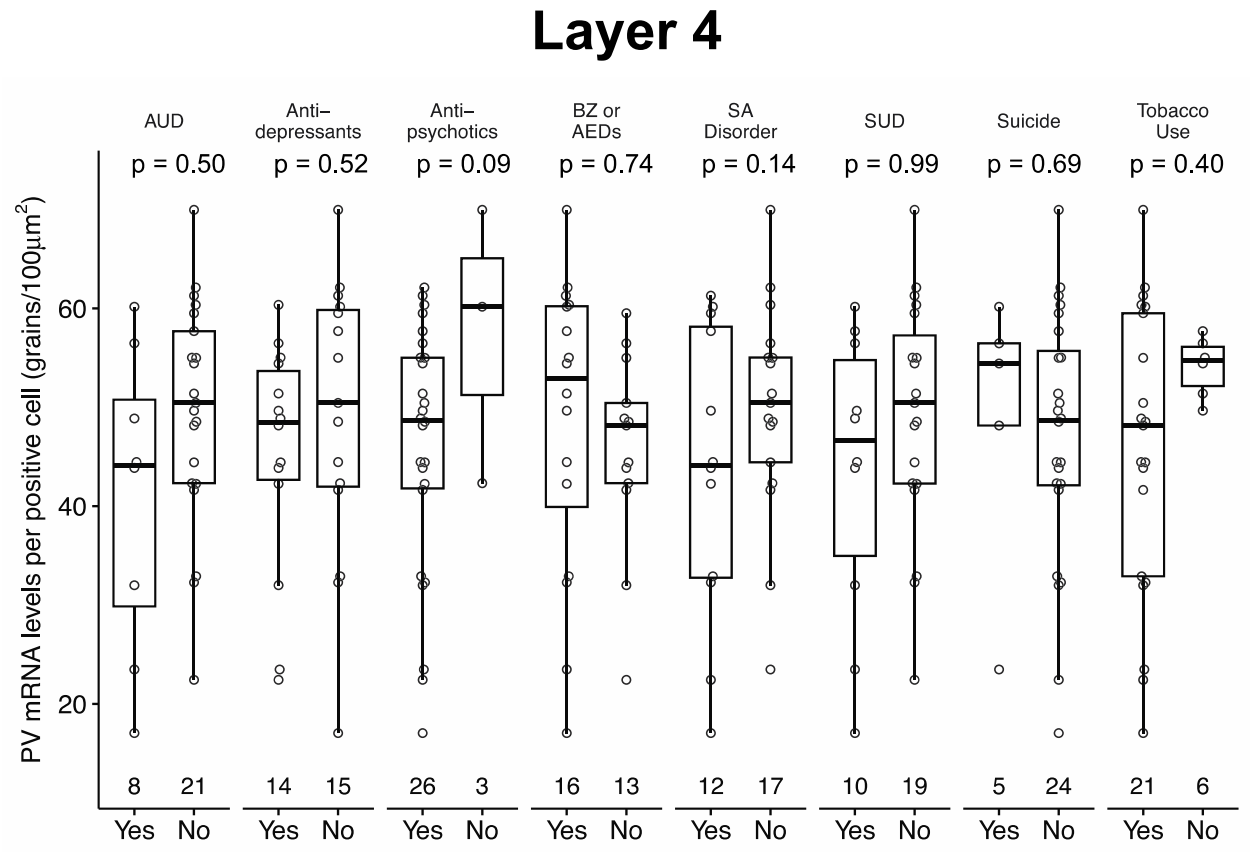

Appendix Figure 6. Comparison of certain comorbid factors on PV levels per positive neuron in layer 4 in individuals with schizophrenia.

P-values shown are corrected for multiple comparisons using false discovery rate of 0.05 across comorbid factors. Values at the bottom indicate the number of schizophrenia subjects with or without a certain comorbid feature. Two individuals with SZ had unknown tobacco use at time of death. Each point represents an individual SZ subject, and boxplots show the median, quartile, and 95% range. AUD = alcohol use disorder, BZ = benzodiazepines, AEDs = antiepileptic drugs, SA = schizoaffective, SUD = substance use disorder (including opioids, cocaine, and sedatives/hallucinogens).

APPENDIX D LAMINAR, CELL TYPE, AND DIAGNOSTIC SPECIFICITY OF LOWER SOMATOSTATIN TRANSCRIPT LEVELS IN THE PREFRONTAL CORTEX OF SCHIZOPHRENIA

APPENDIX D.1 INTRODUCTION

Schizophrenia (SZ) is associated with pronounced deficits in somatostatin (SST) mRNA in the dorsolateral prefrontal cortex (DLPFC) (Fung et al., 2010; Volk et al., 2016; Morris et al., 2008) as demonstrated in multiple postmortem studies using different quantitative methods conducted by several research groups. We recently reported that the deficit in SST mRNA levels in SZ is due to lower gene expression per neuron without a difference in the density of SST neurons. These findings suggest that SZ is associated with a normal complement of functionally altered SST neurons in the DLPFC.

However, no prior findings have addressed the question of which subtypes of SST neurons, which differ in morphology, connectivity, and transcriptome (DeFelipe et al., 2013; Krienen et al., 2020), are affected in SZ. The most striking differences among cortical SST neuron subtypes are evident between those residing in layers 2-superficial 3 (superficial zone) and those located in deep layer 6 and subcortical white matter (deep zone) (Bouras et al., 1987; Hodge et al., 2019). In the primate neocortex, SST neurons in the superficial zone frequently co-express the calcium-binding protein calbindin (CB) (González-Albo et al., 2001; Zaitsev et al., 2009) and give rise to axons that target the distal dendrites of pyramidal neurons in the supragranular layers (Melchitzky & Lewis, 2008). In the deep zone, SST neurons frequently co-express other neuropeptides, including neuropeptide Y (NPY) (Suárez-Solá et al., 2009; Aoki & Pickel, 1990), tachykinin 1 (TAC1; also known as substance P (Jones et al., 1988)), and cortistatin (CORT) (de Lecea et al., 1997; Jones et al., 1988; DeFelipe et al., 1990). These neurons appear to have a role in sleep homeostasis (Kilduff et al., 2011; de Lecea et al., 1996) and regulation of cerebral blood flow (Krawchuk et al., 2020); the latter role is likely related to the high levels of nitric oxide synthase (NOS1) (Yan et al., 1996; Smiley et al., 2000) within these neurons. Thus, the functional consequences of altered SST neuron

function in SZ are certain to be influenced by the relative involvement of SST neurons in the superficial versus deep zones. Finally, lower cortical SST mRNA levels have also been reported in postmortem studies of other psychiatric diagnoses, raising the question of whether alterations in certain subclasses of SST neurons are specific to the disease process(es) of SZ or a reflection in a more general liability to or consequence of a psychiatric diagnosis and accompanying comorbid features.

Consequently, in the present study, we asked a series of questions regarding the nature of the alterations of SST neurons in schizophrenia. First, is the SZ-associated deficit in SST mRNA levels evident in both superficial and deep laminar zones of the DLPFC? Second, are the disease-associated patterns of alterations in SST mRNA also evident for other co-expressed transcripts? Third, are the SZ-associated patterns of SST alterations also evident in bipolar (BP) and major depressive (MD) disorders? Fourth, are alterations in SST neurons attributable to the influence of certain comorbid factors that are frequently observed in individuals living with a psychiatric disorder?

APPENDIX D.2 METHODS

Appendix D.2.1 Human Brain Tissue Specimens

Brain specimens (n = 165) were obtained during routine autopsies conducted at the Office of the Allegheny County of the Medical Examiner (Pittsburgh, PA, USA, n = 154) or the Davidson County Medical Examiner's Office (Nashville, TN, USA, n = 11) after consent was obtained from the next-of-kin. An independent team of clinicians made consensus, lifetime DSM-IV diagnoses for each subject using the results of an expanded psychological autopsy, including structured interviews with family members and review of medical records, as well as toxicological and neuropathology reports (Glausier et al., 2020b). Using the same procedures, unaffected comparison individuals were identified based on the absence of any evidence of a history of psychiatric or neurological disorders except for minor or in remission psychiatric diagnoses in six subjects. The reported race and biological sex of the decedents (**Appendix Table 5**) were corroborated by the final death certificate and next-of-kin interviews. All procedures were approved by the University of Pittsburgh Committee for Oversight of Research and Clinical Training Involving Decedents and Institutional Review Board for Biomedical Research.

Subjects for each diagnostic group were selected with the goal of matching groups as closely as possible for age and biological sex. To optimize tissue quality, only subjects with brain pH >6.1 and brain RNA integrity number (RIN) >7.0 were included. Subject groups did not differ in the distribution of males and females or in mean age, body-mass index (BMI), postmortem interval (PMI), brain pH, or brain RIN (**Appendix Table 5**). The distribution of race did statistically significantly differ across diagnostic groups ($\chi^2(3) = 12.6$, $P = 0.005$), with

significantly more Black individuals in the SZ diagnostic group relative to the BP (unadjusted P = 0.009) and MD (unadjusted P = 0.02) diagnostic groups.

Appendix Table 5. Demographics and tissue characteristics of human postmortem brain tissue specimens.

	PCR Cohort		RNAscope Cohort*		Mood Disorders Cohort	
Characteristic	UC	SZ	UC	SZ	BP	MD
n	43	41	29	29	39	42
Age, years, mean (SD)	47.6 (13.8)	46.4 (12.2)	51.8 (14.4)	50.1 (14.1)	46.2 (12.5)	45.6 (12.1)
Sex, n (%)						
Female	18 (42%)	17 (41%)	8 (28%)	8 (28%)	16 (41%)	18 (43%)
Male	25 (58%)	24 (59%)	21 (72%)	21 (72%)	23 (59%)	24 (57%)
Race, n (%)						
Black	5 (12%)	12 (29%)	5 (17%)	7 (24%)	1 (2.6%)	2 (4.8%)
White	38 (88%)	29 (71%)	24 (83%)	22 (76%)	38 (97%)	40 (95%)
PMI, hours, mean (SD)	19.3 (5.7)	19.6 (7.3)	18.7 (5.6)	18.3 (7.7)	21.8 (6.5)	19.4 (5.8)
RIN, mean (SD)	8.1 (0.6)	8.0 (0.6)	8.1 (0.6)	8.0 (0.7)	7.9 (0.5)	8.1 (0.6)
brain pH, mean (SD)	6.7 (0.2)	6.5 (0.3)	6.7 (0.23)	6.5 (0.3)	6.6 (0.2)	6.5 (0.2)
Tissue storage time at –80°C, months, mean (SD)	173.0 (55.3)	181.8 (64.1)	200.2 (45.4)	203.3 (53.8)	169.8 (60.7)	170.8 (52.2)

*16 schizophrenia and 7 unaffected comparison subjects are represented in both the PCR and RNAscope cohorts. Abbreviations: PCR = polymerase chain reaction, UC = unaffected comparison, BP = bipolar, MD = major depression, SZ = schizophrenia, PMI = postmortem interval, RIN = RNA integrity number

Appendix D.2.2 Laser Microdissection Strategy

Cryostat sections (12 μm) were cut from coronal blocks of the right prefrontal cortex that contained Brodmann area 9. Sections were thaw-mounted onto glass polyethylene naphthalate membrane slides that had been UV treated at 254 nm for 30 minutes, dried briefly, and stored at –80°C. On the day of laser microdissection, slides were immersed in an ethanol-acetic acid fixation solution and stained for thionin, as previously described (Dienel et al., 2021). Using a 5x microscope objective, portions of the tissue section that were cut perpendicular to the pial surface were identified. A cortical traverse, ~3000 μm in distance extending from layer 1 to the white matter boundary, was identified, and two boxes, ~400 μm in thickness, were drawn. The superficial zone was defined as the box that extended 400 μm in depth from the layer 1-layer 2 boundary into the most superficial aspect of layer 3. The deep zone was defined by a 400 μm-thick box that was placed such that ~100 μm of the depth was placed above the layer 6-superficial white matter boundary and ~300 μm extended into the superficial aspect of the white matter. The boxes in superficial and deep zone were placed in the same portion of the tissue section. A total cross-sectional tissue area of ~$5x10^6$ μm^2 per laminar zone for each subject was captured by laser microdissection into tubes and the tissue lysed in RLT Plus Buffer (QIAGEN) with β-mercaptoethanol and frozen. RNA was extracted and purified using the RNeasy Plus Micro Kit (QIAGEN). At the time of microdissection, investigators were blinded to subject diagnosis, and the order of collection of subjects within a tetrad was randomized so the 24 (4 factorial) possibilities were evenly distributed across the full cohort. Both laminar samples and all subjects of a given tetrad were collected on the same day to reduce within-tetrad technical variance.

Appendix D.2.3 qPCR Analysis

Laser microdissection was used to isolate the superficial and deep laminar zones (**Appendix Figure 7A**), and quantitative PCR was used to quantify mRNA levels of SST, NPY, TAC1, CORT, and CB. Levels of these transcripts were normalized to the mean of three housekeeping genes. Although the housekeeping genes did not show significant differences by diagnostic category, levels of these transcripts were different between the superficial and deep laminar zone in all diagnostic groups studied. Thus, we computed separate models for the superficial and deep zone without making comparisons between the two zones.

Total RNA was converted to complementary DNA using the qScript cDNA SuperMix (Quanta Biosciences, Gaithersburg, MD, USA). To reduce technical variance, all samples from a single tetrad (4 subjects x 2 laminar zones) were run on a 384-well quantitative PCR (qPCR) plate in quadruplicate. Forward and reverse primers were designed for each transcript, and all primers showed 90-100% efficiency and each amplified product resulted in a single and specific amplicon. Levels of each transcript were assessed using Power SYBR Green fluorescence and the ViiA™7 Real Time PCR System to determine the cycle threshold (CT). The level of each transcript was normalized to the geometric mean of the 3 housekeeping, or normalizer, genes (beta actin, cyclophilin-A, and GAPDH). The level of each transcript was calculated by subtracting the mean of the three normalizers from the CT values of the gene of interest (difference in CT, or dCT). Because the dCT represents the log2-transformed expression ratio of each target transcript to the mean of the normalizer genes, the relative expression levels of the target transcripts are reported as the more intuitive expression ratio, or the 2-dCT.

Analyses were performed in R (R Core Team, 2018). To compare transcript levels across subject groups, linear models were performed, including transcript level as the dependent variable,

diagnosis as a fixed effect, and age, sex, PMI, brain pH, and RIN as covariates. Tissue storage time at –80ºC did not differ across diagnostic groups and has been previously demonstrated to not influence the expression of many of the neuropeptides studied here; therefore, storage time was not included as a covariate (Morris et al., 2009; Morris et al., 2008). *F* tests were computed from linear models to assess the overall diagnosis effect within a laminar zone, and posthoc comparisons across diagnostic groups within a laminar zone were made using estimated marginal means (Lenth, 2022). Figures generation and analyses were conducted using the 'lme4' (Bates et al., 2015), 'lmerTest' (Kuznetsova et al., 2017), 'tidyverse' (Wickham et al., 2017), and 'rstatix' (Kassambara, 2021) packages in R.

In certain comparisons, especially in instances where we sought to quantify the strength of the evidence in favor of the statistical null hypothesis, Bayes' factors (Keysers et al., 2020) were computed using the BayesFactor package in R (Morey & Rouder, 2018). A Bayes' Factor is a ratio of the likelihood of one particular hypothesis relative to the likelihood of the other hypothesis and provides a quantitative measure of evidence in favor of the alternative or null hypothesis. In the model used to compute the BF value, the true standardized difference is assumed to be 0 under the null hypothesis and follow the Cauchy distribution under the alternative. The prior is described by a Cauchy distribution with a width parameter of 0.707, corresponding to a probability of 80% that the effect size lies between -2 and 2. Here, we use the standard designation of BF_{10} to denote evidence in favor of the alternative hypothesis, or H_1. We use Jeffreys' interpretation (Jeffreys, 1961) of BF of the evidence as follows: 1 to 3 = weak evidence; 3-10 = substantial evidence; 10-100 = strong evidence; >100 = decisive evidence in favor of H_1. A BF value of 1 indicates no evidence favoring either hypothesis, while BF values smaller than 1 suggest evidence in favor of the null hypothesis, or H_0. BF_{10} between 1 and 0.33 = weak evidence in favor of H_0; 0.33 – 0.1 =

substantial evidence; 0.1 – 0.01 = strong evidence, and $BF_{10} < 0.01$ = decisive evidence in favor of H_0.

To provide an estimate of the disease effect (Kraemer, 2019), Cohen's d effect sizes were calculated in R (Torchiano, ; Cohen, 1988) for each subject group in a given comparison. Based on (Coe, 2002), we designated any effect size > 0.60 as 'large' and note these values specifically in the text.

The potential influence of certain comorbid variables, such as concurrent alcohol or substance use disorder, death by suicide, or prescription drug use at time of death (grouped into three categories: benzodiazepines or antiepileptic drugs (AEDs), antidepressants, and antipsychotics) on each transcript of interest was assessed by conducting F tests using the comorbid feature as the main effect and diagnosis, age, sex, PMI, pH, and RIN as covariates, and the z-score of the transcript relative to the UC group as the dependent measure. Benjamini-Hochberg procedure was used to correct for a false discovery rate of 5% for multiple comparisons across comorbid factors.

In SZ and UC individuals, ANCOVA models were used to assess for the main effect of diagnosis while accounting for covariates of age, sex, pH, PMI, and RIN. To provide an estimate of the deficit in SST and other transcripts in SZ relative to the UC group while controlling for significant covariates (i.e., age and brain pH), we provide a 'w-score' that indexes the deviation of SST levels in SZ compared to what would be predicted from a linear model of the UC individuals. First, a linear model using all the UC subjects in a given laminar zone was generated using the influential covariates for SST in that zone (age and pH in superficial zone; pH in the deep zone). This model was used to create a prediction for each SZ individual based on the covariate values

for each SZ subject. We plot the w-score, which is an estimate of the deviation of the SZ subject from the predicted value from the UC model, as described in **4.2.7**.

Composite scores of the four neuropeptides, SST, NPY, TAC1, and CORT, were computed by the average of the normalized (z-score) expression levels for each transcript. Z-scores were computed based on the mean and standard deviation of the UC group, as previously described (Chung et al., 2018).

When comparing measures between all four diagnostic groups, ANCOVA models in each zone were used to assess the main effect of diagnosis across four groups while accounting for covariates of age, sex, pH, PMI, and RIN (**Appendix Table 5**). Posthoc testing using estimated marginal means derived from the overall model were used to assess pairwise differences between diagnostic groups. All statistical analyses were conducted on log-transformed values of the expression ratios, to stabilize the variance.

Cohen's d effect sizes were calculated for each psychiatric diagnosis group relative to the UC group, and positive notation for effect sizes indicate a deficit in the diagnostic group relative to the UC group. Additionally, we computed a Bayes' Factor to provide a quantitative estimate of the strength of the evidence in favor of either the alternative or null statistical hypothesis. All BF values are shown in the notation of evidence for the alternative, or BF_{10}. We rely on Jeffrey's interpretation of BF values such that $BF_{10} > 3$ or < 0.33 indicates substantial evidence in favor of the alternative or null hypothesis, respectively.

APPENDIX D.3 RESULTS

In SZ, SST mRNA levels quantified by PCR were lower in laminar isolates of the superficial zone ($F_{1,77}$ = 9.1, P < 0.01; d = 0.68; 95% CI, 0.23–1.13; **Appendix Figure 7**). To lend further support for this finding, we quantified levels of SST mRNA in a separate cohort of SZ and UC individuals previously studied where 16 of the SZ and 7 of the UC individuals overlapped with the first cohort (**Appendix Table 5**). In this separate cohort, we quantified the laminar fluorescence intensity of SST mRNA signal in the same laminar zones isolated by laser microdissection in the first cohort. Consistent with findings from the first cohort, the fluorescence intensity of SST in the superficial zone in this cohort was significantly lower ($F_{1,51}$ = 16.5, P < 0.01; d = 0.90; 95% CI, 0.35–1.45; **Appendix Figure 7**).

In the deep laminar zone, SST mRNA levels were lower by PCR, with a similar effect size as identified in the superficial zone ($F_{1,77}$ = 6.1, P = 0.02; d = 0.60; 95% CI, 0.16-1.04; **Appendix Figure 7**). Additionally, SST mRNA fluorescence intensity levels were also lower in the deep laminar zone in the partially overlapping cohort, with comparable effect sizes ($F_{1,51}$ = 13.8, P < 0.01; Cohen's d = 0.96; 95% CI, 0.41-1.51; **Appendix Figure 7**). Together, different methods employed in partially overlapping cohorts of SZ and UC individuals support the finding that SZ is associated with lower SST mRNA levels in both superficial and deep laminar zones. However, the within-subject deficits in SZ individuals did not appear to be related between laminar zones. The correlation of within-subject w-scores in the superficial and deep laminar zones was weak for SST quantified by PCR (r = 0.049, p = 0.76) or by fluorescence intensity (r = 0.24, p = 0.22, after removal of a single high leverage point).

Next, we compared the findings in SST to other transcripts that are frequently co-expressed within SST neurons in those with schizophrenia. Levels of NPY were lower in both superficial

($F_{1,77}$ = 4.3, P = 0.05; d = 0.55; 95% CI, 0.10–0.99; **Appendix Figure 8**) and deep ($F_{1,77}$ = 8.4, P < 0.01; d = 0.69; **Appendix Figure 8**). Similarly, levels of TAC1 were lower in both superficial ($F_{1,77}$ = 19.1, P < 0.001; d = 0.97; **Appendix Figure 8**) and deep ($F_{1,77}$ = 4.8, P = 0.03; d = 0.48; **Appendix Figure 8**) laminar zones. Levels of CORT, NOS1, and CB did not differ in SZ. Together, we find that SZ is associated with lower levels of SST, NPY, and TAC1 in both laminar zones studied here.

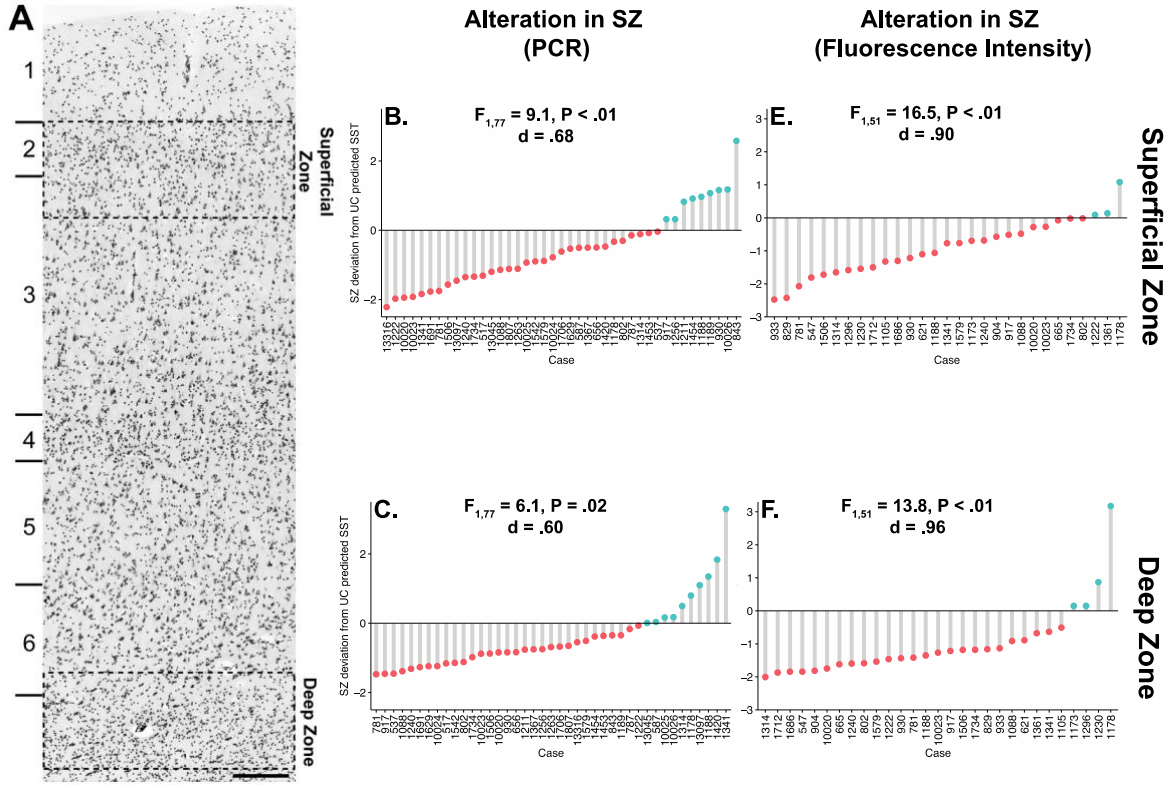

Appendix Figure 7. Laser microdissection strategy and SST levels in superficial and deep laminar zones in schizophrenia.

(A) Illustrative Nissl-labeled area 9 section demonstrating the cortical layers. Dashed-line box indicates the superficial zone, comprising layer 2 and the superficial aspect of layer 3, and the deep zone, comprising the deepest 50% of layer 6 and the subcortical white matter. Scale bar = 200 µm. **(B)** Alterations in schizophrenia (SZ) indexed by w-scores in the superficial laminar zone using qPCR. Red dots indicate a negative w-score, blue dots indicate a positive w-score. **(C)** Same as **(B)** but for the deep laminar zone. **(E)** and **(F)** Alterations in schizophrenia (SZ) indexed by w-scores in the superficial **(E)** and deep **(F)** laminar zones using fluorescent *in situ* hybridization. In all plots, each dot represents a single case number, shown on the x-axis by the human subject number.

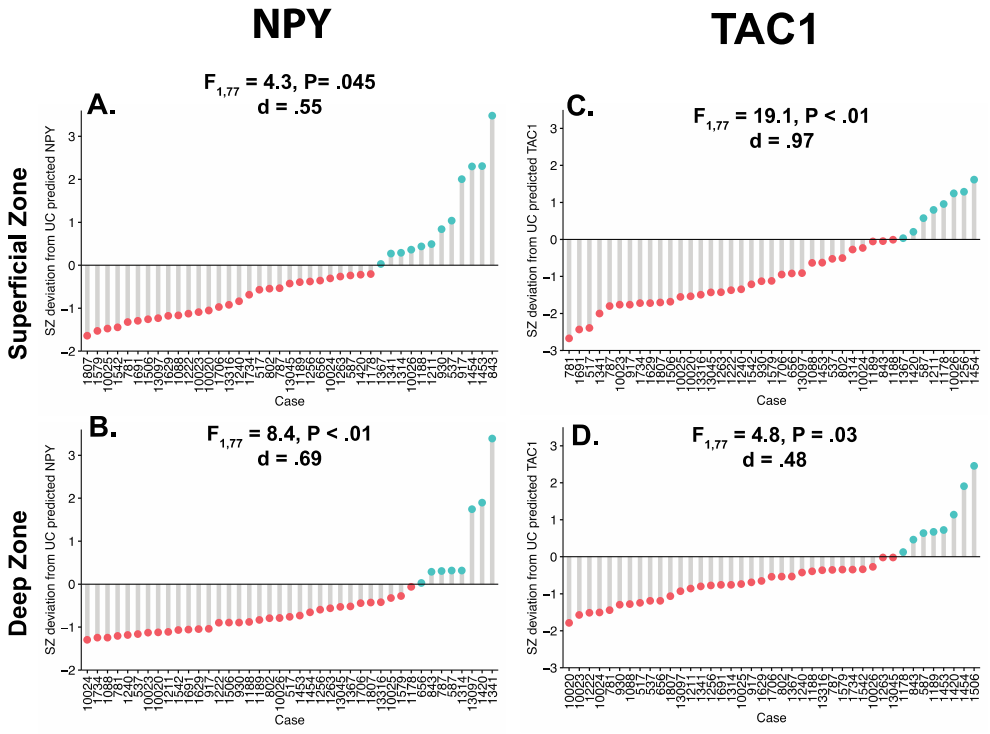

Appendix Figure 8. Alterations in NPY and TAC1 levels in superficial and deep zones in schizophrenia.
(A) NPY alterations in the superficial zone schizophrenia, shown by w-scores, where each represents a single subject with schizophrenia. Dots in blue indicate a positive w-score, while dots in red indicate a negative w-score in schizophrenia. **(B)** NPY w-scores in the deep laminar zone. **(C)** TAC1 w-scores in the superficial laminar zone. **(D)** TAC1 w-scores in the deep laminar zone.

We next compared whether the alterations in SST were also evident in BP and MD disorders in the same laminar pattern. We recomputed an overall ANCOVA model using all four subject groups (UC, SZ, BP, and MD) for SST in a given laminar zone, and posthoc tests using estimated marginal means were conducted to assess pairwise comparisons. SST in the superficial laminar zone was significantly different between diagnostic groups ($F_{3,156}$ = 3.0, P = .03; **Appendix Figure 9A**), with SZ (t-ratio = 2.8, P > 0.01) and MD (t-ratio = 2.0, P = .05) groups significantly different from UC individuals. SST expression in the deep laminar zone did not significant differ between groups ($F_{3,156}$ = 2.3, P = .08; **Appendix Figure 9B**), although SZ was significantly different from the UC group (t-ratio = 2.5, P = .01). By comparing the pattern of SST alterations

in SZ to BP and MD, it appears that only SZ is associated with lower levels of SST in both laminar zones, while MD is associated with SST mRNA deficits only in the superficial laminar zone.

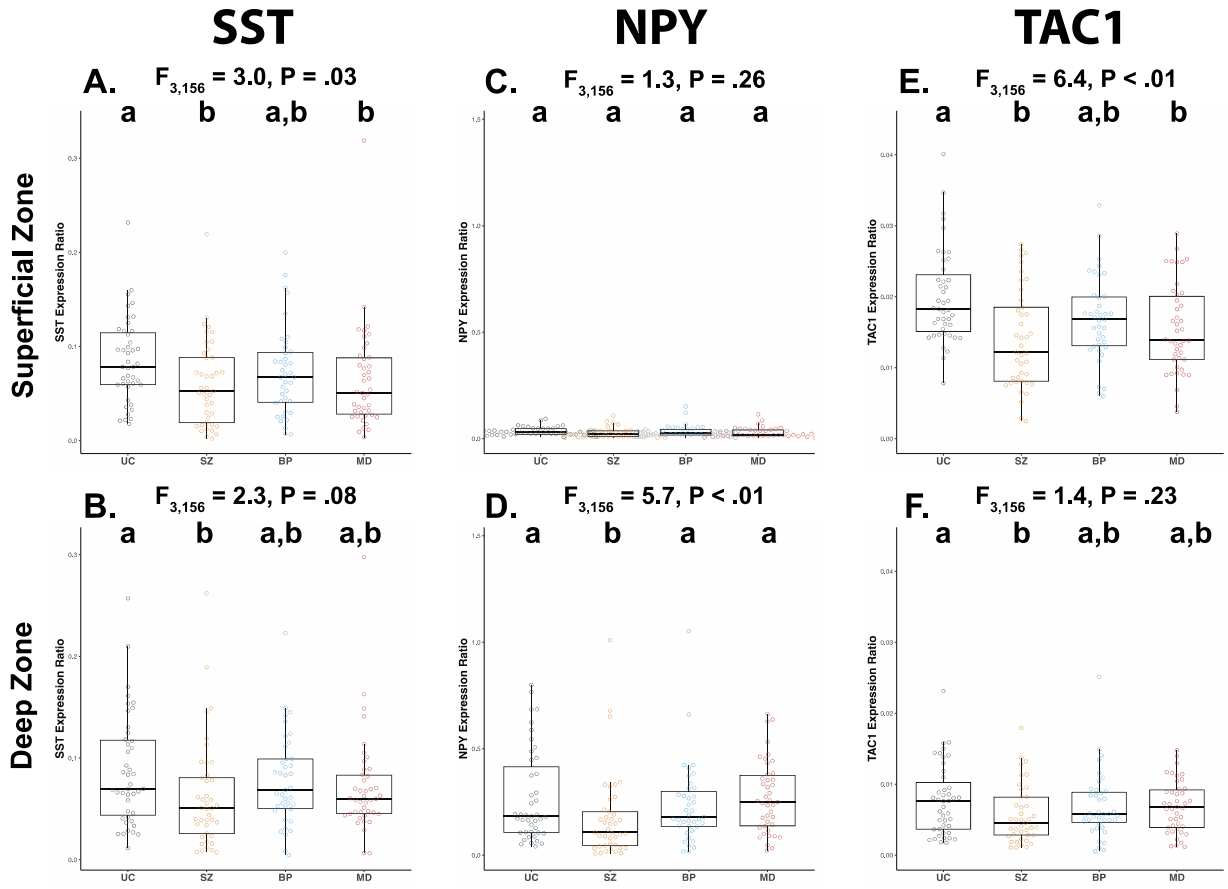

Appendix Figure 9. Alterations in SST, NPY, and TAC1 in across diagnostic groups.

(A) Levels of SST in the superficial zone and **(B)** deep zones across diagnostic groups. Groups are shown on the x-axis and expression ratios on the y-axis. Overall statistical tests are shown at the top, and groups not sharing a letter are statistically significantly different from one another. **(C)** and **(D)** Same as A and B for NPY levels in the superficial and deep zones, respectively. **(E)** and **(F)** Same as A and B for TAC1 levels in the superficial and deep laminar zones, respectively.

To assess the diagnostic specificity of these alterations, we compared findings of NPY and TAC1 in SZ within BP and MD individuals. NPY did not significantly differ across diagnosis groups in the superficial laminar zone ($F_{3,156}$ = 1.3, P = 0.26; **Appendix Figure 9C**). However, levels of NPY were different between groups in the deep laminar zone ($F_{3,156}$ = 5.7, P = 0.001;

Appendix Figure 9D) but the only SZ was significantly different from UC (t-ratio = 3.1, P = 0.003). TAC1 was significantly different between groups in the superficial laminar zone ($F_{3,156}$ = 6.4, P < 0.01; **Appendix Figure 9E**), with both SZ (t-ratio = 4.3, P < 0.01) and MD (t-ratio = 2.7, P = 0.007) individuals exhibited lower levels of TAC1 relative to the UC group. There was no significant difference in TAC1 in the deep laminar zone ($F_{3,156}$ = 1.5, P = 0.23; **Appendix Figure 9F**) and the only diagnostic group difference was between SZ and UC individuals, as noted previously (t-ratio = 1.9, P = 0.05). There was substantial evidence in favor of no difference in expression in SST, TAC1, and NPY in the deep laminar zone in both BP and MD groups.

To assess the overall effect of diagnosis on neuropeptide expression in these two laminar zones, we computed composite scores combining the z-normalized expression ratio for SST, NPY, TAC1 across diagnostic groups relative to the mean and standard deviation of the UC group (**Appendix Figure 10)**. Consistent with the impression from individual transcripts, SZ was associated with lower levels of these neuropeptides in both laminar zones, while MD was associated with lower levels of these neuropeptides only in the superficial laminar zone. There was substantial support for the null hypothesis in the deep laminar zones for both BP and MD.

Finally, in cases where there were significant group differences, we assessed the influence of antemortem comorbid factors present at time of death. Specifically, we assessed the influence of a comorbid alcohol or substance use disorder, antidepressant, antipsychotic, and benzodiazepine or antiepileptic drug use at time of death, death by suicide, or tobacco use at time of death. In the superficial zone, SST levels were lower in SZ and MD. Combining these subject groups, we found that SST mRNA levels were significantly lower in individuals with SZ or MD who were on antidepressants at time of death ($F_{1,76}$ = 5.8, fdr corrected P = 0.05) and in those with a comorbid substance use disorder ($F_{1,76}$ = 5.9, fdr corrected P = 0.05). In contrast, NPY levels in SZ or TAC1

levels in SZ and MD groups did not differ by any of these comorbid factors. Similarly, SST, NPY, and TAC1 levels in the deep laminar zone did not differ in individuals with SZ by any of these comorbid factors.

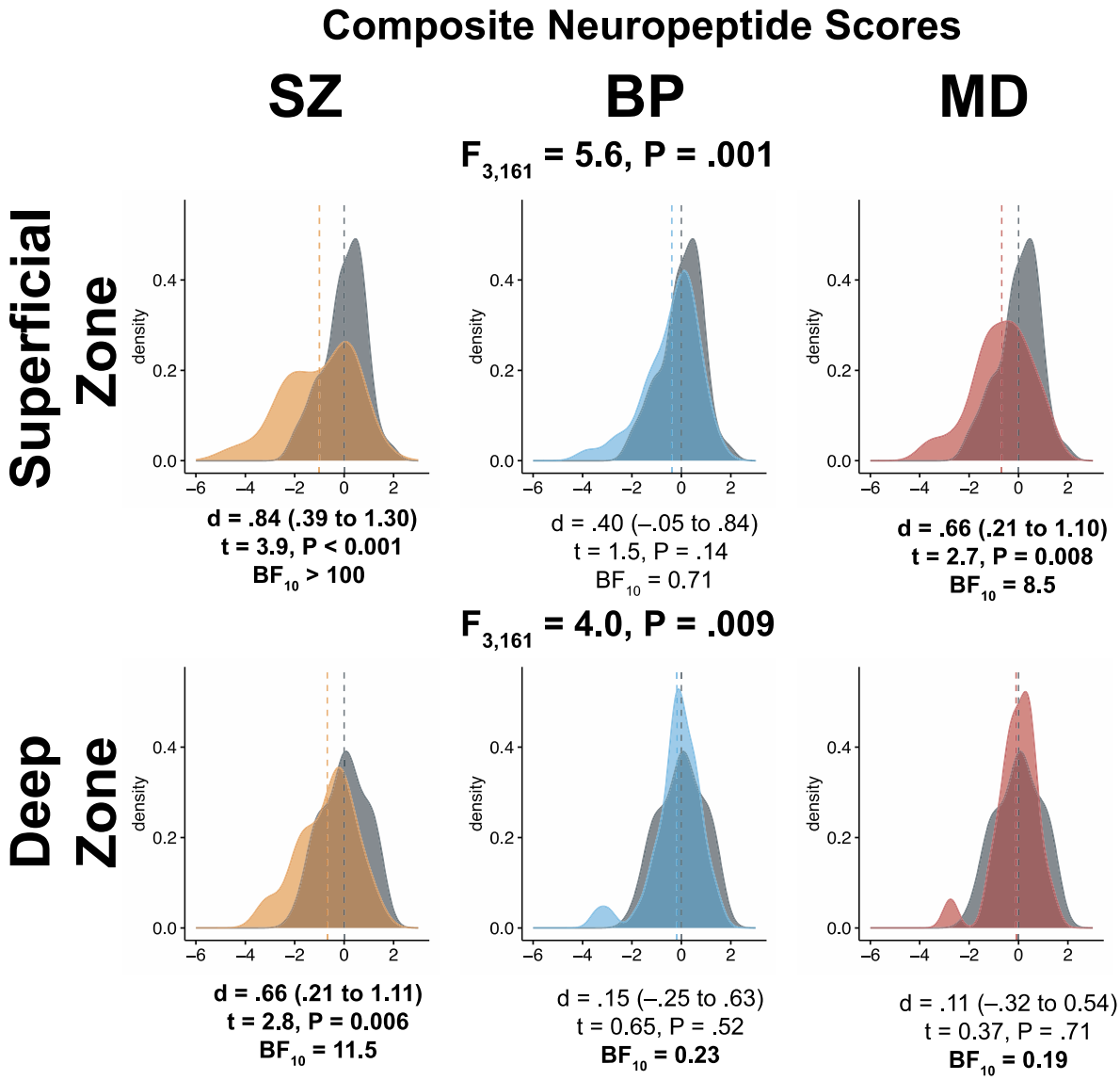

Appendix Figure 10. Composite neuropeptide scores in the superficial and deep laminar zones across diagnoses. On the top row, data are shown for the superficial laminar zone. On the bottom row, data are shown for the deep laminar zone. Data are shown for schizophrenia (SZ), bipolar (BP), and major depressive (MD) disorders. Data are shown as density plots. Gray density distribution is shown for unaffected comparison (UC) individuals. Cohen's d values are show with 95% confidence intervals of the effect size.

BIBLIOGRAPHY

Abbas, A. I., Sundiang, M. J. M., Henoch, B., Morton, M. P., Bolkan, S. S., Park, A. J., Harris, A. Z., Kellendonk, C., & Gordon, J. A. (2018). Somatostatin Interneurons Facilitate Hippocampal-Prefrontal Synchrony and Prefrontal Spatial Encoding. *Neuron*, *100*(4), 926-939.e3. https://doi.org/10.1016/j.neuron.2018.09.029

Addington, A. M., Gornick, M., Duckworth, J., Sporn, A., Gogtay, N., Bobb, A., Greenstein, D., Lenane, M., Gochman, P., Baker, N., Balkissoon, R., Vakkalanka, R. K., Weinberger, D. R., Rapoport, J. L., & Straub, R. E. (2005). GAD1 (2q31.1), which encodes glutamic acid decarboxylase (GAD67), is associated with childhood-onset schizophrenia and cortical gray matter volume loss. *Molecular Psychiatry*, *10*(6), 581-588. https://doi.org/10.1038/sj.mp.4001599

Ahmed, Z., Sheng, H., Xu, Y. F., Lin, W. L., Innes, A. E., Gass, J., Yu, X., Wuertzer, C. A., Hou, H., Chiba, S., Yamanouchi, K., Leissring, M., Petrucelli, L., Nishihara, M., Hutton, M. L., McGowan, E., Dickson, D. W., & Lewis, J. (2010). Accelerated lipofuscinosis and ubiquitination in granulin knockout mice suggest a role for progranulin in successful aging. *Am J Pathol*, *177*(1), 311-324. https://doi.org/10.2353/ajpath.2010.090915

Akaike, H. (1974). A new look at the statistical model identification. *IEEE Transactions on Automatic Control*, *19*(6), 716-723. https://doi.org/10.1109/tac.1974.1100705

Akbarian, S., Bunney, W. E., Potkin, S. G., Wigal, S. B., Hagman, J. O., Sandman, C. A., & Jones, E. G. (1993). Altered distribution of nicotinamide-adenine dinucleotide phosphate-diaphorase cells in frontal lobe of schizophrenics implies disturbances of cortical development. *Arch Gen Psychiatry*, *50*(3), 169-177. https://doi.org/10.1001/archpsyc.1993.01820150007001

Akbarian, S., Kim, J. J., Potkin, S. G., Hagman, J. O., Tafazzoli, A., Bunney, W. E., & Jones, E. G. (1995). Gene expression for glutamic acid decarboxylase is reduced without loss of neurons in prefrontal cortex of schizophrenics. *Arch Gen Psychiatry*, *52*(4), 258-266. https://doi.org/10.1001/archpsyc.1995.03950160008002

Akbarian, S., Kim, J. J., Pothin, S. G., Hetrick, W. P., Bunney, W. E., & Jones, E. G. (1996). Maldistribution of Interstitial Neurons in Prefrontal White Matter of the Brains of Schizophrenic Patients. *Archives of General Psychiatry*, *53*, 425-436.

Albaugh, M. D., Ottino-Gonzalez, J., Sidwell, A., Lepage, C., Juliano, A., Owens, M. M., Chaarani, B., Spechler, P., Fontaine, N., Rioux, P., Lewis, L., Jeon, S., Evans, A., D'Souza, D., Radhakrishnan, R., Banaschewski, T., Bokde, A. L. W., Quinlan, E. B., Conrod, P., . . . IMAGEN, C. (2021). Association of Cannabis Use During Adolescence with Neurodevelopment. *JAMA Psychiatry*. https://doi.org/10.1001/jamapsychiatry.2021.1258

Aleman, A., Hijman, R., de Haan, E. H., & Kahn, R. S. (1999). Memory impairment in schizophrenia: a meta-analysis. *Am J Psychiatry*, *156*(9), 1358-1366. https://doi.org/10.1176/ajp.156.9.1358

Aleman, A., Kahn, R. S., & Selten, J. P. (2003). Sex differences in the risk of schizophrenia: evidence from meta-analysis. *Arch Gen Psychiatry*, *60*(6), 565-571. https://doi.org/10.1001/archpsyc.60.6.565

Ali, A. B., & Thomson, A. M. (2008). Synaptic alpha 5 subunit-containing GABAA receptors mediate IPSPs elicited by dendrite-preferring cells in rat neocortex. *Cereb Cortex*, *18*(6), 1260-1271. https://doi.org/10.1093/cercor/bhm160

Ali, F., Gerhard, D. M., Sweasy, K., Pothula, S., Pittenger, C., Duman, R. S., & Kwan, A. C. (2020). Ketamine disinhibits dendrites and enhances calcium signals in prefrontal dendritic spines. *Nat Commun*, *11*(1), 72. https://doi.org/10.1038/s41467-019-13809-8

Amatrudo, J. M., Weaver, C. M., Crimins, J. L., Hof, P. R., Rosene, D. L., & Luebke, J. I. (2012). Influence of highly distinctive structural properties on the excitability of pyramidal neurons in monkey visual and prefrontal cortices. *J Neurosci*, *32*(40), 13644-13660. https://doi.org/10.1523/JNEUROSCI.2581-12.2012

American Psychiatric Association. (2022). Schizophrenia Spectrum and Other Psychotic Disorders. In *Diagnostic and Statistical Manual of Mental Disorders-5 Text Revision*. American Psychiatric Association Publishing. https://doi.org/10.1176/appi.books.9780890425787.x02_schizophrenia_spectrum

Andreasen, N. C. (1987). The diagnosis of schizophrenia. *Schizophrenia bulletin*, *13*(1), 9-22. https://academic.oup.com/schizophreniabulletin/article-abstract/13/1/9/1854890

Andreasen, N. C. (1995). Symptoms, signs, and diagnosis of schizophrenia. *Lancet*, *346*(8973), 477-481. https://doi.org/10.1016/s0140-6736(95)91325-4

Andressen, C., Blümcke, I., & Celio, M. R. (1993). Calcium-binding proteins: selective markers of nerve cells. *Cell Tissue Res*, *271*(2), 181-208. https://doi.org/10.1007/BF00318606

Anglin, D. M., Ereshefsky, S., Klaunig, M. J., Bridgwater, M. A., Niendam, T. A., Ellman, L. M., DeVylder, J., Thayer, G., Bolden, K., Musket, C. W., Grattan, R. E., Lincoln, S. H., Schiffman, J., Lipner, E., Bachman, P., Corcoran, C. M., Mota, N. B., & van der Ven, E. (2021). From Womb to Neighborhood: A Racial Analysis of Social Determinants of Psychosis in the United States. *Am J Psychiatry*, *178*(7), 599-610. https://doi.org/10.1176/appi.ajp.2020.20071091

Aoki, C., & Pickel, V. M. (1990). Neuropeptide Y in cortex and striatum. Ultrastructural distribution and coexistence with classical neurotransmitters and neuropeptides. *Ann N Y Acad Sci*, *611*, 186-205. https://doi.org/10.1111/j.1749-6632.1990.tb48931.x

Appelbaum, P. S., Robbins, P. C., & Monahan, J. (2000). Violence and delusions: data from the MacArthur Violence Risk Assessment Study. *Am J Psychiatry*, *157*(4), 566-572. https://doi.org/10.1176/appi.ajp.157.4.566

Arion, D., Corradi, J. P., Tang, S., Datta, D., Boothe, F., He, A., Cacace, A. M., Zaczek, R., Albright, C. F., Tseng, G., & Lewis, D. A. (2015). Distinctive transcriptome alterations of prefrontal pyramidal neurons in schizophrenia and schizoaffective disorder. *Mol Psychiatry*, *20*(11), 1397-1405. https://doi.org/10.1038/mp.2014.171

Armstrong, D. M., LeRoy, S., Shields, D., & Terry, R. D. (1985). Somatostatin-like immunoreactivity within neuritic plaques. *Brain Res*, *338*(1), 71-79. https://doi.org/10.1016/0006-8993(85)90249-5

Arnsten, A. F. T., Datta, D., & Wang, M. (2020). The genie in the bottle-magnified calcium signaling in dorsolateral prefrontal cortex. *Mol Psychiatry*. https://pubmed.ncbi.nlm.nih.gov/33319854

Asada, H., Kawamura, Y., Maruyama, K., Kume, H., Ding, R. G., Kanbara, N., Kuzume, H., Sanbo, M., Yagi, T., & Obata, K. (1997). Cleft palate and decreased brain gamma-aminobutyric acid in mice lacking the 67-kDa isoform of glutamic acid decarboxylase. *Proc Natl Acad Sci U S A*, *94*(12), 6496-6499. https://doi.org/10.1073/pnas.94.12.6496

Ascoli, G. A., Alonso-Nanclares, L., Anderson, S. A., Barrionuevo, G., Benavides-Piccione, R., Burkhalter, A., Buzsáki, G., Cauli, B., Defelipe, J., Fairén, A., Feldmeyer, D., Fishell, G., Fregnac, Y., Freund, T. F., Gardner, D., Gardner, E. P., Goldberg, J. H., Helmstaedter, M., Hestrin, S., . . . Yuste, R. (2008). Petilla terminology: nomenclature of features of GABAergic interneurons of the cerebral cortex. *Nat Rev Neurosci*, *9*(7), 557-568. https://doi.org/10.1038/nrn2402

Awh, E., Vogel, E. K., & Oh, S. H. (2006). Interactions between attention and working memory. *Neuroscience*, *139*(1), 201-208. https://doi.org/10.1016/j.neuroscience.2005.08.023

Ayano, G., Tesfaw, G., & Shumet, S. (2019). The prevalence of schizophrenia and other psychotic disorders among homeless people: a systematic review and meta-analysis. *BMC Psychiatry*, *19*(1). https://doi.org/10.1186/s12888-019-2361-7

Azim, E., Jabaudon, D., Fame, R. M., & Macklis, J. D. (2009). SOX6 controls dorsal progenitor identity and interneuron diversity during neocortical development. *Nature Neuroscience*, *12*(10), 1238-1247. https://doi.org/10.1038/nn.2387

Baddeley, A. (2012). Working memory: theories, models, and controversies. *Annu Rev Psychol*, *63*, 1-29. https://doi.org/10.1146/annurev-psych-120710-100422

Baddeley, A. D. (1983). Working Memory. *Philosophical Transactions of the Royal Society of London. Series B, Biological Sciences*, *302*(1110), 311-324.

Ballard, T. M., Knoflach, F., Prinssen, E., Borroni, E., Vivian, J. A., Basile, J., Gasser, R., Moreau, J. L., Wettstein, J. G., Buettelmann, B., Knust, H., Thomas, A. W., Trube, G., & Hernandez, M. C. (2009). RO4938581, a novel cognitive enhancer acting at GABAA alpha5 subunit-containing receptors. *Psychopharmacology (Berl)*, *202*(1-3), 207-223. https://doi.org/10.1007/s00213-008-1357-7

Banasr, M., Lepack, A., Fee, C., Duric, V., Maldonado-Aviles, J., DiLeone, R., Sibille, E., Duman, R. S., & Sanacora, G. (2017). Characterization of GABAergic Marker Expression in the Chronic Unpredictable Stress Model of Depression. *Chronic Stress*, *1*, 247054701772045-247054701772045. https://doi.org/10.1177/2470547017720459

Bankhead, P., Loughrey, M. B., Fernández, J. A., Dombrowski, Y., McArt, D. G., Dunne, P. D., McQuaid, S., Gray, R. T., Murray, L. J., Coleman, H. G., James, J. A., Salto-Tellez, M., & Hamilton, P. W. (2017). QuPath: Open source software for digital pathology image analysis. *Sci Rep*, *7*(1), 16878. https://doi.org/10.1038/s41598-017-17204-5

Barbas, H. (1986). Pattern in the laminar origin of corticocortical connections. *J Comp Neurol*, *252*(3), 415-422. https://doi.org/10.1002/cne.902520310

Barbas, H., & Rempel-Clower, N. (1997). Cortical structure predicts the pattern of corticocortical connections. *Cereb Cortex*, *7*(7), 635-646. https://doi.org/10.1093/cercor/7.7.635

Barch, D. M., Smith, E., Engle, R., Cowan, N., Jonides, J., Braver, T., Frank, M., Robbins, T., Gooding, D., Barch, D., Gold, J., Seidman, L., MacDonald, A., & Ragland, D. (2008). The Cognitive Neuroscience of Working Memory: Relevance to CNTRICS and Schizophrenia. *Biological Psychiatry*, *64*, 11-17. https://doi.org/10.1016/j.biopsych.2008.03.003

Bastos, A. M., Loonis, R., Kornblith, S., Lundqvist, M., & Miller, E. K. (2018). Laminar recordings in frontal cortex suggest distinct layers for maintenance and control of working memory. *Proc Natl Acad Sci U S A*, *115*(5), 1117-1122. https://doi.org/10.1073/pnas.1710323115

Bates, D., Mächler, M., Bolker, B., & Walker, S. (2015). Fitting Linear Mixed-Effects Models Usinglme4. *Journal of Statistical Software*, *67*(1), 1-48. https://doi.org/10.18637/jss.v067.i01

Batista-Brito, R., Rossignol, E., Hjerling-Leffler, J., Denaxa, M., Wegner, M., Lefebvre, V., Pachnis, V., & Fishell, G. (2009). The cell-intrinsic requirement of Sox6 for cortical interneuron development. *Neuron*, *63*(4), 466-481. https://doi.org/10.1016/j.neuron.2009.08.005

Beal, M. F., Mazurek, M. F., Tran, V. T., Chattha, G., Bird, E.D., & Martin, J. B. (1985). Reduced Numbers of Somatostatin Receptors in the Cerebral Cortex in Alzheimer's Disease. *Science, 229, No. 4710*(Jul. 19, 1985), 289-291. https://doi.org/10.2307/1695182

Beal, M. F., Mazurek, M. F., Svendsen, C. N., Bird, E. D., & Martin, J. B. (1986). Widespread reduction of somatostatin-like immunoreactivity in the cerebral cortex in Alzheimer's disease. *Ann Neurol*, *20*(4), 489-495. https://doi.org/10.1002/ana.410200408

Beasley, C. L., & Reynolds, G. P. (1997). Parvalbumin-immunoreactive neurons are reduced in the prefrontal cortex of schizophrenics. *Schizophr Res*, *24*(3), 349-355. https://doi.org/10.1016/s0920-9964(96)00122-3

Beasley, C. L., Zhang, Z. J., Patten, I., & Reynolds, G. P. (2002). Selective deficits in prefrontal cortical GABAergic neurons in schizophrenia defined by the presence of calcium-binding proteins. *Biol Psychiatry*, *52*(7), 708-715. https://doi.org/10.1016/s0006-3223(02)01360-4

Beauchamp, G., & Gagnon, A. (2004). Influence of diagnostic classification on gender ratio in schizophrenia. *Social Psychiatry and Psychiatric Epidemiology*, *39*(12), 1017-1022. https://doi.org/10.1007/s00127-004-0844-3

Benavides, S. H., Monserrat, A. J., Fariña, S., & Porta, E. A. (2002). Sequential histochemical studies of neuronal lipofuscin in human cerebral cortex from the first to the ninth decade of life. *Arch Gerontol Geriatr*, *34*(3), 219-231. https://doi.org/10.1016/s0167-4943(01)00223-0

Benes, F. M., McSparren, J., Bird, E. D., SanGiovanni, J. P., & Vincent, S. L. (1991). Deficits in small interneurons in prefrontal and cingulate cortices of schizophrenic and schizoaffective

patients. *Arch Gen Psychiatry*, *48*(11), 996-1001. https://doi.org/10.1001/archpsyc.1991.01810350036005

Benevento, L. A., Bakkum, B. W., & Cohen, R. S. (1995). Gamma-aminobutyric acid and somatostatin immunoreactivity in the visual cortex of normal and dark-reared rats. *689*(2), 172-182. https://doi.org/10.1016/0006-8993(95)00553-3

Benjamini, Y., & Hochberg, Y. (1995). Controlling the False Discovery Rate: A Practical and Powerful Approach to Multiple Testing. *Journal of the Royal Statistical Society. Series B (Methodological)*, *57*(1), 289-300. http://www.jstor.org/stable/10.2307/2346101

Benson, D. L., Huntsman, M. M., & Jones, E. G. (1994). Activity-dependent changes in GAD and preprotachykinin mRNAs in visual cortex of adult monkeys. *Cereb Cortex*, *4*(1), 40-51. https://doi.org/10.1093/cercor/4.1.40

Bernard, A., Lubbers, L. S., Tanis, K. Q., Luo, R., Podtelezhnikov, A. A., Finney, E. M., McWhorter, M. M., Serikawa, K., Lemon, T., Morgan, R., Copeland, C., Smith, K., Cullen, V., Davis-Turak, J., Lee, C. K., Sunkin, S. M., Loboda, A. P., Levine, D. M., Stone, D. J., . . . Lein, E. S. (2012). Transcriptional architecture of the primate neocortex. *Neuron*, *73*(6), 1083-1099. https://doi.org/10.1016/j.neuron.2012.03.002

Bitanihirwe, B. K., & Woo, T. U. (2014). Transcriptional dysregulation of γ-aminobutyric acid transporter in parvalbumin-containing inhibitory neurons in the prefrontal cortex in schizophrenia. *Psychiatry Res*, *220*(3), 1155-1159. https://doi.org/10.1016/j.psychres.2014.09.016

Black, D. W., & Andreasen, N. C. (2014). *Introductory Textbook of Psychiatry, Sixth Edition*. American Psychiatric Association Publishing. https://books.google.com/books?id=A6iTAwAAQBAJ

Bleuler, E. (1950). Dementia praecox or the group of schizophrenias. https://psycnet.apa.org/record/1951-03305-000

Bloem, B., Poorthuis, R. B., & Mansvelder, H. D. (2014). Cholinergic modulation of the medial prefrontal cortex: the role of nicotinic receptors in attention and regulation of neuronal activity. *Front Neural Circuits*, *8*, 17. https://doi.org/10.3389/fncir.2014.00017

Bloss, E. B., Cembrowski, M. S., Karsh, B., Colonell, J., Fetter, R. D., & Spruston, N. (2016). Structured Dendritic Inhibition Supports Branch-Selective Integration in CA1 Pyramidal Cells. *Neuron*, *89*(5), 1016-1030. https://doi.org/10.1016/j.neuron.2016.01.029

Boehm, S., & Betz, H. (1997). Somatostatin inhibits excitatory transmission at rat hippocampal synapses via presynaptic receptors. *J Neurosci*, *17*(11), 4066-4075. https://doi.org/https://doi.org/10.1523/JNEUROSCI.17-11-04066.1997

Boettcher, L. B., & Menacho, S. T. (2017). The early argument for prefrontal leucotomy: the collision of frontal lobe theory and psychosurgery at the 1935 International Neurological Congress in London. *Neurosurg Focus*, *43*(3), E4. https://doi.org/10.3171/2017.6.FOCUS17249

Bora, E., & Murray, R. M. (2014). Meta-analysis of cognitive deficits in ultra-high risk to psychosis and first-episode psychosis: do the cognitive deficits progress over, or after, the onset of psychosis. *Schizophr Bull*, *40*(4), 744-755. https://doi.org/10.1093/schbul/sbt085

Bouras, C., Magistretti, P. J., Morrison, J. H., & Constantinidis, J. (1987). An immunohistochemical study of pro-somatostatin-derived peptides in the human brain. *Neuroscience, 22*(3), 781-800. https://doi.org/10.1016/0306-4522(87)92959-9

Bowie, C. R., & Harvey, P. D. (2006). Cognitive deficits and functional outcome in schizophrenia. *Neuropsychiatr Dis Treat, 2*(4), 531-536. https://doi.org/10.2147/nedt.2006.2.4.531

Bowie, C. R., Reichenberg, A., Patterson, T. L., Heaton, R. K., & Harvey, P. D. (2006). Determinants of real-world functional performance in schizophrenia subjects: correlations with cognition, functional capacity, and symptoms. *Am J Psychiatry, 163*(3), 418-425. https://doi.org/10.1176/appi.ajp.163.3.418

Braver, T. S., Cohen, J. D., Nystrom, L. E., Jonides, J., Smith, E. E., & Noll, D. C. (1997). A parametric study of prefrontal cortex involvement in human working memory. *Neuroimage, 5*(1), 49-62. https://www.sciencedirect.com/science/article/pii/S1053811996902475

Bredt, D. S., Glatt, C. E., Hwang, P. M., Fotuhi, M., Dawson, T. M., & Snyder, S. H. (1991). Nitric oxide synthase protein and mRNA are discretely localized in neuronal populations of the mammalian CNS together with NADPH diaphorase. *Neuron, 7*(4), 615-624. https://doi.org/10.1016/0896-6273(91)90374-9

Breslaw, B. E. R. N. A. R. D., Barrera, S. E., & Warden, C. A. R. L. J. (1934). The effect of removal of the post-central convolution of the Macacus rhesus monkey upon the delayed response. *Journal of Comparative Psychology, 18*(2), 207-226. https://doi.org/10.1037/h0070359&hl=en&as_sdt=0,39

Bresnahan, M., Begg, M. D., Brown, A., Schaefer, C., Sohler, N., Insel, B., Vella, L., & Susser, E. (2007). Race and risk of schizophrenia in a US birth cohort: another example of health disparity. *International Journal of Epidemiology, 36*(4), 751-758. https://doi.org/10.1093/ije/dym041

Brickner, R. M. (1936). *The intellectual functions of the frontal lobes.* Macmillan. https://psycnet.apa.org/record/1937-00574-000

Brizzee, K. R., Ordy, J. M., & Kaack, B. (1974). Early appearance and regional differences in intraneuronal and extraneuronal lipofuscin accumulation with age in the brain of a nonhuman primate (Macaca mulatta). *J Gerontol, 29*(4), 366-381. https://doi.org/10.1093/geronj/29.4.366

Brockway, D. F., & Crowley, N. A. (2020). Turning the 'Tides on Neuropsychiatric Diseases: The Role of Peptides in the Prefrontal Cortex. *Front Behav Neurosci, 14*, 588400. https://doi.org/10.3389/fnbeh.2020.588400

Brown, K. (2021). 'Schizophrenia' Still Carries a Stigma. Will Changing the Name Help? – *The New York Times*. Retrieved 2022-06-29 from https://www.nytimes.com/2021/12/20/health/schizophrenia-name-change.html

Buckley, M. J., Mansouri, F. A., Hoda, H., Mahboubi, M., Browning, P. G. F., Kwok, S. C., Phillips, A., & Tanaka, K. (2009). Dissociable Components of Rule-Guided Behavior Depend on Distinct Medial and Prefrontal Regions. *Science, 325*(5936), 52-58. https://doi.org/10.1126/science.1172377

Burns, J. (2009). Dispelling a myth: developing world poverty, inequality, violence and social fragmentation are not good for outcome in schizophrenia. *Afr J Psychiatry (Johannesbg)*, *12*(3), 200-205. https://doi.org/10.4314/ajpsy.v12i3.48494

Butler, A., Hoffman, P., Smibert, P., Papalexi, E., & Satija, R. (2018). Integrating single-cell transcriptomic data across different conditions, technologies, and species. *Nat Biotechnol*, *36*(5), 411-420. https://doi.org/10.1038/nbt.4096

Butters, N., Pandya, D., Stein, D., & Rosen, J. (1972). A search for the spatial engram within the frontal lobes of monkeys. *Acta Neurobiol Exp (Wars)*, *32*(2), 305-329. https://pubmed.ncbi.nlm.nih.gov/4627618

Butters, N., & Pandya, D. (1969). Retention of delayed-alternation: effect of selective lesions of sulcus principalis. *Science*, *165*(3899), 1271-1273. https://doi.org/10.2307/1727991

Buzsaki, G., & Wang, X. J. (2012). Mechanisms of gamma oscillations. *Annu Rev Neurosci*, *35*, 203-225. https://doi.org/10.1146/annurev-neuro-062111-150444

Caillard, O., Moreno, H., Schwaller, B., Llano, I., Celio, M. R., & Marty, A. (2000). Role of the calcium-binding protein parvalbumin in short-term synaptic plasticity. *Proc Natl Acad Sci U S A*, *97*(24), 13372-13377. https://doi.org/10.1073/pnas.230362997

Calkins, M. E., Tepper, P., Gur, R. C., Ragland, J. D., Klei, L., Wiener, H. W., Richard, J., Savage, R. M., Allen, T. B., O'Jile, J., Devlin, B., Kwentus, J., Aliyu, M. H., Bradford, L. D., Edwards, N., Lyons, P. D., Nimgaonkar, V. L., Santos, A. B., Go, R. C., . . . Gur, R. E. (2010). Project among African-Americans to explore risks for schizophrenia (PAARTNERS): evidence for impairment and heritability of neurocognitive functioning in families of schizophrenia patients. *Am J Psychiatry*, *167*(4), 459-472. https://doi.org/10.1176/appi.ajp.2009.08091351

Callicott, J. H., Mattay, V. S., Bertolino, A., Finn, K., Coppola, R., Frank, J. A., Goldberg, T. E., & Weinberger, D. R. (1999). Physiological characteristics of capacity constraints in working memory as revealed by functional MRI. *Cerebral cortex*, *9*(1), 20-26. https://academic.oup.com/cercor/article/9/1/20/314918

Campagnola, L., Seeman, S. C., Chartrand, T., Kim, L., Hoggarth, A., Gamlin, C., Ito, S., Trinh, J., Davoudian, P., Radaelli, C., Kim, M. H., Hage, T., Braun, T., Alfiler, L., Andrade, J., Bohn, P., Dalley, R., Henry, A., Kebede, S., . . . Jarsky, T. (2022). Local connectivity and synaptic dynamics in mouse and human neocortex. *Science*, *375*(6585), eabj5861. https://doi.org/10.1126/science.abj5861

Campbell, M. M., Sibeko, G., Mall, S., Baldinger, A., Nagdee, M., Susser, E., & Stein, D. J. (2017). The content of delusions in a sample of South African Xhosa people with schizophrenia. *BMC Psychiatry*, *17*(1). https://doi.org/10.1186/s12888-017-1196-3

Camperi, M., & Wang, X.-J. (1998). A model of visuospatial working memory in prefrontal cortex: recurrent network and cellular bistability. *Journal of computational neuroscience*, *5*(4), 383-405. https://link.springer.com/article/10.1023/A:1008837311948

Canetta, S., Bolkan, S., Padilla-Coreano, N., Song, L. J., Sahn, R., Harrison, N. L., Gordon, J. A., Brown, A., & Kellendonk, C. (2016). Maternal immune activation leads to selective functional deficits in offspring parvalbumin interneurons. *Mol Psychiatry*, *21*(7), 956-968. https://doi.org/10.1038/mp.2015.222

Cao, J. W., Guan, W., Yu, Y. C., & Fu, Y. (2020). Synaptic Transmission from Somatostatin-expressing Interneurons to Excitatory Neurons Mediated by α5-subunit-containing $GABA_A$ Receptors in the Developing Visual Cortex. *Neuroscience*. https://doi.org/10.1016/j.neuroscience.2020.09.008

Carder, R. K., Leclerc, S. S., & Hendry, S. H. (1996). Regulation of calcium-binding protein immunoreactivity in GABA neurons of macaque primary visual cortex. *Cereb Cortex, 6*(2), 271-287. https://doi.org/10.1093/cercor/6.2.271

Cardin, J. A. (2018). Inhibitory Interneurons Regulate Temporal Precision and Correlations in Cortical Circuits. *Trends Neurosci, 41*(10), 689-700. https://doi.org/10.1016/j.tins.2018.07.015

Cardin, J. A., Carlén, M., Meletis, K., Knoblich, U., Zhang, F., Deisseroth, K., Tsai, L.-H., & Moore, C. I. (2009). Driving fast-spiking cells induces gamma rhythm and controls sensory responses. *Nature, 459*(7247), 663-667. https://doi.org/10.1038/nature08002

Carlo, C. N., & Stevens, C. F. (2013). Structural uniformity of neocortex, revisited. *Proceedings of the National Academy of Sciences of the United States of America, 110*(4), 1488-1493. https://doi.org/10.1073/pnas.1221398110

Carter, C. S., Perlstein, W., Ganguli, R., Brar, J., Mintun, M., & Cohen, J. D. (1998). Functional hypofrontality and working memory dysfunction in schizophrenia. *Am J Psychiatry, 155*(9), 1285-1287. https://doi.org/10.1176/ajp.155.9.1285

Cauli, B., Tong, X. K., Rancillac, A., Serluca, N., Lambolez, B., Rossier, J., & Hamel, E. (2004). Cortical GABA interneurons in neurovascular coupling: relays for subcortical vasoactive pathways. *J Neurosci, 24*(41), 8940-8949. https://doi.org/10.1523/JNEUROSCI.3065-04.2004

Cauli, B., & Hamel, E. (2010). Revisiting the role of neurons in neurovascular coupling. *Front Neuroenergetics, 2*, 9. https://doi.org/10.3389/fnene.2010.00009

Chafee, M. V., & Goldman-Rakic, P. S. (2000). Inactivation of parietal and prefrontal cortex reveals interdependence of neural activity during memory-guided saccades. *J Neurophysiol, 83*(3), 1550-1566. https://doi.org/10.1152/jn.2000.83.3.1550

Chao, L. L., & Knight, R. T. (1995). Human prefrontal lesions increase distractibility to irrelevant sensory inputs. *Neuroreport, 6*(12), 1605-1610. https://doi.org/10.1097/00001756-199508000-00005

Charlson, F. J., Ferrari, A. J., Santomauro, D. F., Diminic, S., Stockings, E., Scott, J. G., McGrath, J. J., & Whiteford, H. A. (2018). Global Epidemiology and Burden of Schizophrenia: Findings From the Global Burden of Disease Study 2016. *Schizophr Bull, 44*(6), 1195-1203. https://doi.org/10.1093/schbul/sby058

Chaudhuri, R., Knoblauch, K., Gariel, M. A., Kennedy, H., & Wang, X. J. (2015). A Large-Scale Circuit Mechanism for Hierarchical Dynamical Processing in the Primate Cortex. *Neuron, 88*(2), 419-431. https://doi.org/10.1016/j.neuron.2015.09.008

Chen, C. M., Stanford, A. D., Mao, X., Abi-Dargham, A., Shungu, D. C., Lisanby, S. H., Schroeder, C. E., & Kegeles, L. S. (2014). GABA level, gamma oscillation, and working

memory performance in schizophrenia. *Neuroimage Clin*, *4*, 531-539. https://doi.org/10.1016/j.nicl.2014.03.007

Chen, G., Zhang, Y., Li, X., Zhao, X., Ye, Q., Lin, Y., Tao, H. W., Rasch, M. J., & Zhang, X. (2017). Distinct Inhibitory Circuits Orchestrate Cortical beta and gamma Band Oscillations. *Neuron*, *96*, 1403-1418. http://www.cell.com/neuron/pdf/S0896-6273(17)31086-3.pdf

Chesney, E., Goodwin, G. M., & Fazel, S. (2014). Risks of all-cause and suicide mortality in mental disorders: a meta-review. *World Psychiatry*, *13*(2), 153-160. https://doi.org/10.1002/wps.20128

Chiu, C. Q., Barberis, A., & Higley, M. J. (2019). Preserving the balance: diverse forms of long-term GABAergic synaptic plasticity. *Nat Rev Neurosci*, *20*(5), 272-281. https://doi.org/10.1038/s41583-019-0141-5

Chiu, C. Q., Lur, G., Morse, T. M., Carnevale, N. T., Ellis-Davies, G. C., & Higley, M. J. (2013). Compartmentalization of GABAergic inhibition by dendritic spines. *Science*, *340*(6133), 759-762. https://doi.org/10.1126/science.1234274

Cho, R. Y., Konecky, R. O., & Carter, C. S. (2006). Impairments in frontal cortical gamma synchrony and cognitive control in schizophrenia. *Proceedings of the National Academy of Sciences of the United States of America*, *103*(52), 19878-19883. https://doi.org/10.1073/pnas.0609440103

Choi, K. H., Elashoff, M., Higgs, B. W., Song, J., Kim, S., Sabunciyan, S., Diglisic, S., Yolken, R. H., Knable, M. B., Torrey, E. F., & Webster, M. J. (2008). Putative psychosis genes in the prefrontal cortex: combined analysis of gene expression microarrays. *BMC Psychiatry*, *8*, 87. https://doi.org/10.1186/1471-244X-8-87

Chong, H. Y., Teoh, S. L., Wu, D. B., Kotirum, S., Chiou, C. F., & Chaiyakunapruk, N. (2016). Global economic burden of schizophrenia: a systematic review. *Neuropsychiatr Dis Treat*, *12*, 357-373. https://doi.org/10.2147/NDT.S96649

Chun, J. J., & Shatz, C. J. (1989). Interstitial cells of the adult neocortical white matter are the remnant of the early generated subplate neuron population. *J Comp Neurol*, *282*(4), 555-569. https://doi.org/10.1002/cne.902820407

Chung, D. W., Chung, Y., Bazmi, H. H., & Lewis, D. A. (2018). Altered ErbB4 splicing and cortical parvalbumin interneuron dysfunction in schizophrenia and mood disorders. *Neuropsychopharmacology*, *43*(12), 2478-2486. https://doi.org/10.1038/s41386-018-0169-7

Chung, D. W., Fish, K. N., & Lewis, D. A. (2016a). Pathological Basis for Deficient Excitatory Drive to Cortical Parvalbumin Interneurons in Schizophrenia. *Am J Psychiatry*, *173*(11), 1131-1139. https://doi.org/10.1176/appi.ajp.2016.16010025

Chung, D. W., Volk, D. W., Arion, D., Zhang, Y., Sampson, A. R., & Lewis, D. A. (2016b). Dysregulated ErbB4 Splicing in Schizophrenia: Selective Effects on Parvalbumin Expression. *Am J Psychiatry*, *173*(1), 60-68. https://doi.org/10.1176/appi.ajp.2015.15020150

Clarke, E., & Sherrill-Mix, S. (2017). ggbeeswarm: Categorical Scatter (Violin Point) Plots. https://CRAN.R-project.org/package=ggbeeswarm

Cloutier, M., Aigbogun, M. S., Guerin, A., Nitulescu, R., Ramanakumar, A. V., Kamat, S. A., DeLucia, M., Duffy, R., Legacy, S. N., Henderson, C., Francois, C., & Wu, E. (2016). The economic burden of schizophrenia in the United States in 2013. *Journal of Clinical Psychiatry, 77*(6), 764-771. https://doi.org/10.4088/JCP.15m10278

Clowry, G. J. (2015). An enhanced role and expanded developmental origins for gamma-aminobutyric acidergic interneurons in the human cerebral cortex. *J Anat, 227*(4), 384-393. https://doi.org/10.1111/joa.12198

Coe, R. (2002). *It's the effect size, stupid: what effect size is and why it is important*. In. England.

Cohen, A., Patel, V., Thara, R., & Gureje, O. (2007). Questioning an Axiom: Better Prognosis for Schizophrenia in the Developing World. *Schizophrenia Bulletin, 34*(2), 229-244. https://doi.org/10.1093/schbul/sbm105

Cohen, J. (1988). *Statistical Power Analysis for the Behavioral Sciences*. Routledge. https://doi.org/10.4324/9780203771587

Collins, C. E., Turner, E. C., Sawyer, E. K., Reed, J. L., Young, N. A., Flaherty, D. K., & Kaas, J. H. (2016). Cortical cell and neuron density estimates in one chimpanzee hemisphere. *Proc Natl Acad Sci U S A, 113*(3), 740-745. https://doi.org/10.1073/pnas.1524208113

Compte, A., Brunel, N., Goldman-Rakic, P. S., & Wang, X. J. (2000). Synaptic mechanisms and network dynamics underlying spatial working memory in a cortical network model. *Cereb Cortex, 10*(9), 910-923. https://doi.org/10.1093/cercor/10.9.910

Condé, F., Lund, J. S., Jacobowitz, D. M., Baimbridge, K. G., & Lewis, D. A. (1994). Local circuit neurons immunoreactive for calretinin, calbindin D-28k or parvalbumin in monkey prefrontal cortex: distribution and morphology. *J Comp Neurol, 341*(1), 95-116. https://doi.org/10.1002/cne.903410109

Connor, C. M., Crawford, B. C., & Akbarian, S. (2010). White matter neuron alterations in schizophrenia and related disorders. *Int. J. Devl Neuroscience, 29*, 325-334. https://doi.org/10.1016/j.ijdevneu.2010.07.236

Consens, M. E., Chen, Y., Menon, V., Wang, Y., Schneider, J. A., De Jager, P. L., Bennett, D. A., Tripathy, S. J., & Felsky, D. (2022). Bulk and Single-nucleus Transcriptomics Highlight Intra-telencephalic and Somatostatin Neurons in Alzheimer's Disease. *Front Mol Neurosci.* https://doi.org/10.3389/fnmol.2022.903175.

Constantinidis, C., Funahashi, S., Lee, D., Murray, J. D., Qi, X. L., Wang, M., & Arnsten, A. F. T. (2018). Persistent Spiking Activity Underlies Working Memory. *J Neurosci, 38*(32), 7020-7028. https://doi.org/10.1523/JNEUROSCI.2486-17.2018

Constantinidis, C., Williams, G. V., & Goldman-Rakic, P. S. (2002). A role for inhibition in shaping the temporal flow of information in prefrontal cortex. *Nat Neurosci, 5*(2), 175-180. https://doi.org/10.1038/nn799

Conway, A. R., Cowan, N., & Bunting, M. F. (2001). The cocktail party phenomenon revisited: the importance of working memory capacity. *Psychon Bull Rev*, *8*(2), 331-335. https://doi.org/10.3758/bf03196169

Cotton, S. M., Lambert, M., Schimmelmann, B. G., Foley, D. L., Morley, K. I., McGorry, P. D., & Conus, P. (2009). Gender differences in premorbid, entry, treatment, and outcome characteristics in a treated epidemiological sample of 661 patients with first episode psychosis. *Schizophrenia Research*, *114*(1-3), 17-24. https://doi.org/10.1016/j.schres.2009.07.002

Coyle, J. T. (2012). NMDA Receptor and Schizophrenia: A Brief History. *Schizophrenia Bulletin*, *38*(5), 920-926. https://doi.org/10.1093/schbul/sbs076

Crowe, D. A., Goodwin, S. J., Blackman, R. K., Sakellaridi, S., Sponheim, S. R., MacDonald, A. W., & Chafee, M. V. (2013). Prefrontal neurons transmit signals to parietal neurons that reflect executive control of cognition. *Nat Neurosci*, *16*(10), 1484-1491. https://doi.org/10.1038/nn.3509

Cruikshank, S. J., Lewis, T. J., & Connors, B. W. (2007). Synaptic basis for intense thalamocortical activation of feedforward inhibitory cells in neocortex. *Nature Neuroscience*, *10*(4), 462-468. https://doi.org/10.1038/nn1861

Curley, A. A., Arion, D., Volk, D. W., Asafu-Adjei, J. K., Sampson, A. R., Fish, K. N., & Lewis, D. A. (2011). Cortical deficits of glutamic acid decarboxylase 67 expression in schizophrenia: clinical, protein, and cell type-specific features. *Am J Psychiatry*, *168*(9), 921-929. https://doi.org/10.1176/appi.ajp.2011.11010052

Curley, A. A., & Lewis, D. A. (2012). Cortical basket cell dysfunction in schizophrenia. *J Physiol*, *590*(4), 715-724. https://doi.org/10.1113/jphysiol.2011.224659

Curran, H. V., Freeman, T. P., Mokrysz, C., Lewis, D. A., Morgan, C. J., & Parsons, L. H. (2016). Keep off the grass? Cannabis, cognition and addiction. *Nat Rev Neurosci*, *17*(5), 293-306. https://doi.org/10.1038/nrn.2016.28

D'Esposito, M., Aguirre, G. K., Zarahn, E., Ballard, D., Shin, R. K., & Lease, J. (1998). Functional MRI studies of spatial and nonspatial working memory. *Brain Res Cogn Brain Res*, *7*(1), 1-13. https://doi.org/10.1016/s0926-6410(98)00004-4

D'Esposito, M., & Postle, B. R. (1999). The dependence of span and delayed-response performance on prefrontal cortex. *Neuropsychologia*, *37*(11), 1303-1315. https://doi.org/10.1016/s0028-3932(99)00021-4

Datta, D., Arion, D., Corradi, J. P., & Lewis, D. A. (2015). Altered expression of CDC42 signaling pathway components in cortical layer 3 pyramidal cells in schizophrenia. *Biol Psychiatry*, *78*(11), 775-785. https://doi.org/10.1016/j.biopsych.2015.03.030

Datta, D., Arion, D., Roman, K. M., Volk, D. W., & Lewis, D. A. (2017). Altered Expression of ARP2/3 Complex Signaling Pathway Genes in Prefrontal Layer 3 Pyramidal Cells in Schizophrenia. *Am J Psychiatry*, *174*(2), 163-171. https://doi.org/10.1176/appi.ajp.2016.16020204

Davies, P., Katzman, R., & Terry, R. D. (1980). Reduced somatostatin-like immunoreactivity in cerebral cortex from cases of Alzheimer disease and Alzheimer senile dementa. *Nature, 288*(5788), 279-280. https://doi.org/10.1038/288279a0

Dawson, T. M., Bredt, D. S., Fotuhi, M., Hwang, P. M., & Snyder, S. H. (1991). Nitric oxide synthase and neuronal NADPH diaphorase are identical in brain and peripheral tissues. *Proc Natl Acad Sci U S A, 88*(17), 7797-7801. https://doi.org/10.1073/pnas.88.17.7797

de Jonge, J. C., Vinkers, C. H., Hulshoff Pol, H. E., & Marsman, A. (2017). GABAergic Mechanisms in Schizophrenia: Linking Postmortem and In Vivo Studies. *Frontiers in Psychiatry, 8*, 118-118. https://doi.org/10.3389/fpsyt.2017.00118

de Lecea, L., Criado, J. R., Prospero-Garcia, O., Gautvik, K. M., Schweitzer, P., Danielson, P. E., Dunlop, C. L., Siggins, G. R., Henriksen, S. J., & Sutcliffe, J. G. (1996). A cortical neuropeptide with neuronal depressant and sleep-modulating properties. *Nature, 381*(6579), 242-245. https://doi.org/10.1038/381242a0

de Lecea, L., del Rio, J. A., Criado, J. R., Alcántara, S., Morales, M., Danielson, P. E., Henriksen, S. J., Soriano, E., & Sutcliffe, J. G. (1997). Cortistatin is expressed in a distinct subset of cortical interneurons. *J Neurosci, 17*(15), 5868-5880. https://doi.org/10.1523/jneurosci.17-15-05868.1997

de Lima, A. D., & Morrison, J. H. (1989). Ultrastructural analysis of somatostatin-immunoreactive neurons and synapses in the temporal and occipital cortex of the macaque monkey. *J Comp Neurol, 283*(2), 212-227. https://doi.org/10.1002/cne.902830205

DeFelipe, J. (1993). Neocortical neuronal diversity: chemical heterogeneity revealed by colocalization studies of classic neurotransmitters, neuropeptides, calcium-binding proteins, and cell surface molecules. *Cereb Cortex, 3*(4), 273-289. https://doi.org/10.1093/cercor/3.4.273

DeFelipe, J., Hendry, S. H., Hashikawa, T., Molinari, M., & Jones, E. G. (1990). A microcolumnar structure of monkey cerebral cortex revealed by immunocytochemical studies of double bouquet cell axons. *Neuroscience, 37*(3), 655-673. https://doi.org/10.1016/0306-4522(90)90097-n

DeFelipe, J., López-Cruz, P. L., Benavides-Piccione, R., Bielza, C., Larrañaga, P., Anderson, S., Burkhalter, A., Cauli, B., Fairén, A., Feldmeyer, D., Fishell, G., Fitzpatrick, D., Freund, T. F., González-Burgos, G., Hestrin, S., Hill, S., Hof, P. R., Huang, J., Jones, E. G., . . . Ascoli, G. A. (2013). New insights into the classification and nomenclature of cortical GABAergic interneurons. *Nat Rev Neurosci, 14*(3), 202-216. https://doi.org/10.1038/nrn3444

DeFelipe, J. (1997). Types of neurons, synaptic connections and chemical characteristics of cells immunoreactive for calbindin-D28K, parvalbumin and calretinin in the neocortex. *J Chem Neuroanat, 14*(1), 1-19. https://doi.org/10.1016/s0891-0618(97)10013-8

DeFelipe, J., & Jones, E. G. (1991). Parvalbumin immunoreactivity reveals layer IV of monkey cerebral cortex as a mosaic of microzones of thalamic afferent terminations. *Brain Research, 562*(1), 39-47. https://doi.org/10.1016/0006-8993(91)91184-3

DeFelipe, J., Gonz√°lez-Albo, M. C., del Rio, J. A., & Elston, G. N. (1999). Distribution and patterns of connectivity of interneurons containing calbindin, calretinin, and parvalbumin

in visual areas of the occipital and temporal lobes of the macaque monkey. *The Journal of Comparative Neurology*, *412*(3), 515-526. https://doi.org/10.1002/(sici)1096-9861(19990927)412:3<515::Aid-cne10>3.0.Co;2-1

del Rio, M. R., & DeFelipe, J. (1997). Colocalization of parvalbumin and calbindin D-28k in neurons including chandelier cells of the human temporal neocortex. *J Chem Neuroanat*, *12*(3), 165-173. https://doi.org/10.1016/s0891-0618(96)00191-3

del Río, M. R., & DeFelipe, J. (1996). Colocalization of calbindin D-28k, calretinin, and GABA immunoreactivities in neurons of the human temporal cortex. *J Comp Neurol*, *369*(3), 472-482. https://doi.org/10.1002/(SICI)1096-9861(19960603)369:3<472::AID-CNE11>3.0.CO;2-K

Delfs, J. R., & Dichter, M. A. (1983). Effects of somatostatin on mammalian cortical neurons in culture: physiological actions and unusual dose response characteristics. *J Neurosci*, *3*(6), 1176-1188. https://pubmed.ncbi.nlm.nih.gov/6133919

Deng, S., Li, J., He, Q., Zhang, X., Zhu, J., Li, L., Mi, Z., Yang, X., Jiang, M., Dong, Q., Mao, Y., & Shu, Y. (2020). Regulation of Recurrent Inhibition by Asynchronous Glutamate Release in Neocortex. *Neuron*, *105*(3), 522-533.e4. https://doi.org/10.1016/j.neuron.2019.10.038

di Pellegrino, G., & Wise, S. P. (1993). Visuospatial versus visuomotor activity in the premotor and prefrontal cortex of a primate. *The Journal of Neuroscience*, *13*(3), 1227-1243. https://doi.org/10.1523/jneurosci.13-03-01227.1993

Dienel, S. J., Bazmi, H. H., & Lewis, D. A. (2017). Development of transcripts regulating dendritic spines in layer 3 pyramidal cells of the monkey prefrontal cortex: Implications for the pathogenesis of schizophrenia. *Neurobiol Dis*, *105*, 132-141. https://doi.org/10.1016/j.nbd.2017.05.016

Dienel, S. J., Ciesielski, A. J., Bazmi, H. H., Profozich, E. A., Fish, K. N., & Lewis, D. A. (2021). Distinct Laminar and Cellular Patterns of GABA Neuron Transcript Expression in Monkey Prefrontal and Visual Cortices. *Cereb Cortex*, *31*(5), 2345-2363. https://doi.org/10.1093/cercor/bhaa341

Dienel, S. J., Enwright, J. F., Hoftman, G. D., & Lewis, D. A. (2020). Markers of glutamate and GABA neurotransmission in the prefrontal cortex of schizophrenia subjects: Disease effects differ across anatomical levels of resolution. *Schizophr Res*, *217*, 86-94. https://doi.org/10.1016/j.schres.2019.06.003

Dienel, S. J., & Lewis, D. A. (2017). Cellular Mechanisms of Psychotic Disorders: Human Studies. In D. S. Charney, E. J. Nestler, P. Sklar, & J. D. Buxbaum (Eds.), *Charney & Nestler's Neurobiology of Mental Illness* (pp. 233-244). Oxford University Press. https://books.google.com/books?id=jBBADwAAQBAJ

Dienel, S. J., & Lewis, D. A. (2019). Alterations in cortical interneurons and cognitive function in schizophrenia. *Neurobiol Dis*, *131*, 104208. https://doi.org/10.1016/j.nbd.2018.06.020

Dienel, S. J., Schoonover, K. E., & Lewis, D. A. (2022). Cognitive Dysfunction and Prefrontal Cortical Circuit Alterations in Schizophrenia: Developmental Trajectories. *Biol Psychiatry*, S0006-3223(22)01072. https://doi.org/10.1016/j.biopsych.2022.03.002

Diwan, A., Castine, M., Pomerleau, C. S., Meador-Woodruff, J. H., & Dalack, G. W. (1998). Differential prevalence of cigarette smoking in patients with schizophrenic vs mood disorders. *Schizophr Res*, *33*(1-2), 113-118. https://doi.org/10.1016/s0920-9964(98)00045-0

Dolcos, F., Miller, B., Kragel, P., Jha, A., & McCarthy, G. (2007). Regional brain differences in the effect of distraction during the delay interval of a working memory task. *Brain Res*, *1152*, 171-181. https://doi.org/10.1016/j.brainres.2007.03.059

Donato, F., Rompani, S. B., & Caroni, P. (2013). Parvalbumin-expressing basket-cell network plasticity induced by experience regulates adult learning. *Nature*, *504*(7479), 272-276. https://doi.org/10.1038/nature12866

Dournaud, P., Cervera-Pierot, P., Hirsch, E., Javoy-Agid, F., Kordon, C., Agid, Y., & Epelbaum, J. (1994). Somatostatin messenger RNA-containing neurons in Alzheimer's disease: an in situ hybridization study in hippocampus, parahippocampal cortex and frontal cortex. *Neuroscience*, *61*(4), 755-764. https://doi.org/10.1016/0306-4522(94)90399-9

Dowson, J. H. (1982). Neuronal lipofuscin accumulation in ageing and alzheimer dementia: a pathogenic mechanism. *Br J Psychiatry*, *140*, 142-148. https://doi.org/10.1192/bjp.140.2.142

Duchatel, R. J., Harms, L. R., Meehan, C. L., Michie, P. T., Bigland, M. J., Smith, D. W., Jobling, P., Hodgson, D. M., & Tooney, P. A. (2019a). Reduced cortical somatostatin gene expression in a rat model of maternal immune activation. *Psychiatry Res*, *282*, 112621. https://doi.org/10.1016/j.psychres.2019.112621

Duchatel, R. J., Jobling, P., Graham, B. A., Harms, L. R., Michie, P. T., Hodgson, D. M., & Tooney, P. A. (2016). Increased white matter neuron density in a rat model of maternal immune activation - Implications for schizophrenia. *Prog Neuropsychopharmacol Biol Psychiatry*, *65*, 118-126. https://doi.org/10.1016/j.pnpbp.2015.09.006

Duchatel, R. J., Shannon Weickert, C., & Tooney, P. A. (2019b). White matter neuron biology and neuropathology in schizophrenia. *NPJ Schizophr*, *5*(1), 10. https://doi.org/10.1038/s41537-019-0078-8

Džaja, D., Hladnik, A., Bičanić, I., Baković, M., & Petanjek, Z. (2014). Neocortical calretinin neurons in primates: increase in proportion and microcircuitry structure. *Front Neuroanat*, *8*, 103. https://doi.org/10.3389/fnana.2014.00103

Eack, S. M., Bahorik, A. L., Newhill, C. E., Neighbors, H. W., & Davis, L. E. (2012). Interviewer-perceived honesty as a mediator of racial disparities in the diagnosis of schizophrenia. *Psychiatr Serv*, *63*(9), 875-880. https://doi.org/10.1176/appi.ps.201100388

Ebert, A., & Bär, K. J. (2010). Emil Kraepelin: A pioneer of scientific understanding of psychiatry and psychopharmacology. *Indian J Psychiatry*, *52*(2), 191-192. https://doi.org/10.4103/0019-5545.64591

Egerton, A., Modinos, G., Ferrera, D., & McGuire, P. (2017). Neuroimaging studies of GABA in schizophrenia: a systematic review with meta-analysis. *Transl Psychiatry*, *7*(6), e1147. https://doi.org/10.1038/tp.2017.124

Eggan, S. M., & Lewis, D. A. (2007). Immunocytochemical distribution of the cannabinoid CB1 receptor in the primate neocortex: a regional and laminar analysis. *Cereb Cortex*, *17*(1), 175-191. https://doi.org/10.1093/cercor/bhj136

Eggan, S. M., Melchitzky, D. S., Sesack, S. R., Fish, K. N., & Lewis, D. A. (2010). Relationship of cannabinoid CB1 receptor and cholecystokinin immunoreactivity in monkey dorsolateral prefrontal cortex. *Neuroscience*, *169*(4), 1651-1661. https://doi.org/10.1016/j.neuroscience.2010.06.011

Elbogen, E. B., & Johnson, S. C. (2009). The intricate link between violence and mental disorder: results from the National Epidemiologic Survey on Alcohol and Related Conditions. *Arch Gen Psychiatry*, *66*(2), 152-161. https://doi.org/10.1001/archgenpsychiatry.2008.537

Elston, G. N. (2000). Pyramidal cells of the frontal lobe: all the more spinous to think with. *The Journal of Neuroscience*, *20*(RC95), 1-4. https://doi.org/20004498 [pii]

Elston, G. N. (2002). Cortical heterogeneity: implications for visual processing and polysensory integration. *J Neurocytol*, *31*(3-5), 317-335. https://doi.org/10.1023/a:1024182228103

Enwright Iii, J. F., Huo, Z., Arion, D., Corradi, J. P., Tseng, G., & Lewis, D. A. (2018). Transcriptome alterations of prefrontal cortical parvalbumin neurons in schizophrenia. *Mol Psychiatry*, *23*(7), 1606-1613. https://doi.org/10.1038/mp.2017.216

Enwright, J. F., Sanapala, S., Foglio, A., Berry, R., Fish, K. N., & Lewis, D. A. (2016). Reduced Labeling of Parvalbumin Neurons and Perineuronal Nets in the Dorsolateral Prefrontal Cortex of Subjects with Schizophrenia. *Neuropsychopharmacology*, *41*(9), 2206-2214. https://doi.org/10.1038/npp.2016.24

Erben, L., & Buonanno, A. (2019). Detection and Quantification of Multiple RNA Sequences Using Emerging Ultrasensitive Fluorescent In Situ Hybridization Techniques. *Curr Protoc Neurosci*, *87*(1), e63. https://doi.org/10.1002/cpns.63

Erickson, M., Hahn, B., Leonard, C., Robinson, B., Luck, S., & Gold, J. (2014). Enhanced vulnerability to distraction does not account for working memory capacity reduction in people with schizophrenia. *Schizophrenia Research: Cognition*, *1*(3), 149-154. https://doi.org/10.1016/j.scog.2014.09.001

Estes, M. L., & McAllister, A. K. (2016). Maternal immune activation: Implications for neuropsychiatric disorders. *Science*, *353*(6301), 772-777. https://doi.org/10.1126/science.aag3194

Evensen, S., Wisløff, T., Lystad, J. U., Bull, H., Ueland, T., & Falkum, E. (2016). Prevalence, Employment Rate, and Cost of Schizophrenia in a High-Income Welfare Society: A Population-Based Study Using Comprehensive Health and Welfare Registers. *Schizophrenia Bulletin*, *42*(2), 476-483. https://doi.org/10.1093/schbul/sbv141

Everling, S., Tinsley, C. J., Gaffan, D., & Duncan, J. (2002). Filtering of neural signals by focused attention in the monkey prefrontal cortex. *Nat Neurosci*, *5*(7), 671-676. https://doi.org/10.1038/nn874

Evers, B. M., Rodriguez-Navas, C., Tesla, R. J., Prange-Kiel, J., Wasser, C. R., Yoo, K. S., McDonald, J., Cenik, B., Ravenscroft, T. A., Plattner, F., Rademakers, R., Yu, G., White,

C. L., & Herz, J. (2017). Lipidomic and Transcriptomic Basis of Lysosomal Dysfunction in Progranulin Deficiency. *Cell Rep*, *20*(11), 2565-2574. https://doi.org/10.1016/j.celrep.2017.08.056

Farrant, M., & Nusser, Z. (2005). Variations on an inhibitory theme: phasic and tonic activation of GABA(A) receptors. *Nat Rev Neurosci*, *6*(3), 215-229. https://doi.org/10.1038/nrn1625

Fee, C., Prevot, T. D., Misquitta, K., Knutson, D. E., Li, G., Mondal, P., Cook, J. M., Banasr, M., & Sibille, E. (2021). Behavioral Deficits Induced by Somatostatin-Positive GABA Neuron Silencing Are Rescued by Alpha 5 GABA-A Receptor Potentiation. *Int J Neuropsychopharmacol*, *24*(6), 505-518. https://doi.org/10.1093/ijnp/pyab002

Finn, E. S., Huber, L., Jangraw, D. C., Molfese, P. J., & Bandettini, P. A. (2019). Layer-dependent activity in human prefrontal cortex during working memory. *Nat Neurosci*, *22*(10), 1687-1695. https://doi.org/10.1038/s41593-019-0487-z

Fino, E., & Yuste, R. (2011). Dense inhibitory connectivity in neocortex. *Neuron*, *69*(6), 1188-1203. https://doi.org/10.1016/j.neuron.2011.02.025

Fish, K. N., Rocco, B. R., DeDionisio, A. M., Dienel, S. J., Sweet, R. A., & Lewis, D. A. (2021). Altered Parvalbumin Basket Cell Terminals in the Cortical Visuospatial Working Memory Network in Schizophrenia. *Biol Psychiatry*, *90*(1), 47-57. https://doi.org/10.1016/j.biopsych.2021.02.009

Fish, K. N., Rocco, B. R., & Lewis, D. A. (2018). Laminar Distribution of Subsets of GABAergic Axon Terminals in Human Prefrontal Cortex. *Front Neuroanat*, *12*, 9. https://doi.org/10.3389/fnana.2018.00009

Fish, K. N., Sweet, R. A., & Lewis, D. A. (2011). Differential distribution of proteins regulating GABA synthesis and reuptake in axon boutons of subpopulations of cortical interneurons. *Cereb Cortex*, *21*(11), 2450-2460. https://doi.org/10.1093/cercor/bhr007

Fitzpatrick-McElligott, S., Card, J. P., O'Kane, T. M., & Baldino, F. (1991). Ontogeny of somatostatin mRNA-containing perikarya in the rat central nervous system. *Synapse*, *7*(2), 123-134. https://doi.org/10.1002/syn.890070206

Fleming, K., Goldberg, T. E., Binks, S., Randolph, C., Gold, J. M., & Weinberger, D. R. (1997). Visuospatial working memory in patients with schizophrenia. *Biological Psychiatry*, *41*(1), 43-49. https://doi.org/10.1016/S0006-3223(96)00263-6

Forbes, N. F., Carrick, L. A., McIntosh, A. M., & Lawrie, S. M. (2009). Working memory in schizophrenia: a meta-analysis. *Psychol Med*, *39*(6), 889-905. https://doi.org/10.1017/S0033291708004558

Fox, J., & Weisberg, S. (2019). *An {R} Companion to Applied Regression* (3 ed.). Sage. https://socialsciences.mcmaster.ca/jfox/Books/Companion/

Frankle, W. G., Cho, R. Y., Mason, N. S., Chen, C.-M., Himes, M., Walker, C., Lewis, D. A., Mathis, C. A., & Narendran, R. (2012). [11C] flumazenil Binding Is Increased in a Dose-Dependent Manner with Tiagabine-Induced Elevations in GABA Levels. *PLoS One*, *7*(2), e32443-e32443. https://doi.org/10.1371/journal.pone.0032443

Frankle, W. G., Cho, R. Y., Prasad, K. M., Mason, N. S., Paris, J., Himes, M. L., Walker, C., Lewis, D. A., & Narendran, R. (2015). In Vivo Measurement of GABA Transmission in

Healthy Subjects and Schizophrenia Patients. *The American journal of psychiatry*, *172*(11), 1148-1159. https://doi.org/10.1176/appi.ajp.2015.14081031

Freund, T. F., & Katona, I. (2007). Perisomatic inhibition. *Neuron*, *56*(1), 33-42. https://doi.org/10.1016/j.neuron.2007.09.012

Freund, T. F., Martin, K. A., Soltesz, I., Somogyi, P., & Whitteridge, D. (1989). Arborisation pattern and postsynaptic targets of physiologically identified thalamocortical afferents in striate cortex of the macaque monkey. *J Comp Neurol*, *289*(2), 315-336. https://doi.org/10.1002/cne.902890211

Friedman, H. R., & Goldman-Rakic, P. S. (1994). Coactivation of prefrontal cortex and inferior parietal cortex in working memory tasks revealed by 2DG functional mapping in the rhesus monkey. *Journal of Neuroscience*, *14*(5), 2775-2788. https://doi.org/10.1002/1097-0029(20001001)51:1<54::AID-JEMT6>3.0.CO;2-J

Fromer, M., Pocklington, A. J., Kavanagh, D. H., Williams, H. J., Dwyer, S., Gormley, P., Georgieva, L., Rees, E., Palta, P., Ruderfer, D. M., Carrera, N., Humphreys, I., Johnson, J. S., Roussos, P., Barker, D. D., Banks, E., Milanova, V., Grant, S. G., Hannon, E., . . . O'Donovan, M. C. (2014). De novo mutations in schizophrenia implicate synaptic networks. *Nature*, *506*(7487), 179-184. https://doi.org/10.1038/nature12929

Fromer, M., Roussos, P., Sieberts, S. K., Johnson, J. S., Kavanagh, D. H., Perumal, T. M., Ruderfer, D. M., Oh, E. C., Topol, A., Shah, H. R., Klei, L. L., Kramer, R., Pinto, D., Gümüş, Z. H., Cicek, A. E., Dang, K. K., Browne, A., Lu, C., Xie, L., . . . Sklar, P. (2016). Gene expression elucidates functional impact of polygenic risk for schizophrenia. *Nat Neurosci*, *19*(11), 1442-1453. https://doi.org/10.1038/nn.4399

Froudist-Walsh, S., Bliss, D. P., Ding, X., Rapan, L., Niu, M., Knoblauch, K., Zilles, K., Kennedy, H., Palomero-Gallagher, N., & Wang, X. J. (2021). A dopamine gradient controls access to distributed working memory in the large-scale monkey cortex. *Neuron*, *109*(21), 3500-3520.e13. https://doi.org/10.1016/j.neuron.2021.08.024

Funahashi, S., Bruce, C. J., & Goldman-Rakic, P. S. (1989). Mnemonic coding of visual space in the monkey's dorsolateral prefrontal cortex. *Journal of Neurophysiology*, *61*(2), 331-349. https://doi.org/10.1152/jn.1989.61.2.331

Fung, S. J., Fillman, S. G., Webster, M. J., & Shannon Weickert, C. (2014). Schizophrenia and bipolar disorder show both common and distinct changes in cortical interneuron markers. *Schizophr Res*, *155*(1-3), 26-30. https://doi.org/10.1016/j.schres.2014.02.021

Fung, S. J., Sivagnanasundaram, S., & Weickert, C. S. (2011). Lack of change in markers of presynaptic terminal abundance alongside subtle reductions in markers of presynaptic terminal plasticity in prefrontal cortex of schizophrenia patients. *Biol Psychiatry*, *69*(1), 71-79. https://doi.org/10.1016/j.biopsych.2010.09.036

Fung, S. J., Webster, M. J., Sivagnanasundaram, S., Duncan, C., Elashoff, M., & Weickert, C. S. (2010). Expression of interneuron markers in the dorsolateral prefrontal cortex of the developing human and in schizophrenia. *Am J Psychiatry*, *167*(12), 1479-1488. https://doi.org/10.1176/appi.ajp.2010.09060784

Fuster, J. M., & Alexander, G. E. (1970). Delayed response deficit by cryogenic depression of frontal cortex. *Brain Res*, *20*(1), 85-90. https://doi.org/10.1016/0006-8993(70)90156-3

Fuster, J. M., & Alexander, G. E. (1971). Neuron activity related to short-term memory. *Science*, *173*(3997), 652-654. https://www.science.org/doi/abs/10.1126/science.173.3997.652

Gabbott, P. L., & Bacon, S. J. (1996). Local circuit neurons in the medial prefrontal cortex (areas 24a,b,c, 25 and 32) in the monkey: II. Quantitative areal and laminar distributions. *J Comp Neurol*, *364*(4), 609-636. https://doi.org/10.1002/(SICI)1096-9861(19960122)364:4<609::AID-CNE2>3.0.CO;2-7

Gabbott, P. L. A., Jays, P. R. L., & Bacon, S. J. (1997). Calretinin neurons in human medial prefrontal cortex (areas 24a,b,c, 32?, and 25). *The Journal of Comparative Neurology*, *381*(4), 389-410. https://doi.org/10.1002/(sici)1096-9861(19970519)381:4<389::Aid-cne1>3.0.Co;2-z

Gabriel, S. M., Davidson, M., Haroutunian, V., Powchik, P., Bierer, L. M., Purohit, D. P., Perl, D. P., & Davis, K. L. (1996). Neuropeptide deficits in schizophrenia vs. Alzheimer's disease cerebral cortex. *Biol Psychiatry*, *39*(2), 82-91. https://doi.org/10.1016/0006-3223(95)00066-6

Gage, S. H., Hickman, M., & Zammit, S. (2016). Association Between Cannabis and Psychosis: Epidemiologic Evidence. *Biological Psychiatry*, *79*, 549-556. https://doi.org/10.1016/j.biopsych.2015.08.001

Gara, M. A., Minsky, S., Silverstein, S. M., Miskimen, T., & Strakowski, S. M. (2019). A Naturalistic Study of Racial Disparities in Diagnoses at an Outpatient Behavioral Health Clinic. *Psychiatr Serv*, *70*(2), 130-134. https://doi.org/10.1176/appi.ps.201800223

Garcia-Cabezas, M. A., John, Y. J., Barbas, H., & Zikopoulos, B. (2016). Distinction of Neurons, Glia and Endothelial Cells in the Cerebral Cortex: An Algorithm Based on Cytological Features. *Front Neuroanat*, *10*, 107. https://doi.org/10.3389/fnana.2016.00107

Garey, L. J., Ong, W. Y., Patel, T. S., Kanani, M., Davis, A., Mortimer, A. M., Barnes, T. R., & Hirsch, S. R. (1998). Reduced dendritic spine density on cerebral cortical pyramidal neurons in schizophrenia. *Journal of Neurology Neurosurgery and Psychiatry*, *65*(4), 446-453. https://doi.org/10.1136/jnnp.65.4.446

Gentet, L. J., Kremer, Y., Taniguchi, H., Huang, Z. J., Staiger, J. F., & Petersen, C. C. (2012). Unique functional properties of somatostatin-expressing GABAergic neurons in mouse barrel cortex. *Nat Neurosci*, *15*(4), 607-612. https://doi.org/10.1038/nn.3051

Gidon, A., & Segev, I. (2012). Principles governing the operation of synaptic inhibition in dendrites. *Neuron*, *75*(2), 330-341. https://doi.org/10.1016/j.neuron.2012.05.015

Gidon, A., Zolnik, T. A., Fidzinski, P., Bolduan, F., Papoutsi, A., Poirazi, P., Holtkamp, M., Vida, I., & Larkum, M. E. (2020). Dendritic action potentials and computation in human layer 2/3 cortical neurons. *Science*, *367*(6473), 83-87. https://doi.org/10.1126/science.aax6239

Giguere, M., & Goldman-Rakic, P. S. (1988). Mediodorsal nucleus: areal, laminar, and tangential distribution of afferents and efferents in the frontal lobe of rhesus monkeys. *J Comp Neurol*, *277*(2), 195-213. https://doi.org/10.1002/cne.902770204

Gill, K. M., & Grace, A. A. (2014). The role of α5 GABAA receptor agonists in the treatment of cognitive deficits in schizophrenia. *Curr Pharm Des*, *20*(31), 5069-5076. https://doi.org/10.2174/1381612819666131216114612

Gill, K. M., Lodge, D. J., Cook, J. M., Aras, S., & Grace, A. A. (2011). A novel α5GABA(A)R-positive allosteric modulator reverses hyperactivation of the dopamine system in the MAM model of schizophrenia. *Neuropsychopharmacology*, *36*(9), 1903-1911. https://doi.org/10.1038/npp.2011.76

Gilman, J. P., Medalla, M., & Luebke, J. I. (2017). Area-Specific Features of Pyramidal Neurons-a Comparative Study in Mouse and Rhesus Monkey. *Cereb Cortex*, *27*(3), 2078-2094. https://doi.org/10.1093/cercor/bhw062

Girgenti, M. J., Wang, J., Ji, D., Cruz, D. A., Traumatic, S. B. R. G., Stein, M. B., Gelernter, J., Young, K. A., Huber, B. R., Williamson, D. E., Friedman, M. J., Krystal, J. H., Zhao, H., & Duman, R. S. (2021). Transcriptomic organization of the human brain in post-traumatic stress disorder. *Nat Neurosci*, *24*(1), 24-33. https://doi.org/10.1038/s41593-020-00748-7

Glantz, L. A., & Lewis, D. A. (2000). Decreased dendritic spine density on prefrontal cortical pyramidal neurons in schizophrenia. *Arch Gen Psychiatry*, *57*(1), 65-73. https://doi.org/10.1001/archpsyc.57.1.65

Glausier, J. R., Enwright, J. F., & Lewis, D. A. (2020a). Diagnosis- and Cell Type-Specific Mitochondrial Functional Pathway Signatures in Schizophrenia and Bipolar Disorder. *Am J Psychiatry*, *177*(12), 1140-1150. https://doi.org/10.1176/appi.ajp.2020.19111210

Glausier, J. R., Fish, K. N., & Lewis, D. A. (2014). Altered parvalbumin basket cell inputs in the dorsolateral prefrontal cortex of schizophrenia subjects. *Mol Psychiatry*, *19*(1), 30-36. https://doi.org/10.1038/mp.2013.152

Glausier, J. R., Kelly, M. A., Salem, S., Chen, K., & Lewis, D. A. (2020b). Proxy measures of premortem cognitive aptitude in postmortem subjects with schizophrenia. *Psychol Med*, *50*(3), 507-514. https://doi.org/10.1017/S0033291719000382

Glausier, J. R., Kimoto, S., Fish, K. N., & Lewis, D. A. (2015). Lower glutamic acid decarboxylase 65-kDa isoform messenger RNA and protein levels in the prefrontal cortex in schizoaffective disorder but not schizophrenia. *Biol Psychiatry*, *77*(2), 167-176. https://doi.org/10.1016/j.biopsych.2014.05.010

Glausier, J. R., & Lewis, D. A. (2013). Dendritic spine pathology in schizophrenia. *Neuroscience*, *251*, 90-107. https://doi.org/10.1016/j.neuroscience.2012.04.044

Glorioso, C., Sabatini, M., Unger, T., Hashimoto, T., Monteggia, L. M., Lewis, D. A., & Mirnics, K. (2006). Specificity and timing of neocortical transcriptome changes in response to BDNF gene ablation during embryogenesis or adulthood. *Mol Psychiatry*, *11*(7), 633-648. https://doi.org/10.1038/sj.mp.4001835

Godlewska, B. R., Clare, S., Cowen, P. J., & Emir, U. E. (2017). Ultra-High-Field Magnetic Resonance Spectroscopy in Psychiatry. *Frontiers in Psychiatry*, *8*. https://doi.org/10.3389/fpsyt.2017.00123

Goff, D. C., Henderson, D. C., & Amico, E. (1992). Cigarette smoking in schizophrenia: relationship to psychopathology and medication side effects. *Am J Psychiatry*, *149*(9), 1189-1194. https://doi.org/10.1176/ajp.149.9.1189

Gold, J. M. (2004). Cognitive deficits as treatment targets in schizophrenia. *Schizophrenia Research*, *72*(1), 21-28. https://doi.org/10.1016/j.schres.2004.09.008

Gold, J. M., Bansal, S., Anticevic, A., Cho, Y. T., Repovš, G., Murray, J. D., Hahn, B., Robinson, B. M., & Luck, S. J. (2020). Refining the Empirical Constraints on Computational Models of Spatial Working Memory in Schizophrenia. *Biol Psychiatry Cogn Neurosci Neuroimaging*, *5*(9), 913-922. https://doi.org/10.1016/j.bpsc.2020.05.003

Gold, J. M., Goldberg, R. W., McNary, S. W., Dixon, L. B., & Lehman, A. F. (2002). Cognitive correlates of job tenure among patients with severe mental illness. *Am J Psychiatry*, *159*(8), 1395-1402. https://doi.org/10.1176/appi.ajp.159.8.1395

Goldberg, T. E., Ragland, J. D., Torrey, E. F., Gold, J. M., Bigelow, L. B., & Weinberger, D. R. (1990). Neuropsychological assessment of monozygotic twins discordant for schizophrenia. *Arch Gen Psychiatry*, *47*(11), 1066-1072. https://doi.org/10.1001/archpsyc.1990.01810230082013

Goldman-Rakic, P. S. (1995). Cellular basis of working memory. *Neuron*, *14*(3), 477-485. https://doi.org/10.1016/0896-6273(95)90304-6

Goldman, P. S., & Rosvold, H. E. (1970). Localization of function within the dorsolateral prefrontal cortex of the rhesus monkey. *Experimental Neurology*, *27*(2), 291-304. https://doi.org/10.1016/0014-4886(70)90222-0

González-Albo, M. C., Elston, G. N., & DeFelipe, J. (2001). The human temporal cortex: characterization of neurons expressing nitric oxide synthase, neuropeptides and calcium-binding proteins, and their glutamate receptor subunit profiles. *Cereb Cortex*, *11*(12), 1170-1181. https://doi.org/10.1093/cercor/11.12.1170

González-Burgos, G., Barrionuevo, G., & Lewis, D. A. (2000). Horizontal synaptic connections in monkey prefrontal cortex: an in vitro electrophysiological study. *Cereb Cortex*, *10*(1), 82-92. https://doi.org/10.1093/cercor/10.1.82

Gonzalez-Burgos, G., Cho, R. Y., & Lewis, D. A. (2015). Alterations in cortical network oscillations and parvalbumin neurons in schizophrenia. *Biol Psychiatry*, *77*(12), 1031-1040. https://doi.org/10.1016/j.biopsych.2015.03.010

González-Burgos, G., Krimer, L. S., Urban, N. N., Barrionuevo, G., & Lewis, D. A. (2004). Synaptic efficacy during repetitive activation of excitatory inputs in primate dorsolateral prefrontal cortex. *Cereb Cortex*, *14*(5), 530-542. https://doi.org/10.1093/cercor/bhh015

Gonzalez-Burgos, G., Kroener, S., Zaitsev, A. V., Povysheva, N. V., Krimer, L. S., Barrionuevo, G., & Lewis, D. A. (2008). Functional maturation of excitatory synapses in layer 3 pyramidal neurons during postnatal development of the primate prefrontal cortex. *Cereb Cortex*, *18*(3), 626-637. https://doi.org/10.1093/cercor/bhm095

Gonzalez-Burgos, G., & Lewis, D. A. (2008). GABA neurons and the mechanisms of network oscillations: implications for understanding cortical dysfunction in schizophrenia. *Schizophr Bull*, *34*(5), 944-961. https://doi.org/10.1093/schbul/sbn070

Gonzalez-Burgos, G., Miyamae, T., Krimer, Y., Gulchina, Y., Pafundo, D. E., Krimer, O., Bazmi, H., Arion, D., Enwright, J. F., Fish, K. N., & Lewis, D. A. (2019). Distinct Properties of Layer 3 Pyramidal Neurons from Prefrontal and Parietal Areas of the Monkey Neocortex. *J Neurosci*, *39*(37), 7277-7290. https://doi.org/10.1523/JNEUROSCI.1210-19.2019

Gonzalez-Burgos, G., & Lewis, D. A. (2012). NMDA receptor hypofunction, parvalbumin-positive neurons, and cortical gamma oscillations in schizophrenia. *Schizophrenia Bulletin*, *38*(5), 950-957. https://doi.org/10.1093/schbul/sbs010

Green, M. F. (1996). What are the functional consequences of neurocognitive deficits in schizophrenia. *Am J Psychiatry*, *153*(3), 321-330. https://doi.org/10.1176/ajp.153.3.321

Green, M. F., & Harvey, P. D. (2014). Cognition in schizophrenia: Past, present, and future. *Schizophr Res Cogn*, *1*, e1-e9. https://doi.org/10.1016/j.scog.2014.02.001

Green, M. F., Horan, W. P., & Lee, J. (2019). Nonsocial and social cognition in schizophrenia: current evidence and future directions. *World Psychiatry*, *18*(2), 146-161. https://doi.org/10.1002/wps.20624

Guidotti, A., Auta, J., Davis, J. M., Di-Giorgi-Gerevini, V., Dwivedi, Y., Grayson, D. R., Impagnatiello, F., Pandey, G., Pesold, C., Sharma, R., Uzunov, D., Costa, E., & DiGiorgi Gerevini, V. (2000). Decrease in reelin and glutamic acid decarboxylase67 (GAD67) expression in schizophrenia and bipolar disorder: a postmortem brain study. *Arch Gen Psychiatry*, *57*(11), 1061-1069. https://doi.org/10.1001/archpsyc.57.11.1061

Guimond, S., Padani, S., Lutz, O., Eack, S., Thermenos, H., & Keshavan, M. (2018). Impaired regulation of emotional distractors during working memory load in schizophrenia. *J Psychiatr Res*, *101*, 14-20. https://doi.org/10.1016/j.jpsychires.2018.02.028

Gulyás, A. I., Szabó, G. G., Ulbert, I., Holderith, N., Monyer, H., Erdélyi, F., Szabó, G., Freund, T. F., & Hájos, N. (2010). Parvalbumin-containing fast-spiking basket cells generate the field potential oscillations induced by cholinergic receptor activation in the hippocampus. *J Neurosci*, *30*(45), 15134-15145. https://doi.org/10.1523/JNEUROSCI.4104-10.2010

Gur, R. C., Calkins, M. E., Satterthwaite, T. D., Ruparel, K., Bilker, W. B., Moore, T. M., Savitt, A. P., Hakonarson, H., & Gur, R. E. (2014). Neurocognitive growth charting in psychosis spectrum youths. *JAMA Psychiatry*, *71*(4), 366-374. https://doi.org/10.1001/jamapsychiatry.2013.4190

Hagihara, H., Catts, V. S., Katayama, Y., Shoji, H., Takagi, T., Huang, F. L., Nakao, A., Mori, Y., Huang, K. P., Ishii, S., Graef, I. A., Nakayama, K. I., Shannon Weickert, C., & Miyakawa, T. (2018). Decreased Brain pH as a Shared Endophenotype of Psychiatric Disorders. *Neuropsychopharmacology*, *43*(3), 459-468. https://doi.org/10.1038/npp.2017.167

Hahn, B., Robinson, B. M., Kaiser, S. T., Harvey, A. N., Beck, V. M., Leonard, C. J., Kappenman, E. S., Luck, S. J., & Gold, J. M. (2010). Failure of schizophrenia patients to overcome salient distractors during working memory encoding. *Biol Psychiatry*, *68*(7), 603-609. https://doi.org/10.1016/j.biopsych.2010.04.014

Hahn, B., Robinson, B. M., Kiat, J. E., Geng, J., Bansal, S., Luck, S. J., & Gold, J. M. (2021). Impaired Filtering and Hyperfocusing: Neural Evidence for Distinct Selective Attention

Abnormalities in People with Schizophrenia. *Cereb Cortex*, bhab327. https://doi.org/10.1093/cercor/bhab327

Halim, N. D., Lipska, B. K., Hyde, T. M., Deep-Soboslay, A., Saylor, E. M., Herman, M. M., Thakar, J., Verma, A., & Kleinman, J. E. (2008). Increased lactate levels and reduced pH in postmortem brains of schizophrenics: medication confounds. *J Neurosci Methods*, *169*(1), 208-213. https://doi.org/10.1016/j.jneumeth.2007.11.017

Halvorsrud, K., Nazroo, J., Otis, M., Brown Hajdukova, E., & Bhui, K. (2019). Ethnic inequalities in the incidence of diagnosis of severe mental illness in England: a systematic review and new meta-analyses for non-affective and affective psychoses. *Social Psychiatry and Psychiatric Epidemiology*, *54*(11), 1311-1323. https://doi.org/10.1007/s00127-019-01758-y

Hama, E., & Saido, T. C. (2005). Etiology of sporadic Alzheimer's disease: somatostatin, neprilysin, and amyloid beta peptide. *Med Hypotheses*, *65*(3), 498-500. https://doi.org/10.1016/j.mehy.2005.02.045

Hanlon, M.-C., Campbell, L. E., Single, N., Coleman, C., Morgan, V. A., Cotton, S. M., Stain, H. J., & Castle, D. J. (2017). Men and women with psychosis and the impact of illness-duration on sex-differences: The second Australian national survey of psychosis. *Psychiatry Research*, *256*, 130-143. https://doi.org/10.1016/j.psychres.2017.06.024

Harnett, N. G., & Ressler, K. J. (2021). Structural Racism as a Proximal Cause for Race-Related Differences in Psychiatric Disorders. *Am J Psychiatry*, *178*(7), 579-581. https://doi.org/10.1176/appi.ajp.2021.21050486

Harvey, P. D., Helldin, L., Bowie, C. R., Heaton, R. K., Olsson, A. K., Hjärthag, F., Norlander, T., & Patterson, T. L. (2009). Performance-based measurement of functional disability in schizophrenia: a cross-national study in the United States and Sweden. *Am J Psychiatry*, *166*(7), 821-827. https://doi.org/10.1176/appi.ajp.2009.09010106

Hashimoto, T., Arion, D., Unger, T., Maldonado-Avilés, J. G., Morris, H. M., Volk, D. W., Mirnics, K., & Lewis, D. A. (2008a). Alterations in GABA-related transcriptome in the dorsolateral prefrontal cortex of subjects with schizophrenia. *Mol Psychiatry*, *13*(2), 147-161. https://doi.org/10.1038/sj.mp.4002011

Hashimoto, T., Bazmi, H. H., Mirnics, K., Wu, Q., Sampson, A. R., & Lewis, D. A. (2008b). Conserved regional patterns of GABA-related transcript expression in the neocortex of subjects with schizophrenia. *Am J Psychiatry*, *165*(4), 479-489. https://doi.org/10.1176/appi.ajp.2007.07081223

Hashimoto, T., Bergen, S. E., Nguyen, Q. L., Xu, B., Monteggia, L. M., Pierri, J. N., Sun, Z., Sampson, A. R., & Lewis, D. A. (2005). Relationship of brain-derived neurotrophic factor and its receptor TrkB to altered inhibitory prefrontal circuitry in schizophrenia. *J Neurosci*, *25*(2), 372-383. https://doi.org/10.1523/JNEUROSCI.4035-04.2005

Hashimoto, T., Volk, D. W., Eggan, S. M., Mirnics, K., Pierri, J. N., Sun, Z., Sampson, A. R., & Lewis, D. A. (2003). Gene expression deficits in a subclass of GABA neurons in the prefrontal cortex of subjects with schizophrenia. *J Neurosci*, *23*(15), 6315-6326. https://pubmed.ncbi.nlm.nih.gov/12867516

Hawrylycz, M. J., Lein, E. S., Guillozet-Bongaarts, A. L., Shen, E. H., Ng, L., Miller, J. A., van de Lagemaat, L. N., Smith, K. A., Ebbert, A., Riley, Z. L., Abajian, C., Beckmann, C. F., Bernard, A., Bertagnolli, D., Boe, A. F., Cartagena, P. M., Chakravarty, M. M., Chapin, M., Chong, J., . . . Jones, A. R. (2012). An anatomically comprehensive atlas of the adult human brain transcriptome. *Nature*, *489*(7416), 391-399. https://doi.org/10.1038/nature11405

Hawton, K., Sutton, L., Haw, C., Sinclair, J., & Deeks, J. J. (2005). Schizophrenia and suicide: Systematic review of risk factors. *British Journal of Psychiatry*, *187*(1), 9-20. https://doi.org/10.1192/bjp.187.1.9

Hayashi, M., & Oshima, K. (1986). Neuropeptides in cerebral cortex of macaque monkey (Macaca fuscata fuscata): regional distribution and ontogeny. *Brain Res*, *364*(2), 360-368. https://doi.org/10.1016/0006-8993(86)90848-6

Hayashi, M., Yamashita, A., & Shimizu, K. (1997). Somatostatin and brain-derived neurotrophic factor mRNA expression in the primate brain: decreased levels of mRNAs during aging. *Brain Res*, *749*(2), 283-289. https://doi.org/10.1016/S0006-8993(96)01317-0

Hayes, T. L., Cameron, J. L., Fernstrom, J. D., & Lewis, D. A. (1991). A comparative analysis of the distribution of prosomatostatin-derived peptides in human and monkey neocortex. *J Comp Neurol*, *303*(4), 584-599. https://doi.org/10.1002/cne.903030406

Hebb, D. O. (1945). Man's frontal lobes: A critical review. *Archives of Neurology & Psychiatry*, *54*(1), 10-24. https://jamanetwork.com/journals/archneurpsyc/article-abstract/650111

Hendry, S. H., Schwark, H. D., Jones, E. G., & Yan, J. (1987). Numbers and proportions of GABA-immunoreactive neurons in different areas of monkey cerebral cortex. *J Neurosci*, *7*(5), 1503-1519. https://www.ncbi.nlm.nih.gov/pubmed/3033170

Hendry, S. H., Jones, E. G., & Burstein, N. (1988). Activity-dependent regulation of tachykinin-like immunoreactivity in neurons of monkey visual cortex. *J Neurosci*, *8*(4), 1225-1238. https://pubmed.ncbi.nlm.nih.gov/3162747

Hendry, S. H., Jones, E. G., DeFelipe, J., Schmechel, D., Brandon, C., & Emson, P. C. (1984). Neuropeptide-containing neurons of the cerebral cortex are also GABAergic. *Proc Natl Acad Sci U S A*, *81*(20), 6526-6530. https://doi.org/10.1073/pnas.81.20.6526

Higley, M. J. (2014). Localized GABAergic inhibition of dendritic Ca(2+) signalling. *Nat Rev Neurosci*, *15*(9), 567-572. https://doi.org/10.1038/nrn3803

Hladnik, A., Džaja, D., Darmopil, S., Jovanov-Milošević, N., & Petanjek, Z. (2014). Spatio-temporal extension in site of origin for cortical calretinin neurons in primates. *Front Neuroanat*, *8*, 50. https://doi.org/10.3389/fnana.2014.00050

Hodge, R. D., Bakken, T. E., Miller, J. A., Smith, K. A., Barkan, E. R., Graybuck, L. T., Close, J. L., Long, B., Johansen, N., Penn, O., Yao, Z., Eggermont, J., Höllt, T., Levi, B. P., Shehata, S. I., Aevermann, B., Beller, A., Bertagnolli, D., Brouner, K., . . . Lein, E. S. (2019). Conserved cell types with divergent features in human versus mouse cortex. *Nature*, *573*(7772), 61-68. https://doi.org/10.1038/s41586-019-1506-7

Hof, P. R., Glezer, II, Conde, F., Flagg, R. A., Rubin, M. B., Nimchinsky, E. A., & Vogt Weisenhorn, D. M. (1999). Cellular distribution of the calcium-binding proteins

parvalbumin, calbindin, and calretinin in the neocortex of mammals: phylogenetic and developmental patterns. *J Chem Neuroanat*, *16*(2), 77-116. https://doi.org/10.1016/s0891-0618(98)00065-9

Hofer, A., Baumgartner, S., Bodner, T., Edlinger, M., Hummer, M., Kemmler, G., Rettenbacher, M. A., & Fleischhacker, W. W. (2005). Patient outcomes in schizophrenia II: the impact of cognition. *European Psychiatry*, *20*(5-6), 395-402. https://doi.org/10.1016/j.eurpsy.2005.02.006

Hoftman, G. D., Dienel, S. J., Bazmi, H. H., Zhang, Y., Chen, K., & Lewis, D. A. (2018). Altered Gradients of Glutamate and Gamma-Aminobutyric Acid Transcripts in the Cortical Visuospatial Working Memory Network in Schizophrenia. *Biol Psychiatry*, *83*(8), 670-679. https://doi.org/10.1016/j.biopsych.2017.11.029

Hoftman, G. D., Volk, D. W., Bazmi, H. H., Li, S., Sampson, A. R., & Lewis, D. A. (2015). Altered cortical expression of GABA-related genes in schizophrenia: illness progression vs developmental disturbance. *Schizophr Bull*, *41*(1), 180-191. https://doi.org/10.1093/schbul/sbt178

Holmberg, S. K., & Kane, C. (1999). Health and self-care practices of persons with schizophrenia. *Psychiatr Serv*, *50*(6), 827-829. https://doi.org/10.1176/ps.50.6.827

Hope, B. T., Michael, G. J., Knigget, K. M., & Vincent, S. R. (1991). Neuronal NADPH diaphorase is a nitric oxide synthase. *Proceedings of the National Academy of Sciences USA*, *88*, 2811-2814. http://www.pnas.org/content/pnas/88/7/2811.full.pdf

Hopper, K., & Wanderling, J. (2000). Revisiting the developed versus developing country distinction in course and outcome in schizophrenia: results from ISoS, the WHO collaborative followup project. International Study of Schizophrenia. *Schizophr Bull*, *26*(4), 835-846. https://doi.org/10.1093/oxfordjournals.schbul.a033498

Hor, K., & Taylor, M. (2010). Review: Suicide and schizophrenia: a systematic review of rates and risk factors. *Journal of Psychopharmacology*, *24*(4_suppl), 81-90. https://doi.org/10.1177/1359786810385490

Horn, M. E., & Nicoll, R. A. (2018). Somatostatin and parvalbumin inhibitory synapses onto hippocampal pyramidal neurons are regulated by distinct mechanisms. *Proc Natl Acad Sci U S A*, *115*(3), 589-594. https://doi.org/10.1073/pnas.1719523115

Hornung, J. P., & De Tribolet, N. (1994). Distribution of GABA-containing neurons in human frontal cortex: a quantitative immunocytochemical study. *Anat Embryol (Berl)*, *189*(2), 139-145. https://doi.org/10.1007/BF00185772

Hou, Z. H., & Yu, X. (2013). Activity-regulated somatostatin expression reduces dendritic spine density and lowers excitatory synaptic transmission via postsynaptic somatostatin receptor 4. *Journal of Biological Chemistry*, *288*(4), 2501-2509. https://doi.org/10.1074/jbc.M112.419051

Howard, M. W., Rizzuto, D. S., Caplan, J. B., Madsen, J. R., Lisman, J., Aschenbrenner-Scheibe, R., Schulze-Bonhage, A., & Kahana, M. J. (2003). Gamma oscillations correlate with working memory load in humans. *Cereb Cortex*, *13*(12), 1369-1374. https://doi.org/10.1093/cercor/bhg084

Hubbard, L., Rees, E., Morris, D. W., Lynham, A. J., Richards, A. L., Pardiñas, A. F., Legge, S. E., Harold, D., Zammit, S., Corvin, A. C., Gill, M. G., Hall, J., Holmans, P., O'Donovan, M. C., Owen, M. J., Donohoe, G., Kirov, G., Pocklington, A., & Walters, J. T. R. (2021). Rare Copy Number Variants Are Associated With Poorer Cognition in Schizophrenia. *Biological Psychiatry*, *90*(1), 28-34. https://doi.org/10.1016/j.biopsych.2020.11.025

Hyde, T. M., Lipska, B. K., Ali, T., Mathew, S. V., Law, A. J., Metitiri, O. E., Straub, R. E., Ye, T., Colantuoni, C., Herman, M. M., Bigelow, L. B., Weinberger, D. R., & Kleinman, J. E. (2011). Expression of GABA Signaling Molecules KCC2, NKCC1, and GAD1 in Cortical Development and Schizophrenia. *Journal of Neuroscience*, *31*(30), 11088-11095. https://doi.org/10.1523/JNEUROSCI.1234-11.2011

Inan, M., Petros, T. J., & Anderson, S. A. (2013). Losing your inhibition: Linking cortical GABAergic interneurons to schizophrenia. *Neurobiology of disease*, *53*, 36-48. https://doi.org/10.1016/j.nbd.2012.11.013

Inoue, M., & Yoshii, M. (1992). Modulation of ion channels by somatostatin and acetylcholine. *Prog Neurobiol*, *38*(2), 203-230. https://doi.org/10.1016/0301-0082(92)90040-l

Iwata, N., Tsubuki, S., Takaki, Y., Shirotani, K., Lu, B., Gerard, N. P., Gerard, C., Hama, E., Lee, H. J., & Saido, T. C. (2001). Metabolic regulation of brain Abeta by neprilysin. *Science*, *292*(5521), 1550-1552. https://doi.org/10.1126/science.1059946

Jacob, S. N., & Nieder, A. (2014). Complementary roles for primate frontal and parietal cortex in guarding working memory from distractor stimuli. *Neuron*, *83*(1), 226-237. https://doi.org/10.1016/j.neuron.2014.05.009

Jacob, T. C. (2019). Neurobiology and Therapeutic Potential of α5-GABA Type A Receptors. *Front Mol Neurosci*, *12*, 179. https://doi.org/10.3389/fnmol.2019.00179

Jacobsen, C. F. (1935). Functions of Frontal Association Area in Primates. *Archives of Neurology And Psychiatry*, *33*(3). https://doi.org/10.1001/archneurpsyc.1935.02250150108009

Jacobsen, C. F., Elder, J. H., & Haslerud, G. M. (1936). Studies of cerebral function in primates.

James, S. L., Abate, D., Abate, K. H., Abay, S. M., Abbafati, C., Abbasi, N., Abbastabar, H., Abd-Allah, F., Abdela, J., Abdelalim, A., Abdollahpour, I., Abdulkader, R. S., Abebe, Z., Abera, S. F., Abil, O. Z., Abraha, H. N., Abu-Raddad, L. J., Abu-Rmeileh, N. M. E., Accrombessi, M. M. K., . . . Murray, C. J. L. (2018). Global, regional, and national incidence, prevalence, and years lived with disability for 354 Diseases and Injuries for 195 countries and territories, 1990-2017: A systematic analysis for the Global Burden of Disease Study 2017. *The Lancet*, 1789-1858. https://doi.org/10.1016/S0140-6736(18)32279-7

Jansen, I., Alafaci, C., McCulloch, J., Uddman, R., & Edvinsson, L. (1991). Tachykinins (substance P, neurokinin A, neuropeptide K, and neurokinin B) in the cerebral circulation: vasomotor responses in vitro and in situ. *J Cereb Blood Flow Metab*, *11*(4), 567-575. https://doi.org/10.1038/jcbfm.1991.105

Javitt, D. C., & Zukin, S. R. (1991). Recent advances in the phencyclidine model of schizophrenia. *Am J Psychiatry*, *148*(10), 1301-1308. https://doi.org/10.1176/ajp.148.10.1301

Jeffreys, H. (1961). *The Theory of Probability*. OUP Oxford. https://play.google.com/store/books/details?id=vh9Act9rtzQC&source=gbs_api

Jensen, O., Kaiser, J., & Lachaux, J.-P. (2007). Human gamma-frequency oscillations associated with attention and memory. *Trends in Neurosciences*, *30*(7), 317-324. https://doi.org/10.1016/j.tins.2007.05.001

Johnson, M. K., McMahon, R. P., Robinson, B. M., Harvey, A. N., Hahn, B., Leonard, C. J., Luck, S. J., & Gold, J. M. (2013). The relationship between working memory capacity and broad measures of cognitive ability in healthy adults and people with schizophrenia. *Neuropsychology*, *27*(2), 220-229. https://doi.org/10.1037/a0032060

Jolly, R. D., Palmer, D. N., & Dalefield, R. R. (2002). The analytical approach to the nature of lipofuscin (age pigment). *Archives of gerontology and geriatrics*, *34*(3), 205-217. https://www.sciencedirect.com/science/article/pii/S0167494301002199

Jonas, K., Lian, W., Callahan, J., Ruggero, C. J., Clouston, S., Reichenberg, A., Carlson, G. A., Bromet, E. J., & Kotov, R. (2022). The Course of General Cognitive Ability in Individuals With Psychotic Disorders. *JAMA Psychiatry*. https://doi.org/10.1001/jamapsychiatry.2022.1142

Jones, E. G., & Hendry, S. H. C. (1986). Co-localization of GABA and neuropeptides in neocortical neurons. *Trends in Neurosciences*, *9*, 71-76. https://doi.org/10.1016/0166-2236(86)90026-3

Jones, E. G., DeFelipe, J., Hendry, S. H., & Maggio, J. E. (1988). A study of tachykinin-immunoreactive neurons in monkey cerebral cortex. *J Neurosci*, *8*(4), 1206-1224. https://pubmed.ncbi.nlm.nih.gov/3162746

Jonides, J., Lewis, R. L., Nee, D. E., Lustig, C. A., Berman, M. G., & Moore, K. S. (2008). The mind and brain of short-term memory. *Annu Rev Psychol*, *59*, 193-224. https://doi.org/10.1146/annurev.psych.59.103006.093615

Jonides, J., Smith, E. E., Koeppe, R. A., Awh, E., Minoshima, S., & Mintun, M. A. (1993). Spatial working memory in humans as revealed by PET. *Nature*, *363*(6430), 623-625. https://doi.org/10.1038/363623a0

Joshi, D., Catts, V. S., Olaya, J. C., & Shannon Weickert, C. (2015). Relationship between somatostatin and death receptor expression in the orbital frontal cortex in schizophrenia: a postmortem brain mRNA study. *NPJ Schizophr*, *1*, 14004. https://doi.org/10.1038/npjschz.2014.4

Jung, T., Bader, N., & Grune, T. (2007). Lipofuscin: formation, distribution, and metabolic consequences. *Ann N Y Acad Sci*, *1119*, 97-111. https://doi.org/10.1196/annals.1404.008

Kaar, S. J., Angelescu, I., Marques, T. R., & Howes, O. D. (2019). Pre-frontal parvalbumin interneurons in schizophrenia: a meta-analysis of post-mortem studies. *J Neural Transm (Vienna)*, *126*(12), 1637-1651. https://doi.org/10.1007/s00702-019-02080-2

Kadakia, A., Fan, A., Marden, J., Dembek, C., Catillon, M., Anderson, A., & Williams, R. (2022a). The Economic Burden of Schizophrenia in the United States in 2019. *CNS Spectrums*, *27*(2), 227-227. https://doi.org/10.1017/s1092852922000207

Kadakia, A., Fan, Q., Shepherd, J., Dembek, C., Bailey, H., Walker, C., & Williams, G. R. (2022b). Healthcare resource utilization and quality of life by cognitive impairment in patients with schizophrenia. *Schizophrenia Research: Cognition*, *28*, 100233. https://doi.org/10.1016/j.scog.2021.100233

Kahn, R. S., & Keefe, R. S. (2013). Schizophrenia is a cognitive illness: time for a change in focus. *JAMA Psychiatry*, *70*(10), 1107-1112. https://doi.org/10.1001/jamapsychiatry.2013.155

Kamigaki, T. (2019). Prefrontal circuit organization for executive control. *Neurosci Res*, *140*, 23-36. https://doi.org/10.1016/j.neures.2018.08.017

Kaminski, J., Mascarell-Maricic, L., Fukuda, Y., Katthagen, T., Heinz, A., & Schlagenhauf, F. (2021). Glutamate in the Dorsolateral Prefrontal Cortex in Patients With Schizophrenia: A Meta-analysis of ^{1}H-Magnetic Resonance Spectroscopy Studies. *Biol Psychiatry*, *89*(3), 270-277. https://doi.org/10.1016/j.biopsych.2020.09.001

Kang, S. S., MacDonald, A. W., Chafee, M. V., Im, C. H., Bernat, E. M., Davenport, N. D., & Sponheim, S. R. (2018). Abnormal cortical neural synchrony during working memory in schizophrenia. *Clinical Neurophysiology*, *129*(1), 210-221. https://doi.org/10.1016/j.clinph.2017.10.024

Kao, A. W., McKay, A., Singh, P. P., Brunet, A., & Huang, E. J. (2017). Progranulin, lysosomal regulation and neurodegenerative disease. *Nat Rev Neurosci*, *18*(6), 325-333. https://doi.org/10.1038/nrn.2017.36

Karnani, M. M., Agetsuma, M., & Yuste, R. (2014). A blanket of inhibition: functional inferences from dense inhibitory connectivity. *Curr Opin Neurobiol*, *26*, 96-102. https://doi.org/10.1016/j.conb.2013.12.015

Kass, R. E., & Raftery, A. E. (1995). Bayes Factors. *Journal of the American Statistical Association*, *90*(430), 773-795.

Kassambara, A. (2021) rstatix: Pipe-Friendly Framework for Basic Statistical Tests. *R package version 0.7.0*. https://CRAN.R-project.org/package=rstatix

Keefe, R. S. E., Lees Roitman, S. E., Harvey, P. D., Blum, C. S., Dupre, R. L., Prieto, D. M., Davidson, M., & Davis, K. L. (1995). A pen-and-paper human analogue of a monkey prefrontal cortex activation task: spatial working memory in patients with schizophrenia. *Schizophrenia Research*, *17*(25). http://ac.els-cdn.com/092099649500027J/1-s2.0-092099649500027J-main.pdf?_tid=dad65a1c-576f-11e7-9982-00000aacb35f&acdnat=1498152538_31214d1cc6b5aea75109fd0814ed8bd5

Keefe, R. S., Bilder, R. M., Davis, S. M., Harvey, P. D., Palmer, B. W., Gold, J. M., Meltzer, H. Y., Green, M. F., Capuano, G., Stroup, T. S., McEvoy, J. P., Swartz, M. S., Rosenheck, R. A., Perkins, D. O., Davis, C. E., Hsiao, J. K., Lieberman, J. A., CATIE, I., & Neurocognitive, W. G. (2007). Neurocognitive effects of antipsychotic medications in patients with chronic schizophrenia in the CATIE Trial. *Arch Gen Psychiatry*, *64*(6), 633-647. https://doi.org/10.1001/archpsyc.64.6.633

Keefe, R. S., Buchanan, R. W., Marder, S. R., Schooler, N. R., Dugar, A., Zivkov, M., & Stewart, M. (2013). Clinical trials of potential cognitive-enhancing drugs in schizophrenia:

what have we learned so far. *Schizophr Bull*, *39*(2), 417-435. https://doi.org/10.1093/schbul/sbr153

Keefe, R. S., Eesley, C. E., & Poe, M. P. (2005). Defining a cognitive function decrement in schizophrenia. *Biol Psychiatry*, *57*(6), 688-691. https://doi.org/10.1016/j.biopsych.2005.01.003

Kepecs, A., & Fishell, G. (2014). Interneuron cell types are fit to function. *Nature*, *505*(7483), 318-326. https://doi.org/10.1038/nature12983

Kępińska, A. P., Iyegbe, C. O., Vernon, A. C., Yolken, R., Murray, R. M., & Pollak, T. A. (2020). Schizophrenia and Influenza at the Centenary of the 1918-1919 Spanish Influenza Pandemic: Mechanisms of Psychosis Risk. *Frontiers in Psychiatry*, *11*. https://doi.org/10.3389/fpsyt.2020.00072

Kerns, J. G., Nuechterlein, K. H., Braver, T. S., & Barch, D. M. (2008). Executive Functioning Component Mechanisms and Schizophrenia. *Biological Psychiatry*, *64*, 26-33. http://ac.els-cdn.com/S0006322308005052/1-s2.0-S0006322308005052-main.pdf?_tid=f9d90d6c-55b0-11e7-a7b3-00000aacb362&acdnat=1497960605_be40072e2de74c60b280447f87bce676

Keysers, C., Gazzola, V., & Wagenmakers, E. J. (2020). Using Bayes factor hypothesis testing in neuroscience to establish evidence of absence. *Nat Neurosci*, *23*(7), 788-799. https://doi.org/10.1038/s41593-020-0660-4

Khan, A. G., Poort, J., Chadwick, A., Blot, A., Sahani, M., Mrsic-Flogel, T. D., & Hofer, S. B. (2018). Distinct learning-induced changes in stimulus selectivity and interactions of GABAergic interneuron classes in visual cortex. *Nat Neurosci*, *21*(6), 851-859. https://doi.org/10.1038/s41593-018-0143-z

Kilduff, T. S., Cauli, B., & Gerashchenko, D. (2011). Activation of cortical interneurons during sleep: an anatomical link to homeostatic sleep regulation? *Trends in Neurosciences*, *34*(1), 10-19. https://doi.org/10.1016/J.TINS.2010.09.005

Kim, I. H., Racz, B., Wang, H., Burianek, L., Weinberg, R., Yasuda, R., Wetsel, W. C., & Soderling, S. H. (2013). Disruption of Arp2/3 results in asymmetric structural plasticity of dendritic spines and progressive synaptic and behavioral abnormalities. *J Neurosci*, *33*(14), 6081-6092. https://doi.org/10.1523/JNEUROSCI.0035-13.2013

Kim, Y., Yang, G. R., Pradhan, K., Venkataraju, K. U., Bota, M., Garcia Del Molino, L. C., Fitzgerald, G., Ram, K., He, M., Levine, J. M., Mitra, P., Huang, Z. J., Wang, X. J., & Osten, P. (2017). Brain-wide Maps Reveal Stereotyped Cell-Type-Based Cortical Architecture and Subcortical Sexual Dimorphism. *Cell*, *171*(2), 456-469 e22. https://doi.org/10.1016/j.cell.2017.09.020

Kimoto, S., Zaki, M. M., Bazmi, H. H., & Lewis, D. A. (2015). Altered Markers of Cortical γ-Aminobutyric Acid Neuronal Activity in Schizophrenia: Role of the NARP Gene. *JAMA Psychiatry*, *72*(8), 747-756. https://doi.org/10.1001/jamapsychiatry.2015.0533

Kimoto, S., Bazmi, H. H., & Lewis, D. A. (2014). Lower Expression of Glutamic Acid Decarboxylase 67 in the Prefrontal Cortex in Schizophrenia: Contribution of Altered Regulation by Zif268. *The American journal of psychiatry*, *171*, 969-978. https://ajp-psychiatryonline-org.pitt.idm.oclc.org/doi/pdf/10.1176/appi.ajp.2014.14010004

Kingsbury, A. E., Foster, O. J., Nisbet, A. P., Cairns, N., Bray, L., Eve, D. J., Lees, A. J., & Marsden, C. D. (1995). Tissue pH as an indicator of mRNA preservation in human post-mortem brain. *Brain Res Mol Brain Res*, *28*(2), 311-318. https://doi.org/10.1016/0169-328x(94)00219-5

Kirkbride, J. B., Errazuriz, A., Croudace, T. J., Morgan, C., Jackson, D., Boydell, J., Murray, R. M., & Jones, P. B. (2012). Incidence of Schizophrenia and Other Psychoses in England, 1950–2009: A Systematic Review and Meta-Analyses. *PLoS ONE*, *7*(3), e31660. https://doi.org/10.1371/journal.pone.0031660

Kolb, B. (2021). Brenda Milner: Pioneer of the Study of the Human Frontal Lobes. *Front Hum Neurosci*, *15*, 786167. https://doi.org/10.3389/fnhum.2021.786167

Kolluri, N., Sun, Z., Sampson, A. R., & Lewis, D. A. (2005). Lamina-Specific Reductions in Dendritic Spine Density in the Prefrontal Cortex of Subjects with Schizophrenia. *American Journal of Psychiatry*, *162*(6), 1200-1202. https://doi.org/10.1176/appi.ajp.162.6.1200

Konopaske, G. T., Lange, N., Coyle, J. T., & Benes, F. M. (2014). Prefrontal cortical dendritic spine pathology in schizophrenia and bipolar disorder. *JAMA Psychiatry*, *71*(12), 1323-1331. https://doi.org/10.1001/jamapsychiatry.2014.1582

Konradi, C., Yang, C. K., Zimmerman, E. I., Lohmann, K. M., Gresch, P., Pantazopoulos, H., Berretta, S., & Heckers, S. (2011). Hippocampal interneurons are abnormal in schizophrenia. *Schizophrenia Research*, *131*, 165-173. https://doi.org/10.1016/j.schres.2011.06.007

Kraemer, H. C. (2019). Is It Time to Ban the P Value? *JAMA Psychiatry*, *76*(12), 1219-1220. https://doi.org/10.1001/jamapsychiatry.2019.1965

Kraepelin, E. (1921). *Dementia praecox and paraphrenia* (R. M. Barclay, Trans.). LWW. https://journals.lww.com/jonmd/Citation/1921/10000/Dementia_Praecox_and_Paraphrenia.104.aspx.

Krawchuk, M. B., Ruff, C. F., Yang, X., Ross, S. E., & Vazquez, A. L. (2020). Optogenetic assessment of VIP, PV, SOM and NOS inhibitory neuron activity and cerebral blood flow regulation in mouse somato-sensory cortex. *Journal of Cerebral Blood Flow & Metabolism*, *40*(7), 1427-1440. https://doi.org/10.1177/0271678x19870105

Krienen, F. M., Goldman, M., Zhang, Q., C H Del Rosario, R., Florio, M., Machold, R., Saunders, A., Levandowski, K., Zaniewski, H., Schuman, B., Wu, C., Lutservitz, A., Mullally, C. D., Reed, N., Bien, E., Bortolin, L., Fernandez-Otero, M., Lin, J. D., Wysoker, A., . . . McCarroll, S. A. (2020). Innovations present in the primate interneuron repertoire. *Nature*, *586*(7828), 262-269. https://doi.org/10.1038/s41586-020-2781-z

Kritzer, M. F., & Goldman-Rakic, P. S. (1995). Intrinsic circuit organization of the major layers and sublayers of the dorsolateral prefrontal cortex in the rhesus monkey. *J Comp Neurol*, *359*(1), 131-143. https://doi.org/10.1002/cne.903590109

Kruglikov, I., & Rudy, B. (2008). Perisomatic GABA release and thalamocortical integration onto neocortical excitatory cells are regulated by neuromodulators. *Neuron*, *58*(6), 911-924. https://doi.org/10.1016/j.neuron.2008.04.024

Krystal, J. H., Anticevic, A., Yang, G. J., Dragoi, G., Driesen, N. R., Wang, X. J., & Murray, J. D. (2017). Impaired Tuning of Neural Ensembles and the Pathophysiology of Schizophrenia: A Translational and Computational Neuroscience Perspective. *Biol Psychiatry*, *81*(10), 874-885. https://doi.org/10.1016/j.biopsych.2017.01.004

Krystal, J. H., Karper, L. P., Seibyl, J. P., Freeman, G. K., Delaney, R., Bremner, J. D., Heninger, G. R., Bowers, M. B., & Charney, D. S. (1994). Subanesthetic effects of the noncompetitive NMDA antagonist, ketamine, in humans. Psychotomimetic, perceptual, cognitive, and neuroendocrine responses. *Arch Gen Psychiatry*, *51*(3), 199-214. https://doi.org/10.1001/archpsyc.1994.03950030035004

Krystal, J. H., D'Souza, D. C., Mathalon, D., Perry, E., Belger, A., & Hoffman, R. (2003). NMDA receptor antagonist effects, cortical glutamatergic function, and schizophrenia: toward a paradigm shift in medication development. *Psychopharmacology*, *169*(3-4), 215-233. https://doi.org/10.1007/s00213-003-1582-z

Kubota, Y. (1994). Three distinct subpopulations of GABAergic neurons in rat frontal agranular cortex. *Brain Research*, *649*(1), 159-173.

Kulhara, P., Shah, R., & Grover, S. (2009). Is the course and outcome of schizophrenia better in the 'developing' world. *Asian Journal of Psychiatry*, *2*(2), 55-62. https://doi.org/10.1016/j.ajp.2009.04.003

Kuznetsova, A., Brockhoff, P. B., & Christensen, R. H. B. lmerTest Package: Tests in Linear Mixed Effects Models. *Journal of Statistical Software*, *82*(13).

Kwon, H.-B., & Sabatini, B. L. (2011). Glutamate induces de novo growth of functional spines in developing cortex. *Nature*, *474*(7349), 100-104. https://doi.org/10.1038/nature09986

Lanz, T. A., Reinhart, V., Sheehan, M. J., Rizzo, S. J. S., Bove, S. E., James, L. C., Volfson, D., Lewis, D. A., & Kleiman, R. J. (2019). Postmortem transcriptional profiling reveals widespread increase in inflammation in schizophrenia: a comparison of prefrontal cortex, striatum, and hippocampus among matched tetrads of controls with subjects diagnosed with schizophrenia, bipolar or major depressive disorder. *Transl Psychiatry*, *9*(1), 151. https://doi.org/10.1038/s41398-019-0492-8

Lau, C. G., & Murthy, V. N. (2012). Activity-dependent regulation of inhibition via GAD67. *J Neurosci*, *32*(25), 8521-8531. https://doi.org/10.1523/JNEUROSCI.1245-12.2012

Lawson, J. S., McGhie, A., & Chapman, J. (1967). Distractibility in schizophrenia and organic cerebral disease. *Br J Psychiatry*, *113*(498), 527-535. https://doi.org/10.1192/bjp.113.498.527

Lee, J., & Park, S. (2005). Working memory impairments in schizophrenia: a meta-analysis. *J Abnorm Psychol*, *114*(4), 599-611. https://doi.org/10.1037/0021-843X.114.4.599

Lee, L., Boorman, L., Glendenning, E., Christmas, C., Sharp, P., Redgrave, P., Shabir, O., Bracci, E., Berwick, J., & Howarth, C. (2020). Key Aspects of Neurovascular Control Mediated by Specific Populations of Inhibitory Cortical Interneurons. *Cereb Cortex*, *30*(4), 2452-2464. https://doi.org/10.1093/cercor/bhz251

Lee, S. H., Rosenmund, C., Schwaller, B., & Neher, E. (2000). Differences in Ca2+ buffering properties between excitatory and inhibitory hippocampal neurons from the rat. *J Physiol*, *525 Pt 2*, 405-418. https://doi.org/10.1111/j.1469-7793.2000.t01-3-00405.x

Lennert, T., & Martinez-Trujillo, J. (2011). Strength of response suppression to distracter stimuli determines attentional-filtering performance in primate prefrontal neurons. *Neuron*, *70*(1), 141-152. https://doi.org/10.1016/j.neuron.2011.02.041

Lenth, R. (2022) emmeans: Estimated Marginal Means, aka Least-Squares Mean.

Lesh, T. A., Niendam, T. A., Minzenberg, M. J., & Carter, C. S. (2011). Cognitive control deficits in schizophrenia: Mechanisms and meaning. *Neuropsychopharmacology*, *36*(1), 316-338. https://doi.org/10.1038/npp.2010.156

Letinic, K., Zoncu, R., & Rakic, P. (2002). Origin of GABAergic neurons in the human neocortex. *Nature*, *417*(6889), 645-649. https://doi.org/10.1038/nature00779

Levitt, J. B., Lewis, D. A., Yoshioka, T., & Lund, J. S. (1993). Topography of pyramidal neuron intrinsic connections in macaque monkey prefrontal cortex (areas 9 and 46). *J Comp Neurol*, *338*(3), 360-376. https://doi.org/10.1002/cne.903380304

Lewis, D. A. (2002). The human brain revisited: opportunities and challenges in postmortem studies of psychiatric disorders. *Neuropsychopharmacology*, *26*(2), 143-154. https://doi.org/10.1016/S0893-133X(01)00393-1

Lewis, D. A., Campbell, M. J., & Morrison, J. H. (1986). An immunohistochemical characterization of somatostatin-28 and somatostatin-281-12 in monkey prefrontal cortex. *J Comp Neurol*, *248*(1), 1-18. https://doi.org/10.1002/cne.902480102

Lewis, D. A., & Sweet, R. A. (2009). Schizophrenia from a neural circuitry perspective: advancing toward rational pharmacological therapies. *J Clin Invest*, *119*(4), 706-716. https://doi.org/10.1172/JCI37335

Lewis, D. A., & Lieberman, J. A. (2000). Catching Up on Schizophrenia: Natural History and Neurobiology. *Neuron*, *28*(2), 325-334. http://www.ncbi.nlm.nih.gov/pubmed/11144342

Lewis, S. W., & Murray, R. M. (1987). Obstetric complications, neurodevelopmental deviance, and risk of schizophrenia. *J Psychiatr Res*, *21*(4), 413-421. https://doi.org/10.1016/0022-3956(87)90088-4

Lin, L. C., & Sibille, E. (2015). Somatostatin, neuronal vulnerability and behavioral emotionality. *Molecular psychiatry*, *20*(3), 377-387. https://doi.org/10.1038/mp.2014.184

Lin, L. C., & Sibille, E. (2013). Reduced brain somatostatin in mood disorders: a common pathophysiological substrate and drug target. *Front Pharmacol*, *4*, 110. https://doi.org/10.3389/fphar.2013.00110

Lipska, B. K., Deep-Soboslay, A., Weickert, C. S., Hyde, T. M., Martin, C. E., Herman, M. M., & Kleinman, J. E. (2006). Critical factors in gene expression in postmortem human brain: Focus on studies in schizophrenia. *Biol Psychiatry*, *60*(6), 650-658. https://doi.org/10.1016/j.biopsych.2006.06.019

Lodge, D. J., Behrens, M. M., & Grace, A. A. (2009). A Loss of Parvalbumin-Containing Interneurons Is Associated with Diminished Oscillatory Activity in an Animal Model of

Schizophrenia. *Journal of Neuroscience*, *29*(8), 2344-2354. https://doi.org/10.1523/jneurosci.5419-08.2009

Lorenc, E. S., Mallett, R., & Lewis-Peacock, J. A. (2021). Distraction in Visual Working Memory: Resistance is Not Futile. *Trends Cogn Sci*. https://doi.org/10.1016/j.tics.2020.12.004

Lovett-Barron, M., Turi, G. F., Kaifosh, P., Lee, P. H., Bolze, F., Sun, X. H., Nicoud, J. F., Zemelman, B. V., Sternson, S. M., & Losonczy, A. (2012). Regulation of neuronal input transformations by tunable dendritic inhibition. *Nat Neurosci*, *15*(3), 423-30, S1. https://doi.org/10.1038/nn.3024

Lu, J. T., Li, C. Y., Zhao, J. P., Poo, M. M., & Zhang, X. H. (2007). Spike-timing-dependent plasticity of neocortical excitatory synapses on inhibitory interneurons depends on target cell type. *J Neurosci*, *27*(36), 9711-9720. https://doi.org/10.1523/JNEUROSCI.2513-07.2007

Luck, S. J., Hahn, B., Leonard, C. J., & Gold, J. M. (2019a). The Hyperfocusing Hypothesis: A New Account of Cognitive Dysfunction in Schizophrenia. *Schizophr Bull*, *45*(5), 991-1000. https://doi.org/10.1093/schbul/sbz063

Luck, S. J., Leonard, C. J., Hahn, B., & Gold, J. M. (2019b). Is Attentional Filtering Impaired in Schizophrenia. *Schizophr Bull*, *45*(5), 1001-1011. https://doi.org/10.1093/schbul/sbz045

Luhrmann, T. M., Padmavati, R., Tharoor, H., & Osei, A. (2015). Differences in voice-hearing experiences of people with psychosis in the USA, India and Ghana: Interview-based study. *British Journal of Psychiatry*, *206*(1), 41-44. https://doi.org/10.1192/bjp.bp.113.139048

Luhrmann, T. M., Weisman, K., Aulino, F., Brahinsky, J. D., Dulin, J. C., Dzokoto, V. A., Legare, C. H., Lifshitz, M., Ng, E., Ross-Zehnder, N., & Smith, R. E. (2021). Sensing the presence of gods and spirits across cultures and faiths. *Proceedings of the National Academy of Sciences*, *118*(5). https://doi.org/10.1073/pnas.2016649118

Lund, J. S. (1973). Organization of neurons in the visual cortex, area 17, of the monkey (Macaca mulatta). *J Comp Neurol*, *147*(4), 455-496. https://doi.org/10.1002/cne.901470404

Lund, J. S. (1988). Anatomical organization of macaque monkey striate visual cortex. *Annu Rev Neurosci*, *11*, 253-288. https://doi.org/10.1146/annurev.ne.11.030188.001345

Lundqvist, M., Herman, P., & Miller, E. K. (2018). Working Memory: Delay Activity, Yes! Persistent Activity? Maybe Not. *The Journal of Neuroscience*, *38*(32), 7013-7019. https://doi.org/10.1523/jneurosci.2485-17.2018

Lundqvist, M., Rose, J., Herman, P., Brincat, S. L., Buschman, T. J., & Miller, E. K. (2016). Gamma and Beta Bursts Underlie Working Memory. *Neuron*, *90*(1), 152-164. https://doi.org/10.1016/j.neuron.2016.02.028

Luscher, B., Shen, Q., & Sahir, N. (2011). The GABAergic deficit hypothesis of major depressive disorder. *Mol Psychiatry*, *16*(4), 383-406. https://doi.org/10.1038/mp.2010.120

Ma, T., Wang, C., Wang, L., Zhou, X., Tian, M., Zhang, Q., Zhang, Y., Li, J., Liu, Z., Cai, Y., Liu, F., You, Y., Chen, C., Campbell, K., Song, H., Ma, L., Rubenstein, J. L., & Yang, Z. (2013). Subcortical origins of human and monkey neocortical interneurons. *Nat Neurosci*, *16*(11), 1588-1597. https://doi.org/10.1038/nn.3536

Ma, Y., Hu, H., & Agmon, A. (2012). Short-term plasticity of unitary inhibitory-to-inhibitory synapses depends on the presynaptic interneuron subtype. *J Neurosci*, *32*(3), 983-988. https://doi.org/10.1523/JNEUROSCI.5007-11.2012

MacCabe, J. H., Wicks, S., L√∂fving, S., David, A. S., Berndtsson, √. Ö., Gustafsson, J. E., Allebeck, P., & Dalman, C. (2013). Decline in cognitive performance between ages 13 and 18 years and the risk for psychosis in adulthood: A swedish longitudinal cohort study in males. *JAMA Psychiatry*, *70*(3), 261-270. https://doi.org/10.1001/2013.jamapsychiatry.43

Maddock, R. J., & Buonocore, M. H. (2012). MR Spectroscopic Studies of the Brain in Psychiatric Disorders. In C. S. Carter & W. J. Dalley (Eds.), (Vol. 11, pp. 199-251). Springer. https://doi.org/10.1007/7854_2011_197

Maffei, A., Nelson, S. B., & Turrigiano, G. G. (2004). Selective reconfiguration of layer 4 visual cortical circuitry by visual deprivation. *Nat Neurosci*, *7*(12), 1353-1359. https://doi.org/10.1038/nn1351

Maksymetz, J., Byun, N. E., Luessen, D. J., Li, B., Barry, R. L., Gore, J. C., Niswender, C. M., Lindsley, C. W., Joffe, M. E., & Conn, P. J. (2021). $mGlu_1$ potentiation enhances prelimbic somatostatin interneuron activity to rescue schizophrenia-like physiological and cognitive deficits. *Cell Rep*, *37*(5), 109950. https://doi.org/10.1016/j.celrep.2021.109950

Malmo, R. B. (1942). Interference factors in delayed response in monkeys after removal of frontal lobes. *Journal of Neurophysiology*, *5*(4), 295-308. https://doi.org/10.1152/jn.1942.5.4.295

Maniglio, R. (2009). Severe mental illness and criminal victimization: a systematic review. *Acta Psychiatr Scand*, *119*(3), 180-191. https://doi.org/10.1111/j.1600-0447.2008.01300.x

Manseau, F., Marinelli, S., Mendez, P., Schwaller, B., Prince, D. A., Huguenard, J. R., & Bacci, A. (2010). Desynchronization of neocortical networks by asynchronous release of GABA at autaptic and synaptic contacts from fast-spiking interneurons. *PLoS Biol*, *8*(9), e1000492. https://doi.org/10.1371/journal.pbio.1000492

Marconi, A., Di Forti, M., Lewis, C., Murray, R. M., & Vassos, E. (2016). Meta-analysis of the association between the level of cannabis use and risk of psychosis. *Schizophrenia Bulletin*, 1-8. https://doi.org/10.1093/schbul/sbw003

Marder, S. R., & Cannon, T. D. (2019). Schizophrenia. *N Engl J Med*, *381*(18), 1753-1761. https://doi.org/10.1056/NEJMra1808803

Markram, H., Toledo-Rodriguez, M., Wang, Y., Gupta, A., Silberberg, G., & Wu, C. (2004). Interneurons of the neocortical inhibitory system. *Nat Rev Neurosci*, *5*(10), 793-807. https://doi.org/10.1038/nrn1519

Marlin, J. J., & Carter, A. G. (2014). GABA-A receptor inhibition of local calcium signaling in spines and dendrites. *J Neurosci*, *34*(48), 15898-15911. https://doi.org/10.1523/JNEUROSCI.0869-13.2014

Marshall, C. R., Psychosis, E. I. C., Howrigan, D. P., Merico, D., Thiruvahindrapuram, B., Wu, W., Greer, D. S., Antaki, D., Shetty, A., Holmans, P. A., Pinto, D., Gujral, M., Brandler, W. M., Malhotra, D., Wang, Z., Fajarado, K. V. F., Maile, M. S., Ripke, S., Agartz, I., . . . CNV, A. S. W. G. O. T. P. G. C. (2017). Contribution of copy number variants to

schizophrenia from a genome-wide study of 41,321 subjects. *Nature Genetics*, *49*(1), 27-35. https://doi.org/10.1038/ng.3725

Marshall, L., & Bays, P. M. (2013). Obligatory encoding of task-irrelevant features depletes working memory resources. *J Vis*, *13*(2). https://doi.org/10.1167/13.2.21

Marsman, A., Mandl, R. C., Klomp, D. W., Bohlken, M. M., Boer, V. O., Andreychenko, A., Cahn, W., Kahn, R. S., Luijten, P. R., & Hulshoff Pol, H. E. (2014). GABA and glutamate in schizophrenia: a 7 T ^{1}H-MRS study. *Neuroimage Clin*, *6*, 398-407. https://doi.org/10.1016/j.nicl.2014.10.005

Marty, S., & Onténiente, B. (1997). The expression pattern of somatostatin and calretinin by postnatal hippocampal interneurons is regulated by activity-dependent and -independent determinants. *Neuroscience*, *80*(1), 79-88. https://doi.org/10.1016/s0306-4522(97)00134-6

Marty, S. (2000). Differences in the regulation of neuropeptide Y, somatostatin, and parvalbumin levels in hippocampal interneurons by neuronal activity and BDNF. *Progress in Brain Research*, *128*, 193-202.

Marwaha, S., Johnson, S., Bebbington, P., Stafford, M., Angermeyer, M. C., Brugha, T., Azorin, J. M., Kilian, R., Hansen, K., & Toumi, M. (2007). Rates and correlates of employment in people with schizophrenia in the UK, France and Germany. *Br J Psychiatry*, *191*, 30-37. https://doi.org/10.1192/bjp.bp.105.020982

Maxwell, K. E., Matthews, T. R., Sheehy, M. R. J., Bertelsen, R. D., & Derby, C. D. (2007). Neurolipofuscin is a measure of age in Panulirus argus, the Caribbean spiny lobster, in Florida. *The Biological Bulletin*, *213*(1), 55-66. https://www.journals.uchicago.edu/doi/pdf/10.2307/25066618

Mayer, J. S., Fukuda, K., Vogel, E. K., & Park, S. (2012). Impaired contingent attentional capture predicts reduced working memory capacity in schizophrenia. *PLoS One*, *7*(11), e48586. https://doi.org/10.1371/journal.pone.0048586

McCarthy, G., Puce, A., Constable, T., Krystal, J. H., Gore, J. C., & Goldman-Rakic, P. (1996). Activation of human prefrontal cortex during spatial and nonspatial working memory tasks measured by functional MRI. *Cerebral cortex*, *6*(4), 600-611. https://academic.oup.com/cercor/article-abstract/6/4/600/309917

McGrath, J., Saha, S., Chant, D., & Welham, J. (2008). Schizophrenia: a concise overview of incidence, prevalence, and mortality. *Epidemiol Rev*, *30*, 67-76. https://doi.org/10.1093/epirev/mxn001

McGrath, J. J. (2005a). Variations in the Incidence of Schizophrenia: Data Versus Dogma. *Schizophrenia Bulletin*, *32*(1), 195-197. https://doi.org/10.1093/schbul/sbi052

McGrath, J. J. (2005b). Myths and plain truths about schizophrenia epidemiology - the NAPE lecture 2004. *Acta Psychiatrica Scandinavica*, *111*(1), 4-11. https://doi.org/10.1111/j.1600-0447.2004.00467.x

McNab, F., & Dolan, R. J. (2014). Dissociating distractor-filtering at encoding and during maintenance. *J Exp Psychol Hum Percept Perform*, *40*(3), 960-967. https://doi.org/10.1037/a0036013

McNab, F., Zeidman, P., Rutledge, R. B., Smittenaar, P., Brown, H. R., Adams, R. A., & Dolan, R. J. (2015). Age-related changes in working memory and the ability to ignore distraction. *Proc Natl Acad Sci U S A, 112*(20), 6515-6518. https://doi.org/10.1073/pnas.1504162112

Medalla, M., & Barbas, H. (2009). Synapses with inhibitory neurons differentiate anterior cingulate from dorsolateral prefrontal pathways associated with cognitive control. *Neuron, 61*(4), 609-620. https://doi.org/10.1016/j.neuron.2009.01.006

Melchitzky, D. S., Sesack, S. R., & Lewis, D. A. (1999). Parvalbumin-immunoreactive axon terminals in macaque monkey and human prefrontal cortex: Laminar, regional, and target specificity of type I and type II synapses. *Journal of Comparative Neurology*, *408*(1), 11-22. https://doi.org/10.1002/(SICI)1096-9861(19990524)408:1<11::AID-CNE2>3.0.CO;2-T

Melchitzky, D. S., González-Burgos, G., Barrionuevo, G., & Lewis, D. A. (2001). Synaptic targets of the intrinsic axon collaterals of supragranular pyramidal neurons in monkey prefrontal cortex. *J Comp Neurol, 430*(2), 209-221. https://doi.org/10.1002/1096-9861(20010205)430:2<209::aid-cne1026>3.0.co;2-#

Melchitzky, D. S., & Lewis, D. A. (2003). Pyramidal neuron local axon terminals in monkey prefrontal cortex: differential targeting of subclasses of GABA neurons. *Cereb Cortex, 13*(5), 452-460. https://doi.org/10.1093/cercor/13.5.452

Melchitzky, D. S., & Lewis, D. A. (2008). Dendritic-targeting GABA neurons in monkey prefrontal cortex: comparison of somatostatin- and calretinin-immunoreactive axon terminals. *Synapse*, *62*(6), 456-465. https://doi.org/10.1002/syn.20514

Mellios, N., Huang, H. S., Baker, S. P., Galdzicka, M., Ginns, E., & Akbarian, S. (2009). Molecular determinants of dysregulated GABAergic gene expression in the prefrontal cortex of subjects with schizophrenia. *Biol Psychiatry*, *65*(12), 1006-1014. https://doi.org/10.1016/j.biopsych.2008.11.019

Mendonça, P. R. F., Tagliatti, E., Langley, H., Kotzadimitriou, D., Zamora-Chimal, C. G., Timofeeva, Y., & Volynski, K. E. (2022). Asynchronous glutamate release is enhanced in low release efficacy synapses and dispersed across the active zone. *Nature Communications*, *13*(1), 1-17. https://doi.org/10.1038/s41467-022-31070-4

Meriney, S. D., Gray, D. B., & Pilar, G. R. (1994). Somatostatin-induced inhibition of neuronal Ca2+ current modulated by cGMP-dependent protein kinase. *Nature*, *369*(6478), 336-339. https://doi.org/10.1038/369336a0

Merritt, K., McGuire, P. K., Egerton, A., 1H-MRS, I. S. I., Aleman, A., Block, W., Bloemen, O. J. N., Borgan, F., Bustillo, J. R., Capizzano, A. A., Coughlin, J. M., De la Fuente-Sandoval, C., Demjaha, A., Dempster, K., Do, K. Q., Du, F., Falkai, P., Galinska-Skok, B., Gallinat, J., . . . Yamasue, H. (2021). Association of Age, Antipsychotic Medication, and Symptom Severity in Schizophrenia With Proton Magnetic Resonance Spectroscopy Brain Glutamate Level: A Mega-analysis of Individual Participant-Level Data. *JAMA Psychiatry*. https://doi.org/10.1001/jamapsychiatry.2021.0380

Meskenaite, V. (1997). Calretinin-immunoreactive local circuit neurons in area 17 of the cynomolgus monkey, Macaca fascicularis. *J Comp Neurol, 379*(1), 113-132. https://doi.org/10.1002/(SICI)1096-9861(19970303)379:1<113::AID-CNE8>3.0.CO;2-7

Metzl, J. M. (2010). *The Protest Psychosis: How Schizophrenia Became a Black Disease*. Beacon Press. https://books.google.com/books?id=L9utU61499UC

Michels, L., Martin, E., Klaver, P., Edden, R., Zelaya, F., Lythgoe, D. J., Lüchinger, R., Brandeis, D., & O'Gorman, R. L. (2012). Frontal GABA levels change during working memory. *PLoS One*, *7*(4), e31933. https://doi.org/10.1371/journal.pone.0031933

Miller, E. K., Erickson, C. A., & Desimone, R. (1996). Neural Mechanisms of Visual Working Memory in Prefrontal Cortex of the Macaque. *The Journal of Neuroscience*, *16*(16), 5154-5167. http://www.jneurosci.org/content/jneuro/16/16/5154.full.pdf

Miller, E. K., Lundqvist, M., & Bastos, A. M. (2018). Working Memory 2.0. *Neuron*, *100*(2), 463-475. https://doi.org/10.1016/j.neuron.2018.09.023

Milner, B. (1963). Effects of different brain lesions on card sorting: The role of the frontal lobes. *Archives of neurology*, *9*(1), 90-100. https://jamanetwork.com/journals/jamaneurology/article-abstract/564510

Minamoto, T., Osaka, M., & Osaka, N. (2010). Individual differences in working memory capacity and distractor processing: possible contribution of top-down inhibitory control. *Brain Res*, *1335*, 63-73. https://doi.org/10.1016/j.brainres.2010.03.088

Minzenberg, M. J., Firl, A. J., Yoon, J. H., Gomes, G. C., Reinking, C., & Carter, C. S. (2010). Gamma Oscillatory Power is Impaired During Cognitive Control Independent of Medication Status in First-Episode Schizophrenia. *Neuropsychopharmacology*, *35*(13), 2590-2599. https://doi.org/10.1038/npp.2010.150

Minzenberg, M. J., Laird, A. R., Thelen, S., Carter, C. S., & Glahn, D. C. (2009). Meta-analysis of 41 functional neuroimaging studies of executive function in schizophrenia. *Archives of General Psychiatry*, *66*(8), 811-822. https://doi.org/10.1001/archgenpsychiatry.2009.91.Meta-analysis

Mishara, A. L., & Goldberg, T. E. (2004). A meta-analysis and critical review of the effects of conventional neuroleptic treatment on cognition in schizophrenia: opening a closed book. *Biological Psychiatry*, *55*(10), 1013-1022. https://doi.org/10.1016/j.biopsych.2004.01.027

Mitchell, A. C., Jiang, Y., Peter, C., & Akbarian, S. (2015). Transcriptional regulation of GAD1 GABA synthesis gene in the prefrontal cortex of subjects with schizophrenia. *Schizophr Res*, *167*(1-3), 28-34. https://doi.org/10.1016/j.schres.2014.10.020

Mohan, A., Thalamuthu, A., Mather, K. A., Zhang, Y., Catts, V. S., Weickert, C. S., & Sachdev, P. S. (2018). Differential expression of synaptic and interneuron genes in the aging human prefrontal cortex. *Neurobiol Aging*, *70*, 194-202. https://doi.org/10.1016/j.neurobiolaging.2018.06.011

Mollon, J., David, A. S., Zammit, S., Lewis, G., & Reichenberg, A. (2018). Course of cognitive development from infancy to early adulthood in the psychosis spectrum. *JAMA Psychiatry*, *75*(3), 270-279. https://doi.org/10.1001/jamapsychiatry.2017.4327

Monahan, J. (2002). The MacArthur studies of violence risk. *Crim. Behav. & Mental Health S67*, *12*. https://heinonline.org/hol-cgi-bin/get_pdf.cgi?handle=hein.journals/cbmh12&section=45

Monoranu, C. M., Apfelbacher, M., Grünblatt, E., Puppe, B., Alafuzoff, I., Ferrer, I., Al-Saraj, S., Keyvani, K., Schmitt, A., Falkai, P., Schittenhelm, J., Halliday, G., Kril, J., Harper, C., McLean, C., Riederer, P., & Roggendorf, W. (2009). pH measurement as quality control on human post mortem brain tissue: a study of the BrainNet Europe consortium. *Neuropathol Appl Neurobiol*, *35*(3), 329-337. https://doi.org/10.1111/j.1365-2990.2008.01003a.x

Moreno-García, A., Kun, A., Calero, O., Medina, M., & Calero, M. (2018). An Overview of the Role of Lipofuscin in Age-Related Neurodegeneration. *Front Neurosci*, *12*, 464. https://doi.org/10.3389/fnins.2018.00464

Morey, R. D., & Rouder, J. N. (2018). BayesFactor: Computation of Bayes Factors for Common Designs. https://CRAN.R-project.org/package=BayesFactor

Morris, H. M., Hashimoto, T., & Lewis, D. A. (2008). Alterations in somatostatin mRNA expression in the dorsolateral prefrontal cortex of subjects with schizophrenia or schizoaffective disorder. *Cereb Cortex*, *18*(7), 1575-1587. https://doi.org/10.1093/cercor/bhm186

Morris, H. M., Stopczynski, R. E., & Lewis, D. A. (2009). NPY mRNA expression in the prefrontal cortex: Selective reduction in the superficial white matter of subjects with schizoaffective disorder. *Schizophr Res*, *115*(2-3), 261-269. https://doi.org/10.1016/j.schres.2009.09.014

Morrison, J. H., Rogers, J., Scherr, S., Benoit, R., & Bloom, F. E. (1985). Somatostatin immunoreactivity in neuritic plaques of Alzheimer's patients. *Nature*, *314*(6006), 90-92. https://www.nature.com/articles/314090a0

Murray, J. D., Bernacchia, A., Freedman, D. J., Romo, R., Wallis, J. D., Cai, X., Padoa-Schioppa, C., Pasternak, T., Seo, H., Lee, D., & Wang, X. J. (2014a). A hierarchy of intrinsic timescales across primate cortex. *Nat Neurosci*, *17*(12), 1661-1663. https://doi.org/10.1038/nn.3862

Murray, J. D., Anticevic, A., Gancsos, M., Ichinose, M., Corlett, P. R., Krystal, J. H., & Wang, X. J. (2014b). Linking microcircuit dysfunction to cognitive impairment: effects of disinhibition associated with schizophrenia in a cortical working memory model. *Cereb Cortex*, *24*(4), 859-872. https://doi.org/10.1093/cercor/bhs370

Murray, R. M., Englund, A., Abi-Dargham, A., Lewis, D. A., Di Forti, M., Davies, C., Sherif, M., McGuire, P., & D'Souza, D. C. (2017). Cannabis-associated psychosis: Neural substrate and clinical impact. *Neuropharmacology*, *124*, 89-104. https://doi.org/10.1016/j.neuropharm.2017.06.018

Naskar, S., Qi, J., Pereira, F., Gerfen, C. R., & Lee, S. (2021). Cell-type-specific recruitment of GABAergic interneurons in the primary somatosensory cortex by long-range inputs. *Cell Reports*, *34*(8), 108774. https://doi.org/10.1016/j.celrep.2021.108774

Neighbors, H. W., Jackson, J. S., Campbell, L., & Williams, D. (1989). The influence of racial factors on psychiatric diagnosis: a review and suggestions for research. *Community Ment Health J*, *25*(4), 301-311. https://doi.org/10.1007/BF00755677

Nemeroff, C. B., Youngblood, W. W., Manberg, P. J., Prange Jr, A. J., & Kizer, J. S. (1983). Regional brain concentrations of neuropeptides in Huntington's chorea and schizophrenia. *Science*, *221*(4614), 972-975. https://doi.org/10.2307/1691904

Niendam, T. A., Ray, K. L., Iosif, A. M., Lesh, T. A., Ashby, S. R., Patel, P. K., Smucny, J., Ferrer, E., Solomon, M., Ragland, J. D., & Carter, C. S. (2018). Association of Age at Onset and Longitudinal Course of Prefrontal Function in Youth With Schizophrenia. *JAMA Psychiatry*, *75*(12), 1252-1260. https://doi.org/10.1001/jamapsychiatry.2018.2538

Nusser, Z., Sieghartt, W., Benket, D., Fritschyt, J.-M., & Somogyi, P. (1996). Differential synaptic localization of two major y-aminobutyric acid type A receptor alpha subunits on hippocampal pyramidal cells. *Proceedings of the National Academy of Sciences*, *93*, 11939-11944. http://www.pnas.org/content/93/21/11939.long

Obermayer, J., Heistek, T. S., Kerkhofs, A., Goriounova, N. A., Kroon, T., Baayen, J. C., Idema, S., Testa-Silva, G., Couey, J. J., & Mansvelder, H. D. (2018). Lateral inhibition by Martinotti interneurons is facilitated by cholinergic inputs in human and mouse neocortex. *Nat Commun*, *9*(1), 4101. https://doi.org/10.1038/s41467-018-06628-w

Oeth, K. M., & Lewis, D. A. (1990). Cholecystokinin innervation of monkey prefrontal cortex: an immunohistochemical study. *J Comp Neurol*, *301*(1), 123-137. https://doi.org/10.1002/cne.903010112

Oh, H., Piantadosi, S. C., Rocco, B. R., Lewis, D. A., Watkins, S. C., & Sibille, E. (2019). The Role of Dendritic Brain-Derived Neurotrophic Factor Transcripts on Altered Inhibitory Circuitry in Depression. *Biol Psychiatry*, *85*(6), 517-526. https://doi.org/10.1016/j.biopsych.2018.09.026

Oh, W. C., Lutzu, S., Castillo, P. E., & Kwon, H. B. (2016). De novo synaptogenesis induced by GABA in the developing mouse cortex. *Science*, *353*(6303), 1037-1040. https://doi.org/10.1126/science.aaf5206

Olbert, C. M., Nagendra, A., & Buck, B. (2018). Meta-analysis of Black vs. White racial disparity in schizophrenia diagnosis in the United States: Do structured assessments attenuate racial disparities. *J Abnorm Psychol*, *127*(1), 104-115. https://doi.org/10.1037/abn0000309

Olesen, P. J., Macoveanu, J., Tegnér, J., & Klingberg, T. (2007). Brain activity related to working memory and distraction in children and adults. *Cereb Cortex*, *17*(5), 1047-1054. https://doi.org/10.1093/cercor/bhl014

Olfson, M., Gerhard, T., Huang, C., Crystal, S., & Stroup, T. S. (2015). Premature Mortality Among Adults With Schizophrenia in the United States. *JAMA Psychiatry*, *72*(12), 1172. https://doi.org/10.1001/jamapsychiatry.2015.1737

Oltmanns, T. F. (1978). Selective attention in schizophrenic and manic psychoses: the effect of distraction on information processing. *J Abnorm Psychol*, *87*(2), 212-225. https://doi.org/10.1037//0021-843x.87.2.212

Oltmanns, T. F., & Neale, J. M. (1975). Schizophrenic performance when distractors are present: attentional deficit or differential task difficulty. *J Abnorm Psychol*, *84*(3), 205-209. https://doi.org/10.1037/h0076721

Otsuka, T., & Kawaguchi, Y. (2009). Cortical Inhibitory Cell Types Differentially Form Intralaminar and Interlaminar Subnetworks withExcitatory Neurons. *Journal of Neuroscience*, *29*(34), 10533-10540. https://doi.org/10.1523/jneurosci.2219-09.2009

Pala, A., & Petersen, C. (2015). In Vivo Measurement of Cell-Type-Specific Synaptic Connectivity and Synaptic Transmission in Layer 2/3 Mouse Barrel Cortex. *Neuron*, *85*(1), 68-75. https://doi.org/10.1016/j.neuron.2014.11.025

Palmer, B. W., Heaton, R. K., Gladsjo, J. A., Evans, J. D., Patterson, T. L., Golshan, S., & Jeste, D. V. (2002). Heterogeneity in functional status among older outpatients with schizophrenia: employment history, living situation, and driving. *Schizophrenia research*, *55*(3), 205-215. https://www.sciencedirect.com/science/article/pii/S0920996401002183

Pan, N. C., Fang, A., Shen, C., Sun, L., Wu, Q., & Wang, X. (2019). Early Excitatory Activity-Dependent Maturation of Somatostatin Interneurons in Cortical Layer 2/3 of Mice. *Cereb Cortex*, *29*(10), 4107-4118. https://doi.org/10.1093/cercor/bhy293

Pantazopoulos, H., Wiseman, J. T., Markota, M., Ehrenfeld, L., & Berretta, S. (2017). Decreased Numbers of Somatostatin-Expressing Neurons in the Amygdala of Subjects With Bipolar Disorder or Schizophrenia: Relationship to Circadian Rhythms. *Biol Psychiatry*, *81*(6), 536-547. https://doi.org/10.1016/j.biopsych.2016.04.006

Papadopoulos, G. C., Cavanagh, M. E., Antonopoulos, J., Michaloudi, H., & Parnavelas, J. G. (1993). Postnatal development of somatostatin-containing neurons in the visual cortex of normal and dark-reared rats. *Exp Brain Res*, *92*(3), 473-478. https://doi.org/10.1007/BF00229035

Park, H. J., Choi, I., & Leem, K. H. (2021). Decreased Brain pH and Pathophysiology in Schizophrenia. *Int J Mol Sci*, *22*(16), 8358. https://doi.org/10.3390/ijms22168358

Park, H. J., Kong, J. H., Kang, Y. S., Park, W. M., Jeong, S. A., Park, S. M., Lim, J. K., & Jeon, C. J. (2002). The distribution and morphology of calbindin D28K- and calretinin-immunoreactive neurons in the visual cortex of mouse. *Mol Cells*, *14*(1), 143-149. https://pubmed.ncbi.nlm.nih.gov/12243344

Park, S., & Holzman, P. S. (1992). Schizophrenics show spatial working memory deficits. *Arch Gen Psychiatry*, *49*(12), 975-982. https://doi.org/10.1001/archpsyc.1992.01820120063009

Passingham, R. E. (1985). Memory of monkeys (Macaca mulatta) with lesions in prefrontal cortex. *Behav Neurosci*, *99*(1), 3-21. https://doi.org/10.1037//0735-7044.99.1.3

Patel, A. B., de Graaf, R. A., Martin, D. L., Battaglioli, G., & Behar, K. L. (2006a). Evidence that GAD₆₅mediates increased GABA synthesis during intense neuronal activityin vivo. *Journal of Neurochemistry*, *97*(2), 385-396. https://doi.org/10.1111/j.1471-4159.2006.03741.x

Patel, V., Cohen, A., Thara, R., & Gureje, O. (2006b). Is the outcome of schizophrenia really better in developing countries. *Braz J Psychiatry*, *28*(2), 149-152. https://doi.org/10.1590/s1516-44462006000200014

Peng, M., Li, Y., Wamsley, B., Wei, Y., & Roeder, K. (2021). Integration and transfer learning of single-cell transcriptomes via cFIT. *Proceedings of the National Academy of Sciences*, *118*(10), e2024383118. https://www.pnas.org/doi/full/10.1073/pnas.2024383118

Pérez-Santiago, J., Diez-Alarcia, R., Callado, L. F., Zhang, J. X., Chana, G., White, C. H., Glatt, S. J., Tsuang, M. T., Everall, I. P., Meana, J. J., & Woelk, C. H. (2012). A combined analysis of microarray gene expression studies of the human prefrontal cortex identifies

genes implicated in schizophrenia. *J Psychiatr Res*, *46*(11), 1464-1474. https://doi.org/10.1016/j.jpsychires.2012.08.005

Perlstein, W. M., Carter, C. S., Noll, D. C., & Cohen, J. D. (2001). Relation of prefrontal cortex dysfunction to working memory and symptoms in schizophrenia. *Am J Psychiatry*, *158*(7), 1105-1113. https://doi.org/10.1176/appi.ajp.158.7.1105

Petanjek, Z., Berger, B., & Esclapez, M. (2009). Origins of cortical GABAergic neurons in the cynomolgus monkey. *Cereb Cortex*, *19*(2), 249-262. https://doi.org/10.1093/cercor/bhn078

Peters, A., Leahu, D., Moss, M. B., & McNally, K. J. (1994). The effects of aging on area 46 of the frontal cortex of the rhesus monkey. *Cereb Cortex*, *4*(6), 621-635. https://doi.org/10.1093/cercor/4.6.621

Petrides, M., Alivisatos, B., Meyer, E., & Evans, A. C. (1993). Functional activation of the human frontal cortex during the performance of verbal working memory tasks. *Proceedings of the National Academy of Sciences*, *90*(3), 878-882. https://www.pnas.org/content/90/3/878.short

Pfeffer, C. K., Xue, M., He, M., Josh Huang, Z., & Scanziani, M. (2013). Inhibition of inhibition in visual cortex: the logic of connections between molecularly distinct interneurons. *Nature Neuroscience*, *16*, 1068-1076. https://doi.org/10.1038/nn.3446

Pierri, J. N., Volk, C. L., Auh, S., Sampson, A., & Lewis, D. A. (2001). Decreased somal size of deep layer 3 pyramidal neurons in the prefrontal cortex of subjects with schizophrenia. *Arch Gen Psychiatry*, *58*(5), 466-473. https://doi.org/10.1001/archpsyc.58.5.466

Pierri, J. N., Chaudry, A. S., Woo, T.-U. W., & Lewis, D. A. (1999). Alterations in Chandelier Neuron Axon Terminals in the Prefrontal Cortex of Schizophrenic Subjects. *American Journal of Psychiatry*, *156*(11), 1709-1719.

Pocklington, A., Rees, E., Walters, J., Han, J., Kavanagh, D., Chambert, K., Holmans, P., Moran, J., McCarroll, S., Kirov, G., O'Donovan, M., & Owen, M. (2015). Novel Findings from CNVs Implicate Inhibitory and Excitatory Signaling Complexes in Schizophrenia. *Neuron*, *86*(5), 1203-1214. https://doi.org/10.1016/j.neuron.2015.04.022

Pouille, F., & Scanziani, M. (2001). Enforcement of temporal fidelity in pyramidal cells by somatic feed-forward inhibition. *Science*, *293*(5532), 1159-1163. https://doi.org/10.1126/science.1060342

Prevot, T. D., Sumitomo, A., Tomoda, T., Knutson, D. E., Li, G., Mondal, P., Banasr, M., Cook, J. M., & Sibille, E. (2021). Reversal of Age-Related Neuronal Atrophy by α5-GABAA Receptor Positive Allosteric Modulation. *Cereb Cortex*, *31*(2), 1395-1408. https://doi.org/10.1093/cercor/bhaa310

Prevot, T. D., Sumitomo, A., Tomoda, T., Knutson, D. E., Li, G., Cook, J. M., & Sibille, E. (2020). Chronic administration of a positive allosteric modulator at the α5-GABAA receptor reverses age-related dendritic shrinkage. https://doi.org/10.1101/2020.02.28.964742

Price, A. J., Jaffe, A. E., & Weinberger, D. R. (2021). Cortical cellular diversity and development in schizophrenia. *Mol Psychiatry*, *26*(1), 203-217. https://doi.org/10.1038/s41380-020-0775-8

Psychiatric Genomics Consortium. (2009). Common polygenic variation contributes to risk of schizophrenia and bipolar disorder. *Nature*, *460*(7256), 748-752. https://doi.org/10.1038/nature08185

Psychiatric Genomics Consortium. (2018). Genomic Dissection of Bipolar Disorder and Schizophrenia, Including 28 Subphenotypes. *Cell*, *173*(7), 1705-1715.e16. https://doi.org/10.1016/j.cell.2018.05.046

Pucak, M. L., Levitt, J. B., Lund, J. S., & Lewis, D. A. (1996). Patterns of intrinsic and associational circuitry in monkey prefrontal cortex. *J Comp Neurol*, *376*(4), 614-630. https://doi.org/10.1002/(SICI)1096-9861(19961223)376:4<614::AID-CNE9>3.0.CO;2-4

Puig, E., Tolchard, J., Riera, A., & Carulla, N. (2020). Somatostatin, an In Vivo Binder to Aβ Oligomers, Binds to βPFO_{Aβ(1–42)} Tetramers. *ACS Chemical Neuroscience*, *11*(20), 3358-3365. https://doi.org/10.1021/acschemneuro.0c00470

Purcell, S. M., Moran, J. L., Fromer, M., Ruderfer, D., Solovieff, N., Roussos, P., O,ÄôDushlaine, C., Chambert, K., Bergen, S. E., K√§hler, A., Duncan, L., Stahl, E., Genovese, G., Fern√°ndez, E., Collins, M. O., Komiyama, N. H., Choudhary, J. S., Magnusson, P. K. E., Banks, E., . . . Sklar, P. (2014). A polygenic burden of rare disruptive mutations in schizophrenia. *Nature*, *506*(7487), 185-190. https://doi.org/10.1038/nature12975

Qi, X. L., Katsuki, F., Meyer, T., Rawley, J. B., Zhou, X., Douglas, K. L., & Constantinidis, C. (2010). Comparison of neural activity related to working memory in primate dorsolateral prefrontal and posterior parietal cortex. *Front Syst Neurosci*, *4*, 12. https://doi.org/10.3389/fnsys.2010.00012

R Core Team. (2018). R: A language and environment for statistical computing. https://www.R-project.org/

Rainer, G., Asaad, W. F., & Miller, E. K. (1998). Selective representation of relevant information by neurons in the primate prefrontal cortex. *Nature*, *393*(6685), 577-579. https://doi.org/10.1038/31235

Rajkowska, G., Selemon, L. D., & Goldman-Rakic, P. S. (1998). Neuronal and Glial Somal Size in the Prefrontal Cortex: A Postmortem Morphometric Study of Schizophrenia and Huntington Disease. *Archives of General Psychiatry*, *55*(3), 215-215. https://doi.org/10.1001/archpsyc.55.3.215

Rao, S. G., Williams, G. V., & Goldman-Rakic, P. S. (1999). Isodirectional tuning of adjacent interneurons and pyramidal cells during working memory: evidence for microcolumnar organization in PFC. *J Neurophysiol*, *81*(4), 1903-1916. https://doi.org/10.1152/jn.1999.81.4.1903

Rao, S. G., Williams, G. V., & Goldman-Rakic, P. S. (2000). Destruction and creation of spatial tuning by disinhibition: GABAA blockade of prefrontal cortical neurons engaged by working memory. *Journal of Neuroscience*, *20*(1), 485-494. https://www.jneurosci.org/content/20/1/485.short

Reichenberg, A., Caspi, A., Harrington, H., Houts, R., Keefe, R. S., Murray, R. M., Poulton, R., & Moffitt, T. E. (2010). Static and dynamic cognitive deficits in childhood preceding adult

schizophrenia: a 30-year study. *Am J Psychiatry*, *167*(2), 160-169. https://doi.org/10.1176/appi.ajp.2009.09040574

Reyes, A., Lujan, R., Rozov, A., Burnashev, N., Somogyi, P., & Sakmann, B. (1998). Target-cell-specific facilitation and depression in neocortical circuits. *Nat Neurosci*, *1*(4), 279-285. https://doi.org/10.1038/1092

Reynolds, G. P. (2021). The neurochemical pathology of schizophrenia: post-mortem studies from dopamine to parvalbumin. *J Neural Transm (Vienna)*. https://doi.org/10.1007/s00702-021-02453-6

Reynolds, G. P., & Beasley, C. L. (2001). GABAergic neuronal subtypes in the human frontal cortex--development and deficits in schizophrenia. *J Chem Neuroanat*, *22*(1-2), 95-100. https://doi.org/10.1016/s0891-0618(01)00113-2

Riedemann, T., & Sutor, B. (2019). Long-lasting actions of somatostatin on pyramidal cell excitability in the mouse cingulate cortex. *Neurosci Lett*, *698*, 217-223. https://doi.org/10.1016/j.neulet.2019.01.034

Riley, M. R., & Constantinidis, C. (2015). Role of Prefrontal Persistent Activity in Working Memory. *Front Syst Neurosci*, *9*, 181. https://doi.org/10.3389/fnsys.2015.00181

Ritsher, J. B., Otilingam, P. G., & Grajales, M. (2003). Internalized stigma of mental illness: psychometric properties of a new measure. *Psychiatry Res*, *121*(1), 31-49. https://doi.org/10.1016/j.psychres.2003.08.008

Roberts, G. W., Crow, T. J., & Polak, J. M. (1985). Location of neuronal tangles in somatostatin neurones in Alzheimer's disease. *Nature*, *314*(6006), 92-94. https://doi.org/10.1038/314092a0

Robertson, C. E., Ratai, E. M., & Kanwisher, N. (2016). Reduced GABAergic Action in the Autistic Brain. *Curr Biol*, *26*(1), 80-85. https://doi.org/10.1016/j.cub.2015.11.019

Rocco, B. R., Lewis, D. A., & Fish, K. N. (2016a). Markedly Lower Glutamic Acid Decarboxylase 67 Protein Levels in a Subset of Boutons in Schizophrenia. *Biol Psychiatry*, *79*(12), 1006-1015. https://doi.org/10.1016/j.biopsych.2015.07.022

Rocco, B. R., Sweet, R. A., Lewis, D. A., & Fish, K. N. (2016b). GABA-Synthesizing Enzymes in Calbindin and Calretinin Neurons in Monkey Prefrontal Cortex. *Cereb Cortex*, *26*(5), 2191-2204. https://doi.org/10.1093/cercor/bhv051

Rockel, A. J., Hiorns, R. W., & Powell, T. P. (1980). The basic uniformity in structure of the neocortex. *Brain*, *103*(2), 221-244. https://doi.org/10.1093/brain/103.2.221

Rofo, F., Ugur Yilmaz, C., Metzendorf, N., Gustavsson, T., Beretta, C., Erlandsson, A., Sehlin, D., Syvänen, S., Nilsson, P., & Hultqvist, G. (2021). Enhanced neprilysin-mediated degradation of hippocampal Aβ42 with a somatostatin peptide that enters the brain. *Theranostics*, *11*(2), 789-804. https://doi.org/10.7150/thno.50263

Roux, F., Wibral, M., Mohr, H. M., Singer, W., & Uhlhaas, P. J. (2012). Gamma-band activity in human prefrontal cortex codes for the number of relevant items maintained in working memory. *J Neurosci*, *32*(36), 12411-12420. https://doi.org/10.1523/JNEUROSCI.0421-12.2012

Rudolph, U., & Knoflach, F. (2011). Beyond classical benzodiazepines: novel therapeutic potential of GABAA receptor subtypes. *Nat Rev Drug Discov*, *10*(9), 685-697. https://doi.org/10.1038/nrd3502

Rueckert, L., & Grafman, J. (1996). Sustained attention deficits in patients with right frontal lesions. *Neuropsychologia*, *34*(10), 953-963. https://doi.org/10.1016/0028-3932(96)00016-4

Ruff, C. (2021). *Tacr1 marks a population of long-range inhibitory neurons that regulate neurovascular coupling*. University of Pittsburgh. http://d-scholarship.pitt.edu/41066.

Runyan, C. A., Schummers, J., Van Wart, A., Kuhlman, S. J., Wilson, N. R., Huang, Z. J., & Sur, M. (2010). Response features of parvalbumin-expressing interneurons suggest precise roles for subtypes of inhibition in visual cortex. *Neuron*, *67*(5), 847-857. https://doi.org/10.1016/j.neuron.2010.08.006

Saha, S., Chant, D., Welham, J., & McGrath, J. (2005). A systematic review of the prevalence of schizophrenia. *PLoS Med*, *2*(5), e141. https://doi.org/10.1371/journal.pmed.0020141

Saito, T., Iwata, N., Tsubuki, S., Takaki, Y., Takano, J., Huang, S. M., Suemoto, T., Higuchi, M., & Saido, T. C. (2005). Somatostatin regulates brain amyloid beta peptide Abeta42 through modulation of proteolytic degradation. *Nat Med*, *11*(4), 434-439. https://doi.org/10.1038/nm1206

Sakai, K., Rowe, J. B., & Passingham, R. E. (2002). Active maintenance in prefrontal area 46 creates distractor-resistant memory. *Nat Neurosci*, *5*, 479-484. https://doi.org/10.1038/nn846

Sakai, T., Oshima, A., Nozaki, Y., Ida, I., Haga, C., Akiyama, H., Nakazato, Y., & Mikuni, M. (2008). Changes in density of calcium-binding-protein-immunoreactive GABAergic neurons in prefrontal cortex in schizophrenia and bipolar disorder. *Neuropathology*, *28*(2), 143-150. https://doi.org/10.1111/j.1440-1789.2007.00867.x

Sánchez-Muñoz, I., Sánchez-Franco, F., Vallejo, M., Fernández, A., Palacios, N., Fernández, M., & Cacicedo, L. (2010). Activity-dependent somatostatin gene expression is regulated by cAMP-dependent protein kinase and Ca2+-calmodulin kinase pathways. *J Neurosci Res*, *88*(4), 825-836. https://doi.org/10.1002/jnr.22264

Sariaslan, A., Arseneault, L., Larsson, H., Lichtenstein, P., & Fazel, S. (2020). Risk of Subjection to Violence and Perpetration of Violence in Persons With Psychiatric Disorders in Sweden. *JAMA Psychiatry*, *77*(4), 359-367. https://doi.org/10.1001/jamapsychiatry.2019.4275

Sartorius, N., Chiu, H., Heok, K. E., Lee, M. S., Ouyang, W. C., Sato, M., Yang, Y. K., & Yu, X. (2014). Name change for schizophrenia. *Schizophr Bull*, *40*(2), 255-258. https://doi.org/10.1093/schbul/sbt231

Sartorius, N., Jablensky, A., Korten, A., Ernberg, G., Anker, M., Cooper, J. E., & Day, R. (1986). Early manifestations and first-contact incidence of schizophrenia in different cultures. A preliminary report on the initial evaluation phase of the WHO Collaborative Study on determinants of outcome of severe mental disorders. *Psychol Med*, *16*(4), 909-928. https://doi.org/10.1017/s0033291700011910

Savalia, N. K., Shao, L. X., & Kwan, A. C. (2021). A Dendrite-Focused Framework for Understanding the Actions of Ketamine and Psychedelics. *Trends Neurosci*, *44*(4), 260-275. https://doi.org/10.1016/j.tins.2020.11.008

Sawaguchi, T., Matsumura, M., & Kubota, K. (1989). Delayed response deficits produced by local injection of bicuculline into the dorsolateral prefrontal cortex in Japanese macaque monkeys. *Exp Brain Res*, *75*(3), 457-469. https://doi.org/10.1007/BF00249897

Schmidt, B. F., Chao, J., Zhu, Z., DeBiasio, R. L., & Fisher, G. (1997). Signal amplification in the detection of single-copy DNA and RNA by enzyme-catalyzed deposition (CARD) of the novel fluorescent reporter substrate Cy3.29-tyramide. *J Histochem Cytochem*, *45*(3), 365-373. https://doi.org/10.1177/002215549704500304

Schmidt, U., Weigert, M., Broaddus, C., & Myers, G. (2018). Cell Detection with Star-Convex Polygons. In A. F. Frangi, J. A. Schnabel, C. Davatzikos, C. Alberola-López, & G. Fichtinger (Eds.), *Medical Image Computing and Computer Assisted Intervention – MICCAI* (pp. 265-273). Springer International Publishing. https://doi.org/10.1007/978-3-030-00934-2_30

Schoonover, K. E., Dienel, S. J., & Lewis, D. A. (2020). Prefrontal cortical alterations of glutamate and GABA neurotransmission in schizophrenia: Insights for rational biomarker development. *Biomark Neuropsychiatry*, *3*. https://doi.org/10.1016/j.bionps.2020.100015

Schulz, J. M., Knoflach, F., Hernandez, M. C., & Bischofberger, J. (2018). Dendrite-targeting interneurons control synaptic NMDA-receptor activation via nonlinear α5-$GABA_A$ receptors. *Nat Commun*, *9*(1), 3576. https://doi.org/10.1038/s41467-018-06004-8

Schwartz, R. C. (2014). Racial disparities in psychotic disorder diagnosis: A review of empirical literature. *World Journal of Psychiatry*, *4*(4), 133. https://doi.org/10.5498/wjp.v4.i4.133

Shao, L. X., Liao, C., Gregg, I., Davoudian, P. A., Savalia, N. K., Delagarza, K., & Kwan, A. C. (2021). Psilocybin induces rapid and persistent growth of dendritic spines in frontal cortex in vivo. *Neuron*, *109*(16), 2535-2544.e4. https://doi.org/10.1016/j.neuron.2021.06.008

Sheehy, M. R. J., Greenwood, J. G., & Fielder, D. R. (1994). More accurate chronological age determination of crustaceans from field situations using the physiological age marker, lipofuscin. *Marine Biology*, *121*(2), 237-245. https://link.springer.com/article/10.1007/BF00346731

Silberberg, G., & Markram, H. (2007). Disynaptic inhibition between neocortical pyramidal cells mediated by Martinotti cells. *Neuron*, *53*(5), 735-746. https://doi.org/10.1016/j.neuron.2007.02.012

Silberstein, J., & Harvey, P. D. (2019). Cognition, social cognition, and Self-assessment in schizophrenia: prediction of different elements of everyday functional outcomes. *CNS Spectrums*, *24*(1), 88-93. https://doi.org/10.1017/s1092852918001414

Silver, H., & Feldman, P. (2005). Evidence for sustained attention and working memory in schizophrenia sharing a common mechanism. *J Neuropsychiatry Clin Neurosci*, *17*(3), 391-398. https://doi.org/10.1176/jnp.17.3.391

Silver, H., Feldman, P., Bilker, W., & Gur, R. C. (2003). Working memory deficit as a core neuropsychological dysfunction in schizophrenia. *Am J Psychiatry*, *160*(10), 1809-1816. https://doi.org/10.1176/appi.ajp.160.10.1809

Singh, T., INTERVAL, S., Walters, J. T. R., Johnstone, M., Curtis, D., Suvisaari, J., Torniainen, M., Rees, E., Iyegbe, C., Blackwood, D., McIntosh, A. M., Kirov, G., Geschwind, D., Murray, R. M., Di Forti, M., Bramon, E., Gandal, M., Hultman, C. M., Sklar, P., . . . UK10K, C. (2017). The contribution of rare variants to risk of schizophrenia in individuals with and without intellectual disability. *Nature Genetics*, *49*(8), 1167-1173. https://doi.org/10.1038/ng.3903

Skene, N. G., Bryois, J., Bakken, T. E., Breen, G., Crowley, J. J., Gaspar, H. A., Giusti-Rodriguez, P., Hodge, R. D., Miller, J. A., Muñoz-Manchado, A. B., O'Donovan, M. C., Owen, M. J., Pardiñas, A. F., Ryge, J., Walters, J. T. R., Linnarsson, S., Lein, E. S., Major, D. D. W. G. O. T. P. G. C., Sullivan, P. F., . . . Hjerling-Leffler, J. (2018). Genetic identification of brain cell types underlying schizophrenia. *Nat Genet*, *50*(6), 825-833. https://doi.org/10.1038/s41588-018-0129-5

Smiley, J. F., McGinnis, J. P., & Javitt, D. C. (2000). Nitric oxide synthase interneurons in the monkey cerebral cortex are subsets of the somatostatin, neuropeptide Y, and calbindin cells. *863*, 205-212. www.elsevier.com/locate/bres

Smith, M. L., Leonard, G., Crane, J., & Milner, B. (1995). The effects of frontal- or temporal-lobe lesions on susceptibility to interference in spatial memory. *Neuropsychologia*, *33*(3), 275-285. https://doi.org/10.1016/0028-3932(94)00120-e

Smucny, J., Carter, C. S., & Maddock, R. J. (2021). Medial Prefrontal Cortex Glutamate Is Reduced in Schizophrenia and Moderated by Measurement Quality: A Meta-analysis of Proton Magnetic Resonance Spectroscopy Studies. *Biol Psychiatry*, *90*(9), 643-651. https://doi.org/10.1016/j.biopsych.2021.06.008

Smucny, J., Dienel, S. J., Lewis, D. A., & Carter, C. S. (2022). Mechanisms underlying dorsolateral prefrontal cortex contributions to cognitive dysfunction in schizophrenia. *Neuropsychopharmacology*, *47*(1), 292-308. https://doi.org/10.1038/s41386-021-01089-0

Smucny, J., Lesh, T. A., Zarubin, V. C., Niendam, T. A., Ragland, J. D., Tully, L. M., & Carter, C. S. (2020). One-Year Stability of Frontoparietal Cognitive Control Network Connectivity in Recent Onset Schizophrenia: A Task-Related 3T fMRI Study. *Schizophrenia Bulletin*, *46*(5), 1249-1258. https://doi.org/10.1093/schbul/sbz122

Sohal, V. S. (2022). Transforming Discoveries About Cortical Microcircuits and Gamma Oscillations Into New Treatments for Cognitive Deficits in Schizophrenia. *Am J Psychiatry*, *179*(4), 267-276. https://doi.org/10.1176/appi.ajp.20220147

Sohal, V. S., Zhang, F., Yizhar, O., & Deisseroth, K. (2009). Parvalbumin neurons and gamma rhythms enhance cortical circuit performance. *Nature*, *459*(7247), 698-702. https://doi.org/10.1038/nature07991

Sokoloff, L., Reivich, M., Kennedy, C., Rosiers, M. H. D., Patlak, C. S., Pettigrew, K. D. E. A., Sakurada, O., & Shinohara, M. (1977). The [14C] deoxyglucose method for the measurement of local cerebral glucose utilization: theory, procedure, and normal values in

the conscious and anesthetized albino rat. *Journal of neurochemistry*, *28*(5), 897-916. https://onlinelibrary.wiley.com/doi/abs/10.1111/j.1471-4159.1977.tb10649.x

Sommer, I. E., Tiihonen, J., van Mourik, A., Tanskanen, A., & Taipale, H. (2020). The clinical course of schizophrenia in women and men—a nation-wide cohort study. *npj Schizophrenia*, *6*(1). https://doi.org/10.1038/s41537-020-0102-z

Song, Y. H., Hwang, Y. S., Kim, K., Lee, H. R., Kim, J. H., Maclachlan, C., Dubois, A., Jung, M. W., Petersen, C. C. H., Knott, G., Lee, S. H., & Lee, S. H. (2020). Somatostatin enhances visual processing and perception by suppressing excitatory inputs to parvalbumin-positive interneurons in V1. *Sci Adv*, *6*(17), eaaz0517. https://doi.org/10.1126/sciadv.aaz0517

Song, Y. H., Yoon, J., & Lee, S. H. (2021). The role of neuropeptide somatostatin in the brain and its application in treating neurological disorders. *Exp Mol Med*, *53*(3), 328-338. https://doi.org/10.1038/s12276-021-00580-4

Southwell, D. G., Nicholas, C. R., Basbaum, A. I., Stryker, M. P., Kriegstein, A. R., Rubenstein, J. L., & Alvarez-Buylla, A. (2014). Interneurons from embryonic development to cell-based therapy. *Science*, *344*(6180), 1240622. https://doi.org/10.1126/science.1240622

Stamm, J. S. (1969). Electrical stimulation of monkeys' prefrontal cortex during delayed-response performance. *Journal of Comparative and Physiological Psychology*, *67*(4), 535. https://psycnet.apa.org/record/1969-10874-001

Stan, A. D., & Lewis, D. A. (2012). Altered cortical GABA neurotransmission in schizophrenia: insights into novel therapeutic strategies. *Curr Pharm Biotechnol*, *13*(8), 1557-1562. https://doi.org/10.2174/138920112800784925

Stansfield, K. H., Ruby, K. N., Soares, B. D., McGlothan, J. L., Liu, X., & Guilarte, T. R. (2015). Early-life lead exposure recapitulates the selective loss of parvalbumin-positive GABAergic interneurons and subcortical dopamine system hyperactivity present in schizophrenia. *Transl Psychiatry*, *5*, e522. https://doi.org/10.1038/tp.2014.147

Starc, M., Murray, J. D., Santamauro, N., Savic, A., Diehl, C., Cho, Y. T., Srihari, V., Morgan, P. T., Krystal, J. H., Wang, X. J., Repovs, G., & Anticevic, A. (2017). Schizophrenia is associated with a pattern of spatial working memory deficits consistent with cortical disinhibition. *Schizophr Res*, *181*, 107-116. https://doi.org/10.1016/j.schres.2016.10.011

Steadman, H. J., Monahan, J., Pinals, D. A., Vesselinov, R., & Robbins, P. C. (2015). Gun Violence and Victimization of Strangers by Persons With a Mental Illness: Data From the MacArthur Violence Risk Assessment Study. *Psychiatr Serv*, *66*(11), 1238-1241. https://doi.org/10.1176/appi.ps.201400512

Stirling, D. R., Swain-Bowden, M. J., Lucas, A. M., Carpenter, A. E., Cimini, B. A., & Goodman, A. (2021). CellProfiler 4: improvements in speed, utility and usability. *BMC Bioinformatics*, *22*(1), 433. https://doi.org/10.1186/s12859-021-04344-9

Stokes, C. C., Teeter, C. M., & Isaacson, J. S. (2014). Single dendrite-targeting interneurons generate branch-specific inhibition. *Front Neural Circuits*, *8*, 139. https://doi.org/10.3389/fncir.2014.00139

Strakowski, S. M., Keck, P. E., Arnold, L. M., Collins, J., Wilson, R. M., Fleck, D. E., Corey, K. B., Amicone, J., & Adebimpe, V. R. (2003). Ethnicity and diagnosis in patients with affective disorders. *The Journal of Clinical Psychiatry*, *64*(7), 747-754. https://doi.org/10.4088/JCP.v64n0702

Strassnig, M., Bowie, C., Pinkham, A. E., Penn, D., Twamley, E. W., Patterson, T. L., & Harvey, P. D. (2018). Which levels of cognitive impairments and negative symptoms are related to functional deficits in schizophrenia. *J Psychiatr Res*, *104*, 124-129. https://doi.org/10.1016/j.jpsychires.2018.06.018

Straub, R. E., Lipska, B. K., Egan, M. F., Goldberg, T. E., Callicott, J. H., Mayhew, M. B., Vakkalanka, R. K., Kolachana, B. S., Kleinman, J. E., & Weinberger, D. R. (2007). Allelic variation in GAD1 (GAD67) is associated with schizophrenia and influences cortical function and gene expression. *Mol Psychiatry*, *12*(9), 854-869. https://doi.org/10.1038/sj.mp.4001988

Suárez-Solá, M. L., González-Delgado, F. J., Pueyo-Morlans, M., Medina-Bolívar, O. C., Hernández-Acosta, N. C., González-Gómez, M., & Meyer, G. (2009). Neurons in the white matter of the adult human neocortex. *Front Neuroanat*, *3*, 7. https://doi.org/10.3389/neuro.05.007.2009

Sum, M. Y., Chan, S. K. W., Tse, S., Bola, J. R., & Chen, E. Y. H. (2021). Internalized stigma as an independent predictor of employment status in patients with schizophrenia. *Psychiatric Rehabilitation Journal*, *44*(3), 299-302. https://doi.org/10.1037/prj0000451

Suzuki, M., & Gottlieb, J. (2013). Distinct neural mechanisms of distractor suppression in the frontal and parietal lobe. *Nat Neurosci*, *16*(1), 98-104. https://doi.org/10.1038/nn.3282

Sweet, R. A., Hamilton, R. L., Butters, M. A., Mulsant, B. H., Pollock, B. G., Lewis, D. A., Lopez, O. L., DeKosky, S. T., & Reynolds, C. F. (2004). Neuropathologic Correlates of Late-Onset Major Depression. *Neuropsychopharmacology*, *29*(12), 2242-2250. https://doi.org/10.1038/sj.npp.1300554

Sydnor, V. J., & Roalf, D. R. (2020). A meta-analysis of ultra-high field glutamate, glutamine, GABA and glutathione 1HMRS in psychosis: Implications for studies of psychosis risk. *Schizophr Res*, *226*, 61-69. https://doi.org/10.1016/j.schres.2020.06.028

Szczepanski, S. M., & Knight, R. T. (2014). Insights into human behavior from lesions to the prefrontal cortex. *Neuron*, *83*(5), 1002-1018. https://doi.org/10.1016/j.neuron.2014.08.011

Szkultecka-Dębek, M., Miernik, K., Stelmachowski, J., Jakovljević, M., Jukić, V., Aadamsoo, K., Janno, S., Bitter, I., Jarema, M., & Jankovic, S. (2016). SCHIZOPHRENIA CAUSES SIGNIFICANT BURDEN TO PATIENTS'AND CAREGIVERS'LIVES. *Psychiatria Danubina*, *28*(2), 104-110. https://hrcak.srce.hr/file/258533

Taylor, S. F., & Tso, I. F. (2015). GABA abnormalities in schizophrenia: a methodological review of in vivo studies. *Schizophr Res*, *167*(1-3), 84-90. https://doi.org/10.1016/j.schres.2014.10.011

Teplin, L. A., McClelland, G. M., Abram, K. M., & Weiner, D. A. (2005). Crime victimization in adults with severe mental illness: comparison with the National Crime Victimization Survey. *Arch Gen Psychiatry*, *62*(8), 911-921. https://doi.org/10.1001/archpsyc.62.8.911

Tepper, J. M., Koós, T., Ibanez-Sandoval, O., Tecuapetla, F., Faust, T. W., & Assous, M. (2018). Heterogeneity and Diversity of Striatal GABAergic Interneurons: Update 2018. *Front Neuroanat*, *12*, 91. https://doi.org/10.3389/fnana.2018.00091

Tepper, J. M., & Koós, T. (2017). GABAergic Interneurons of the Striatum. In *Handbook of Basal Ganglia Structure and Function* (Vol. 24, pp. 157-178). Academic Press. https://doi.org/10.1016/B978-0-12-802206-1.00008-8

Terman, A., & Brunk, U. T. (2004). Lipofuscin. *The International Journal of Biochemistry & Cell Biology*, *36*(8), 1400-1404. https://doi.org/10.1016/j.biocel.2003.08.009

Teuber, H. L. (2009). The riddle of frontal lobe function in man. 1964. *Neuropsychol Rev*, *19*(1), 25-46. https://doi.org/10.1007/s11065-009-9088-z

Thakkar, K. N., Rösler, L., Wijnen, J. P., Boer, V. O., Klomp, D. W., Cahn, W., Kahn, R. S., & Neggers, S. F. (2017). 7T Proton Magnetic Resonance Spectroscopy of Gamma-Aminobutyric Acid, Glutamate, and Glutamine Reveals Altered Concentrations in Patients With Schizophrenia and Healthy Siblings. *Biol Psychiatry*, *81*(6), 525-535. https://doi.org/10.1016/j.biopsych.2016.04.007

Thompson-Schill, S. L., Jonides, J., Marshuetz, C., Smith, E. E., D'Esposito, M., Kan, I. P., Knight, R. T., & Swick, D. (2002). Effects of frontal lobe damage on interference effects in working memory. *Cogn Affect Behav Neurosci*, *2*, 109-120. https://doi.org/10.3758/cabn.2.2.109

Thune, J. J., Uylings, H. B., & Pakkenberg, B. (2001). No deficit in total number of neurons in the prefrontal cortex in schizophrenics. *J Psychiatr Res*, *35*(1), 15-21. https://doi.org/10.1016/s0022-3956(00)00043-1

Tomioka, R., & Rockland, K. S. (2007). Long-distance corticocortical GABAergic neurons in the adult monkey white and gray matter. *J Comp Neurol*, *505*(5), 526-538. https://doi.org/10.1002/cne.21504

Tomoda, T., Sumitomo, A., Newton, D., & Sibille, E. (2022). Molecular origin of somatostatin-positive neuron vulnerability. *Mol Psychiatry*, *27*(4), 2304-2314. https://doi.org/10.1038/s41380-022-01463-4

Tooney, P. A., & Chahl, L. A. (2004). Neurons expressing calcium-binding proteins in the prefrontal cortex in schizophrenia. *Progress in Neuro-Psychopharmacology and Biological Psychiatry*, *28*(2), 273-278. https://doi.org/10.1016/j.pnpbp.2003.10.004

Torchiano, M. (2020) effsize - A Package For Efficient Effect Size Computation. https://doi.org/10.5281/zenodo.1480624

Torres-Gomez, S., Blonde, J. D., Mendoza-Halliday, D., Kuebler, E., Everest, M., Wang, X. J., Inoue, W., Poulter, M. O., & Martinez-Trujillo, J. (2020). Changes in the Proportion of Inhibitory Interneuron Types from Sensory to Executive Areas of the Primate Neocortex: Implications for the Origins of Working Memory Representations. *Cereb Cortex*, *30*(8), 4544-4562. https://doi.org/10.1093/cercor/bhaa056

Torrey, E. F., Barci, B. M., Webster, M. J., Bartko, J. J., Meador-Woodruff, J. H., & Knable, M. B. (2005). Neurochemical markers for schizophrenia, bipolar disorder, and major

depression in postmortem brains. *Biol Psychiatry*, *57*(3), 252-260. https://doi.org/10.1016/j.biopsych.2004.10.019

Torrey, E. F., & Yolken, R. H. (2019). Schizophrenia as a pseudogenetic disease: A call for more gene-environmental studies. *Psychiatry Res*, *278*, 146-150. https://doi.org/10.1016/j.psychres.2019.06.006

Tremblay, R., Lee, S., & Rudy, B. (2016). GABAergic Interneurons in the Neocortex: From Cellular Properties to Circuits. *Neuron*, *91*(2), 260-292. https://doi.org/10.1016/j.neuron.2016.06.033

Trubetskoy, V., Pardiñas, A. F., Qi, T., Panagiotaropoulou, G., Awasthi, S., Bigdeli, T. B., Bryois, J., Chen, C. Y., Dennison, C. A., Hall, L. S., Lam, M., Watanabe, K., Frei, O., Ge, T., Harwood, J. C., Koopmans, F., Magnusson, S., Richards, A. L., Sidorenko, J., . . . Schizophrenia, W. G. O. T. P. G. C. (2022). Mapping genomic loci implicates genes and synaptic biology in schizophrenia. *Nature*. https://doi.org/10.1038/s41586-022-04434-5

Tsubomoto, M., Kawabata, R., Zhu, X., Minabe, Y., Chen, K., Lewis, D. A., & Hashimoto, T. (2019). Expression of Transcripts Selective for GABA Neuron Subpopulations across the Cortical Visuospatial Working Memory Network in the Healthy State and Schizophrenia. *Cereb Cortex*, *29*(8), 3540-3550. https://doi.org/10.1093/cercor/bhy227

Tuncdemir, S. N., Wamsley, B., Stam, F. J., Callaway, E. M., Rudy, B., & Fishell, G. (2016). Early Somatostatin Interneuron Connectivity Mediates the Maturation of Deep Layer Cortical Circuits. *Neuron*, *89*, 521-535. https://doi.org/10.1016/j.neuron.2015.11.020

Uhlhaas, P. J., & Singer, W. (2010). Abnormal neural oscillations and synchrony in schizophrenia. *Nature Reviews. Neuroscience*, *11*(2), 100-113. https://doi.org/10.1038/nrn2774

Urban-Ciecko, J., & Barth, A. L. (2016). Somatostatin-expressing neurons in cortical networks. *Nat Rev Neurosci*, *17*(7), 401-409. https://doi.org/10.1038/nrn.2016.53

Urban-Ciecko, J., Fanselow, E. E., & Barth, A. L. (2015). Neocortical somatostatin neurons reversibly silence excitatory transmission via GABAb receptors. *Curr Biol*, *25*(6), 722-731. https://doi.org/10.1016/j.cub.2015.01.035

Urban-Ciecko, J., Jouhanneau, J. S., Myal, S. E., Poulet, J. F. A., & Barth, A. L. (2018). Precisely Timed Nicotinic Activation Drives SST Inhibition in Neocortical Circuits. *Neuron*, *97*(3), 611-625.e5. https://doi.org/10.1016/j.neuron.2018.01.037

van Os, J., Kenis, G., & Rutten, B. P. F. (2010). The environment and schizophrenia. *Nature*, *468*(7321), 203-212. https://doi.org/10.1038/nature09563

Vaucher, E., Tong, X. K., Cholet, N., Lantin, S., & Hamel, E. (2000). GABA neurons provide a rich input to microvessels but not nitric oxide neurons in the rat cerebral cortex: a means for direct regulation of local cerebral blood flow. *J Comp Neurol*, *421*(2), 161-171. https://pubmed.ncbi.nlm.nih.gov/10813779

Vawter, M. P., Crook, J. M., Hyde, T. M., Kleinman, J. E., Weinberger, D. R., Becker, K. G., & Freed, W. J. (2002). Microarray analysis of gene expression in the prefrontal cortex in schizophrenia: a preliminary study. *Schizophrenia Research*, *58*, 11-20. http://ac.els-

cdn.com/S0920996401003772/1-s2.0-S0920996401003772-main.pdf?_tid=93fe821c-7174-11e7-a900-00000aab0f26&acdnat=1501013297_8db15eca7b2611c51c3564c6ec807ad6

Veit, J., Hakim, R., Jadi, M. P., Sejnowski, T. J., & Adesnik, H. (2017). Cortical gamma band synchronization through somatostatin interneurons. *Nature Neuroscience, 20*(7), 951-959. https://doi.org/10.1038/nn.4562

Verrico, C. D., Liu, S., Asafu-Adjei, J. K., Sampson, A. R., Bradberry, C. W., & Lewis, D. A. (2011). Acquisition and baseline performance of working memory tasks by adolescent rhesus monkeys. *Brain Res, 1378*, 91-104. https://doi.org/10.1016/j.brainres.2010.12.081

Vincent, S. L., Peters, A., & Tigges, J. (1989). Effects of aging on the neurons within area 17 of rhesus monkey cerebral cortex. *Anat Rec, 223*(3), 329-341. https://doi.org/10.1002/ar.1092230312

Viollet, C., Lepousez, G., Loudes, C., Videau, C., Simon, A., & Epelbaum, J. (2008). Somatostatinergic systems in brain: networks and functions. *Mol Cell Endocrinol, 286*(1-2), 75-87. https://doi.org/10.1016/j.mce.2007.09.007

Vogel, E. K., McCollough, A. W., & Machizawa, M. G. (2005). Neural measures reveal individual differences in controlling access to working memory. *Nature, 438*(7067), 500-503. https://doi.org/10.1038/nature04171

Volk, D., Austin, M., Pierri, J., Sampson, A., & Lewis, D. (2001). GABA transporter-1 mRNA in the prefrontal cortex in schizophrenia: decreased expression in a subset of neurons. *Am J Psychiatry, 158*(2), 256-265. https://doi.org/10.1176/appi.ajp.158.2.256

Volk, D. W., Edelson, J. R., & Lewis, D. A. (2014). Cortical inhibitory neuron disturbances in schizophrenia: Role of the ontogenetic transcription factor Lhx6. *Schizophrenia Bulletin, 40*(5), 1053-1061. https://doi.org/10.1093/schbul/sbu068

Volk, D. W., Pierri, J. N., Fritschy, J.-M., Auh, S., Sampson, A. R., & Lewis, D. A. (2002). Reciprocal Alterations in Pre- and Postsynaptic Inhibitory Markers at Chandelier Cell Inputs to Pyramidal Neurons in Schizophrenia. *Cerebral Cortex, 12*, 1063-1070. https://doi.org/10.1093/cercor/12.10.1063

Volk, D. W., Austin, M. C., Pierri, J. N., Sampson, A. R., & Lewis, D. A. (2000). Decreased glutamic acid decarboxylase67 messenger RNA expression in a subset of prefrontal cortical gamma-aminobutyric acid neurons in subjects with schizophrenia. *Arch Gen Psychiatry, 57*(3), 237-245. https://doi.org/10.1001/archpsyc.57.3.237

Volk, D. W., Matsubara, T., Li, S., Sengupta, E. J., Georgiev, D., Minabe, Y., Sampson, A., Hashimoto, T., & Lewis, D. A. (2012). Deficits in transcriptional regulators of cortical parvalbumin neurons in schizophrenia. *Am J Psychiatry, 169*(10), 1082-1091. https://doi.org/10.1176/appi.ajp.2012.12030305

Volk, D. W., Sampson, A. R., Zhang, Y., Edelson, J. R., & Lewis, D. A. (2016). Cortical GABA markers identify a molecular subtype of psychotic and bipolar disorders. *Psychol Med, 46*(12), 2501-2512. https://doi.org/10.1017/S0033291716001446

Volman, V., Behrens, M. M., & Sejnowski, T. J. (2011). Downregulation of parvalbumin at cortical GABA synapses reduces network gamma oscillatory activity. *J Neurosci*, *31*(49), 18137-18148. https://doi.org/10.1523/JNEUROSCI.3041-11.2011

Vruwink, M., Schmidt, H. H., Weinberg, R. J., & Burette, A. (2001). Substance P and nitric oxide signaling in cerebral cortex: anatomical evidence for reciprocal signaling between two classes of interneurons. *J Comp Neurol*, *441*(4), 288-301. https://doi.org/10.1002/cne.1413

Wahle, P. (1993). Differential regulation of substance P and somatostatin in Martinotti cells of the developing cat visual cortex. *J Comp Neurol*, *329*(4), 519-538. https://doi.org/10.1002/cne.903290408

Walker, A. E. (1940). A cytoarchitectural study of the prefrontal area of the macaque monkey. *The Journal of Comparative Neurology*, *73*(1), 59-86. https://doi.org/10.1002/cne.900730106

Wallis, J. D., Anderson, K. C., & Miller, E. K. (2001). Single neurons in prefrontal cortex encode abstract rules. *Nature*, *411*(6840), 953-956. https://doi.org/10.1038/35082081

Wang, F., Flanagan, J., Su, N., Wang, L. C., Bui, S., Nielson, A., Wu, X., Vo, H. T., Ma, X. J., & Luo, Y. (2012). RNAscope: a novel in situ RNA analysis platform for formalin-fixed, paraffin-embedded tissues. *J Mol Diagn*, *14*(1), 22-29. https://doi.org/10.1016/j.jmoldx.2011.08.002

Wang, H., Muiznieks, L. D., Ghosh, P., Williams, D., Solarski, M., Fang, A., Ruiz-Riquelme, A., Pomès, R., Watts, J. C., Chakrabartty, A., Wille, H., Sharpe, S., & Schmitt-Ulms, G. (2017). Somatostatin binds to the human amyloid β peptide and favors the formation of distinct oligomers. *Elife*, *6*. https://doi.org/10.7554/eLife.28401

Wang, H. X., & Gao, W. J. (2009). Cell type-specific development of NMDA receptors in the interneurons of rat prefrontal cortex. *Neuropsychopharmacology*, *34*(8), 2028-2040. https://doi.org/10.1038/npp.2009.20

Wang, X.-J. (2021). 50 years of mnemonic persistent activity: quo vadis. *Trends in Neurosciences*, *44*(11), 888-902. https://doi.org/10.1016/j.tins.2021.09.001

Wang, X. J. (2020). Macroscopic gradients of synaptic excitation and inhibition in the neocortex. *Nat Rev Neurosci*, *21*(3), 169-178. https://doi.org/10.1038/s41583-020-0262-x

Wang, X. J., Tegnér, J., Constantinidis, C., & Goldman-Rakic, P. S. (2004). Division of labor among distinct subtypes of inhibitory neurons in a cortical microcircuit of working memory. *Proc Natl Acad Sci U S A*, *101*(5), 1368-1373. https://doi.org/10.1073/pnas.0305337101

Wehring, H. J., & Carpenter, W. T. (2011). Violence and schizophrenia. *Schizophr Bull*, *37*(5), 877-878. https://doi.org/10.1093/schbul/sbr094

Weickert, C. S., Hyde, T. M., Lipska, B. K., Herman, M. M., Weinberger, D. R., & Kleinman, J. E. (2003). Reduced brain-derived neurotrophic factor in prefrontal cortex of patients with schizophrenia. *Mol Psychiatry*, *8*(6), 592-610. https://doi.org/10.1038/sj.mp.4001308

Weinberger, D. R., Berman, K. F., & Zec, R. F. (1986). Physiological Dysfunction of Dorsolateral Prefrontal Cortex in Schizophrenia I. Regional Cerebral Blood Flow

Evidence. *Archives of General Psychiatry, 43*, 114-124. https://doi.org/10.1001/archpsyc.1988.01800310020002

Welch, J. D., Kozareva, V., Ferreira, A., Vanderburg, C., Martin, C., & Macosko, E. Z. (2019). Single-Cell Multi-omic Integration Compares and Contrasts Features of Brain Cell Identity. *Cell*, *177*(7), 1873-1887.e17. https://doi.org/10.1016/j.cell.2019.05.006

Wickham, H. (2016). *ggplot2: Elegant Graphics for Data Analysis*. Springer-Verlag.

Wickham, H., Averick, M., Bryan, J., Chang, W., McGowan, L., François, R., Grolemund, G., Hayes, A., Henry, L., Hester, J., Kuhn, M., Pedersen, T., Miller, E., Bache, S., Müller, K., Ooms, J., Robinson, D., Seidel, D., Spinu, V., . . . Yutani, H. (2017). tidyverse: Easily Install and Load the 'Tidyverse'. *R package version 1.2.1*. https://CRAN.R-project.org/package=tidyverse

Wiener, H. W., Klei, L., Irvin, M. D., Perry, R. T., Aliyu, M. H., Allen, T. B., Bradford, L. D., Calkins, M. E., Devlin, B., Edwards, N., Gur, R. E., Gur, R. C., Kwentus, J., Lyons, P. D., McEvoy, J. P., Nasrallah, H. A., Nimgaonkar, V. L., O'Jile, J., Santos, A. B., . . . Go, R. C. P. (2009). Linkage analysis of schizophrenia in African-American families. *Schizophrenia Research*, *109*(1-3), 70-79. https://doi.org/10.1016/j.schres.2009.02.007

Williams, S. M., Goldman-Rakic, P. S., & Leranth, C. (1992). The synaptology of parvalbumin-immunoreactive neurons in the primate prefrontal cortex. *J Comp Neurol*, *320*(3), 353-369. https://doi.org/10.1002/cne.903200307

Willoughby, C. D. E. (2018). Running Away from Drapetomania: Samuel A. Cartwright, Medicine, and Race in the Antebellum South. *Journal of Southern History*, *84*(3), 579-614. https://doi.org/10.1353/soh.2018.0164

Wilson, F. A. W., Scalaidhe, S. P. √., & Goldman-Rakic, P. S. (1994). Functional synergism between putative y-aminobutyrate-containing neurons and pyramidal neurons in prefrontal cortex. *Proceedings of the National Academy of Sciences USA*, *91*, 4009-4013. http://www.pnas.org/content/91/9/4009.long

Wonders, C. P., & Anderson, S. A. (2006). The origin and specification of cortical interneurons. *Nat Rev Neurosci*, *7*(9), 687-696. https://doi.org/10.1038/nrn1954

Wong, F. K., Bercsenyi, K., Sreenivasan, V., Portalés, A., Fernández-Otero, M., & Marín, O. (2018a). Pyramidal cell regulation of interneuron survival sculpts cortical networks. *Nature*, *557*(7707), 668-673. https://doi.org/10.1038/s41586-018-0139-6

Wong, Y. I., Kong, D., Tu, L., & Frasso, R. (2018b). "My bitterness is deeper than the ocean": understanding internalized stigma from the perspectives of persons with schizophrenia and their family caregivers. *Int J Ment Health Syst*, *12*, 14. https://doi.org/10.1186/s13033-018-0192-4

Woo, T.-U., Whitehead, R. E., Melchitzky, D. S., & Lewis, D. A. (1998). A subclass of prefrontal gamma-aminobutyric acid axon terminals are selectively altered in schizophrenia. *Proceedings of the National Academy of Sciences USA*, *95*, 5341-5346. http://www.pnas.org/content/95/9/5341.full.pdf

Woo, T. U., Kim, A. M., & Viscidi, E. (2008). Disease-specific alterations in glutamatergic neurotransmission on inhibitory interneurons in the prefrontal cortex in schizophrenia. *Brain Res, 1218,* 267-277. https://doi.org/10.1016/j.brainres.2008.03.092

Woo, T. U., Miller, J. L., & Lewis, D. A. (1997). Schizophrenia and the parvalbumin-containing class of cortical local circuit neurons. *Am J Psychiatry, 154*(7), 1013-1015. https://doi.org/10.1176/ajp.154.7.1013

Woodruff, A. R., Anderson, S. A., & Yuste, R. (2010). The enigmatic function of chandelier cells. *Front Neurosci, 4*, 201. https://doi.org/10.3389/fnins.2010.00201

Wu, E. Q., Birnbaum, H. G., Shi, L., Ball, D. E., Kessler, R. C., Moulis, M., & Aggarwal, J. (2005). The economic burden of schizophrenia in the United States in 2002. *Journal of Clinical Psychiatry, 66*(9), 1122-1129.

Xu, H., Jeong, H. Y., Tremblay, R., & Rudy, B. (2013). Neocortical somatostatin-expressing GABAergic interneurons disinhibit the thalamorecipient layer 4. *Neuron, 77*(1), 155-167. https://doi.org/10.1016/j.neuron.2012.11.004

Xu, M. Y., & Wong, A. H. C. (2018). GABAergic inhibitory neurons as therapeutic targets for cognitive impairment in schizophrenia. *Acta Pharmacol Sin, 39*(5), 733-753. https://doi.org/10.1038/aps.2017.172

Xu, X., Roby, K. D., & Callaway, E. M. (2006). Mouse Cortical Inhibitory Neuron Type that Coexpresses Somatostatin and Calretinin. *The Journal of Comparative Neurology, 499,* 144-160. https://doi.org/10.1002/cne

Xue, M., Atallah, B. V., & Scanziani, M. (2014). Equalizing excitation-inhibition ratios across visual cortical neurons. *Nature, 511*(7511), 596-600. https://doi.org/10.1038/nature13321

Yamashita, A., Hayashi, M., Shimizu, K., & Oshima, K. (1989). Ontogeny of somatostatin in cerebral cortex of macaque monkey: an immunohistochemical study. *Brain Res Dev Brain Res, 45*(1), 103-111. https://doi.org/10.1016/0165-3806(89)90012-6

Yan, X. X., Jen, L. S., & Garey, L. J. (1996). NADPH-Diaphorase-Positive Neurons in Primate Cerebral Cortex Colocalize with GABA and Calcium-Binding Proteins. *Cerebral Cortex, 6,* 524-529. https://academic.oup.com/cercor/article-abstract/6/3/524/385595

Yang, G. R., Murray, J. D., & Wang, X. J. (2016). A dendritic disinhibitory circuit mechanism for pathway-specific gating. *Nat Commun, 7,* 12815. https://doi.org/10.1038/ncomms12815

Yang, L. H., & Kleinman, A. (2008). 'Face'and the embodiment of stigma in China: The cases of schizophrenia and AIDS. *Social science & medicine, 67*(3), 398-408. https://www.sciencedirect.com/science/article/pii/S0277953608001445

Yang, Y., Fung, S. J., Rothwell, A., Tianmei, S., & Weickert, C. S. (2011). Increased interstitial white matter neuron density in the dorsolateral prefrontal cortex of people with schizophrenia. *Biol Psychiatry, 69*(1), 63-70. https://doi.org/10.1016/j.biopsych.2010.08.020

Yoon, J. H., Grandelis, A., & Maddock, R. J. (2016). Dorsolateral Prefrontal Cortex GABA Concentration in Humans Predicts Working Memory Load Processing Capacity. *The Journal of Neuroscience, 36*(46), 11788-11794. https://doi.org/10.1523/JNEUROSCI.1970-16.2016

Yoon, J. H., Minzenberg, M. J., Ursu, S., Walters, R., Carter Wendelken, B., Daniel Ragland, J., & Carter, C. S. (2008). Association of Dorsolateral Prefrontal Cortex Dysfunction With Disrupted Coordinated Brain Activity in Schizophrenia: Relationship With Impaired Cognition, Behavioral Disorganization, and Global Function. *American Journal of Psychiatry, 165*, 1006-1014. http://ajp.psychiatryonline.org/doi/pdfplus/10.1176/appi.ajp.2008.07060945

Yoshimura, Y., & Callaway, E. M. (2005). Fine-scale specificity of cortical networks depends on inhibitory cell type and connectivity. *Nature Neuroscience, 8*(11), 1552-1559. https://doi.org/10.1038/nn1565

Zaitsev, A. V., Povysheva, N. V., Gonzalez-Burgos, G., Rotaru, D., Fish, K. N., Krimer, L. S., & Lewis, D. A. (2009). Interneuron diversity in layers 2-3 of monkey prefrontal cortex. *Cereb Cortex, 19*(7), 1597-1615. https://doi.org/10.1093/cercor/bhn198

Zanelli, J., Reichenberg, A., Sandin, S., Morgan, C., Dazzan, P., Pilecka, I., Marques, T. R., Morgan, K., Young, A. H., & Mollon, J. (2022). Dynamic and Static Cognitive Deficits in Schizophrenia and Bipolar Disorder After the First Episode. *Schizophrenia Bulletin*. https://doi.org/10.1093/schbul/sbab150

Zanto, T. P., & Gazzaley, A. (2009). Neural suppression of irrelevant information underlies optimal working memory performance. *J Neurosci, 29*(10), 3059-3066. https://doi.org/10.1523/JNEUROSCI.4621-08.2009

Zhou, X., Zhu, D., Qi, X. L., Li, S., King, S. G., Salinas, E., Stanford, T. R., & Constantinidis, C. (2016). Neural correlates of working memory development in adolescent primates. *Nat Commun, 7*, 13423. https://doi.org/10.1038/ncomms13423

Zhou, X., Katsuki, F., Qi, X.-L., & Constantinidis, C. (2012). Neurons with inverted tuning during the delay periods of working memory tasks in the dorsal prefrontal and posterior parietal cortex. *Journal of Neurophysiology*, *108*(1), 31-38. https://doi.org/10.1152/jn.01151.2011

Zilberter, Y., Kaiser, K. M., & Sakmann, B. (1999). Dendritic GABA release depresses excitatory transmission between layer 2/3 pyramidal and bitufted neurons in rat neocortex. *Neuron, 24*(4), 979-988. https://doi.org/10.1016/S0896-6273(00)81044-2